NONLINEAR DYNAMICS AND SEISMIC RESPONSE OF POWER TRANSMISSION LINES

BY

MOHAMED MOHSEN EL-ATTAR, B. Sc., M. Sc.

A Thesis

Submitted to the School of Graduate Studies

in Partial Fulfilment of the Requirements

for the Degree of

Doctor of Philosophy

McMaster University

TO MY FAMILY

NONLINEAR DYNAMICS AND SEISMIC RESPONSE OF POWER TRANSMISSION LINES

DOCTOR OF PHILOSOPHY (1997)
(Civil Engineering Department)

McMaster University
Hamilton, Ontario

TITLE: Nonlinear Dynamics and Seismic Response of Power Transmission Lines

AUTHOR: Mohamed Mohsen El-Attar, B.Sc. Cairo University
M.Sc. Cairo University

SUPERVISOR: Professor T.S. Aziz
Professor A. Ghobarah

NUMBER OF PAGES: xx, 254

ABSTRACT

Electric power transmission lines have been traditionally designed for wind and ice loads. The earthquake load has not been considered in the analysis of transmission lines. During recent earthquakes, there have been indications of damage to transmission lines. Due to the complex nature of the problem, there is a lack of research work in the area of seismic analysis of transmission lines.

The objective of this study is to evaluate the response of transmission lines to earthquake ground motion in order to evaluate the current design code methodology. The scope of this research program includes: 1) Modelling of different parts of the transmission line to analyze its seismic response, 2) comparison between the forces generated in the transmission tower members by wind, ice and earthquake loads, and 3) analyzing the probabilistic characteristics of the cable response to earthquake ground motion in order to establish a seismic design procedure for transmission lines.

An intermediate span of a typical transmission line is chosen for the analysis. The tower members are modelled as truss elements. The cables are modelled by two node elements that retain their geometric nonlinearity. The dynamic characteristics of different components of the line (towers and cables) are determined in order to obtain a better understanding of the line behaviour. The in-plane and out-of-plane vibrations of the line are

analyzed. The transmission line response to multiple support as well as uniform support excitations is evaluated. A closed form analytical solution for the cable vibration is carried out for a more detailed study of the cable nonlinear behaviour.

It is concluded from the analysis that earthquake ground motion may cause substantial displacements and internal forces in the transmission line elements. The forces in transmission tower members due to the earthquake load may exceed those caused by the wind loads specified by the National Electrical Safety Code (NESC, 1993). Seismic ground motion may cause large displacement in the transmission line cables. This suggests that the cable motion during earthquakes should be included in the design of the line clearances to avoid having cables touch each other, which may cause power failure.

ACKNOWLEDGEMENTS

I would like to express my sincere appreciation to my research supervisors, Dr. A. Ghobarah and Dr. T. S. Aziz, for their guidance during every stage of this research work. Their persistent support combined with their constructive criticism and praise has contributed abundantly in putting this thesis in its final shape.

I would like also to express my sincere gratitude to Dr. W. K. Tso and Dr. M. Elbestawi, the other members of my supervisory committee, for their valuable comments and suggestions.

Finally, this thesis is dedicated to my parents, my wife and my children for their understanding and continuous encouragements. Their love is the backbone in my persistence to excel.

TABLE OF CONTENTS

		Page
ABSTRACT		iii
ACKNOWLEDGEMENTS		v
TABLE OF CONTENTS		vi
LIST OF FIGURES		xi
LIST OF TABLES		xviii
CHAPTER 1 INTRODUCTION		
1.1	GENERAL	1
1.2	REVIEW OF PREVIOUS WORK	2
1.2.1	Modelling of Different Elements of Transmission Lines	2
1.2.1.1	Modelling of cables	3
1.2.1.2	Modelling of towers	5
1.2.2	Transmission Line Analysis for Various Load Conditions	6
1.2.3	Multiple Support Excitation of Structures	7
1.3	OBJECTIVES AND SCOPE	8
1.4	ORGANIZATION	10
CHAPTER 2 FINITE ELEMENT APPROACH FOR SEISMIC ANALYSIS OF CABLES		
2.1	GENERAL	12
2.2	ANALYSIS PROCEDURE	13

Page

2.2.1 Formulation of Element Matrices 13
2.2.2 Element Verification 17

2.3 SELECTION OF PARAMETERS 18
2.3.1 Cable Characteristics 19
2.3.2 Ground Motion Characteristics 19

2.4 FREE VIBRATION CHARACTERISTICS OF CABLES 20

2.5 SEISMIC RESPONSE OF CABLES 22
2.5.1 Effect of the Frequency Content of Ground Motion 22
2.5.2 Effect of the Cable Sag to Span Ratio 24
2.5.3 Effect of the Cable Damping Ratio 25
2.5.4 Effect of Difference in Elevation between Cable Supports 26

2.6 SUMMARY 28

CHAPTER 3 SEISMIC ANALYSIS OF TRANSMISSION LINE SYSTEMS

3.1 GENERAL 63

3.2 SEISMIC ANALYSIS OF TRANSMISSION TOWERS 65

3.3 SEISMIC RESPONSE OF TRANSMISSION LINES 68
3.3.1 Modelling of Transmission Lines for Seismic Analysis 70
3.3.1.1 Transverse excitation 70
3.3.1.2 Vertical excitation 72
3.3.2 Effect of Cable Insulator on the Seismic Response of Transmission Lines 72

3.4 COMPARISON BETWEEN WIND AND EARTHQUAKE EFFECTS 74
3.4.1 Code Specifications 74
3.4.2 Design Procedure 75

Page

3.4.3 Evaluation of Combined Wind and Ice Loading (Case I) 77
3.4.3.1 Loads from the conductors 77
3.4.3.2 Loads from the tower itself 77
3.4.4 Evaluation of Extreme Wind Loading (Case II) 78
3.4.5 Numerical Example 79

3.5 SUMMARY 80

CHAPTER 4 MULTIPLE SUPPORT EXCITATION OF TRANSMISSION LINES

4.1 GENERAL 116

4.2 GENERATION OF ARTIFICIAL GROUND DISPLACEMENT 117
4.2.1 Power Spectral Density of Ground Motion 118
4.2.2 Coherency Models 120
4.2.3 Method for Generating Ground Displacement 122
4.2.4 Wave Travel Effect 125
4.2.5 Generated Ground Displacement 126

4.3 ANALYSIS APPROACH 127
4.3.1 Equations of Motion 127
4.3.2 Simplified Approach for the analysis 129

4.4 RESPONSE OF TRANSMISSION LINES TO TRANSVERSE GROUND MOTION 130
4.4.1 Transverse Cable Displacement 131
4.4.2 Internal Forces in Transmission Line Elements 133
4.4.3 Effect of Choice of a Specific Coherency Model 134
4.4.4 Incoherency Versus Wave Travel Effects 135

4.5 RESPONSE OF TRANSMISSION LINES TO VERTICAL GROUND MOTION 136

Page

4.5.1 Vertical Cable Displacement 136
4.5.2 Internal Forces in Transmission Line Elements 137
4.5.3 Effect of the Coherency Model 138
4.5.4 Incoherency Versus Wave Travel Effects 138

4.6 SUMMARY 139

CHAPTER 5 ANALYTICAL SOLUTION OF CABLE VIBRATION

5.1 GENERAL 168

5.2 EQUATIONS OF CABLE VIBRATION 170
5.2.1 Response of Cables to Support Excitation 173
5.2.2 Solution of the Equations of Motion 177
5.2.3 Transverse Excitation 179
5.2.4 Vertical Excitation 183

5.3 STABILITY OF STEADY STATE SOLUTION 184

5.4 NUMERICAL EXAMPLES 185
5.4.1 Verification of the Results 186
5.4.2 Effect of the Cable Sag to Span Ratio 188
5.4.3 Effect of Damping Ratio on the Response 189

5.5 EFFECT OF PHASE DIFFERENCE BETWEEN SUPPORT EXCITATIONS 189
5.5.1 Transverse Excitation 189
5.5.1.1 Symmetric modes 189
5.5.1.2 Anti-symmetric modes 190
5.5.2 Vertical Excitation 190
5.5.2.1 Symmetric modes 190
5.5.2.2 Anti-symmetric modes 190
5.5.3 Discussion 191

5.6 SUMMARY 192

Page

CHAPTER 6 RELIABILITY ASSESSMENT OF CABLE VIBRATION

6.1 GENERAL 207

6.2 GROUND MOTION MODELLING 209
6.2.1 Power Spectral Density Function 210
6.2.2 Temporal Shape of Ground Motion 211

6.3 ANALYSIS PROCEDURE 211

6.4 ANALYSIS RESULTS 213
6.4.1 Statistical Properties of the Cable Response 213
6.4.2 Comparison between the Results Using Actual and Artificial Earthquakes 215
6.4.3 Probability Distribution Curves for the Cable Response 216

6.5 SENSITIVITY ANALYSIS 217
6.5.1 Effect of the Cable Sag to Span Ratio 218
6.5.2 Effect of Strong Ground Motion Duration 219
6.5.3 Effect of Probability Distribution Type of Earthquake Predominant Frequency 219

6.6 SUMMARY 220

CHAPTER 7 SUMMARY AND CONCLUSIONS

7.1 SUMMARY 242

7.2 CONCLUSIONS 243

7.3 RECOMMENDATIONS 245

REFERENCES 247

LIST OF FIGURES

Figure	Title	Page
2.1	Cable configuration	37
2.2	Transverse displacement time history of cable mid-point under suddenly applied load	38
2.3	Cable seismic response to the 1952 Taft earthquake	39
2.4	Frequency-response relationship for Cable I (sag to span ratio of 0.03) in the transverse direction: (a) displacement and (b) tension	42
2.5	Frequency-response relationship for Cable I (sag to span ratio of 0.03) in the vertical direction: (a) displacement and (b) tension	43
2.6	Frequency-response relationship for Cable II (sag to span ratio of 0.01) in the transverse direction: (a) displacement and (b) tension	44
2.7	Frequency-response relationship for Cable II (sag to span ratio of 0.01) in the vertical direction: (a) displacement and (b) tension	45
2.8	Frequency-response relationship for Cable III (sag to span ratio of 0.003) in the transverse direction: (a) displacement and (b) tension	46
2.9	Frequency-response relationship for Cable III (sag to span ratio of 0.003) in the vertical direction: (a) displacement and (b) tension	47
2.10	Transverse displacement of cable mid-point due to the horizontal component of ground motion	48
2.11	Vertical displacement of cable mid-point due to the vertical component of ground motion	50
2.12	Vertical displacement at cable ¼ span due to the longitudinal component of ground motion	52

Figure	Title	Page
2.13	Cable supports at different elevations	54
2.14	Transverse displacement of cable mid-point due to the Horizontal component of the Mexico earthquake for different values of h/L	55
2.15	Transverse displacement of cable mid-point due to the transverse component of the San Fernando earthquake for different values of h/L	57
2.16	Vertical displacement of cable mid-point due to the vertical component of the Mexico earthquake for different values of h/L	59
2.17	Vertical displacement of cable mid-point due to the vertical component of the San Fernando earthquake for different values of h/L	61
3.1	Transmission Tower I	92
3.2	Transmission Tower II	93
3.3	First three mode shapes for Tower I and Tower II	94
3.4	Displacement of point (X) in Tower I for different values of excitation frequency	95
3.5	Displacement of point (X) in Tower II for different values of excitation frequency	95
3.6	Displacement of point (X) in transmission Tower I due to horizontal ground motion	96
3.7	Displacement of point (X) in transmission Tower II due to horizontal ground motion	98
3.8	Transmission line system	100
3.9	Envelopes of maximum response to transverse excitation for transmission lines with Tower I	101

Figure	Title	Page
3.10	Envelopes of maximum response to transverse excitation for transmission lines with Tower II	103
3.11	Envelopes of maximum response to vertical excitation for transmission lines with Tower I	105
3.12	Envelopes of maximum response to vertical excitation for transmission lines with Tower II	107
3.13	Transmission line system with suspension insulators	109
3.14	Effect of suspension insulator on the vibration of cable mid-point due to the horizontal component of the 1985 Mexico earthquake	110
3.15	Effect of suspension insulator on the vibration of cable mid-point due to the horizontal component of the 1971 San Fernando earthquake	111
3.16	Effect of suspension insulator on the vibration of cable mid-point due to the vertical component of ground motion	112
3.17	General wind and ice loading map of the United States for transmission lines (NESC, 1993)	113
3.18	Basic wind speed in miles per hour (NESC, 1993)	113
3.19	Maximum forces in tower members for different load combinations and for cable diameter of 3.5 cm	114
3.20	Maximum forces in tower members for different load combinations and for cable diameter of 2.0 cm	115
4.1	Power spectral density function for the horizontal component of ground motion	144
4.2	Power spectral density function for the vertical component of ground motion	144
4.3	Change in coherency with the frequency of ground motion using model I	145

Figure	Title	Page
4.4	Change in coherency with the frequency of ground motion using model II	145
4.5	Generated horizontal ground displacement using model I and considering incoherency effect only	146
4.6	Generated horizontal ground displacement using model I and considering both incoherency and wave travel effects	147
4.7	Generated horizontal ground displacement using model II and considering incoherency effect only	148
4.8	Generated horizontal ground displacement using model II and considering both incoherency and wave travel effects	149
4.9	Generated vertical ground displacement using model I and considering incoherency effect only	150
4.10	Generated vertical ground displacement using model I and considering both incoherency and wave travel effects	151
4.11	Generated vertical ground displacement using model II and considering incoherency effect only	152
4.12	Generated vertical ground displacement using model II and considering both incoherency and wave travel effects	153
4.13	Simplified approach for ground motion application	154
4.14	Transverse displacement time history of the cable mid-point due to sinusoidal ground motion with 1 Hz frequency	155
4.15	Vertical displacement time history of the cable mid-point due to sinusoidal ground motion with 1 Hz frequency	155
4.16	Envelopes of total peak cable transverse displacement considering incoherency effect only	156
4.17	Envelopes of total peak cable transverse displacement considering wave travel effect only	156

Figure	Title	Page
4.18	Envelopes of total peak cable transverse displacement considering incoherency and wave travel effects (model I)	157
4.19	Envelopes of total peak cable transverse displacement considering incoherency and wave travel effects (model II)	157
4.20	Transverse displacement of cable mid-point considering incoherency effect only (model I)	158
4.21	Transverse displacement of cable mid-point considering incoherency effect only (model II)	159
4.22	Transverse displacement of cable mid-point considering wave travel effect only	160
4.23	Effect of propagation velocity and coherency model on the maximum cable displacement due to transverse ground motion	161
4.24	Envelopes of total peak cable vertical displacement considering incoherency effect only	162
4.25	Envelopes of total peak cable vertical displacement considering wave travel effect only	162
4.26	Envelopes of total peak cable vertical displacement considering incoherency and wave travel effects (model I)	163
4.27	Envelopes of total peak cable vertical displacement considering incoherency and wave travel effects (model II)	163
4.28	Vertical displacement of cable mid-point considering incoherency effect only (model I)	164
4.29	Vertical displacement of cable mid-point considering incoherency effect only (model II)	165
4.30	Vertical displacement of cable mid-point considering wave travel effect only	166
4.31	Effect of propagation velocity and coherency model on the maximum cable displacement due to vertical ground motion	167

Figure	Title	Page
5.1	Coordinate axes and components of cable motion	196
5.2	Transverse displacement time history of cable mid-point due to transverse excitation (Cable I)	197
5.3	Vertical displacement time history of cable mid-point due to vertical excitation (Cable I)	198
5.4	Transverse displacement time history of cable mid-point due to transverse excitation (Cable II)	199
5.5	Vertical displacement time history of cable mid-point due to vertical excitation (Cable II)	200
5.6	Transverse displacement time history of cable mid-point due to transverse excitation (Cable III)	201
5.7	Vertical displacement time history of cable mid-point due to vertical excitation (Cable III)	202
5.8	Frequency response curves for different cables due to vertical excitation, (a) Cable I, (b) Cable II and © Cable III	203
5.9	Effect of damping on the frequency response relationship of Cable I	204
5.10	Effect of phase difference between transverse support excitation on the frequency response relationship of Cable I	205
5.11	Effect of phase difference between vertical support excitation on the frequency response relationship of Cable I	206
6.1	Envelop function for the ground motion acceleration time history	228
6.2	Maximum transverse displacement of cables due to transverse excitation	229
6.3	Maximum vertical displacement of cables due to vertical excitation	230

Figure	Title	Page
6.4	Maximum ratio of dynamic to static tension due to transverse excitation	231
6.5	Maximum ratio of dynamic to static tension due to vertical excitation	232
6.6	Comparison between the effect of the transverse component of actual and artificial ground motion	233
6.7	Comparison between the effect of the vertical component of actual and artificial ground motion	234
6.8	Probability of exceedance of maximum transverse cable displacement due to transverse excitation	235
6.9	Probability of exceedance of maximum vertical cable displacement due to vertical excitation	236
6.10	Probability of exceedance of maximum dynamic to static cable tension due to vertical excitation	237
6.11	Effect of cable sag to span ratio on the mean value of the maximum cable displacement	238
6.12	Effect of strong ground motion duration on the mean value of the maximum cable displacement	239
6.13	Effect of strong ground motion duration on the mean value of the ratio of dynamic to static cable tension due to vertical excitation	240
6.14	Effect of the probability distribution type of the ground motion predominant frequency on the maximum cable displacement	241

LIST OF TABLES

Table	Title	Page
2.1	Selected earthquake records	30
2.2	Out-of-plane symmetric frequencies of free vibration	31
2.3	In-plane symmetric frequencies of free vibration	31
2.4	Maximum response of Cable I	32
2.5	Maximum cable response to transverse excitation	33
2.6	Maximum cable response to vertical excitation	33
2.7	Maximum cable response to transverse excitation for different damping ratios	34
2.8	Maximum cable response to vertical excitation for different damping ratios	34
2.9	Effect of difference of cable levels on the natural frequencies	35
2.10	Maximum response in the cable due to various components of the Mexico Earthquake for different h/L ratios	36
2.11	Maximum response in the cable due to various components of the San Fernando Earthquake for different h/L ratios	36
3.1	Maximum displacement response of transmission lines with Tower I due to transverse excitation	82
3.2	Maximum forces of transmission lines with Tower I due to transverse excitation	82
3.3	Maximum displacement response of transmission lines with Tower II due to transverse excitation	83

Table	Title	Page
3.4	Maximum forces of transmission lines with Tower II due to transverse excitation	83
3.5	Maximum displacement response of transmission lines with Tower I due to vertical excitation	84
3.6	Maximum forces of transmission lines with Tower I due to vertical excitation	84
3.7	Maximum displacement response of transmission lines with Tower II due to vertical excitation	85
3.8	Maximum forces of transmission lines with Tower II due to vertical excitation	85
3.9	Effect of the suspension insulator on cable response to transverse excitation	86
3.10	Effect of the suspension insulator on cable response to vertical excitation	86
3.11	Ice and wind loading factors (NESC, 1993)	87
3.12	Overload capacity factors for metal towers (NESC, 1993)	87
3.13	Maximum forces in tower members in kN due to wind on cables (Case I)	88
3.14	Maximum forces in tower members in kN due to wind on tower (Case I)	89
3.15	Maximum forces in tower members in kN due to wind pressure of 0.60 kPa on cables (Case II)	90
3.16	Maximum forces in tower members in kN due to wind pressure of 0.60 kPa on tower (Case II)	90
3.17	Maximum forces in tower members in kN due to the 1940 Imperial Valley earthquake (cable diameter = 3.5 cm)	91

Table	Title	Page
3.18	Maximum forces in tower members in kN due to the 1940 Imperial Valley earthquake (cable diameter = 2.0 cm)	91
4.1	Power spectral density filter parameters for horizontal ground motion (Der Kiureghian and Neuenhofer 1991)	141
4.2	Power spectral density filter parameters for vertical ground motion (Elghadamsi et al. 1988)	141
4.3	Maximum forces in tower members due to transverse ground motion (kN)	142
4.4	Maximum tension in cables due to transverse ground motion (kN)	142
4.5	Maximum forces in tower members due to vertical ground motion (kN)	143
4.6	Maximum tension in cables due to vertical ground motion (kN)	143
5.1	Properties of the example cables	194
5.2	Constants for different cable types	195
6.1	Statistics for the Clough-Penzien power spectral density function	221
6.2	Statistics for the cable maximum transverse displacement	222
6.3	Statistics for the cable maximum vertical displacement	222
6.4	Statistics for the ratio of dynamic to static cable tension due to transverse excitation	223
6.5	Statistics for the ratio of dynamic to static cable tension due to vertical excitation	223
6.6	Description of the used ground motion records (Naumoski et al. 1988)	224

CHAPTER 1

INTRODUCTION

1.1 GENERAL

Transmission lines are vital for an industrial society as they transmit electric power from power generating plants to cities and industrial facilities. They extend thousands of kilometres and cost billions of dollars to construct and maintain. Understanding the actual behaviour of transmission lines under various loading conditions may result in safer designs that save millions of dollars in construction cost as well as minimize costly line failures.

The design of transmission lines is governed by codes such as the National Electrical Safety Code (NESC, 1993) in the United States. In Canada, the CSA Standard S37-M86 (1986) deals with the design of antenna towers and antenna supporting structures and the CSA Standard C22.3-M87 (1987) deals with the design of transmission towers. The general trend in the design of overhead power transmission lines is to analyze the transmission line for dead weight, wind load, and ice load in the vertical and transverse directions. In the longitudinal direction, transmission lines are designed for the loads resulting from a broken conductor. During the 1992 Landers and the 1994 Northridge earthquakes (Northridge earthquake reconnaissance report, 1995) there were several cases of power line failures. In spite of this, there are no code provisions for earthquake design of transmission lines. This emphasizes the importance of the seismic analysis and design of transmission lines.

During earthquakes, the transmission towers vibrate which causes cable vibration. In the design of transmission lines, two issues should be addressed. The first issue is that the internal forces in the tower members and the tension in the cables should not exceed their strength capacity. The second issue is that during conditions of extreme cable displacement, the cables should not touch each other or any surrounding objects causing power failure. Several difficulties arise in the seismic analysis of transmission lines. The cables have geometric nonlinearity as the large cable displacement changes its stiffness. In such cases, nonlinear dynamic analyses should be carried out. Due to the long line spans, the ground motion at various supporting towers can not be assumed identical and therefore multiple support excitation should be considered instead of uniform support excitation.

1.2 REVIEW OF PREVIOUS WORK

Research work related to the seismic analysis of overhead transmission lines can be divided into three categories: first, research work related to the modelling of various elements of the line; second, analysis of transmission lines response to various types of loads; and third, research work related to ground motion modelling studies.

1.2.1 Modelling of Different Elements of Transmission Lines

A typical intermediate span of a transmission line consists of two towers with cables extending between them. The cables are suspended from the towers by insulators. The vibration of the system may be damped using different types of vibration dampers. Modelling of different components of the transmission line for the dynamic analysis attracted the

attention of several researchers. The use of a specific model for the line elements depends mainly on the purpose of the analysis and the required level of accuracy and simplicity.

1.2.1.1 Modelling of cables

Two approaches are generally used to analyze the static and dynamic behaviour of cables. The first approach is numerical using the finite element or the finite difference methods. The second approach is analytical intended to obtain a closed form solution for the differential equation representing the cable static or dynamic equilibrium.

Various numerical schemes were used to model the cables for the static and dynamic analysis. A review of some of the research work on cable modelling was presented by Migliore and Webster (1979 and 1982). Winget and Houston (1976) used a finite segment approach to model the cable. Their formulation was limited to cables with small motion only. Ali (1986) used the finite difference approach to study the dynamic response of cables under a suddenly applied uniform load; a sinusoidal load; and a prescribed support motion. The results agreed well with the results of other research work specially for the case of taut cables.

Various types of finite elements have been used to model the cable. Two-node elements were used by Argyris et al. (1973) and Mote and Chu (1978). These elements are simple and easy to use but a large number of elements is required to accurately model the cable. When a large number of elements is used, the straight elements can be accurate enough for the analysis of moderately sagged cables. For heavily sagged cables, the use of two-node curved elements is preferable (Gambhir and Batchelor, 1977). Three-node curved elements were also used to model cables (Desai et al., 1988). The use of three-node curved elements

is required in the case of cables with a very large sag to span ratio which is not common in transmission lines.

Henghold and Russell (1976) developed a family of finite elements for use in cable problems. These elements retain all geometric nonlinearities and allow for elastic deformation. The stiffness matrices were derived in terms of the deformed global coordinates. Later, Henghold et al. (1977) and Russell et al. (1978) used a three-node element to study the free vibration characteristics and the cable equilibrium in wind load, respectively.

The simplest theoretical approach is to consider the cable as a shallow catenary as was done by Irvine and Caughey (1974) and Simpson (1966 and 1970) who studied the in-plane free vibration of a shallow catenary. A better solution can be achieved by considering the nonlinear vibration of cables. Various methods for obtaining a closed form solution for the cable differential equation were reviewed by Nayfeh and Mook (1979) and Hagedorn (1981). The choice of a specific method depends on the form of the equilibrium equations.

The planar nonlinear vibration of cables was analyzed by a few researchers. For example, Hagedorn and Schafer (1980) used the perturbation method to study the effect of cable nonlinearities on its normal modes. Luongo et al. (1984) used the perturbation method and Galerkin's method to study the planar non-linear free vibration of an elastic cable. Other researchers such as Iyengar and Rao (1988), Perkins and Mote (1987), Benedettini et al. (1986), Luongo et al. (1982), and Yamaguchi et al. (1982), studied the three dimensional nonlinear free vibration of cables.

Few studies were conducted to obtain an analytical solution for the forced vibration of cables. Takahashi and Konishi (1987a, b) studied the free vibration characteristics and the out-of-plane vibrations due to in-plane sinusoidally time varying load using the harmonic balance method. They obtained the unstable solution regions. Rao and Iyengar (1991b) studied the nonlinear vibration of cables under periodic loads. Takahashi (1991) analyzed the stability of cables subjected to an axial periodic load using Galerkin's method. There has been no attempt to obtain a closed form solution for the seismic response of cables. The response of a cable to earthquake ground motion may be different from its response to other types of loads.

1.2.1.2 Modelling of towers

The dynamic behaviour of transmission towers has been well studied both analytically and experimentally. A simplified analysis to obtain the fundamental natural frequency of towers by Dunkerley's method was performed by Trainor et al. (1986). This method is a simple numerical procedure that provides a reasonable estimate of the system's fundamental frequency. The finite element method was also used in the analysis of transmission towers (Kotsubo et al., 1983 and Suzuki et al., 1992).

Experimental testing on transmission towers is usually carried out on full scale towers. Kempner et al. (1981) performed static and dynamic tests on transmission towers. The obtained mode shapes and natural frequencies were compared with the results of a finite element analysis. They concluded that the experimental results agree well with the results of the truss model.

1.2.2 Transmission Line Analysis for Various Load Conditions

The response of cables to wind and galloping loads was studied both theoretically and experimentally. Myerscough (1973 and 1975) studied the wind-induced oscillations in overhead lines using Krylov & Bogoliubov method. He also studied the existence and stability of limit cycles. Wind and galloping vibrations of overhead lines were also studied by Hagedorn (1982) and Schafer (1984). Currie et al. (1989) carried out an experimental research program to study the aeolian wind power imparted to the bundled conductors of overhead power lines. Foata et al. (1989) presented the principal features of the aeolian vibration models developed at Hydro-Quebec.

The dynamic behaviour of transmission lines as a coupled system of towers and cables was recently studied. Ozono et al. (1988) introduced a method for the in-plane dynamic analysis of tower and conductor coupled system. The method was used to study the characteristics of the in-plane free vibration of the system. Each tower was also modelled as a simple mass-spring system and each conductor as a massless spring. They found that the dynamic behaviour of the simplified model is similar to that of the actual model. Ozono and Maeda (1992) used the same model to study the in-plane dynamic interaction between towers and conductors at varying support stiffness. They evaluated the contribution of the normal modes of vibration of the conductor to the dynamic tension transmitted to the tower.

Suzuki et al. (1992) applied the frequency response method to analyze the seismic response of transmission towers due to the phase difference between seismic ground motion at various supports. McClure and Tinawi (1987) carried out a nonlinear dynamic analysis to evaluate the transient dynamic response of transmission lines due to conductor breakage.

A distinctive characteristic of seismic ground motion is their random nature, which suggests that the use of probabilistic seismic analysis is preferable than the deterministic approach. Ang et al. (1996) performed a reliability analysis on a power transmission line system in order to evaluate the probability of substations blackout. They used Monte Carlo simulation in the analysis. However, they concentrated their analysis on the substations while the cable vibrations were ignored.

It appears that there is lack of deterministic and probabilistic studies on the seismic response of transmission lines. Further analysis is needed to examine the forces created in transmission towers and the maximum cable displacements and to compare them with the response of the line to the code loads.

1.2.3 Multiple Support Excitation of Structures

A major problem that arises in the analysis of long span structures such as bridges, dams, pipelines and transmission lines is the difference among the ground motion components affecting various support points of the structure. The principal factors that affect the seismic ground motion variation are three. First, the wave travel effect that results from the finite speed of the seismic waves that creates a phase shift between the seismic excitations at various supports. The second factor is the incoherency effect that results from reflection and refraction of seismic waves. The third factor is the local site effects.

There are two fundamental approaches to account for the variation in seismic ground motion. The seismological approach follows the propagation of seismic waves from the epicentre to the supports of the structure (Rassem et al., 1996). The other is a stochastic

approach based on random vibration analysis. This approach is adopted by Ramadan and Novak (1994); Loh and Lin (1990); and Hao et al. (1989).

Multiple support excitation has been applied to various structures. Abdel-Ghaffar and Stringfellow (1984a and b) studied the response of suspension bridges to travelling earthquake excitations. They concluded that the assumed shear wave velocity can have a significant effect on the response of the structure. Nazmy and Abdel-Ghaffar (1992) studied the response of cable stayed bridges to multiple support excitation. Ramadan and Novak (1992) studied the response of concrete gravity dams to multiple support excitation. Zerva (1990) studied the response of multi-span beams to spatially incoherent ground motions. Zerva (1994) studied the effect of the incoherency and the wave velocity on the seismic response of buried and above ground lifelines. He found that the most significant effect of multiple support excitation is the introduction of high quasi-static forces in the structures. Multiple support excitation of transmission lines has not been previously studied, although they represent long span structures which could be affected by this type of excitation.

1.3 OBJECTIVES AND SCOPE

From the review of previous research work, it is concluded that there is a significant gap in research in the area of seismic analysis of overhead transmission lines. The response of transmission lines to earthquake loading has not been evaluated yet, and therefore it is unrealistic for the design code to assume that this response is small. The analysis of the transmission line response to various types of loads will establish a rational approach to determine the overloading factors and thus may reduce the line cost.

The objectives of this investigation are to model the transmission line system and evaluate its response during earthquake ground motion including multiple support excitation. Moreover, it is required to evaluate the current design methodology and develop seismic design recommendations for transmission lines.

The scope of work in the current research program includes:

1. The analysis of the seismic response of transmission lines in order to obtain a better understanding of the behaviour of the line during earthquakes and to identify the important parameters that have a significant influence on the response.
2. The modelling of different parts of the transmission line (towers, cables and suspension insulator) and to analyze the dynamic behaviour characteristics of each component of the line.
3. The development of an accurate yet simple model of the transmission lines to be used in their seismic analysis.
4. The comparison of the internal forces created in the transmission tower by earthquake ground motion to the forces produced by the wind/ice loads as specified in the code provisions in order to assess the adequacy of the current code for the design of transmission lines.
5. The analysis of the effect of multiple support excitation on the response of transmission lines.
6. The analysis of the effect of the different assumptions used to model the earthquake ground motion such as the coherency model and the wave velocity on the response of the transmission line to transverse and vertical excitations.

7. The analysis of some aspects of nonlinear cable dynamic-behaviour using analytical solutions.

8. The analysis of the probabilistic characteristic of cable response to earthquake ground motion in order to develop a basis for the clearances of the line from the seismic point of view.

In the theoretical and analytical solutions presented in the current research, some assumptions were adopted. The tension in the cable due to its own weight and its vibration is assumed to be below the elastic limit so that the cable will remain elastic during the earthquake. Vibration dampers and spacers are not considered in the analysis. An intermediate span of the transmission line is considered in the analysis. The end spans and the corner spans represent special cases that are not considered in this investigation.

1.4 ORGANIZATION

The thesis is divided into seven Chapters. In Chapter two the cable finite element model is presented. The free vibration characteristics of cables with different sag to span ratios are determined. The seismic response of different cables is analyzed and the effects of different cable properties and ground motion characteristics are determined.

Dynamic characteristics of transmission towers are determined in Chapter three. The seismic behaviour of transmission lines is analyzed and a simplified model for the line is proposed to determine the cable response. The internal member forces in transmission towers due to earthquakes are compared to the forces caused by the code specified loads. In Chapter

four, the response of transmission lines to multiple support excitation is analyzed. The effect of different assumptions in modelling the ground motion on the response is determined.

The analytical solution of the cable dynamic behaviour is presented in Chapter five. Galerkin's method along with the method of multiple time scales are used in the analysis. The stability of the steady state solution is examined. The results of the analytical solution are compared to those of the finite element solution to assess their accuracy. The effect of multiple support excitation and the internal resonance are analyzed.

Probabilistic analysis of the seismic response of transmission lines is presented in Chapter six. The statistical characteristics of the cable tension and maximum displacement are evaluated. Finally, Chapter seven contains a summary of the research program and the main conclusions and recommendations for further research.

CHAPTER 2

FINITE ELEMENT APPROACH FOR SEISMIC ANALYSIS OF CABLES

2.1 GENERAL

Seismic behaviour of transmission lines is determined from the dynamic analysis of towers and cables when the system is subjected to earthquake ground motion. Cables have geometric nonlinearity because large displacement of the cable changes its stiffness and hence its frequencies of free vibrations.

Different kinds of finite elements were developed to model the cable taking into account the cable geometric nonlinearity. Some researchers (Mote and Chu, 1978 and Gambhir and Batchelor, 1978) believe that if a large enough number of straight elements is used to model the cable, adequate accuracy of the analysis can be achieved. Other researchers believe that straight elements are inadequate to model strongly curved cables (McClure and Tinawi, 1987). However, since transmission line cables are generally with small to moderate sag to span ratios, the use of straight elements is adequate to model the cables provided that the cable is divided into sufficient number of elements.

In this chapter, a two-node nonlinear element is developed to model the cable. The element is verified and incorporated in the PC-ANSR computer program which is a program for nonlinear static and dynamic analysis of structures. Different cable examples with

different sag to span ratios are selected for the analysis. Free vibration characteristics of the different cables are determined. The cable response to different components of ground motion is analyzed. The effect of different cable properties and ground motion characteristics on the response is investigated. The effect of the difference in elevation between cable supports is also analyzed.

2.2 ANALYSIS PROCEDURE

The problem of cable vibration was studied extensively. Some researchers used analytical procedures based on mathematical solutions of the differential equations of cable vibration (Perkins, 1992, for example). Other researchers used the finite difference approach (Ali, 1986). The finite element method was used extensively to study cable vibration with different kinds of elements to model the cable (Leonard and Recker, 1972; and Russell et al., 1978). The use of straight elements to model the cable is appropriate for cables with small sag to span ratios to avoid the complexity that results from using curved elements.

2.2.1 Formulation of Element Matrices

The equation of motion of a sagging cable fixed at both ends under earthquake loading can be written in the following matrix form:

$$[M]\{\ddot{u}\} + [C]\{\dot{u}\} + [K_T]\{u\} = -[M]\ddot{u}_g \qquad (2.1)$$

where $\ddot{u}_g$ is the ground acceleration; {u}, {$\dot{u}$} and {$\ddot{u}$} are the nodal displacement, velocity and acceleration, respectively; [M] is the lumped mass matrix; [C] is the damping matrix; and

$[K_T]$ is the total stiffness matrix which is defined as:

$$[K_T] = [K_E] + [K_L] \tag{2.2}$$

where $[K_L]$ is the conventional symmetric stiffness matrix that accounts for the large deflection of the cable and $[K_E]$ is the geometric stiffness matrix.

Assuming large deflections but small deformations in the cable and neglecting its bending rigidity, the stiffness matrices $[K_E]$ and $[K_L]$ are defined by Henghold and Russell (1976) as follows:

$$[K_E] = \frac{1}{2}\int_0^L EA\,(\{U_N\}^T [N']^T [N'] \{U_N\} - 1)\,[N']^T [N']\,ds \tag{2.3}$$

$$[K_L] = \int_0^L EA\,[N']^T [N'] \{U_N\} \{U_N\}^T [N']^T [N']\,ds \tag{2.4}$$

where, E is Young's modulus of the cable material; A is the cross sectional area of the cable; L is the element length; $\{U_N\}$ is the nodal coordinate vector; and [N] is the shape function.

Henghold and Russell (1976) developed a class of three-node elements based on the previous equations and used it in their analysis. In the present analysis, a straight two-node element is developed to model the cable. The shape function of the element [N] is given by:

$$[N] = \begin{bmatrix} (1-\eta) & 0 & 0 & \eta & 0 & 0 \\ 0 & (1-\eta) & 0 & 0 & \eta & 0 \\ 0 & 0 & (1-\eta) & 0 & 0 & \eta \end{bmatrix} \tag{2.5}$$

where $\eta = x / L$ and it varies from 0 to 1, and

$$[N'] = \frac{1}{L} \lfloor -[I] \; [I] \rfloor \tag{2.6}$$

where [I] is the unit matrix. On the basis of equations (2.3) through (2.6), the stiffness matrix $[K_L]$ is written in the form:

$$[K_L] = \frac{EA}{L^3} \begin{bmatrix} [K] & -[K] \\ -[K] & [K] \end{bmatrix} \tag{2.7}$$

where,

$$[K] = \begin{bmatrix} (\Delta X)^2 & \Delta X \Delta Y & \Delta X \Delta Z \\ \Delta X \Delta Y & (\Delta Y)^2 & \Delta Y \Delta Z \\ \Delta X \Delta Z & \Delta Y \Delta Z & (\Delta Z)^2 \end{bmatrix} \tag{2.8}$$

where X_i, Y_i and Z_i are the coordinates of the i'th node at any instant; and $\Delta X = X_{i+1} - X_i$; $\Delta Y = Y_{i+1} - Y_i$ and $\Delta Z = Z_{i+1} - Z_i$. The cable configuration is shown in figure 2.1.

The stiffness matrix $[K_E]$ is given by:

$$[K_E] = \frac{EA\left((\Delta X)^2 + (\Delta Y)^2 + (\Delta Z)^2 - L^2\right)}{2L^3} \begin{bmatrix} [I] & -[I] \\ -[I] & [I] \end{bmatrix} \tag{2.9}$$

The developed element is incorporated in the PC-ANSR computer program (Maison, 1992). The PC-ANSR is a program for the nonlinear static and dynamic analyses of structures. The program uses the Newton-Raphson method to achieve equilibrium within each load step. It also uses the Newmark-β algorithm for numerical integration in the dynamic analysis. The numerical procedures for the static and dynamic analysis were presented by Mondkar and Powell (1975 and 1977) and by El-Attar et al. (1995b). The procedures can be summarized as follows:

Static analysis:

(a) The stiffness matrix $[K^j_T]$ is determined using equations 2.5 through 2.9 from the cable geometry at the end of step (j-1).

(b) The joint displacement and elastic forces are calculated using Newton-Raphson method.

(c) The out-of-balance load vector $\{R_u\}$ is determined.

(d) If the components of $\{R_u\}$ are within a given tolerance, then the answer is achieved and the next step is started, otherwise the forces and displacement vectors are updated and the steps should be repeated starting with step (a).

Dynamic analysis:

(a) The mass matrix [M] and the stiffness matrix $[K_T]$ are evaluated.

(b) The damping matrix [C] is evaluated using $[C] = \alpha [M] + \beta_0 [K_0] + \beta_T [K_T]$ where $[K_0]$ is the initial stiffness matrix, α, β_0, and β_T are the Rayleigh damping coefficients.

(c) Using Newmark-β method, the changes in displacement, velocity and acceleration are evaluated at each node.

(d) The member forces are computed and the stiffness matrix is updated.

(e) $[R_u]$ is evaluated and the equilibrium is checked as in the static case.

(f) A reasonable time step is selected to ensure convergence. In this analysis, the time step is selected to be 0.005 s.

It should be noted that the cable is a tension member. Therefore, it is important to adjust the element such that when the member force is negative, the stiffness matrix $[K_T]$ is set to zero.

2.2.2 Element Verification

To examine the accuracy of the results of the dynamic analysis using the developed element, the results are compared to the available solutions. Two examples are considered to verify the accuracy of the developed element. The first example examines the cable response to dynamic loads, while the second example examines its response to earthquake ground motion. The first example is a problem reported by Leonard and Recker (1972) in their finite element analysis of cable vibration. The same problem was used by Ali (1986) in his finite difference analysis of the dynamic response of sagged cables. The data of the verification problem is as follows :

Cable span	= 254 m	Young's modulus	= 13.8×10^7 KPa
Sag to span ratio	= 0.019	Weight	= 3.5 N/m
Cross sectional area	= 42 mm^2	Damping ratio	= 0%

The cable was subjected to a uniformly distributed load with intensity 17.5 N/m in the transverse direction. The cable is divided into 12 straight elements and a parabolic shape is assumed as a first approximation for the static equilibrium position. The results of the static

analysis showed that the parabolic shape is an accurate representation for the cable deformed shape under its own weight. The results of the dynamic analysis using the finite element method developed in this analysis, Leonard and Recker (1972) solution and Ali's finite difference solution are compared in figure 2.2. This figure shows that the developed element agrees well with both the finite element and the finite difference results.

The second problem was solved by Rao and Iyengar (1991a) using the normal modes approach. The data of the cable considered is as follows:

Cable span	= 1000 m	Young's modulus	= 20.0×10^4 MPa
Sag to span ratio	= 0.09	Weight	= 28.0 N/m
Cross sectional area	= 50 mm^2	Damping ratio	= 0.5%

The cable is subjected to the three components of the 1952 Taft earthquake. The cable is divided into 32 elements. The time history of the cable tension as a percentage of the static tension is shown in figure 2.3. This figure shows that the results of the current analysis agree well with those of Rao and Iyengar in both the maximum response and the frequency of vibration.

2.3 SELECTION OF PARAMETERS

The cable properties have a significant effect on its free and forced vibration characteristics. Moreover, the ground motion characteristics may affect the seismic response of cables. In the analysis, the cable properties are varied in a range similar to that used in transmission lines. It is also of interest to determine the ground motion characteristics that have significant influence on the cable seismic response.

2.3.1 Cable Characteristics

An actual transmission line cable is used in the analysis with the following properties:

Cable span	= 400 m	Young's modulus	= 55×10^3 MPa
Weight	= 22.23 N/m	Cross sectional area	= 10^{-3} m^2

Damping of the cable is assumed to be of the Rayleigh type. The effect of the cable damping on the response is studied, however in all other cases of the analysis, the cable damping ratio is assumed equal to 1%.

The sag to span ratio of cables is the principal parameter that affects the dynamic behaviour. In general, transmission line cables have a sag to span ratio less than 5%. Three cable examples Cable I, Cable II and Cable III with sag to span ratios of 0.03, 0.01 and 0.003, respectively are used in the analysis.

Cables I and II are typical sagged cables that are in actual use in transmission lines. On the other hand, Cable III is an example of taut cables which are not used in transmission lines because very high tension will be created in the cable. The main reason for choosing Cable III is to provide a comparison between the dynamic behaviour of sagged and taut cables.

2.3.2 Ground Motion Characteristics

Earthquake ground motion may be categorized according to their peak ground acceleration (A), peak ground velocity (V), frequency content, and / or strong ground motion duration. However, one important method of categorizing ground motion is the use of A/V ratio where A is in g and V is in m/s. This method was used by several researchers (Tso et

al., 1992 and Hodhod, 1993). It is also adopted and used in the National Building Code of Canada (NBCC, 1995). Low A/V ground motion records represent low frequency content which may be associated with large earthquakes occurring at far epicentral distances. High A/V ground motion records represent high frequency content which may be associated with small earthquakes at short epicentral distances.

Six ground motion records are selected to be used in the analysis. The records have different frequency content as represented by the ratio A/V. Scaling of ground motion is required to be able to compare between the effect of various earthquakes on the cable. The horizontal component of ground motion is scaled to 0.34 g which represents the level of excitation for the city of Victoria on Canada's west coast according to NBCC (1995). According to NBCC 1995, the ratio of vertical to horizontal peak ground acceleration ranges from ⅔ to ¾. Therefore, in this analysis, the vertical component of ground motion is scaled to a peak value of ⅔ of that of the corresponding horizontal component. The details of the selected earthquake records are shown in table 2.1.

2.4 FREE VIBRATION CHARACTERISTICS OF CABLES

To determine the free vibration characteristics of cables, the three cable examples Cables I, II and III, are subjected to a sinusoidal ground acceleration with a peak acceleration of 0.1 g in the vertical and transverse directions. The maximum displacement of various points along the cable span and the cable tension are plotted in figures 2.4 to 2.9 for the three cable examples and for the transverse and vertical directions.

Figures 2.4(a), 2.6(a) and 2.8(a) show that, in the transverse direction, the displacements of various cable points are mainly governed by the first mode, specially for the cable mid-point, where the contribution of the higher modes is small. In the vertical direction, figures 2.7(a) and 2.9(a) show that for Cables II and III, the displacements of cable points in the vertical direction are also governed by the first mode. On the other hand, figure 2.5(a) shows that for Cable I, with higher sag to span ratio, the contribution of higher modes to the displacement may be significant.

The analysis showed that the tension in the cable is almost constant throughout the cable span, and therefore the average value of the tension in the cable is shown in figures 2.4(b) to 2.9(b). The tension in Cable II and Cable III due to transverse or vertical excitation is dominated by the first mode. For Cable I, the contribution of the second symmetric mode is significant specially due to vertical excitation.

It was also found from figures 2.4 through 2.9 that due to the application of a similar excitation at both supports, only the symmetric modes were excited which is expected due to symmetry. The out-of-plane symmetric frequencies are well separated. The in-plane symmetric frequencies for sagged cables (Cable I) are closely spaced, while for taut cables (Cable III) they are well separated.

The first three symmetric out-of-plane natural frequencies are listed in table 2.2. The first three symmetric in-plane natural frequencies are shown in table 2.3. The out-of-plane frequencies reported in table 2.2 are in good agreement with those calculated by the equations derived by Irvine and Caughey (1974) based on their linear theory of cable vibrations given as :

$$\omega_n = (2n - 1)\frac{\pi}{L}\sqrt{\frac{H}{m}} \qquad (2.10)$$

This agreement can be explained by the fact that for sag to span ratio up to 3% the nonlinear geometry effects in the cable are small. The first three symmetric in-plane frequencies for Cable I shown in table 2.3 are compared with the corresponding values reported by Rao and Iyengar (1991) which were 0.40, 0.54 and 0.80 Hz, respectively. The agreement with the present analysis is acceptable.

By comparing table 2.2 with table 2.3, it is observed that for Cable III which is a taut cable, the in-plane natural frequencies are similar to the out-of-plane ones. Similar conclusions were reached by Henghold et al. (1977) and Irvine (1981).

2.5 SEISMIC RESPONSE OF CABLES

This analysis is performed on Cable I which represents a typical example for transmission line cables. Other cables are considered only when the effect of sag to span on the seismic response is analyzed. Damping ratio of the cable is assumed to be 1% unless otherwise stated.

2.5.1 Effect of the Frequency Content of Ground Motion

The A/V ratio of the ground motion records is used as a measure of the frequency content. Low values of A/V (less than 0.8) represent low frequency content ground motion records, intermediate values of A/V (0.8 - 1.2) represent intermediate frequency content

records, and high values of A/V (more than 1.2) represent high frequency content ground motion records.

Cable I is subjected to the vertical and horizontal components of the six earthquakes given in table 2.1. The maximum values of cable displacements and tension due to transverse, vertical, and longitudinal ground motions are shown in table 2.4. Figures 2.10 and 2.11 show the displacement time history of the cable mid-point due to transverse and vertical excitations, respectively. The vertical displacement time history of a point at ¼ cable span due to longitudinal excitation is shown in figure 2.12.

The results of the analysis show that for the transverse component of ground motion, the maximum response in the cable results from earthquakes with low A/V ratio, i.e. low frequency content. This is expected since the first three frequencies of the cable are less than 0.8 Hz. It is also observed that while the cable displacements can be as high as 205 cm for the Mexico earthquake, the cable tension does not exceed 2.8 kN which is small when compared to the tension developed in the cable due to its own weight (37.1 kN). The reason for the small values of cable tension is that the cable transverse vibrations are of a swinging type and do not cause change in length and therefore do not produce significant strains and stresses.

For the vertical ground motion, the records with low A/V ratio caused the maximum response in the cable. The maximum displacement and tension in the cable result from the Mexico earthquake. The maximum displacement is approximately 150 cm and the maximum tension is approximately 17.0 kN which is almost half the static tension.

On the other hand, the ground motion component in the longitudinal direction does not cause significant displacement or tension in the cable. The maximum vertical displacement in the cable is only 25.0 cm and it results from the Mexico earthquake. The maximum tension in the cable due to the longitudinal ground motion is 3.6 kN.

Comparing the cable response to various components of ground motion indicates that the displacements in the cable due to the transverse component of ground motion are quite significant. Vertical displacements, as well as tension in the cable due to vertical excitation are also significant. Cable response to the longitudinal component of ground motion is insignificant and will not be considered in the rest of the analysis. While the cable tension is small in comparison to the tension developed in the cable under its own weight, the displacements of the cable are significant and may govern the design of transmission line clearance.

2.5.2 Effect of the Cable Sag to Span Ratio

To study the effect of cable sag to span ratio, the three cable examples were subjected to the horizontal and vertical components of the Mexico and the San Fernando earthquakes. These two specific earthquakes are chosen because they cause the maximum response in the cable. The results of the analysis are presented in tables 2.5 and 2.6 for the transverse and vertical excitations, respectively.

The results indicate that there are large differences in the magnitude of the response for cables of different sag to span ratios. For example, the vertical displacement of Cable I due to the vertical component of the Mexico earthquake is 150.9 cm, while the vertical

displacement of Cable II is 274.4 cm. The main reason for the large differences in the response is the difference in frequencies between different cable examples which causes amplification of the response in some cases (Cable II) and attenuation of the response in other cases (Cable III).

Comparing the response of different cables to the sinusoidal ground acceleration as shown in figures 2.4 to 2.9, indicates that the response of sagged cables is generally larger than the response of taut cables. The only exception is the response of Cable II to vertical excitation which is larger than the response of Cable I. For example, the maximum displacement of Cable I due to vertical excitation is 5.5 m, while the maximum displacement of Cable II due to vertical excitation is 9.4 m.

2.5.3 Effect of the Cable Damping Ratio

Cable damping is an uncertain quantity. Little research work was conducted to evaluate the damping characteristics of cables. Traditionally, the damping of cables is very small. However, there is a new trend in transmission line design to use self damping conductors to damp the cable vibrations instead of using vibration dampers (McCulloch et al., 1980). The damping ratio of the self damping cables can be as high as 5 times the damping ratio of the ordinary cables (Jones et al., 1988).

Cable I is used in the analysis with different damping ratios 0, 1, 2 and 4%. The cable is subjected to the vertical and horizontal components of the Mexico and the San Fernando earthquakes. Results of the analysis are presented in tables 2.7 and 2.8 for the transverse and vertical excitations, respectively.

The maximum cable response data in tables 2.7 and 2.8 indicate that the damping ratio of the cable has a significant effect on the cable response to ground motion. For example, considering a small damping ratio such as 1% rather than neglecting the damping, reduces the vertical cable displacement due to the Mexico earthquake by 35%. The use of self damping cables also reduce the cable response significantly. The maximum effect is associated with the vertical component of the Mexico earthquake where the maximum displacement is reduced from 205.9 cm to 127.3 cm with a percentage decrease of 38% when the damping ratio increases from 1% to 4%. This result suggests that the use of self damping cables is an excellent solution to attenuate the vibrations of transmission lines due to earthquakes.

2.5.4 Effect of the Difference in Elevation between Cable Supports

In general, transmission lines extend over long distances of different topography. It is common that the supports of the line are not at the same level. Therefore, it is important to examine the effect of the difference in elevation between cable supports on the seismic response of cables.

First, the effect of the difference in elevations on the natural frequency of cables is examined. Cable I is considered in the analysis with a difference of "h" in elevation between its supports and a mid-point sag of "d" as shown in figure 2.13. The values of the first and second symmetric in-plane and out-of-plane frequencies are presented in table 2.9 for different values of h/L ranging from zero to 1.0.

Table 2.9 indicates that, the fundamental frequency of cables decreases with the increase of h/L. Similar conclusion was arrived at by Gambhir and Batchelor (1978). While the decrease in the out-of-plane frequencies is small, the decrease in the in-plane frequencies is significant. For example, the first frequency decreases from 0.38 Hz to 0.24 Hz as h/L increases from 0 to 1.0, with a percentage decrease of 37%. Moreover, for small values of h/L (up to 0.4) the natural frequencies of the cable are almost unaffected by the change in h/L as found by Gambhir and Batchelor (1978).

The effect of the difference in elevations on the seismic response of cable I when subjected to the vertical and horizontal components of the Mexico and the San Fernando earthquakes was studied. Values of the maximum response in the cable are presented in tables 2.10 and 2.11. The displacement time histories of cable mid-point for different h/L values due to the ground motion components are shown in figures 2.14 to 2.17.

The results presented in tables 2.10 and 2.11 show that the ratio h/L has a significant effect on the cable response to vertical excitation, however the effect on the response to transverse (out-of-plane) excitation is not that significant. For example, the maximum displacement in the cable due to the vertical component of the Mexico earthquake is 234.4 cm for h/L = 0.4, while the minimum response is 73.1 cm for h/L = 1.0 with a percentage change of 70%. For the transverse component, the maximum displacement is 205.9 at h/L = 0, while the minimum displacement is 177.0 cm at h/L = 0.8 with a percentage change of 14%.

The main reason for the difference is that the change in the in-plane frequencies due to the increase in h/L is much larger than the change in the out-of-plane frequencies. This is

also clear from figures 2.13 and 2.14 where it appears that the frequency of the out-of-plane vibration is not changed except for the case of h/L = 0.8. Figures 2.16 and 2.17 show that the change in the in-plane frequencies , in some cases, is significant which agrees with the data in table 2.9.

2.6 SUMMARY

A two-node element which accounts for the cable geometric nonlinearity is developed. The element is incorporated in the PC-ANSR for the nonlinear static and dynamic analysis of structures. The element is checked against other available solutions to determine its accuracy. The free vibration characteristics of cables are determined. Finally a parametric analysis is carried out to study the effect of different ground motion characteristics and different cable parameters on the response.

The following conclusions may be arrived at from the analysis:

1. In the vertical direction, the frequencies for taut cables are widely spaced and the response is mainly dominated by the first mode. For sagged cables the frequencies of free vibration are closely spaced and higher modes may contribute significantly to the cable response.
2. In the transverse direction, the modes are widely spaced and the response is governed by the fundamental mode.
3. The response of cables to the earthquakes with low A/V ratio is much higher than their response to earthquakes with higher A/V ratio.

4. Significant displacements may result in cables due to earthquake ground motion in the vertical and transverse directions. These calculated displacements may form the basis to develop criteria for line separation. The displacements caused by the longitudinal component of ground motion are insignificant.

5. The tension in the cable due to the selected earthquakes scaled to the peak ground acceleration of Victoria B.C. location does not exceed approximately half that of the static cable tension.

6. Cable sag to span ratio, damping ratio, and the difference in elevation between cable supports, are important parameters that may have significant effects on the cable response to earthquake ground motion.

Table 2.1 Selected earthquake records

Date & Event	Station	Horizontal Component				Vertical Component		
		Comp.	A (g)	V (m/s)	A/V	A (g)	V (m/s)	A/V
1985 Mexico	Mesa Vibradora	N90W	0.040	0.11	0.36	0.021	0.084	0.24
1971 San Fernando	800 W first St., L.A.	N37E	0.088	0.179	0.49	0.062	0.087	0.71
1979 Monte Negro	Albatros Hotel, Ulcinj	N00E	0.171	0.194	0.88	0.163	0.118	1.38
1940 Imperial Valley	El Centro	S00E	0.348	0.334	1.04	0.21	0.108	1.95
1966 Parkfield	Temblor No. 2	N65W	0.269	0.145	1.86	0.132	0.040	3.31
1970 Lytle Creek	Wrightwood, California	S25W	0.198	0.096	2.06	0.054	0.032	1.69

Table 2.2 Out-of-plane symmetric frequencies of free vibration

Cable type	Frequency (Hz)					
	Calculated using finite element			Linear theory Irvine and Caughey (1974)		
	first	second	third	first	second	third
Cable I	0.15	0.48	0.80	0.16	0.49	0.80
Cable II	0.30	0.83	1.39	0.28	0.83	1.39
Cable III	0.50	1.51	2.50	0.51	1.51	2.50

Table 2.3 In-plane symmetric frequencies of free vibration

Cable type	Frequency (Hz)					
	Calculated using finite element			Rao and Iyengar (1991a)		
	first	second	third	first	second	third
Cable I	0.38	0.52	0.80	0.40	0.54	0.80
Cable II	0.32	0.83	1.37			
Cable III	0.51	1.51	2.50			

Table 2.4 Maximum response of Cable I

Event	Transverse ground motion		Vertical ground motion		Longitudinal ground motion	
	Tension (kN)	Transverse displ. (cm)	Tension (kN)	Vertical displ. (cm)	Tension (kN)	Vertical displ. (cm)
Mexico	2.4	205.9	17	151	1.3	24.8
San Fernando	1.6	95.7	4	32	3.2	13.2
Monte Negro	0.4	27.5	2	15	3.6	5.3
Imperial Valley	0.3	45.4	2	9	1.8	4.3
Parkfield	0.3	8.7	1	7	2.4	2
Lytle Creek	0.2	4.6	1	4	2.1	0.3

Table 2.5 Maximum cable response to transverse excitation

Cable example	Mexico Earthquake		San Fernando Earthquake	
	Tension (kN)	Displacement (cm)	Tension (kN)	Displacement (cm)
Cable I	2.4	205.9	1.6	95.7
Cable II	1.4	130.5	1.6	140.6
Cable III	1.1	114.2	0.1	38.7

Table 2.6 Maximum cable response to vertical excitation

Cable example	Mexico Earthquake		San Fernando Earthquake	
	Tension (kN)	Displacement (cm)	Tension (kN)	Displacement (cm)
Cable I	17.1	151	4.4	31.5
Cable II	20.9	274.4	3.8	51.9
Cable III	1.3	51.7	0.3	13.5

Table 2.7 Maximum Cable (I) response to transverse excitation for different damping ratios

Damping ratio	Mexico Earthquake		San Fernando Earthquake	
	Tension (kN)	Displacement (cm)	Tension (kN)	Displacement (cm)
0 %	4.2	261	2	100.4
1 %	2.4	206	1.6	95.7
2 %	1.6	171	1.3	91.6
4 %	1	127	1	84.8

Table 2.8 Maximum Cable (I) response to vertical excitation for different damping ratios

Damping ratio	Mexico Earthquake		San Fernando Earthquake	
	Tension (kN)	Displacement (cm)	Tension (kN)	Displacement (cm)
0 %	26.5	230	5.7	44
1 %	17.1	151	4.4	31.5
2 %	16.1	127	3.7	24.1
4 %	15	106	3.4	21.1

Table 2.9 Effect of difference of cable end levels on the natural frequencies

h/L	In-plane symmetric frequencies (Hz)		Out-of-plane symmetric frequencies (Hz)	
	First	Second	First	Second
0	0.38	0.53	0.15	0.50
0.1	0.37	0.53	0.15	0.50
0.2	0.36	0.51	0.14	0.49
0.4	0.34	0.51	0.14	0.49
0.8	0.27	0.49	0.14	0.47
1.0	0.24	0.46	0.13	0.46

Table 2.10 Maximum response in the cable due to various components of the Mexico Earthquake for different h/L ratios

h/L	Transverse component		Vertical component	
	Displacement (cm)	Tension (kN)	Displacement (cm)	Tension (kN)
0	205.9	2.4	150.9	17.1
0.1	205.6	2.4	152.0	17.1
0.2	204.3	2.4	162.9	18.9
0.4	194.3	3.7	234.4	27.5
0.8	177.0	4.2	90.0	10.1
1.0	178.3	2.6	73.1	7.7

Table 2.11 Maximum response in the cable due to various components of the San Fernando Earthquake for different h/L ratios

h/L	Transverse component		Vertical component	
	Displacement (cm)	Tension (kN)	Displacement (cm)	Tension (kN)
0	95.7	1.6	31.5	4.4
0.1	95.7	1.7	30.6	4.3
0.2	95.8	1.7	28.3	3.8
0.4	96.4	1.5	32.4	3.8
0.8	97.7	0.6	42.9	5.4
1.0	95.7	0.6	48.1	5.0

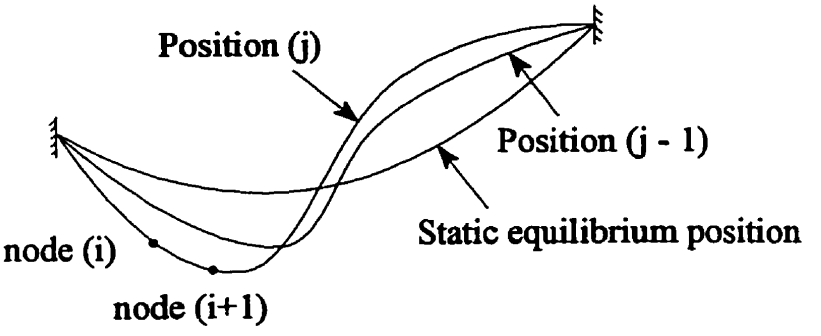

Figure 2.1 Cable configuration

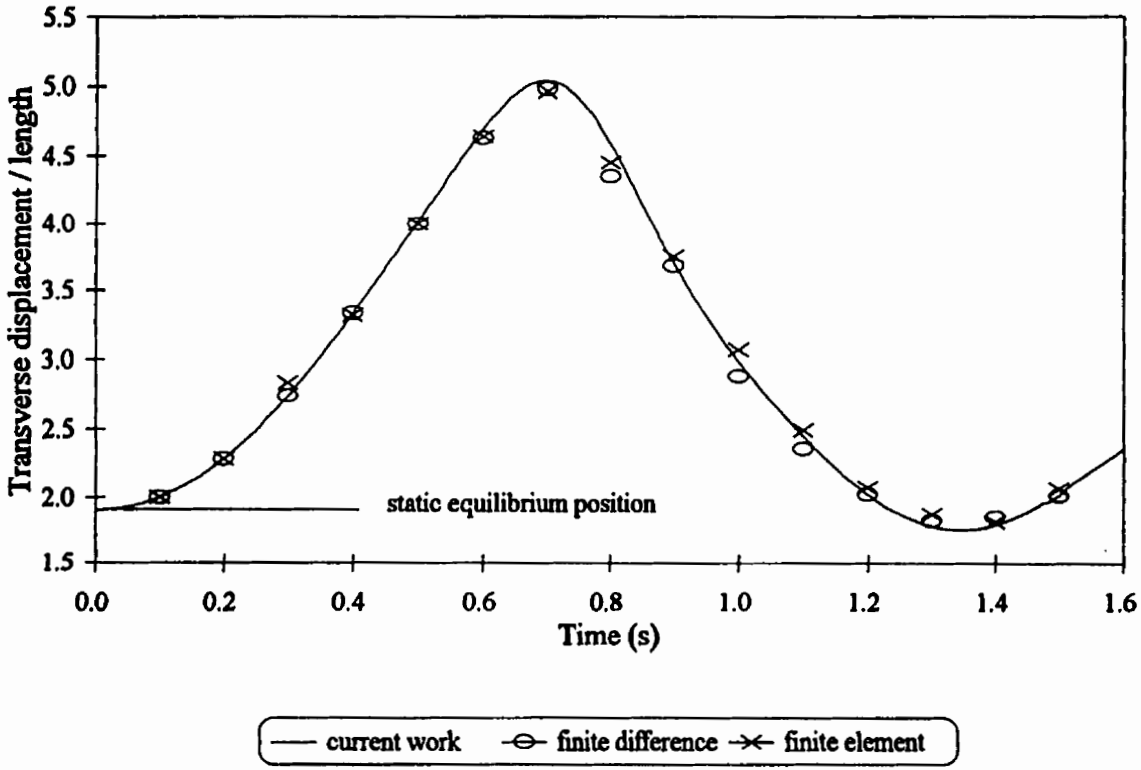

Figure 2.2 Transverse displacement time history of cable mid-point under suddenly applied load

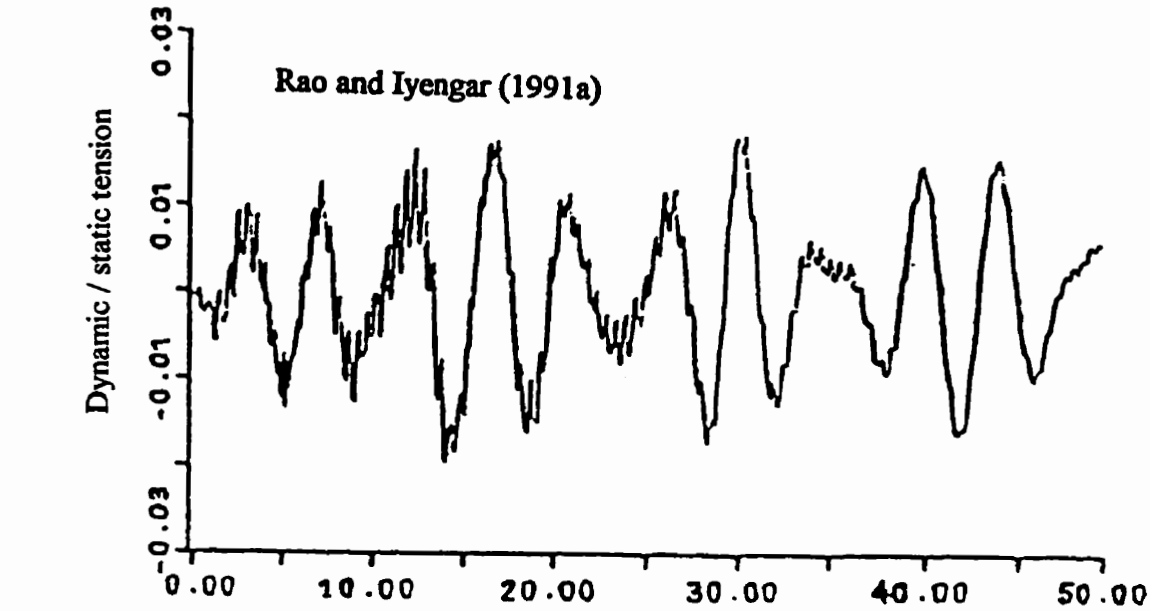

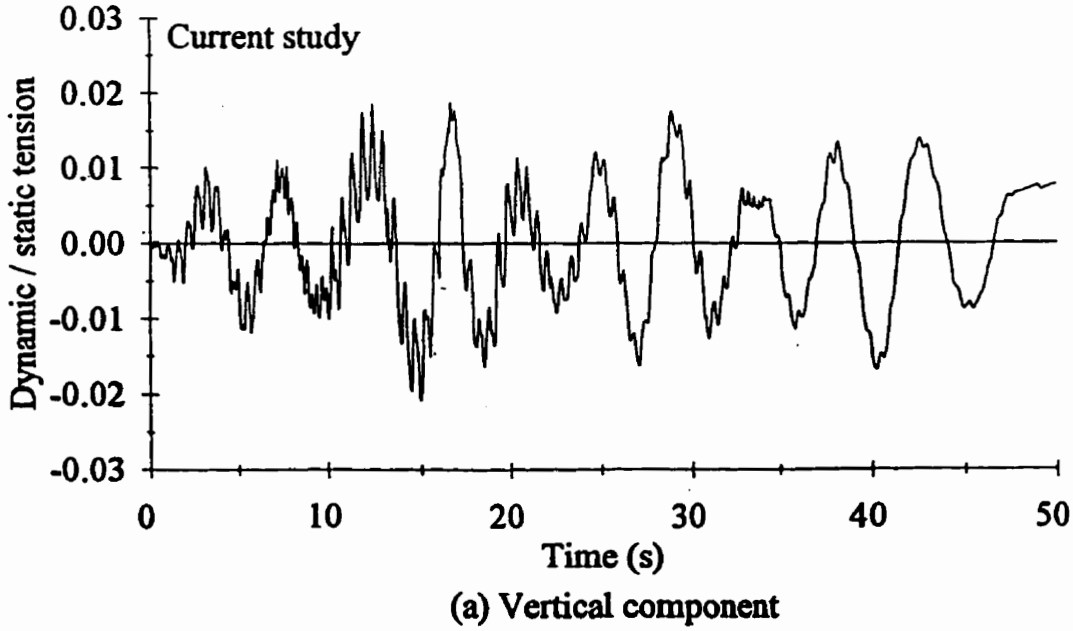

(a) Vertical component

Figure 2.3 Cable seismic response to the 1952 Taft earthquake

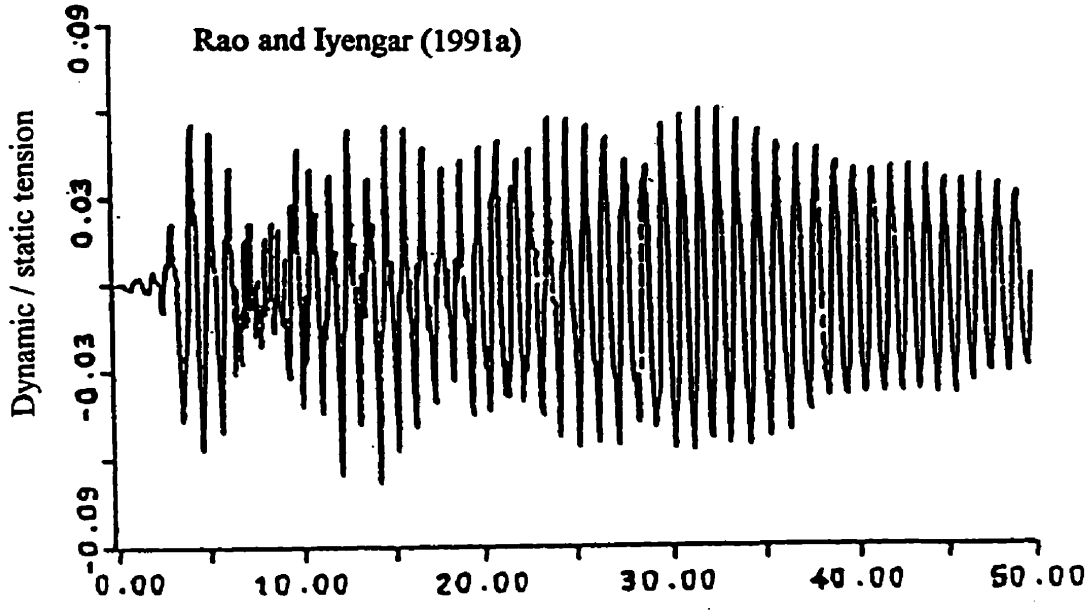

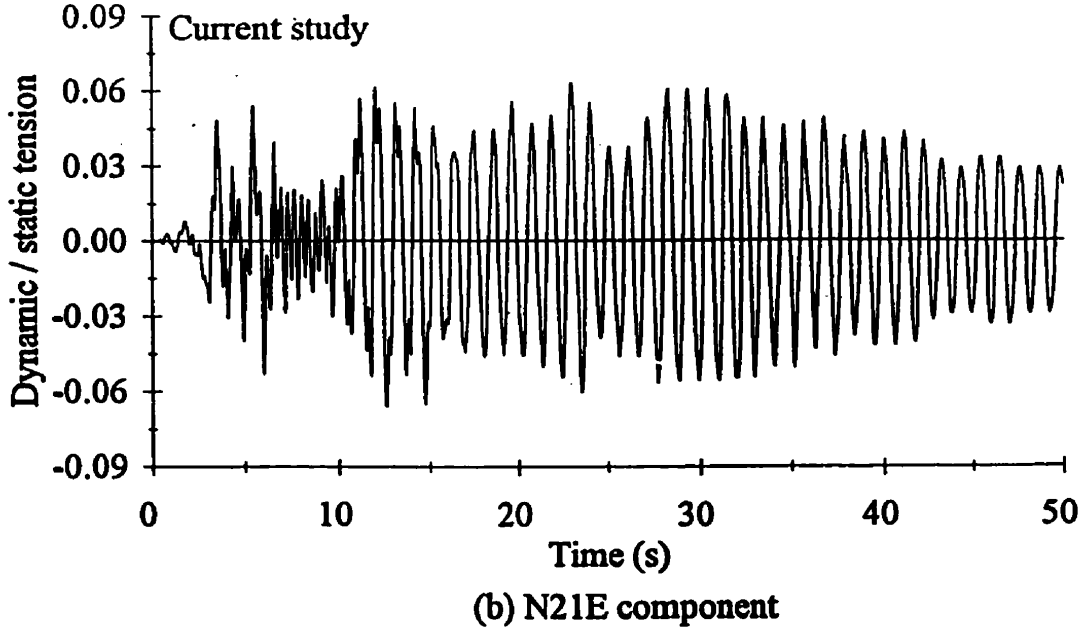

(b) N21E component

Figure 2.3 (cont.) Cable seismic response to the 1952 Taft earthquake

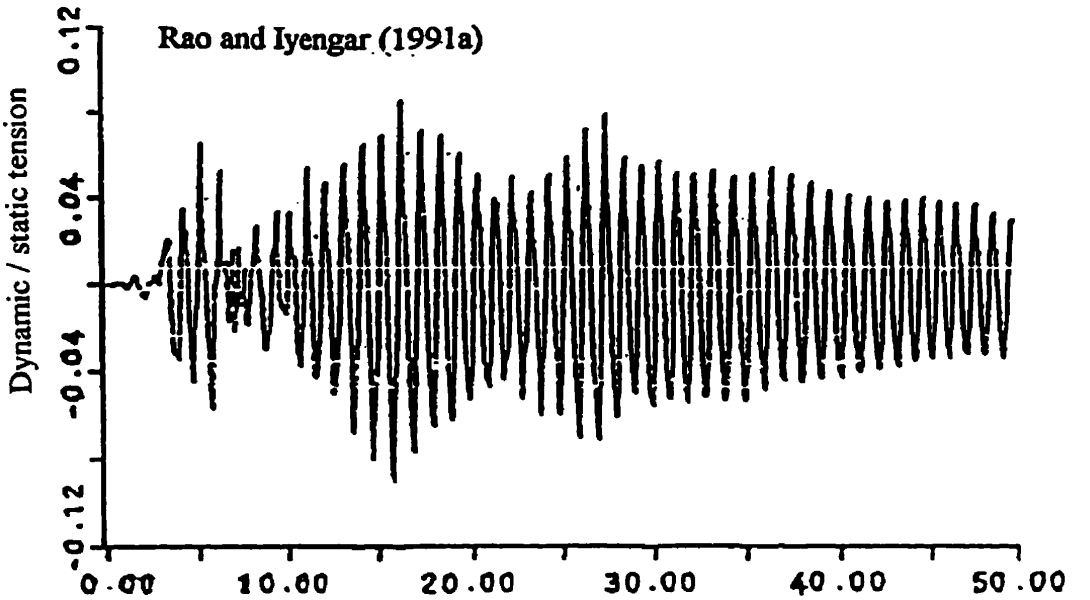

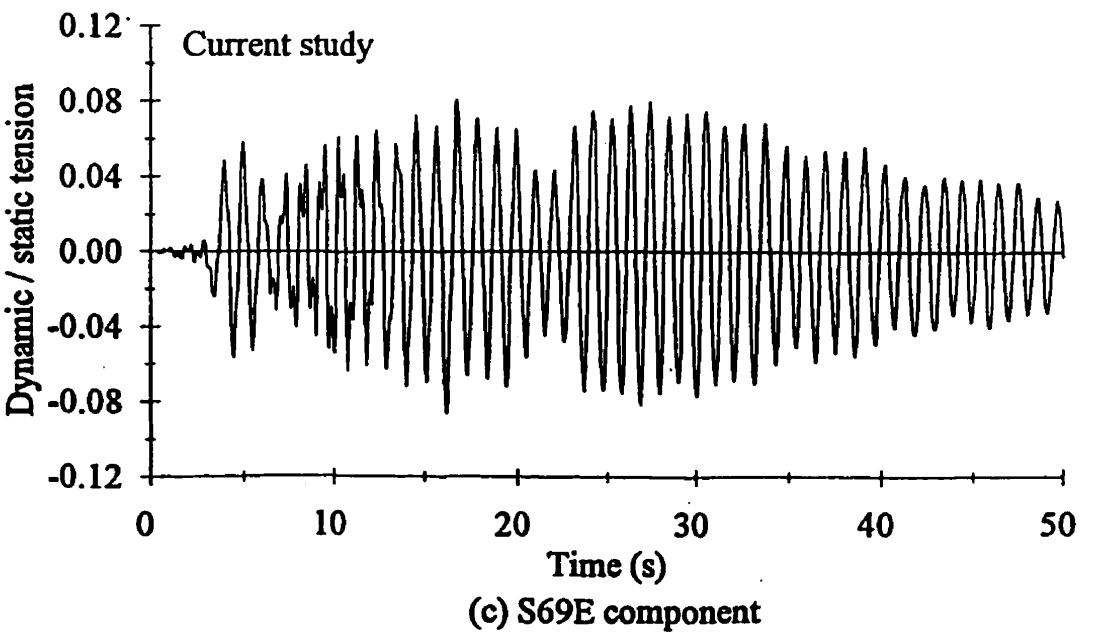

(c) S69E component

Figure 2.3 (cont.) Cable seismic response to the 1952 Taft earthquake

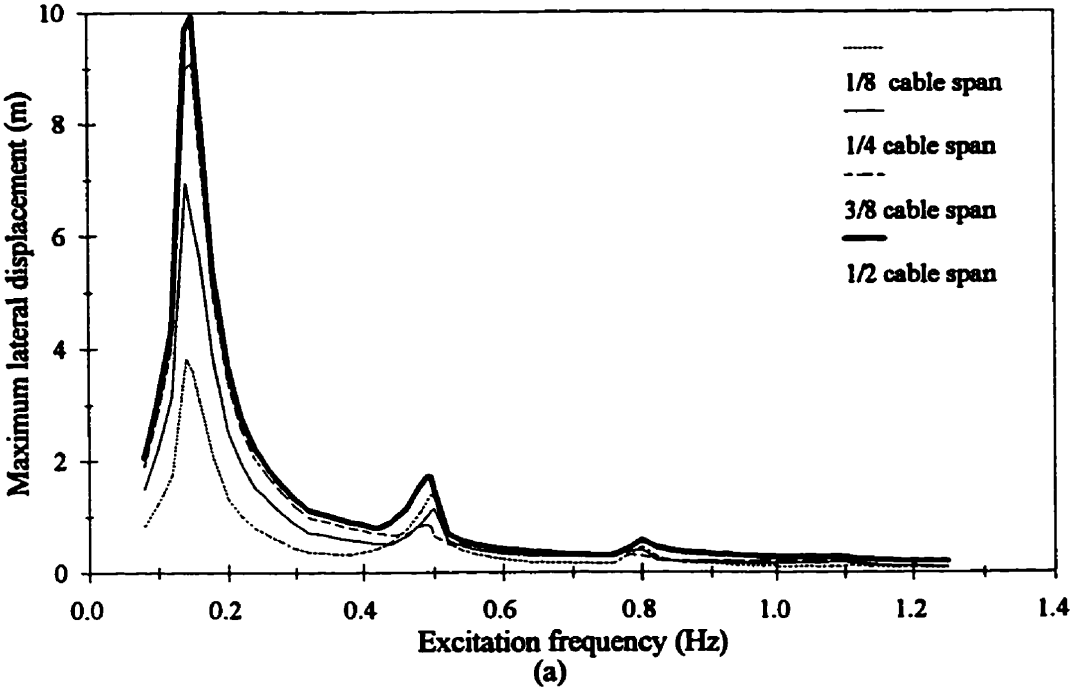

(a)

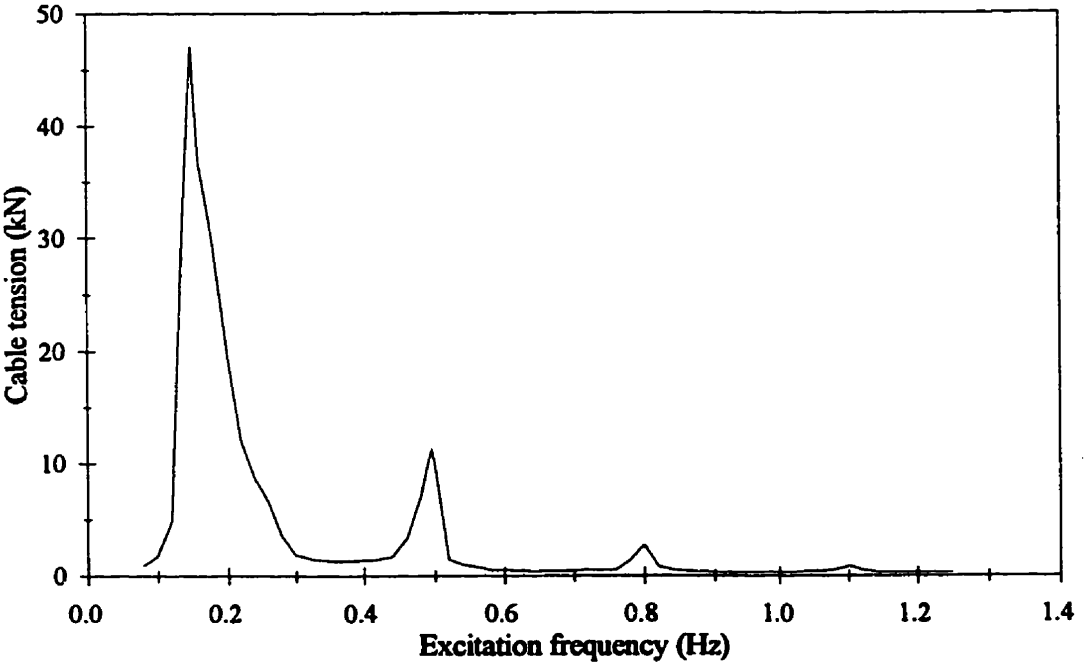

(b)

Figure 2.4 Frequency-response relationship for Cable I (sag / span ratio of 0.03) in the transverse direction : (a) displacement and (b) tension

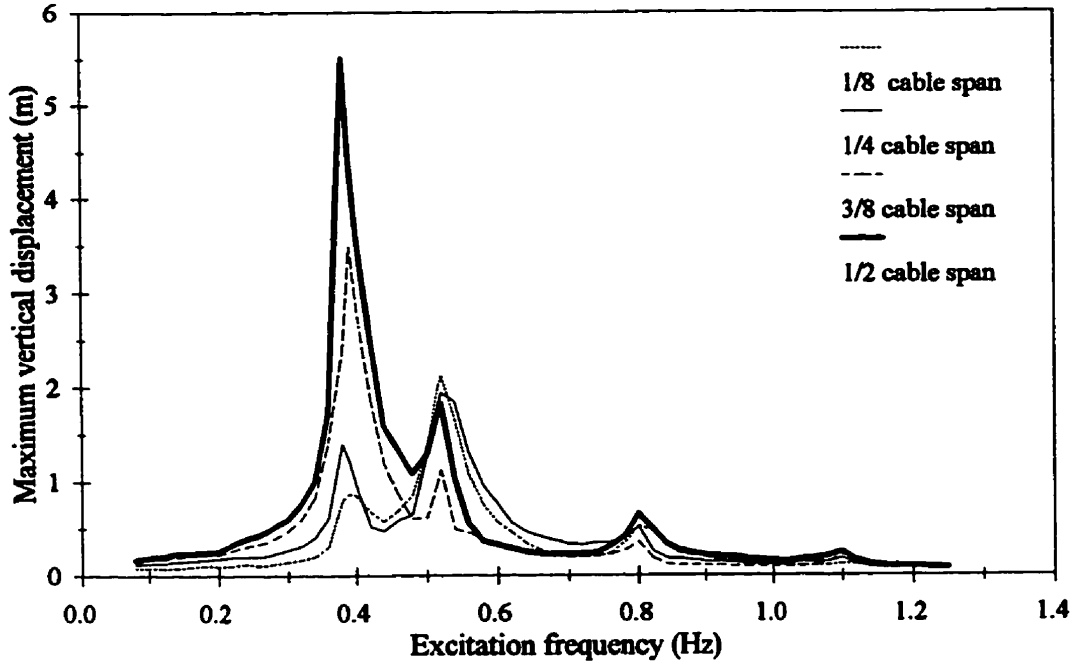

(a)

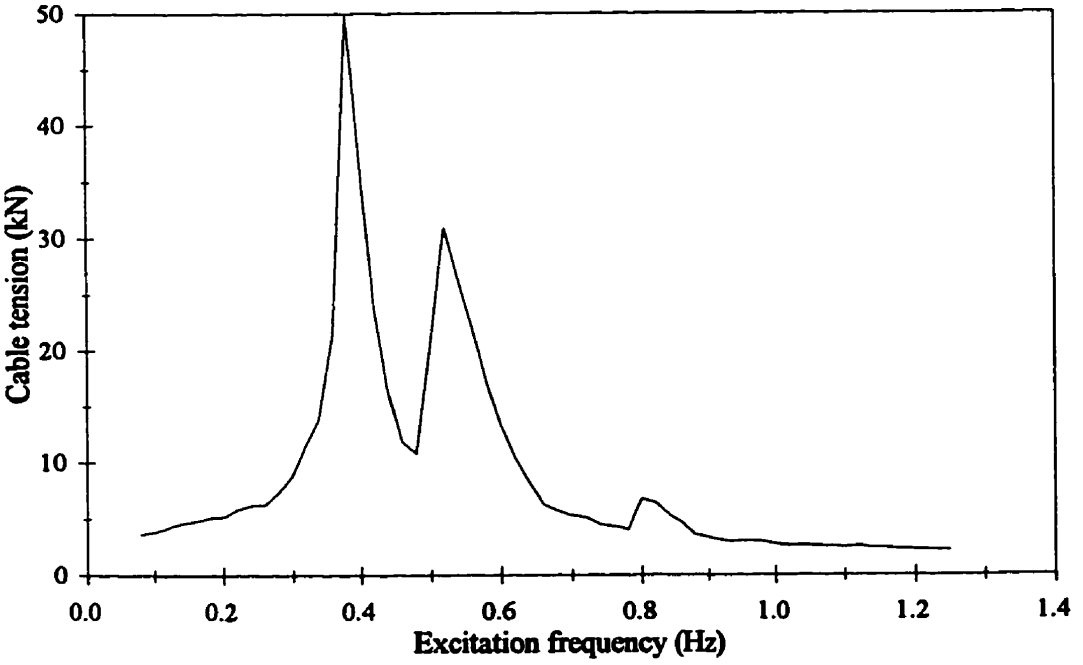

(b)

Figure 2.5 Frequency-response relationship for Cable I in the vertical direction: (a) displacement and (b) tension

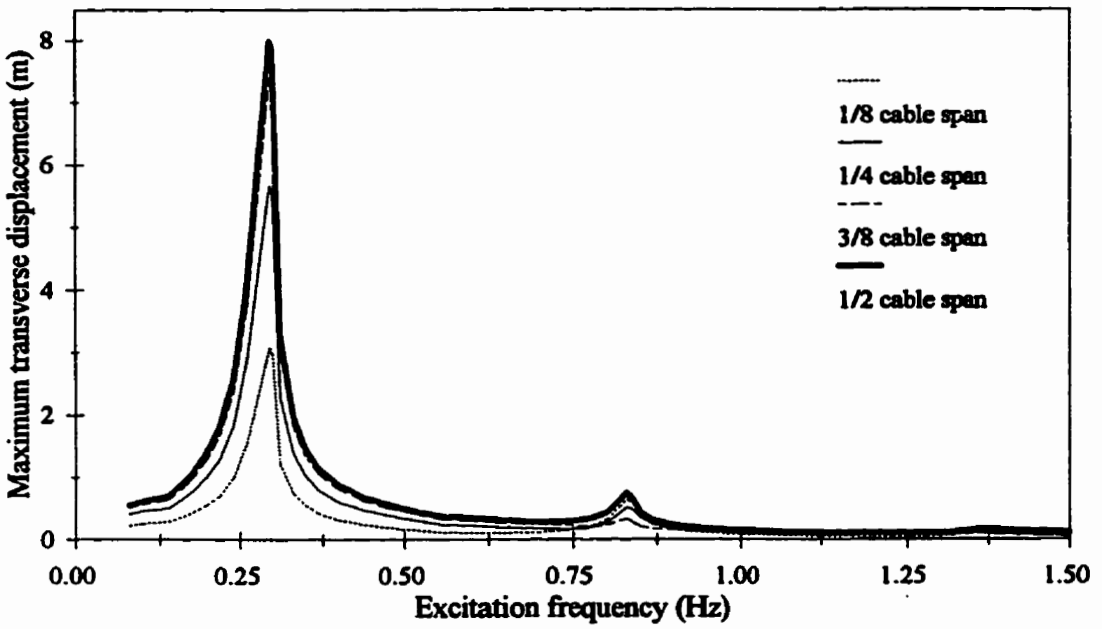

(a)

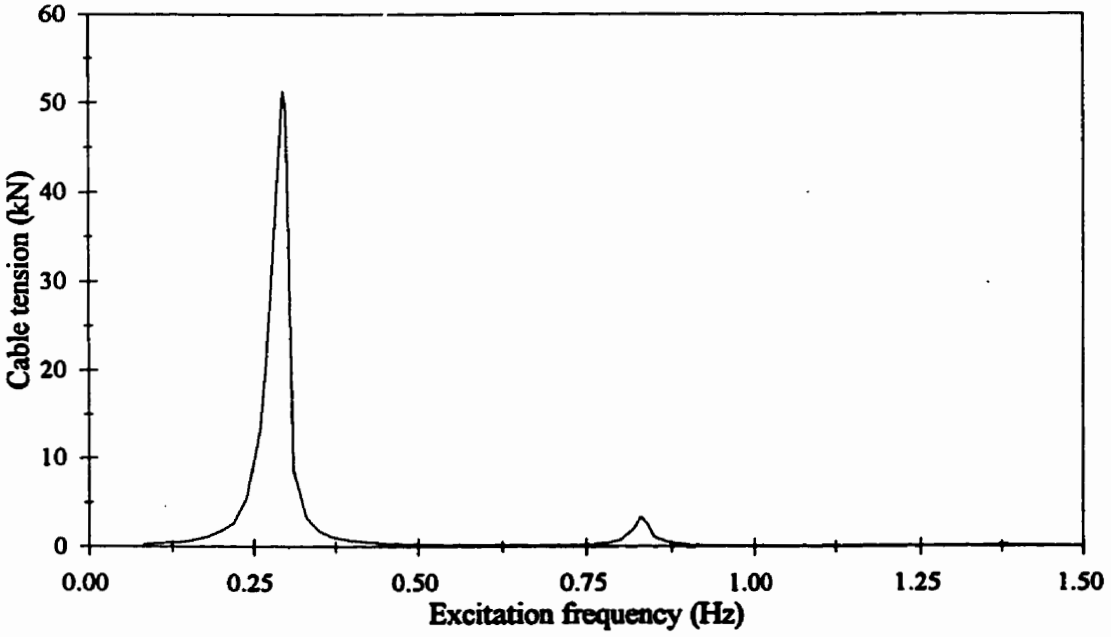

(b)

Figure 2.6 Frequency-response relationship for Cable II (sag / span ratio of 0.01) in the transverse direction : (a) displacement and (b) tension

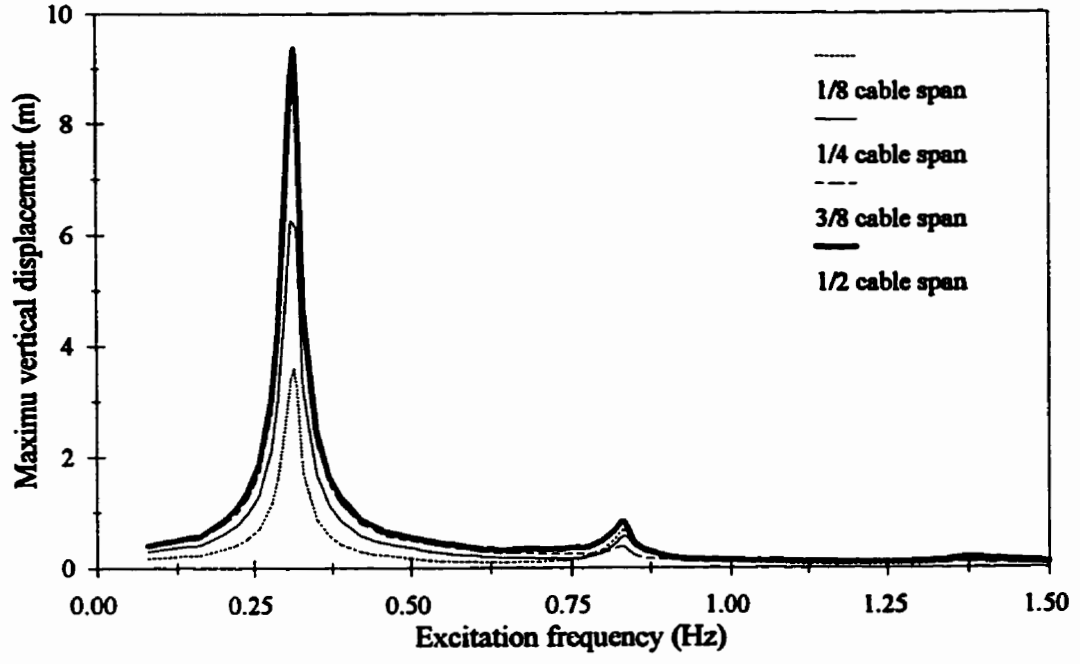

(a)

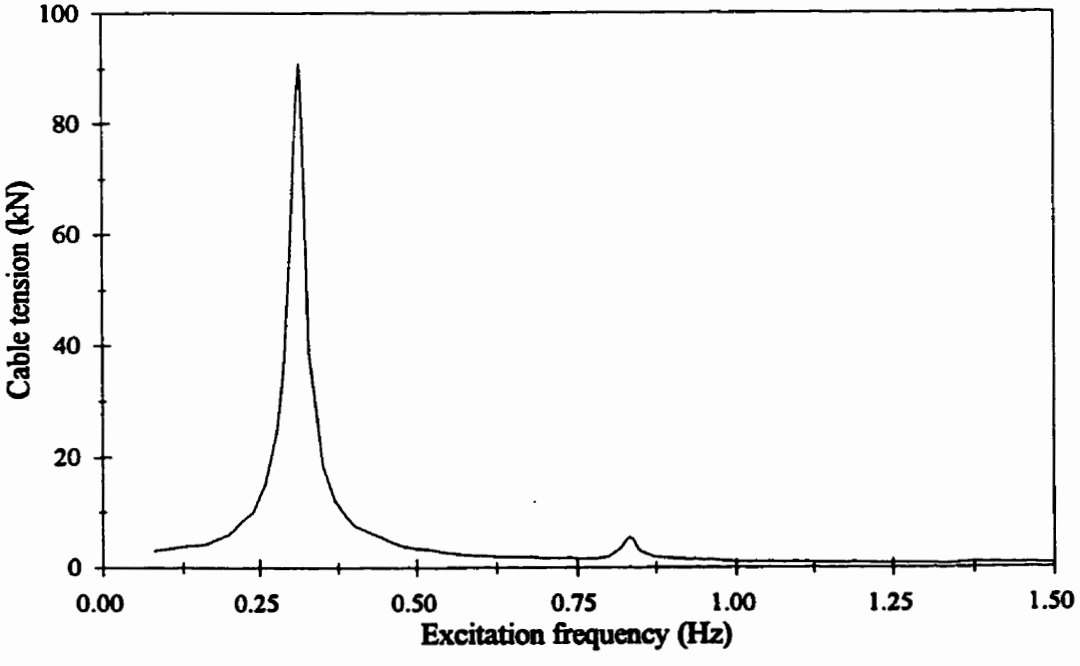

(b)

Figure 2.7 Frequency-response relationship for Cable II in the vertical direction: (a) displacement and (b) tension

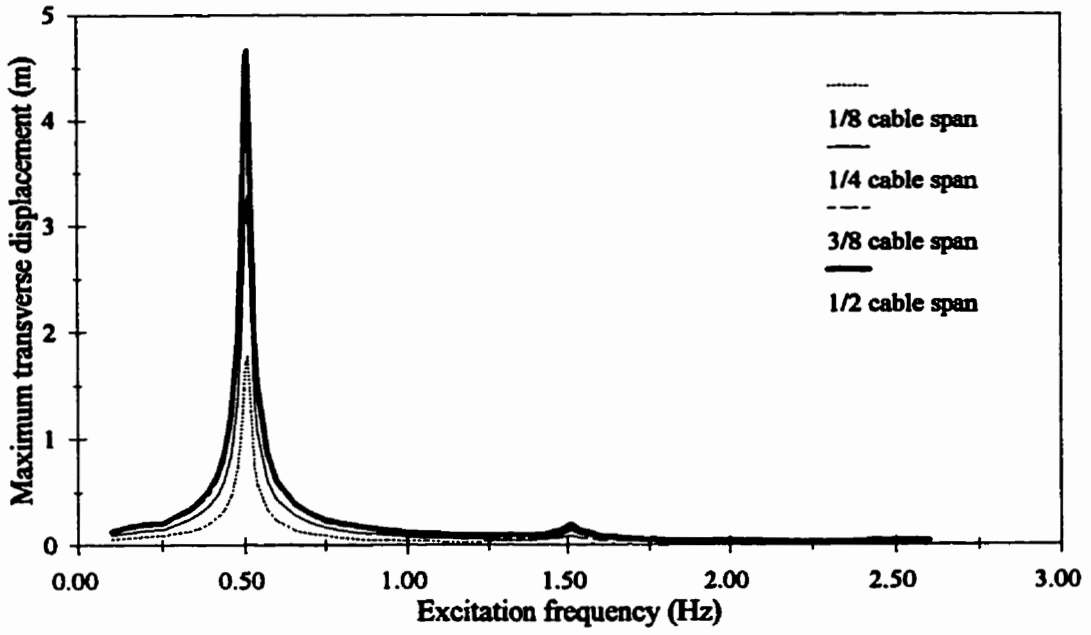

(a)

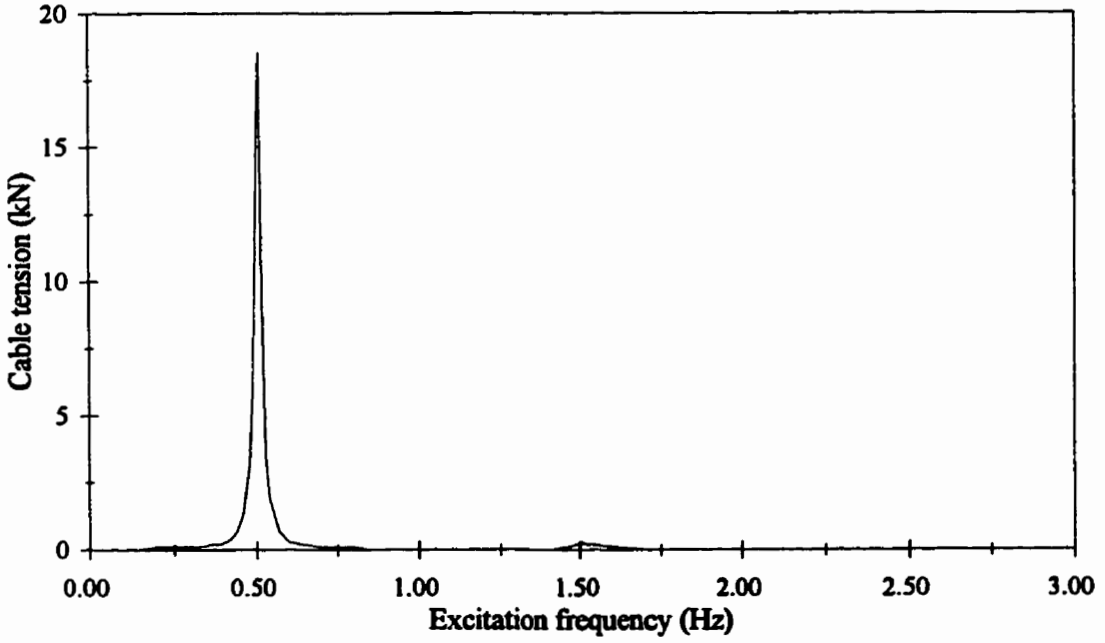

(b)

Figure 2.8 Frequency-response relationship for Cable III (sag / span ratio of 0.003) in the transverse direction : (a) displacement and (b) tension

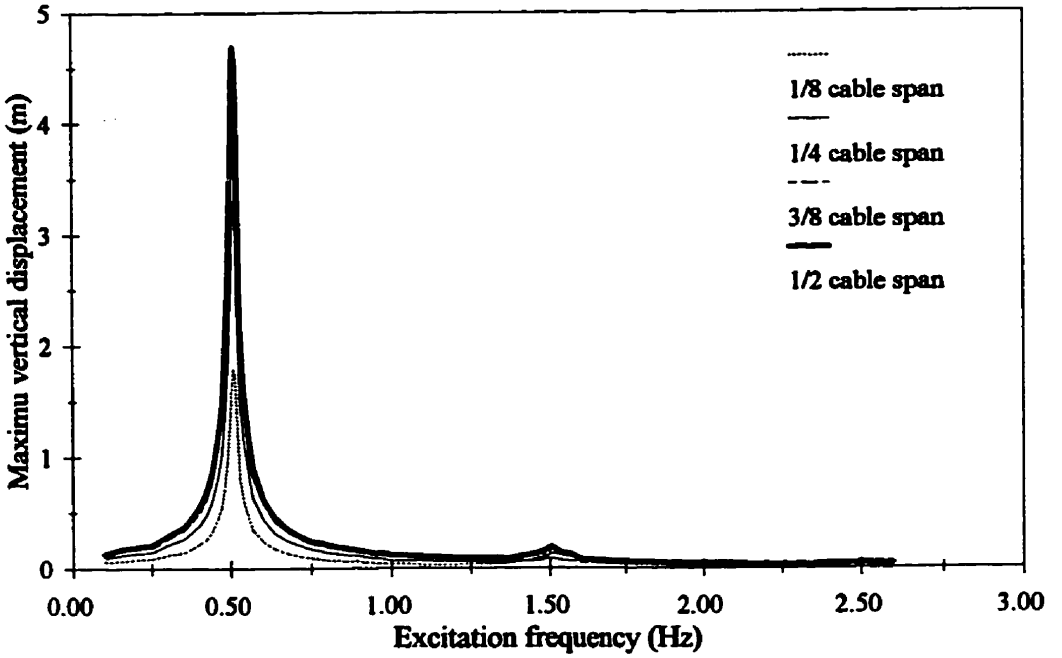

(a)

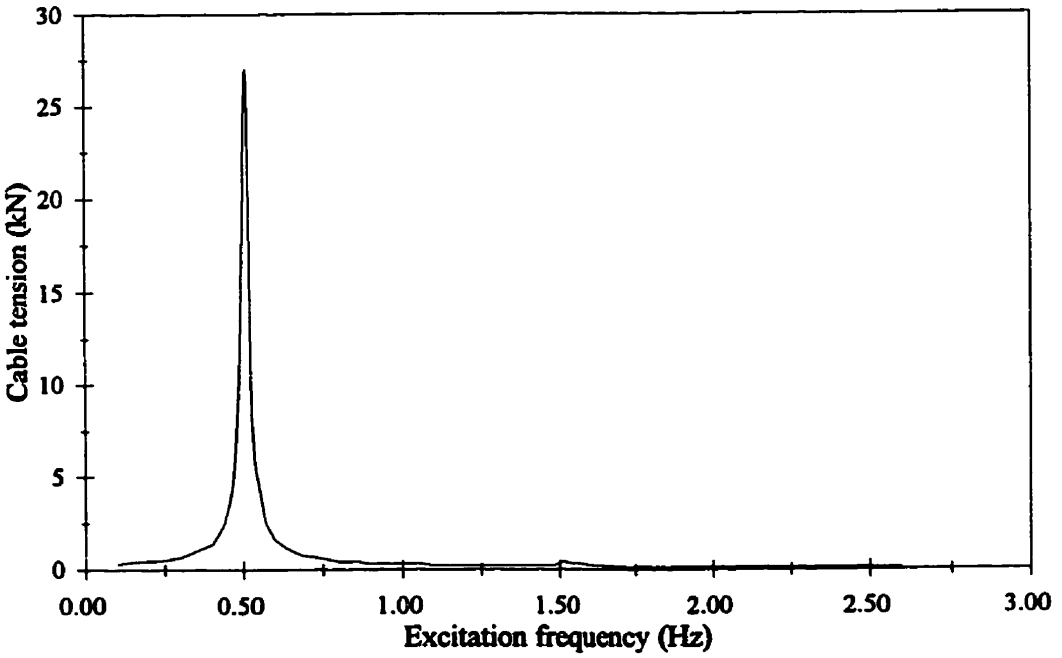

(b)

Figure 2.9 Frequency-response relationship for Cable III in the vertical direction: (a) displacement and (b) tension

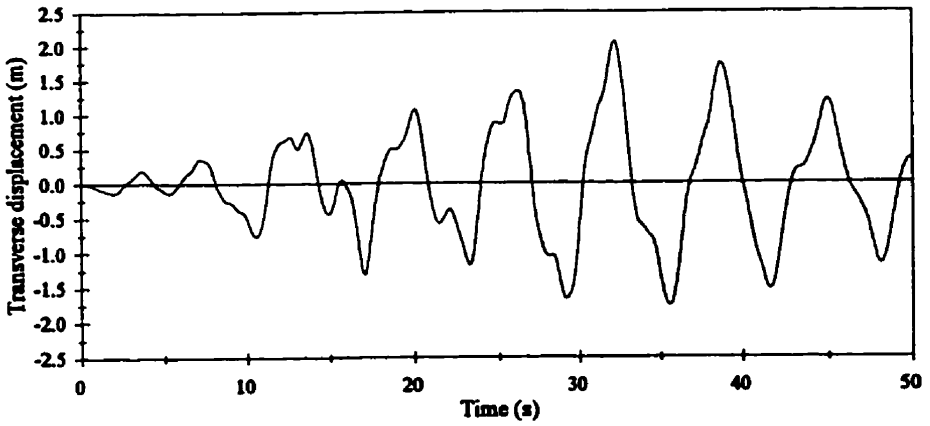

(a) Mexico Earthquake

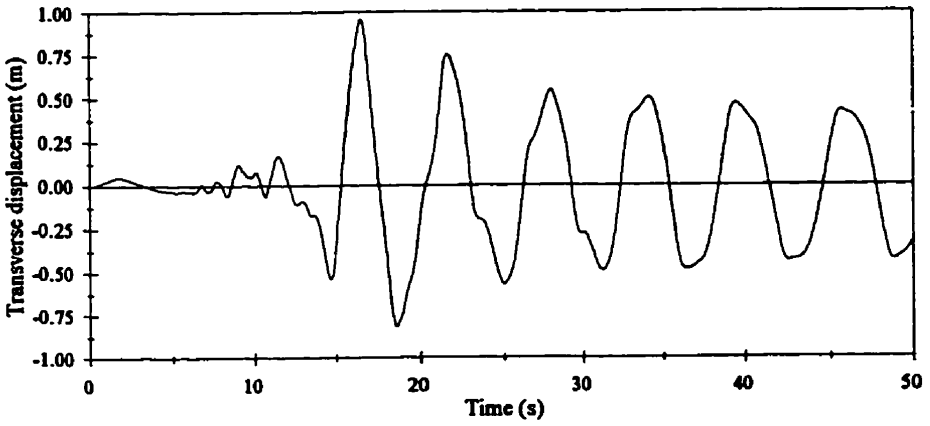

(b) San Fernando Earthquake

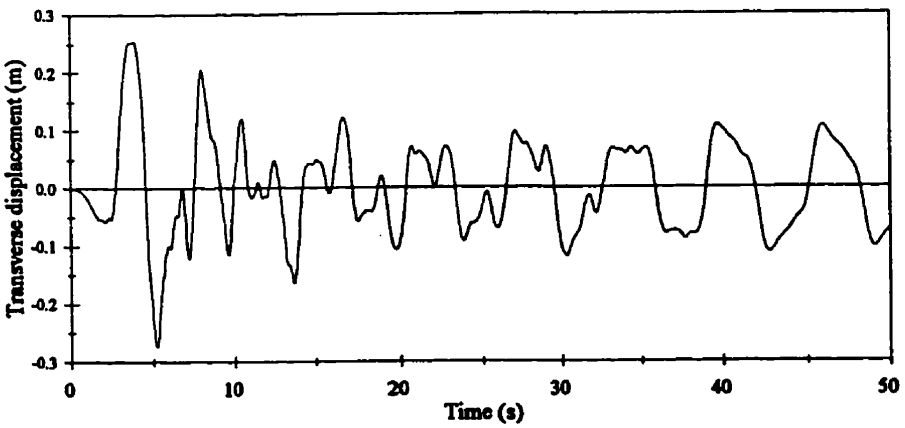

(c) Monte Negro Earthquake

Figure 2.10 Transverse displacement of cable mid-point due to the horizontal component of ground motion

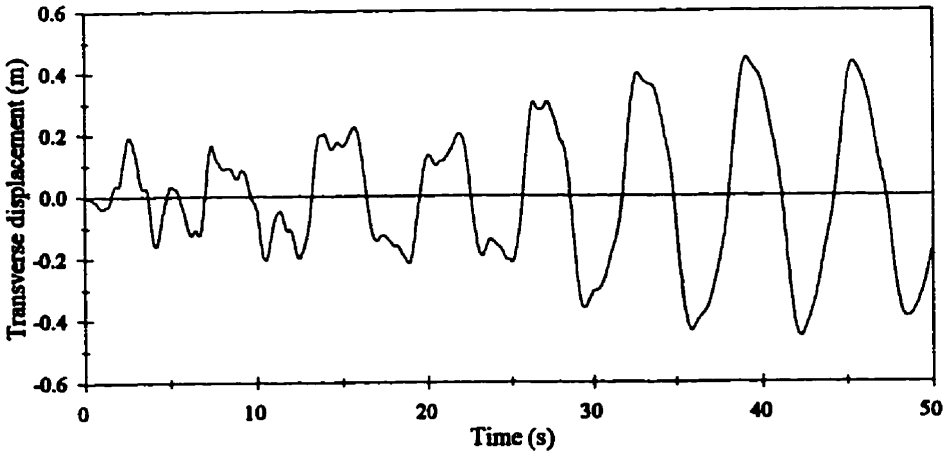

(d) Imperial Valley Earthquake

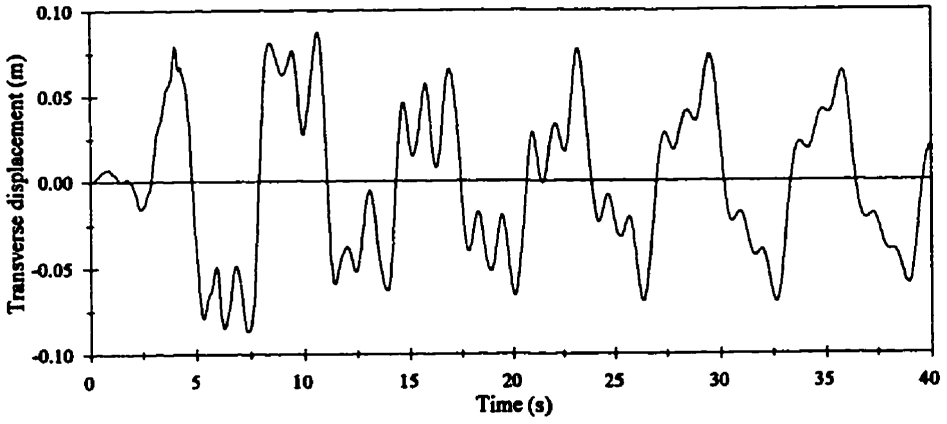

(e) Parkfield Earthquake

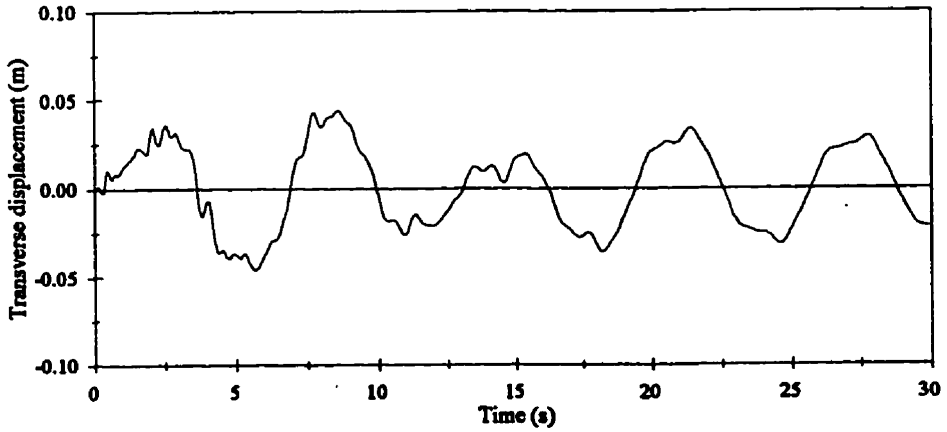

(f) Lytle Creek Earthquake

Figure 2.10 (cont.) Transverse displacement of cable mid-point due to the horizontal component of ground motion

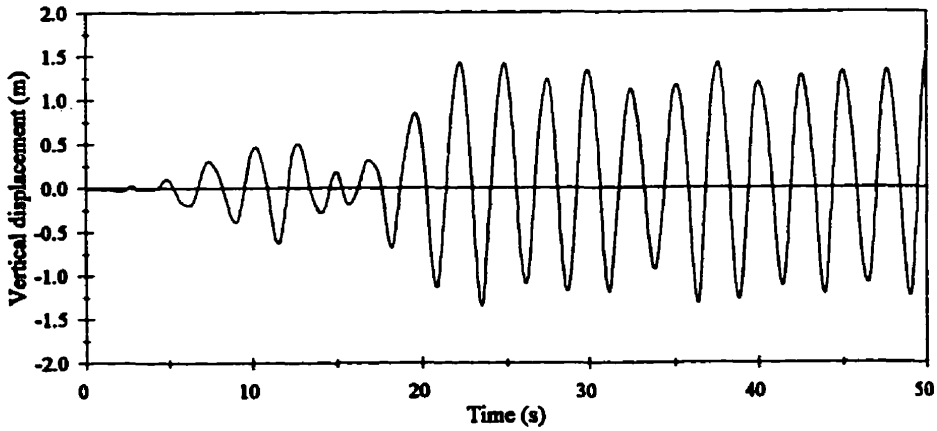

(a) Mexico Earthquake

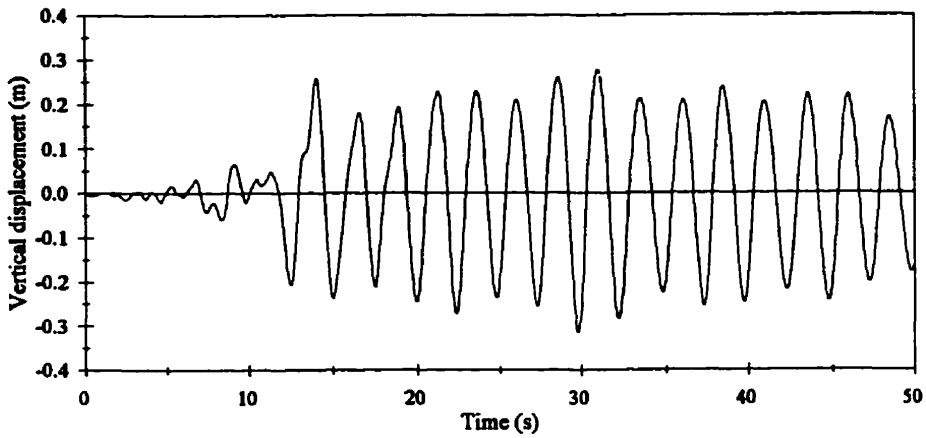

(b) San Fernando Earthquake

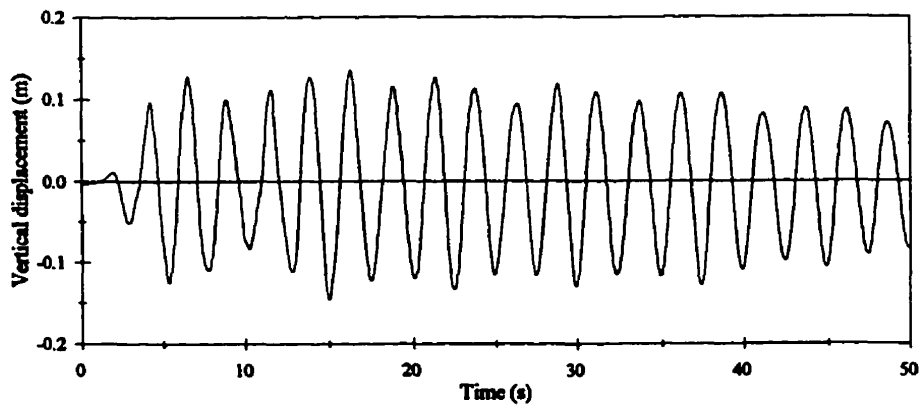

(c) Monte Negro Earthquake

Figure 2.11 Vertical displacement of cable mid-point due to the vertical component of ground motion

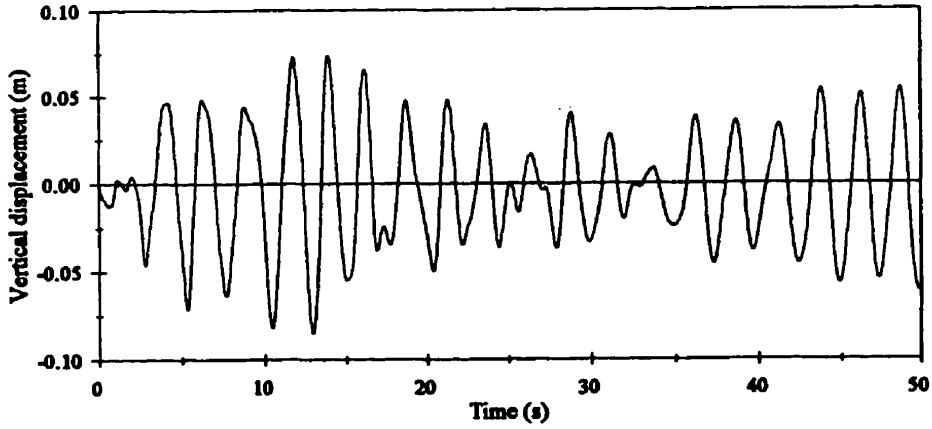

(d) Imperial Valley Earthquake

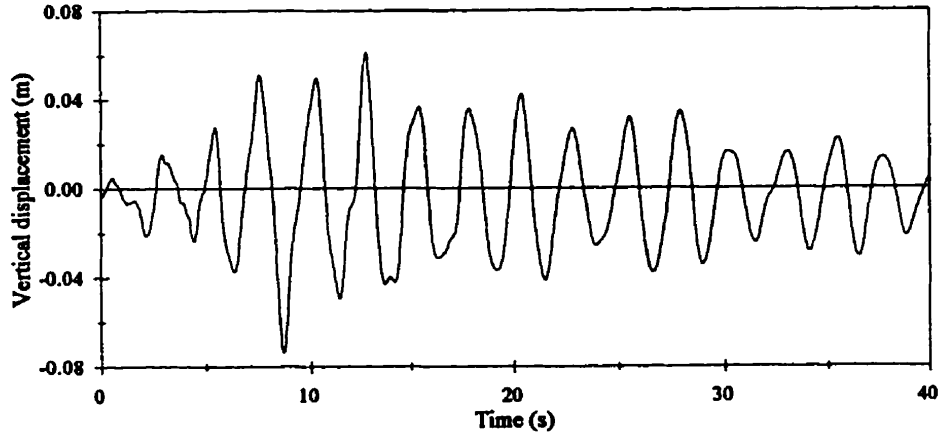

(e) Parkfield Earthquake

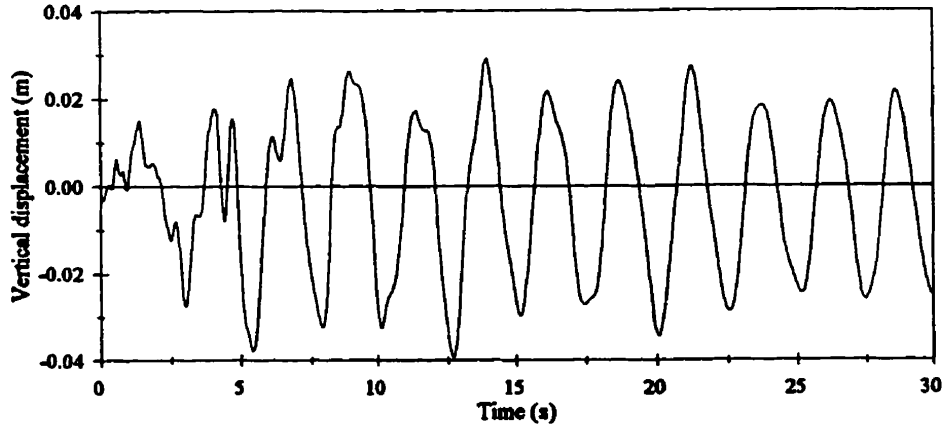

(f) Lytle Creek Earthquake

Figure 2.11 (cont.) Vertical displacement of cable mid-point due to the vertical component of ground motion

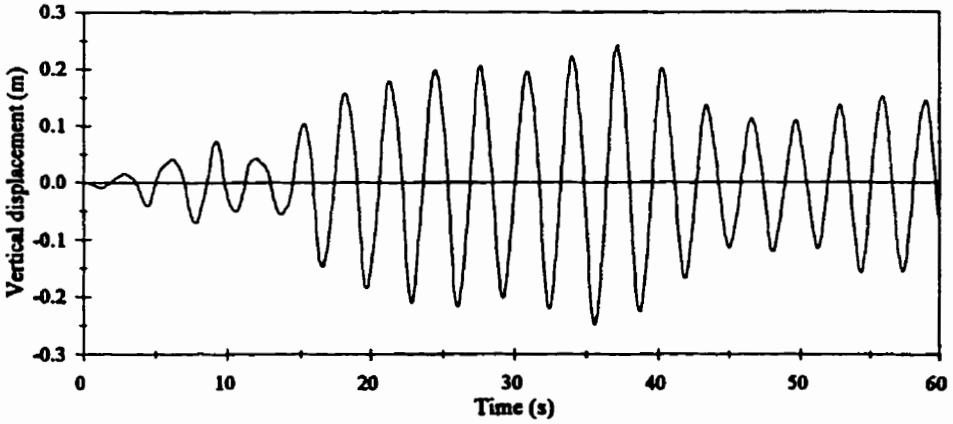

(a) Mexico Earthquake

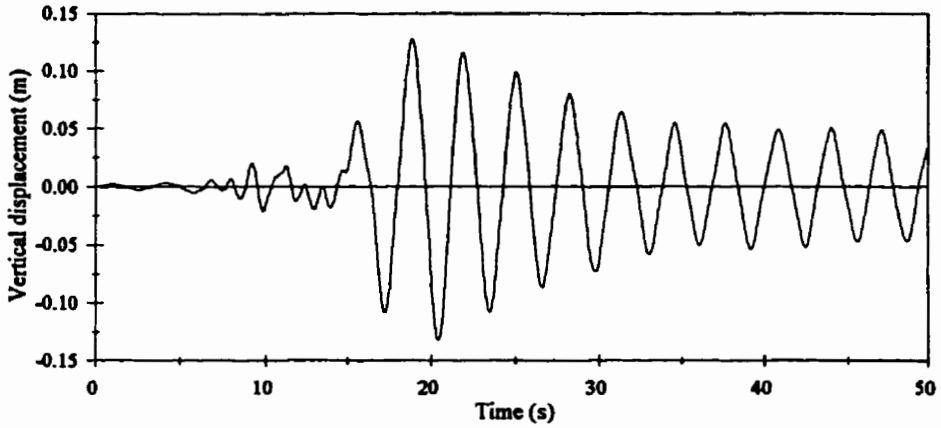

(b) San Fernando Earthquake

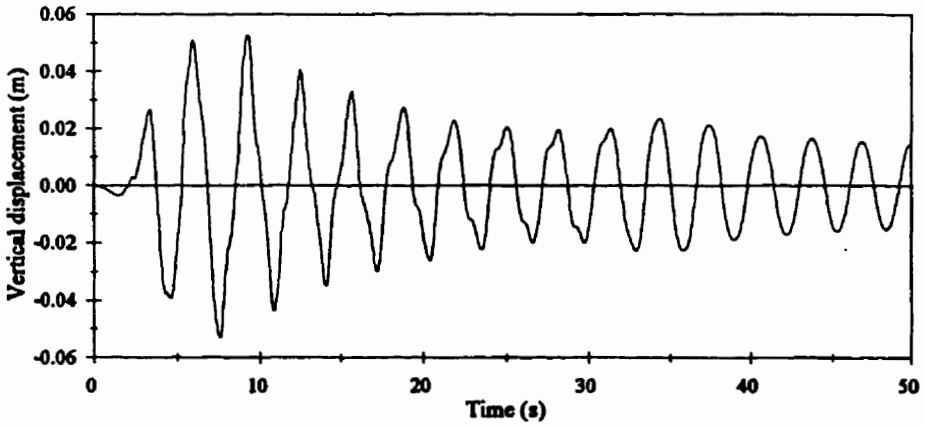

(c) Monte Negro Earthquake

Figure 2.12 Vertical displacement at cable 1/4 span point due to the longitudinal component of ground motion

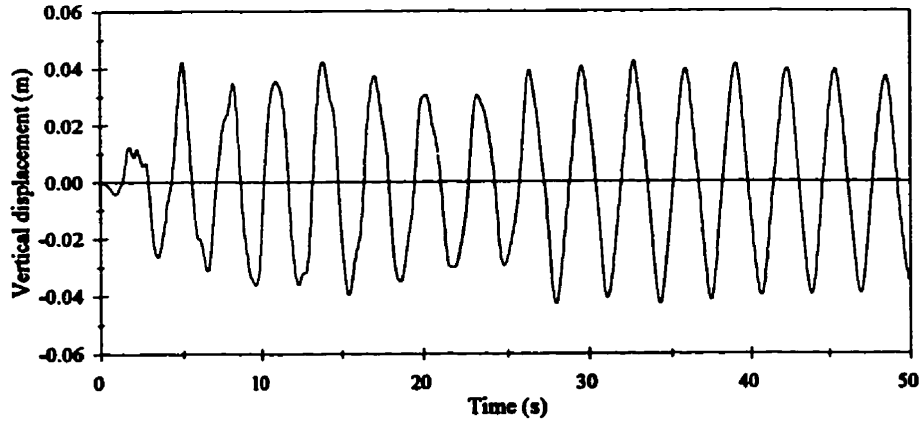

(d) Imperial Valley Earthquake

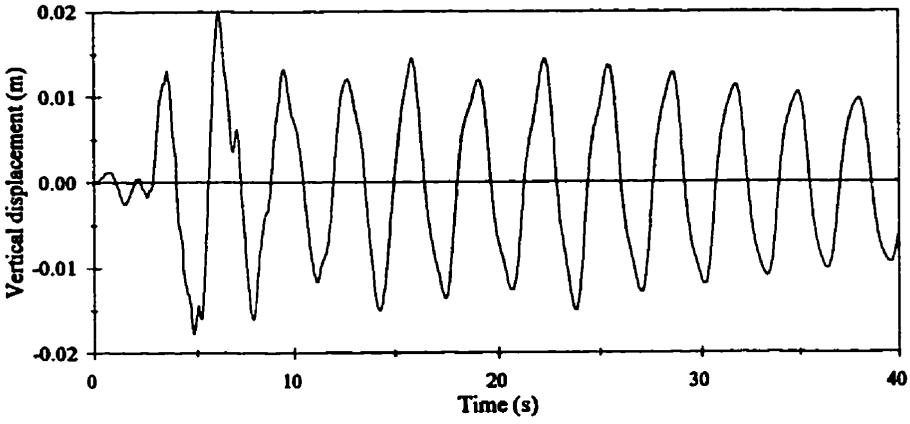

(e) Parkfield Earthquake

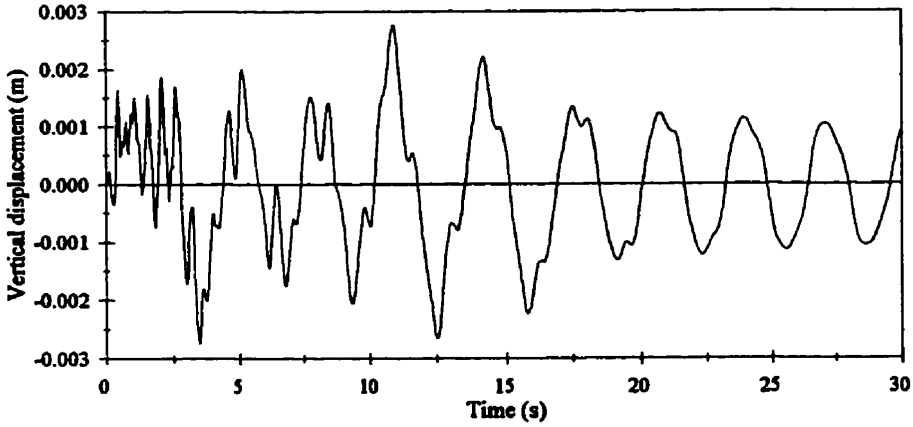

(f) Lytle Creek Earthquake

Figure 2.12 (cont.) Vertical displacement at cable 1/4 span point due to the longitudinal component of ground motion

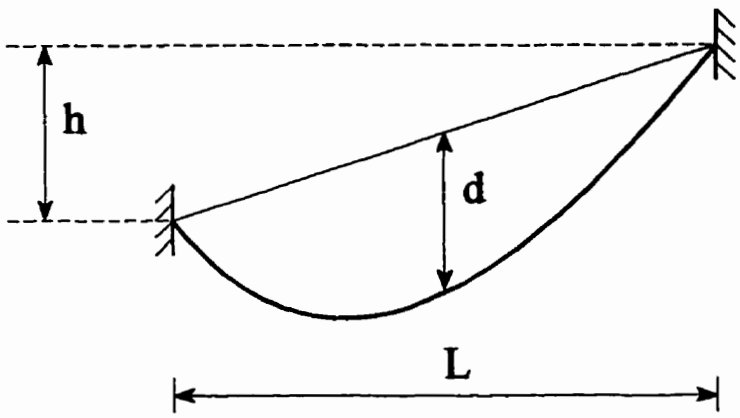

Figure 2.13 Cable supports at different elevations

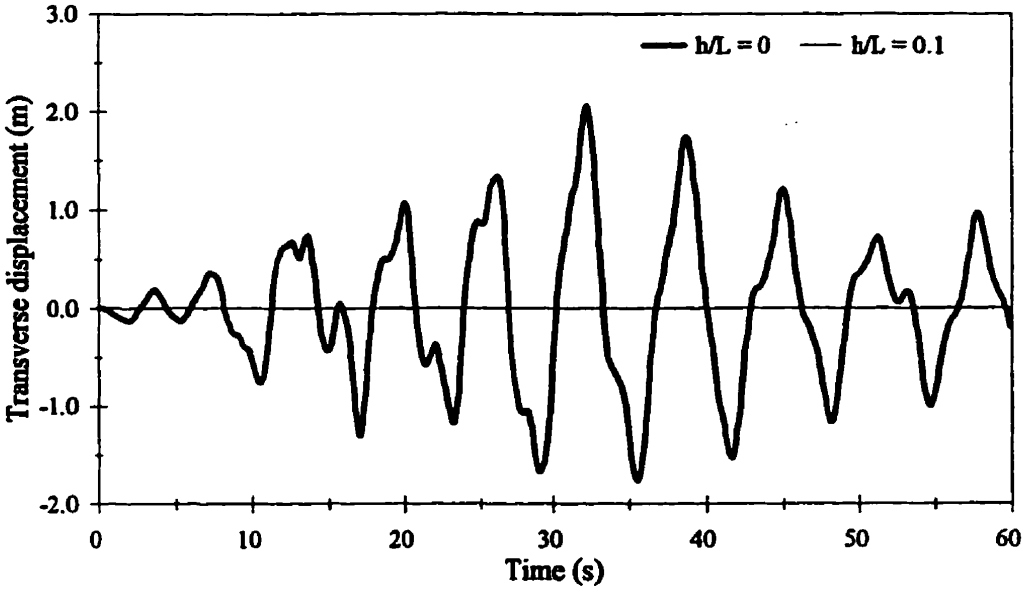

(a)

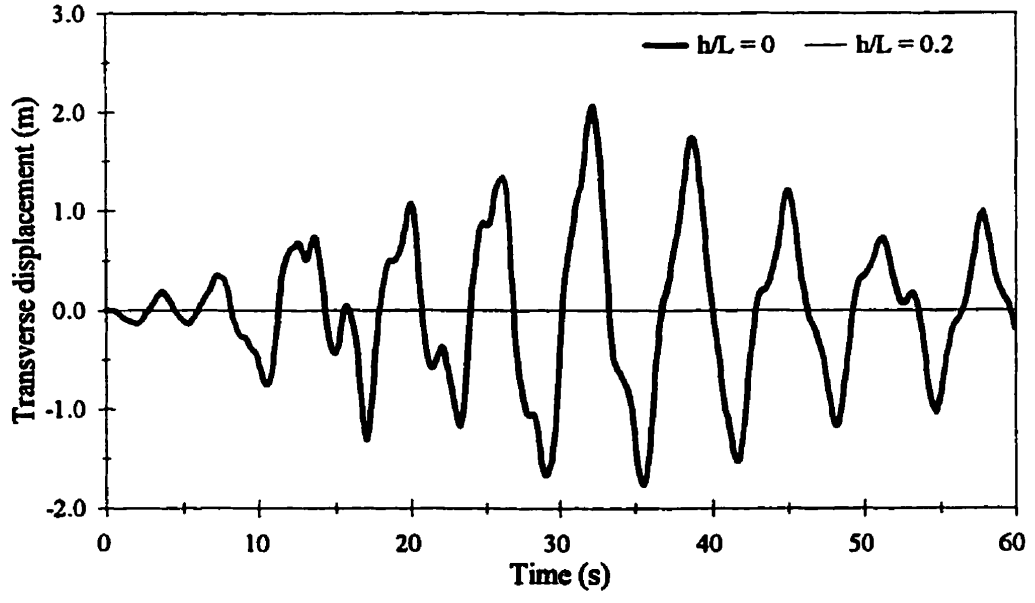

(b)

Figure 2.14 Transverse displacement of cable mid-point due to the horizontal component of the Mexico earthquake for different values of h/L

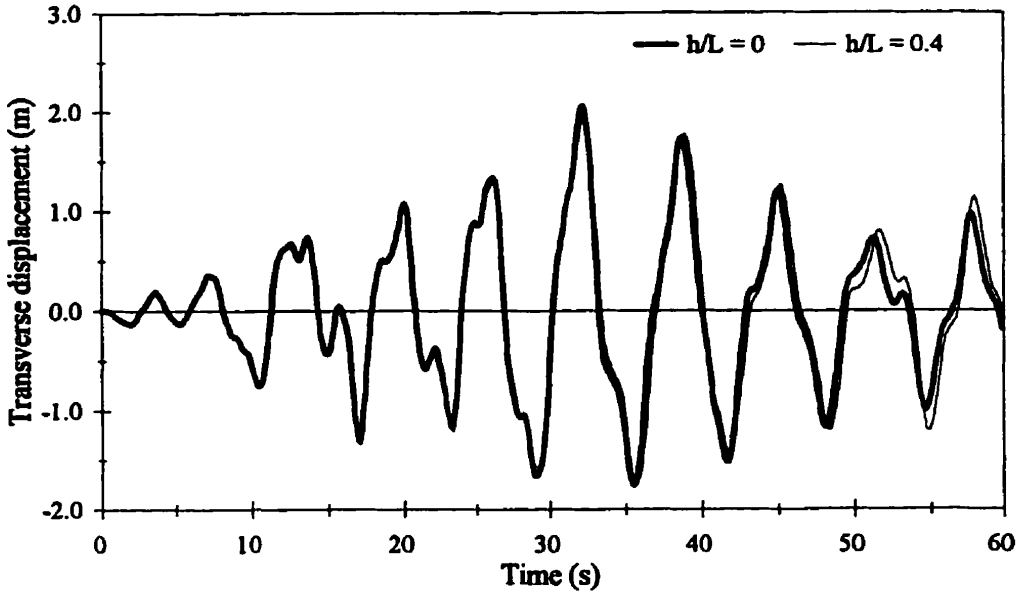

(c)

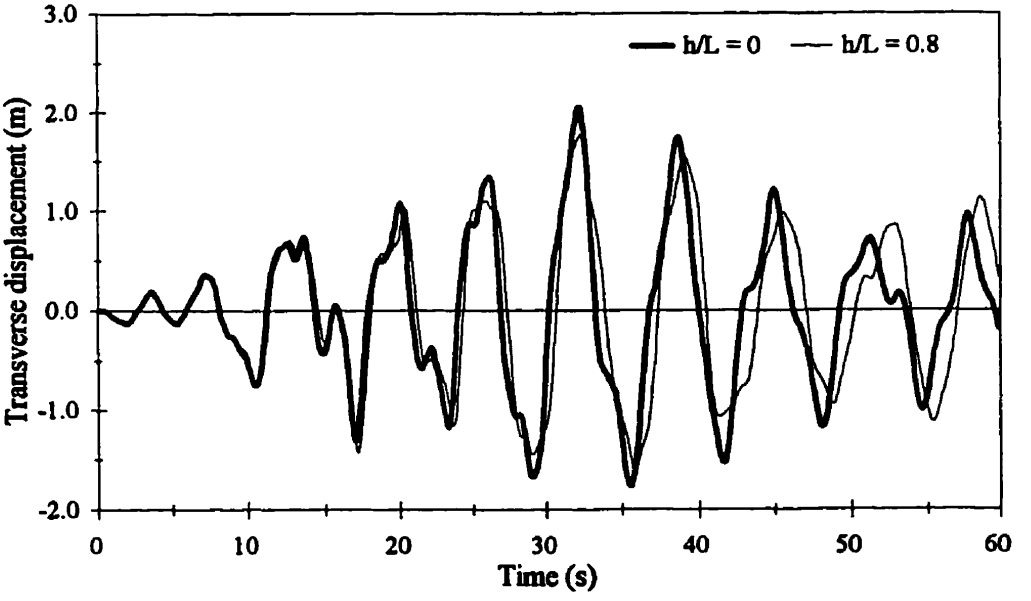

(d)

Figure 2.14 (cont.) Transverse displacement of cable mid-point due to the horizont component of the Mexico earthquake for different values of h/L

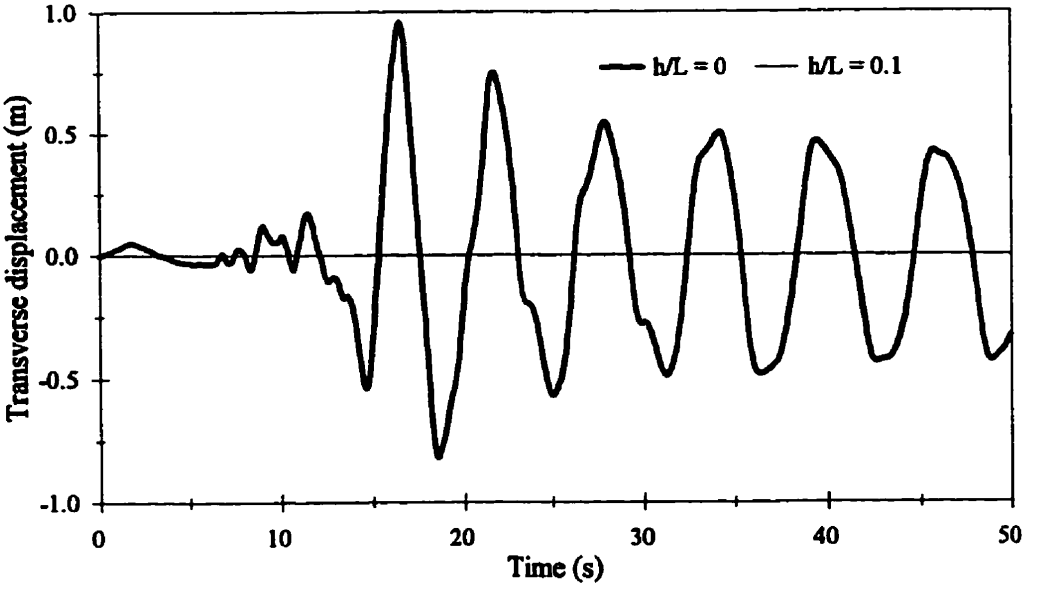

(a)

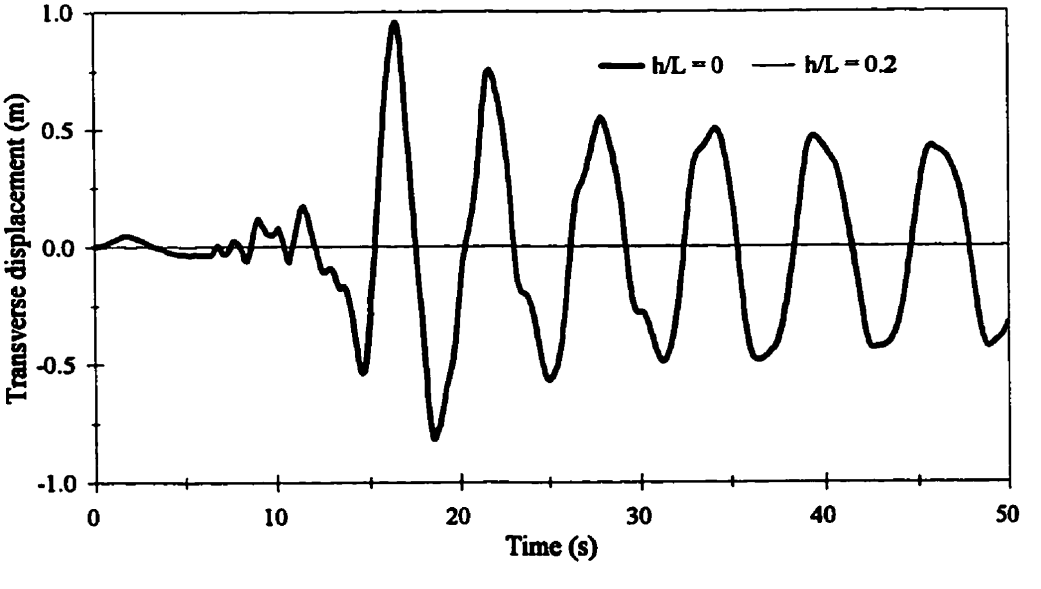

(b)

Figure 2.15 Transverse displacement of cable mid-point due to the horizontal component of the San Fernando earthquake for different values of h/L

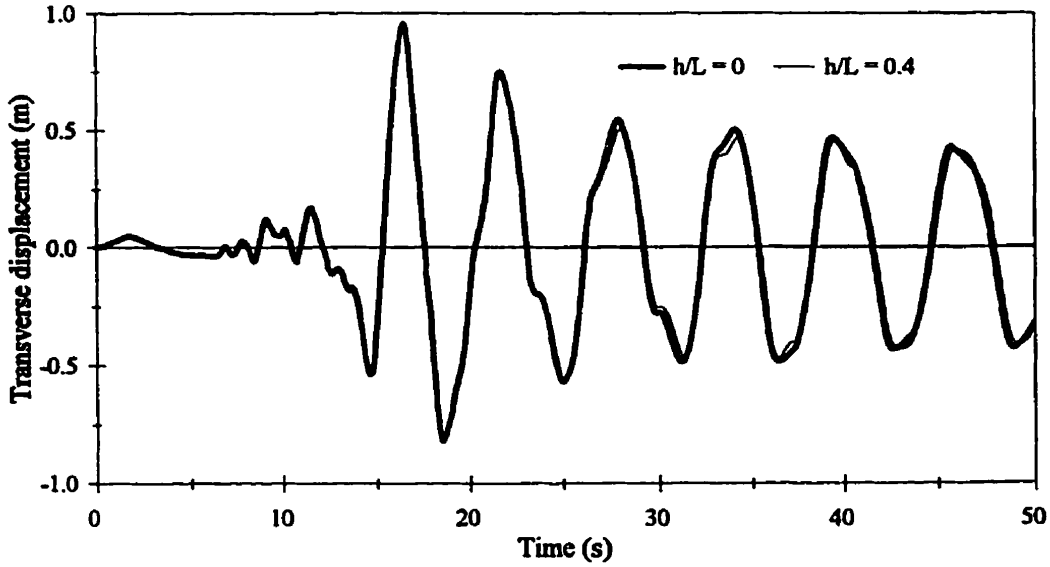

(c)

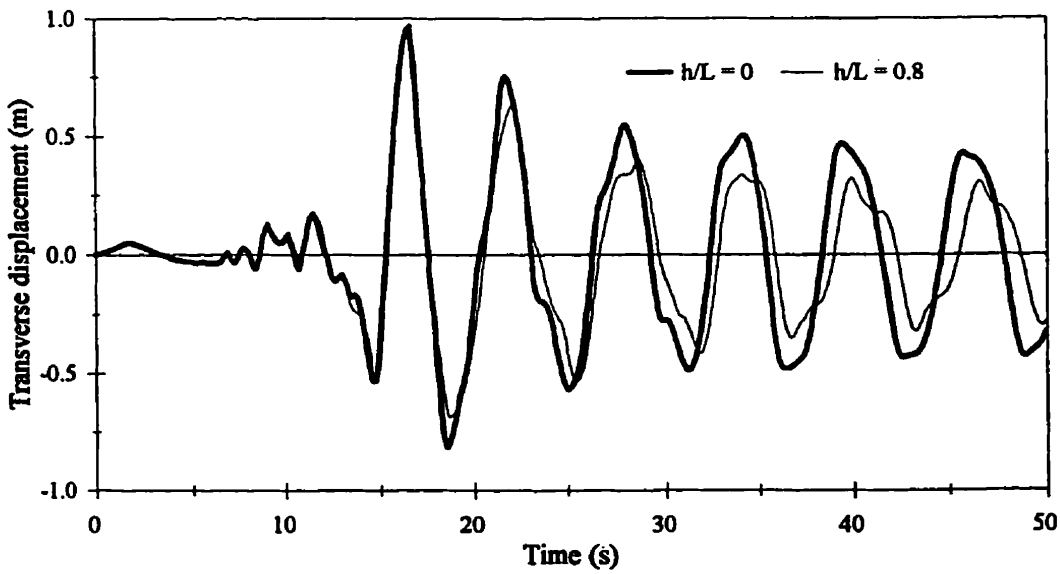

(d)

Figure 2.15 (cont.) Transverse displacement of cable mid-point due to the horizontal component of the San Fernando earthquake for different values of h/L

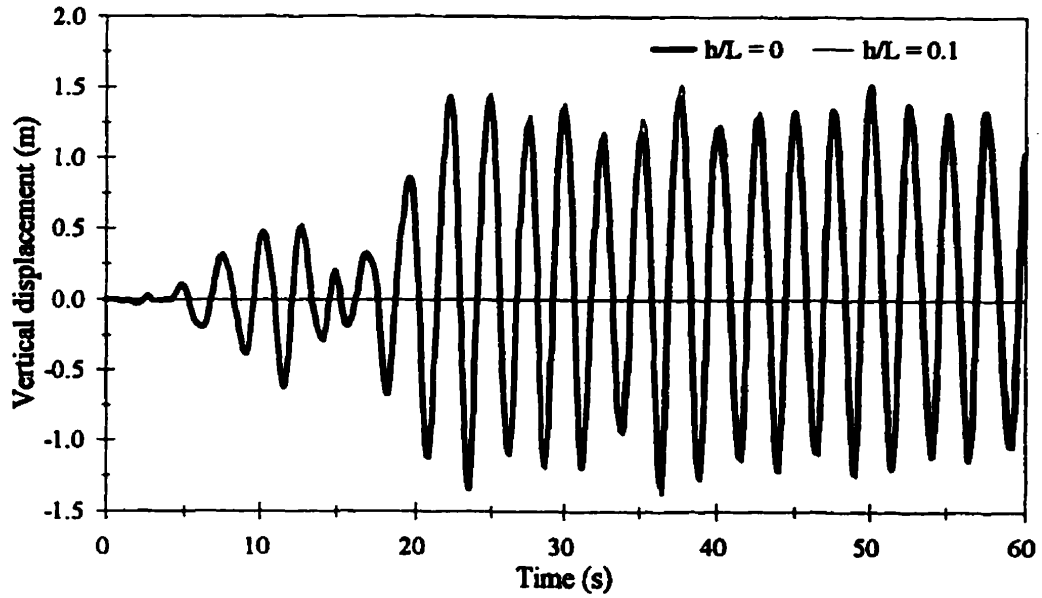

(a)

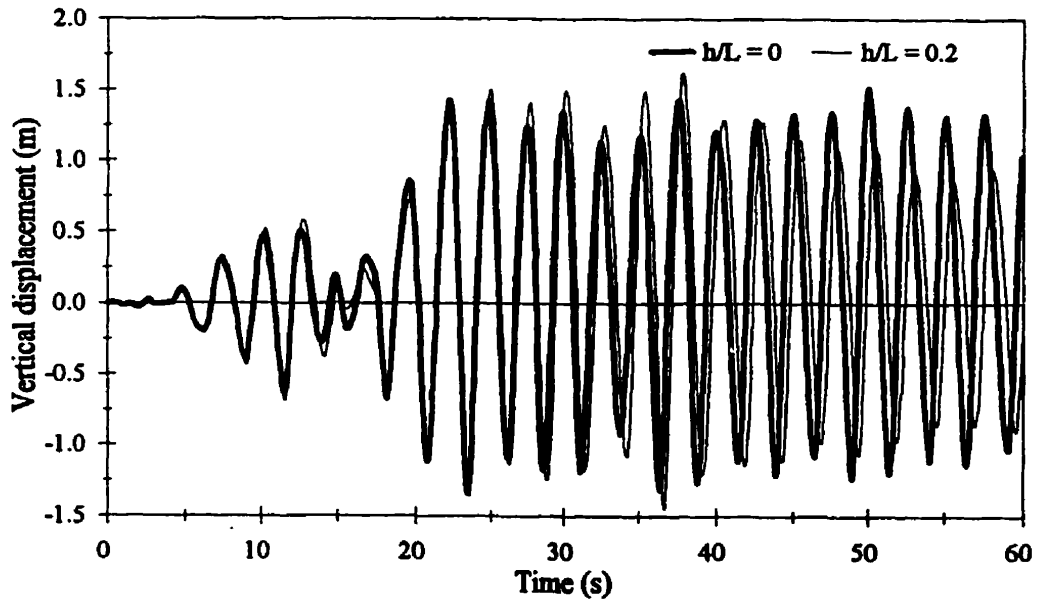

(b)

Figure 2.16 Vertical displacement of cable mid-point due to the vertical component of the Mexico earthquake for different values of h/L

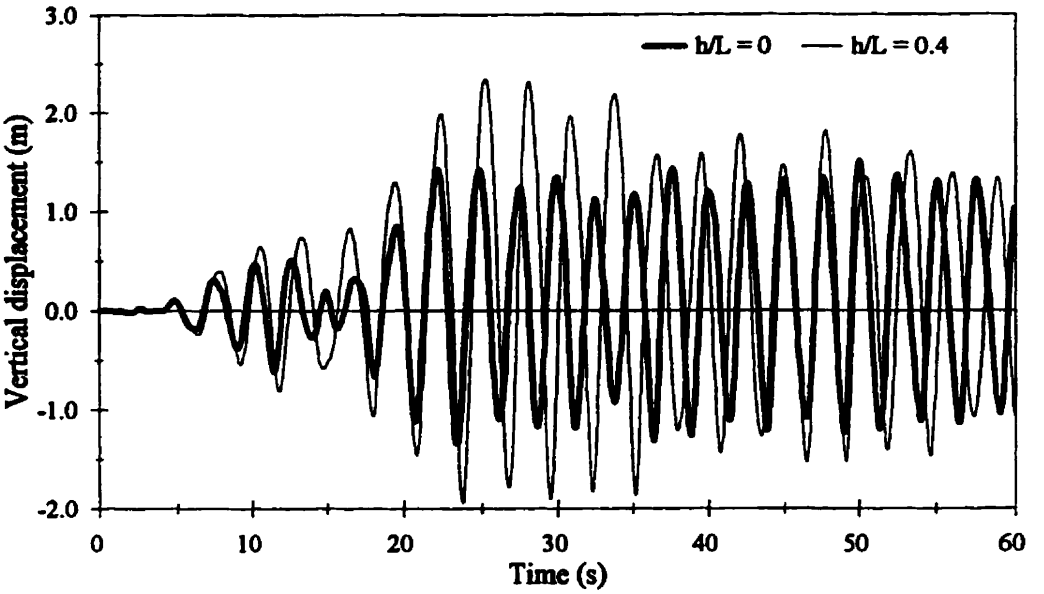

(c)

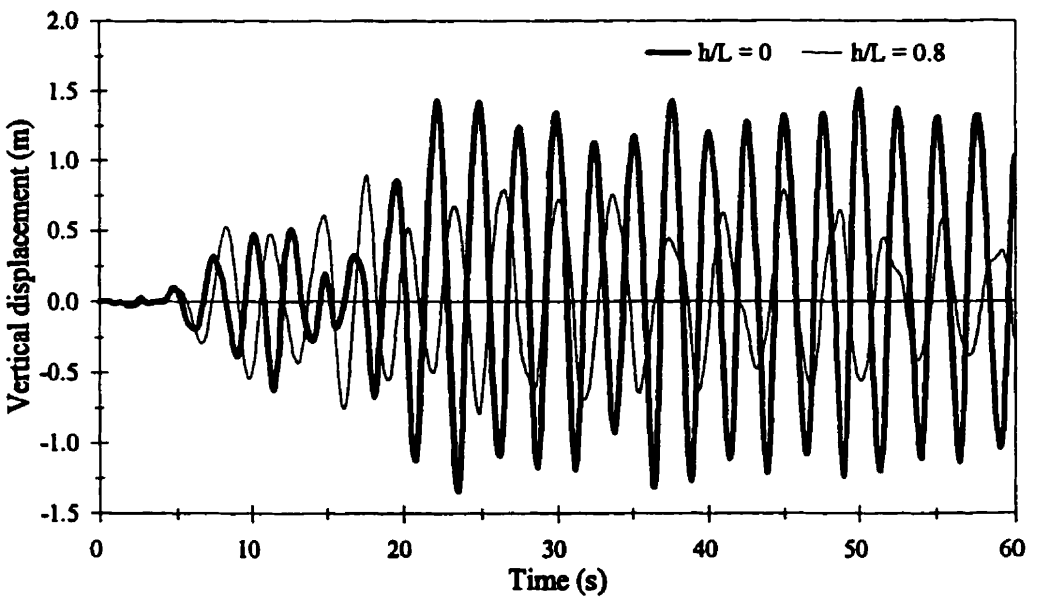

(d)

Figure 2.16 (cont.) Vertical displacement of cable mid-point due to vertical component of the Mexico earthquake for different values of h/L

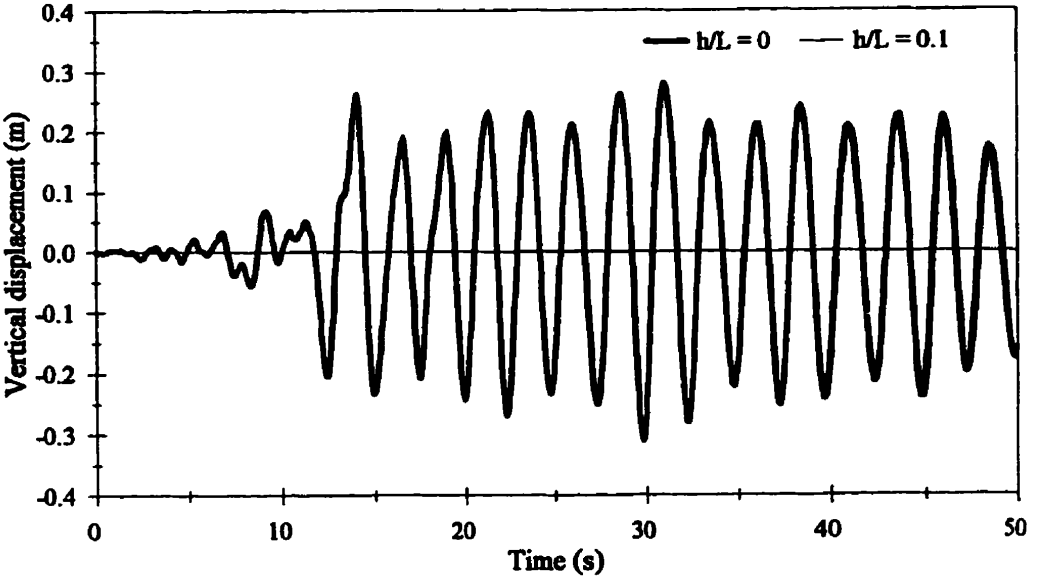

(a)

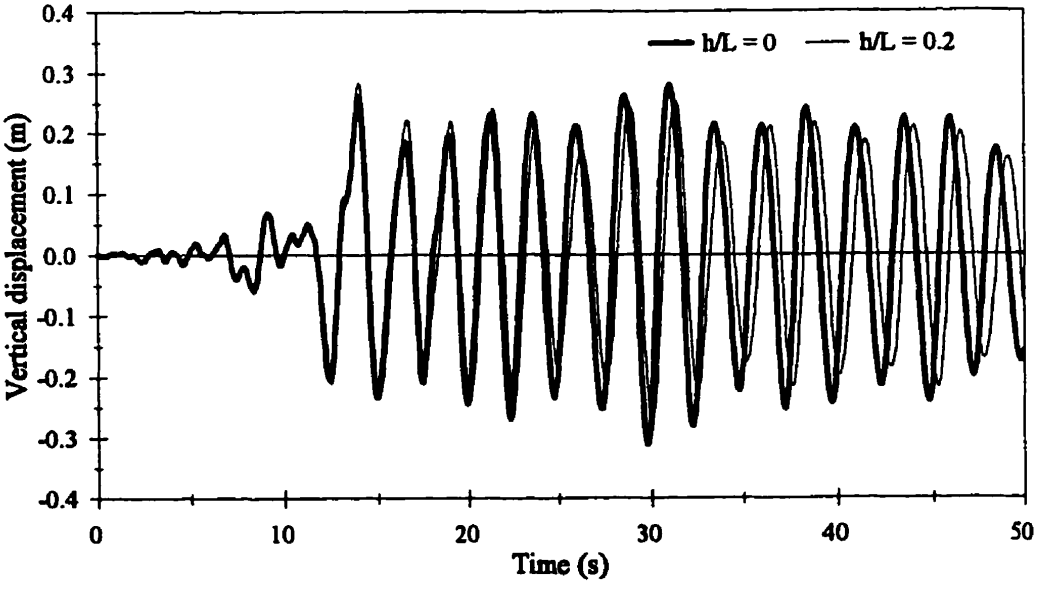

(b)

Figure 2.17 Vertical displacement of cable mid-point due to the vertical component of the San Fernando Earthquake for different values of h/L

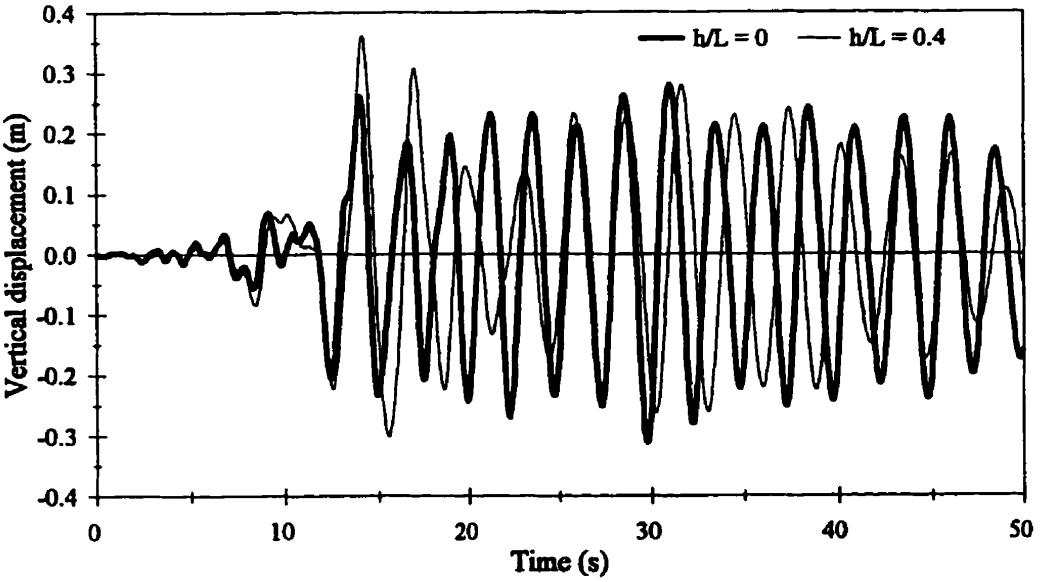

(c)

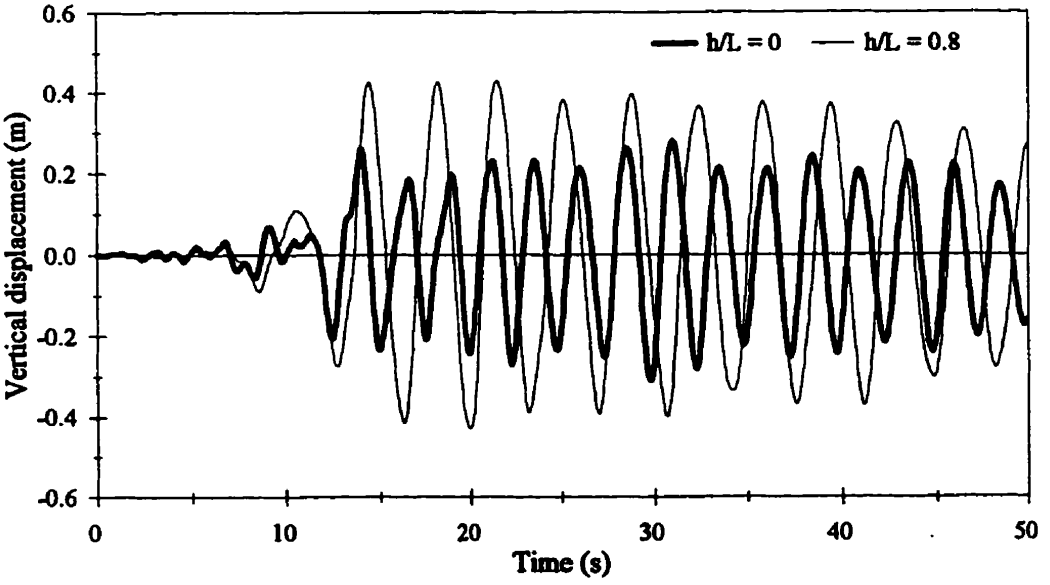

(d)

Figure 2.17 (cont.) Vertical displacement of cable mid-point due to the vertical component of the San Fernando Earthquake for different values of h/L

CHAPTER 3

SEISMIC ANALYSIS OF TRANSMISSION LINE SYSTEMS

3.1 GENERAL

Transmission lines are normally designed for wind and ice loads in the transverse direction. In the absence of seismic code provisions, it is not the practice to take earthquake loads into account. However, seismic loads may be important in cases where the transmission line extends in areas of low wind forces and high seismicity. When subjected to ground motion, the transmission line towers and cables may be subjected to significant forces and stresses. However of major concern in the response of transmission lines during earthquakes is that large cable displacements do not cause the cables to touch each other or any surrounding object, thus causing power failure

The analysis of cables presented in Chapter 2 indicated that seismic excitation can cause large displacements of the cables. The displacements of the transmission line cables are the main concern in this analysis. However, cable tension and the transmission tower displacements and internal forces are also reported.

A transmission line consists of several towers with cables extending between them. The cables are connected to the towers using suspension insulators. To control the cable vibrations, various kinds of dampers may be used such as the Stockbridge dampers and spacer

dampers in case of bundle conductors. In the present analysis, damping of vibrations due to the use of dampers is not considered.

Since power transmission lines are normally designed for wind loads, little research has been conducted to investigate the effect of earthquakes on the design. It is the conception of designers in the industry that higher safety factors in design eliminate the need to take earthquakes into account. There are several recent cases of damage to power lines during earthquakes. During the 1994 Northridge earthquake, 85 power line cables were damaged and two transmission towers collapsed due to high ground motion (Northridge earthquake-reconnaissance report, 1995). During the 1992 Landers earthquake, there were over 100 cases of line burn-downs.

In this chapter, two typical transmission towers are analyzed to determine their free vibration characteristics as well as their behaviour when subjected to earthquake ground motion. The effect of the suspension insulator and its characteristics on the seismic behaviour of the transmission line is also analyzed. The seismic behaviour of an intermediate span transmission line is analyzed due to the effect of vertical and transverse excitations. A simplified model for the transmission line for seismic analysis is developed. The internal member forces in the towers due to earthquake ground motion are compared to the forces caused by the code specified loads. The design code considered is the National Electrical Safety Code (NESC, 1993) which specifies wind and ice loads as the design loads in the transverse and vertical directions.

3.2 SEISMIC ANALYSIS OF TRANSMISSION TOWERS

Towers are the main supporting structural elements of a power transmission line. Different kinds of transmission towers can be used depending on the line voltage, the spacing between towers, and the clearance required above ground. The choice of a specific type of towers will have a direct effect on the cost of the line. The main types of transmission towers are wood poles, steel poles, steel latticed towers, and reinforced concrete poles.

Steel latticed towers are usually used for high voltage transmission lines where longer spans are used and considerable height is necessary to provide ground clearance for the conductors. The current analysis deals primarily with high voltage transmission lines with steel latticed wide base towers. However, the main conclusions regarding cable displacements and cable tensions are valid for lines with various voltage rating using other types of towers.

Two typical examples of steel transmission towers are selected for the analysis. The first tower (Tower I) has a total height of 41.6 m, a base width of 7.5 m and a weight of 11.1 tons. The dimensions of Tower I are shown in figure 3.1 (Lomas, 1993). The second tower (Tower II) has a total height of 29.6 m, a base width of 7.1 m and a weight of 7.0 tons. The shape of Tower II is shown in figure 3.2. All the base points of both towers are assumed to be totally fixed at the foundation level. Maeno et al. (1984) showed that this assumption resulted in frequencies of vibration that agreed with experimental results.

In this analysis, the tower members are modelled using truss elements. It was shown by Kotsubo et al. (1983) that it is sufficient to model the tower using truss elements. They

concluded that good accuracy in both the free and forced vibration responses can be achieved by using plane truss elements to model the tower members.

A free vibration analysis is carried out to determine the first three transverse natural frequencies and mode shapes of the two towers. The analysis is performed using the SAP IV computer program which is a general purpose finite element program for the linear static and dynamic analysis of structures. The first three frequencies of Tower I were found to be 1.8 Hz, 8.5 Hz, and 14.7 Hz. The first three mode shapes of this tower are shown in figure 3.3. The first three transverse natural frequencies of Tower II were found to be 3.5 Hz, 12.8 Hz, and 18.0 Hz. The mode shapes of Tower II are similar in shape to those of Tower I showed in figure 3.3, which are the first three mode shapes of a cantilever.

The frequency response relationships of transmission Towers I and II are shown in figures 3.4 and 3.5, respectively. The towers are subjected to a sinusoidal ground acceleration with different frequencies and the maximum response of the point of cable suspension (X) is plotted against the excitation frequency. The ground acceleration is scaled to a peak value of 0.34 g to represent the city of Victoria in Canada according to the National Building Code of Canada (NBCC, 1995). Damping ratio of the tower is assumed to be 2% for all modes. Figures 3.4 and 3.5 show that the tower response to the transverse excitation is mainly dominated by the first mode which agrees with the conclusions of Suzuki et al. (1992).

The seismic analysis of a free standing tower is conducted using the PC-ANSR computer program. The two towers are subjected to the horizontal and vertical components of the six selected ground motion records listed in table 2.1 with different A/V ratios. The

ground motion records are scaled to a peak ground acceleration of 0.34 g. The maximum displacement of the cable suspension point (X) and the maximum internal forces in Tower I members due to horizontal excitation are given in tables 3.1 and 3.2, respectively for the case of a free tower. The results of the seismic response of Tower II due to horizontal excitation are shown in tables 3.3 and 3.4 for the case of a free tower.

The results of tables 3.1 to 3.4 indicate that the transverse component of ground motion can cause significant internal forces in the transmission tower specially for Tower I. For example, the maximum force in Tower I members is about 253.2 kN when subjected to the horizontal component of the Monte Negro earthquake. For Tower II, the maximum force is about 95.4 kN and it results from the Monte Negro earthquake as well. The maximum internal forces in both towers were in the lower part of the tower leg for all the earthquake ground motion records used in the analysis. The displacement of the cable suspension point in Tower I is much larger than in Tower II. The maximum displacement in Tower I is 12.9 cm due to the Monte Negro earthquake, while the maximum displacement in Tower II is 2.6 cm for the same earthquake.

The results of the seismic response of the two towers due to vertical excitation are shown in tables 3.5 to 3.8. These tables indicate that both the vertical displacement of tower points (tables 3.5 and 3.7) and the internal forces in tower members (tables 3.6 and 3.8) are small and insignificant.

Figures 3.6 and 3.7 show the transverse displacement time history of the cable suspension point due to the horizontal component of various earthquakes in Tower I and Tower II, respectively. The fundamental frequency of vibration of this point is relatively high

(1.8 Hz for Tower I and 3.5 Hz for Tower II) as compared to the frequencies of vibration of the cable (0.16 Hz to 0.51 Hz for Cables I to III as shown in Chapter 2). This observation suggests that the fundamental frequencies of the transmission tower and the cables are widely separated.

3.3 SEISMIC RESPONSE OF TRANSMISSION LINES

To analyze the response of transmission lines during earthquakes, an intermediate span of the line is selected for the analysis as shown in figure 3.8. The analysis of an end span transmission line can be carried out in a similar way to this investigation. The analysis is applied to the Cable-Tower I and Cable-Tower II systems. In this analysis the typical span is chosen to be typically 400 m unless otherwise stated. The cable used in this analysis is Cable I with EA = 55 x 10^6 N and mass / unit length = 22.23 N/m. Damping ratio of the cable is selected as 1% while the damping ratio of the tower is selected to be 2%. Both values are considered typical for transmission lines.

In the present chapter, it is assumed that the same ground motion component is applied at all the base points of all the transmission towers. The effect of multiple support excitation on the seismic response of transmission lines will be addressed in Chapter 4. Only the effect of the transverse and vertical ground motion components on transmission lines are taken into account. The longitudinal excitation has been shown earlier to have only a very limited effect on cable vibration and cable tension and therefore, it is not considered in the analysis.

The PC-ANSR computer program is used in the dynamic analysis of the transmission line. The time step is taken equal to 0.005 s which was found to be small enough to achieve convergence of the solution. Each cable is divided into 32 finite elements. The number of theses elements was established to accurately model the dynamic behaviour of the cable. The tower is modelled by truss elements. The base points of the transmission tower are assumed fixed at the foundation level.

The transmission lines response to transverse excitation are shown in tables 3.1 to 3.4. The results are presented in terms of the maximum displacement of point (X) in the transmission tower (figures 3.1 and 3.2), the maximum displacement of the cable mid-point, the maximum force in the tower, and the maximum tension in the cable. Similar results are presented for the vertical component of ground motion in tables 3.5 to 3.8. In tables 3.1 to 3.8, the response of a single cable with the ground motion applied directly at both ends is compared to the response of the same cable in a cable-tower transmission line system.

The results of the analysis indicate that the transverse excitation can have a significant effect on the cable vibration. Earthquakes with low A/V ratio such as the Mexico and the San Fernando earthquakes, cause the largest displacement in the cable for both types of towers. For example, the maximum transverse displacement in the cable mid-point is 209.8 cm due to the Mexico earthquake.

The cable tension due to transverse excitation is insignificant as the maximum value is only 2.7 kN which is small as compared to the value of the static tension due to its own weight (37.1 kN). The tension in the cable is almost constant throughout the cable span. The maximum internal force in tower members is 229.0 kN in tower I due to the Monte

Negro earthquake. The maximum force occurred in the lower part of the tower leg. These seismic forces in the tower will be compared later to the design forces of the tower due to wind and ice loads.

In the vertical direction, the maximum cable displacement for Tower I can be as much as 150.8 cm for the Mexico earthquake. The tower forces due to vertical excitation are generally small and insignificant. However, The maximum cable tension due to vertical ground motion may be significant. The tension in the cable resulting from the vertical component of the Mexico earthquake is about 17.1 kN which represents 46% of the tension in the cable due to its own weight.

3.3.1 Modelling of Transmission Lines for Seismic Analysis

The purpose of this section is to propose a simplified model for the transmission lines in order to analyze their seismic response. In tables 3.1 to 3.8, the results of the analysis performed on a single cable fixed at both ends are compared to those of a transmission line system as shown in figure 3.8. The forces and displacement of a tower in a cable tower system are compared to those of a free standing tower in tables 3.1 to 3.8.

3.3.1.1 Transverse excitation

The envelopes of the maximum cable displacement due to transverse excitation are shown in figures 3.9 and 3.10 when using Tower I and Tower II, respectively. These figures along with tables 3.1 and 3.3 show that the effect of the transmission tower on cable vibrations is not significant. Earthquakes with low A/V ratio cause large displacement in the

cable while the tower is moving as a rigid body. The reason for this is that the frequency content of the records with low A/V ratio is much less than the tower's fundamental frequency.

Earthquakes that have a strong effect on the tower such as the Monte Negro earthquake, cause insignificant cable displacement due to the decoupling of the frequencies of free vibration of the cable and the tower in the transverse direction (figures 3.9d and 3.10d).

By comparing the resulting forces in a free tower with the forces in the tower in a transmission line system given in table 3.2 for Tower I, some differences are observed. The maximum difference in internal forces is approximately 17% for the Imperial Valley earthquake. For Tower II, the maximum difference in tower forces is much smaller as indicated from table 3.4. The maximum cable tension due to transverse excitation is insignificant and the change in cable tension is therefore insignificant. On the basis of these results and observations, the intermediate spans of a transmission line can be modelled in the transverse direction by separate cables fixed at both ends. This simplification yields excellent results especially in cable displacement calculations. The tower forces calculated from a free standing tower model are within a maximum difference of only 17% from the force in the towers of a transmission line system. These observations agree with the conclusions of Kotsubo et al. (1983) who found that the dynamic interaction between cables and towers is weak and that the effect of cables on the natural frequencies of the tower may be neglected.

3.3.1.2 Vertical excitation

The envelopes of the maximum cable displacement due to the vertical component of ground motion are shown in figures 3.11 and 3.12 when using Tower I and Tower II in the analysis of the transmission line system, respectively. Tables 3.5 and 3.7 along with figures 3.11 and 3.12 show that the effect of the tower on the cable vibration due to vertical ground motion is insignificant. The tower is very stiff in the vertical direction, and therefore it transmits the ground motion without any change to the cable suspension point. Tables 3.6 and 3.8 show that the cable tension is not affected by the existence of the towers. Comparing the force in the tower for the case of a free tower with the force in a tower in a transmission line system indicates that the tower forces are unaffected by the interaction between the tower and the cables in case of vertical excitation. A free standing tower is a good model to obtain the forces in the tower due to vertical ground motion.

3.3.2 Effect of Cable Insulator on the Seismic Response of Transmission line

Cables are connected to transmission towers by insulators. The insulators are usually designed to withstand extreme and sudden temperature changes, rain, smoke, dust, and chemical fumes without chemical, deterioration, mechanical or electrical failure. Suspension insulators are a class of insulators that is used widely for all type of transmission lines specially high voltage lines. Under transverse ground motion, the insulators will swing in the out-of-plane direction and thus affecting the cable vibration. However, under vertical excitation it is expected that the cable vibrations will not be affected by the existence of the insulators. In this section, the effect of the insulators on cable vibration is analyzed.

A porcelain suspension insulator is selected for the analysis with an average diameter of 4.0 cm and a modulus of elasticity $E = 10^4$ MPa. Two different lengths are selected for the insulator, 2.0 m to be used for high voltage transmission lines and 1.0 m for low voltage transmission lines.

The transmission line model shown in figure 3.13 is used with Tower I in this analysis. The only difference between this model and the model given in figure 3.8 is the existence of the suspension insulator. The insulator is modelled by a linear truss element. The transmission line is subjected to the horizontal and vertical components of the 1985 Mexico and the 1971 San Fernando earthquakes. These two specific earthquakes are selected because they cause the maximum response in the transmission line.

The maximum displacements of the cable as well as the maximum tension in the cable are presented in tables 3.9 and 3.10 for transverse and vertical excitations, respectively. These tables show that for transverse excitation, the cable tension is not affected significantly by the presence of the suspension insulators. For vertical excitation, the presence of the suspension insulator does not have any effect on the cable displacement or tension.

Figures 3.14 and 3.15 show the displacement time history of the cable mid-point due to the horizontal component of the Mexico and the San Fernando earthquakes, respectively. It is noted that the displacement time history of the cable mid-point is affected by the presence of the insulators. The main reason for this is the swinging motion of the insulator. This effect increases with the increase in the insulator length. However, the maximum value of the cable displacement as shown in figures 3.14 and 3.15 and table 3.9 is not affected significantly by

the insulator. In the vertical direction, the displacement of the cable is unaffected by the presence of the insulator as shown in figure 3.16.

3.4 COMPARISON BETWEEN WIND AND EARTHQUAKE EFFECTS

Transmission lines are designed in the transverse and vertical directions for the dead load in addition to wind and ice loads (Kravitz, 1982, for example). None of the codes used to design transmission lines contains seismic provisions. The relative importance of wind / ice and earthquake loads in transmission line design is a complex issue. The relative importance of loads in design depends on the wind and seismic zones where the transmission line is to be constructed.

In this section an attempt is made to compare between the design forces in the transmission towers due to wind and earthquake loads. It is proposed that in seismic analysis of transmission lines, the main concern is the large cable displacement which may cause the cables to touch each other. In this section, line forces due to earthquake loads will be compared with the design code provisions for wind and ice loads.

3.4.1 Code Specifications

Some of the specifications available for the design of transmission lines include the "Guidelines for Transmission Line Structural Loading " prepared by the Committee on Electrical Transmission Structures of the Structural Division of the American Society of Civil Engineers (ASCE, 1991) and the State of the art report " Wind Loading and Wind-Induced Structural Response" by the Committee on Wind Effects (1987). In this analysis the design

procedure for transmission lines of the "National Electrical Safety Code ", (NESC, 1993) is used. The NESC code considers the dead load and the combination of ice and wind loads for the design of transmission lines in the vertical and transverse directions. Loads from conductor breakage are included in the design in the longitudinal direction.

3.4.2 Design Procedure

According to the NESC (1993) code, two critical wind loading conditions should be considered in the vertical and transverse directions of transmission lines. The first load condition is the combined wind and ice loading on transmission lines (Case I). The second load condition is the extreme wind loading on the transmission line system without ice (Case II).

For the combined wind and ice loads, the United States is divided into three districts according to the ice conditions. Table 3.11 shows the minimum radial ice thicknesses and the horizontal wind pressure to be used in load calculation for each district. According to this table, the country is divided into three districts of heavy, medium, and light ice loadings as shown in figure 3.17 (NESC, 1993). The design loads on cables are increased by the factors given in table 3.11 to take into consideration the wind and ice loads. The values of extreme wind pressure (Case II) are based on the 50 year isotachs. The contours of extreme wind speeds in miles per hour are shown in figure 3.18 (NESC, 1993). These values of wind speeds can be converted into wind pressures using the following relations (NESC, 1993):

pressure in lb/ft^2 $= 0.00256\,(v_{miles/h})^2$

or pressure in Pascals $= 0.613\,(v_{m/s})^2$ (3.1)

The vertical loads on the towers include their dead weight, the weight of cables, insulators, and ice on cable. Transverse loading on transmission towers consists of two components: transverse loading from the conductor and transverse loading from the tower itself. The transverse loading from the conductor is calculated according to table 3.11 for all the conductors carried by the transmission tower if their number is less than 10. The transverse loading on the tower itself is calculated using the wind pressure values in table 3.11 acting on the tower face without ice covering and applying a shape factor of 2.0 for cylindrical members and 3.2 for flat surfaced members (NESC, 1993). The total load, however, should not exceed the load which would occur on a solid structure with the same outside dimensions.

Overload capacity factors are used in the design of transmission lines for the case of combined wind and ice loading as an added design safety. Values of these factors depend on the kind of load under consideration and the grade of construction. The overload capacity factors for metal towers specified by the NESC (1993) are listed in table 3.12. For the extreme wind loading case, this factor is 1.0 for the supporting towers. In the current analysis the forces due to earthquake ground motion will be compared to the forces due to the code specified loads without using the overload capacity factors. This is because earthquakes induced forces may be subjected to overload capacity factors as well.

3.4.3 Evaluation of Combined Wind and Ice Loading (Case I)

Wind loading is calculated for the transmission line system shown in figure 3.8 using Tower I. The loads on the tower are divided into loads from the conductors and loads from the tower itself. The total loads are the summation of both cases

3.4.3.1 Loads from the conductors

The loads are calculated for a range of different parameters to check the effect of their variation on the maximum forces in the tower members. The cable diameter is varied from 2.0 cm to 3.5 cm and the typical span of the line is taken to range from 300 m to 500 m. The number of cables hanging on an intermediate tower is 6 from each side. Internal forces in tower members are shown in table 3.13 for different loading districts. As expected, the maximum internal forces are in the heavy ice loading district. In all loading combinations, the maximum force resulted in the lower part of the tower leg.

From the maximum forces in the medium and heavy ice loading districts, the span of the line has a more substantial effect on the forces than the cable diameter. However, in the light ice loading district both the cable diameter and the line span have effects of the same order of magnitude on the forces in the transmission tower members.

3.4.3.2 Loads from the tower itself

The load on the tower face is calculated for a latticed steel tower with flat surface members which means that the shape factor equals to 3.2 (NESC, 1993). To calculate the load for a general tower, the shape of the tower side face is assumed to be triangular with

equals to 41.6 m and a variable base width and solidity ratio. The base width is varied from 7.5 m which represents a square base to 6.5 m, while the solidity ratio is varied from 0.05 to 0.20. Values of the maximum forces in tower members are shown in table 3.14 for different ice loading districts.

Comparing tables 3.13 and 3.14 shows that in the light ice loading district, both the wind on the cables and the wind on the tower produce forces in the tower members of the same order of magnitude. However, in the medium and heavy ice loading districts, the wind on cables produces forces in the tower members that are much larger than the wind on the tower itself. The reason is that according to the NESC (1993) the ice covering is considered only on the cables and not on the tower itself.

3.4.4 Evaluation of Extreme Wind Loading (Case II)

On the map shown in figure 3.18, the extreme wind speed in each zone in the United States is indicated. The minimum value of wind pressure using equation (3.1) is 0.60 kPa in the Los Angeles area and the maximum value is 1.48 kPa in the south-east of the United States. The maximum values of forces in tower members due to an extreme wind pressure of 0.60 kPa are shown in tables 3.15 and 3.16 due to wind on the cables and on the tower, respectively. Since the problem under consideration is a linear problem, then for any value of wind pressure higher than 0.60 kPa, the internal forces in tower members are linearly proportional to the value of wind pressure.

3.4.5 Numerical Example

A numerical example is chosen to compare between the wind and earthquake effects on transmission lines. The base width is taken equal to 7.5 m to represent a tower with a square base and the solidity ratio is chosen equal to 0.15 which is a reasonable value for transmission towers. Two values of cable diameters are selected: 3.5 cm and 2.0 cm to represent heavy cables and light cables, respectively. The cable span is varied from 300 m to 500 m.

For seismic analysis, the Imperial Valley earthquake is used because it produces the largest forces in tower members next only to the Monte Negro earthquake as shown previously in table 3.2 This event has the advantage of being a California earthquake and represents a more realistic earthquake loading for towers in the California area.

The horizontal component of the Imperial Valley earthquake has a peak ground acceleration of 0.35 g. In the analysis, the earthquake is used once without scaling, then it is scaled to peak ground accelerations of 0.2 g and 0.5 g to cover a range of possible earthquakes. The maximum forces in tower members due to the Imperial Valley earthquake for various span lengths of the transmission line are given in tables 3.17 and 3.18 for cable diameter equal to 3.5 cm and 2.0 cm, respectively. From the forces shown in tables 3.17 and 3.18, it is observed that the change in the tower force due to the difference in line span and cable diameter is insignificant.

A comparison between the maximum forces in tower members due to different load combinations for cable diameter of 3.5 cm and 2.0 cm, is shown in figures 3.19 and 3.20, respectively. Two values of extreme wind pressure are used in this analysis, 0.60 kPa and

0.78 kPa (13 lb/ft^2 and 16 lb/ft^2, respectively). In this comparison, the overload capacity factor for the case of combined wind and ice loading is not used. The earthquake load used in this figures is the Imperial Valley earthquake without scaling.

From the data shown in figures 3.19 and 3.20, it is observed that the code specified loads are not always the critical loads for the design of transmission towers and that the forces due to earthquake loading may exceed those due to wind loading. For smaller cable diameters and smaller line spans, the earthquake loading becomes more critical than the wind loading. In the light and medium ice loading districts for the case of combined wind and ice loading, the earthquake loading may become more significant than the wind loading.

Consider a specific example for a transmission line in the area of Los Angeles where the extreme wind pressure is 0.60 kPa and the area is in the light ice loading district. For the case of a small cable diameter (2.0 cm), the force induced in the tower due to wind loading is smaller than the force induced in the tower by the Imperial Valley earthquake.

3.5 SUMMARY

In this chapter, the dynamic behaviour of transmission towers is analyzed, then their seismic response is evaluated. The seismic behaviour of transmission lines is evaluated and a simplified model for the analysis of the line when subjected to earthquake ground motion is presented. The forces in tower members due to earthquake loading are compared to the forces caused by the design loads in the National Electrical Safety Code (NESC, 1993).

The following conclusions are arrived at from the analysis:

1. The displacement of tower points due to transverse excitation is governed by the first mode.
2. The transverse excitation can have a significant effect on the tower forces, while the vertical excitation does not produce any significant forces in tower members.
3. The contribution of the towers to the seismic performance of transmission lines can be neglected. For simplicity, the line can be modelled by cables fixed at both ends.
4. The forces developed in tower members due to seismic loading can exceed the loads developed by wind and ice loads and extreme wind loads particularly for smaller cable diameters and for shorter spans.

Table 3.1 Maximum displacement response of transmission lines with Tower I due to transverse excitation

Event	Tower displacement (cm)		Cable mid-point displacement (cm)	
	Free tower	Transmission line	Single cable	Transmission line
Mexico	6.0	5.7	205.9	209.8
San Fernando	5.2	4.6	95.7	97.9
Monte Negro	12.9	11.6	27.5	33.7
Imperial Valley	9.5	7.8	45.4	47.1
Parkfield	2.1	2.0	8.7	10.9
Lytle Creek	4.8	4.2	4.6	9.3

Table 3.2 Maximum forces of transmission lines with Tower I due to transverse excitation

Event	Tower internal force (kN)		Cable tension (kN)	
	Free tower	Transmission line	Single cable	Transmission line
Mexico	118.3	113.4	2.4	2.7
San Fernando	101.9	88.8	1.6	1.9
Monte Negro	253.2	229.0	0.4	1.6
Imperial Valley	186.9	155.4	0.3	1.4
Parkfield	41.0	39.7	0.3	0.4
Lytle Creek	92.1	85.2	0.2	0.6

Table 3.3 Maximum displacement response of transmission lines with Tower II due to transverse excitation

Event	Tower displacement (cm)		Cable mid-point displacement (cm)	
	Free tower	Transmission line	Single cable	Transmission line
Mexico	2.0	0.7	205.9	207.2
San Fernando	0.7	2.0	95.7	96.4
Monte Negro	2.6	2.6	27.5	27.8
Imperial Valley	1.4	1.3	45.4	45.6
Parkfield	1.6	1.6	8.7	9.0
Lytle Creek	1.9	4.2	4.6	4.7

Table 3.4 Maximum forces of transmission lines with Tower II due to transverse excitation

Event	Tower internal force (kN)		Cable tension (kN)	
	Free tower	Transmission line	Single cable	Transmission line
Mexico	23.4	24.8	2.4	2.4
San Fernando	72.0	73.2	1.6	1.7
Monte Negro	95.4	94.8	0.4	0.6
Imperial Valley	42.4	42.2	0.3	0.4
Parkfield	65.4	65.4	0.3	0.4
Lytle Creek	54.6	54.8	0.2	0.4

Table 3.5 Maximum displacement response of transmission lines with Tower I due to vertical excitation

Event	Tower displacement (cm)		Cable mid-point displacement (cm)	
	Free tower	Transmission line	Single cable	Transmission line
Mexico	0.2	0.3	150.9	150.8
San Fernando	0.2	0.3	31.5	31.7
Monte Negro	0.2	0.3	14.6	14.9
Imperial Valley	0.2	0.3	8.5	8.8
Parkfield	0.2	0.3	7.4	7.6
Lytle Creek	0.2	0.3	3.9	4.2

Table 3.6 Maximum forces of transmission lines with Tower I due to vertical excitation

Event	Tower internal force (kN)		Cable tension (kN)	
	Free tower	Transmission line	Single cable	Transmission line
Mexico	6.0	10.7	17.1	17.1
San Fernando	6.3	6.7	4.4	4.4
Monte Negro	5.8	10.1	2.1	2.1
Imperial Valley	8.4	12.8	1.7	1.7
Parkfield	6.4	10.8	1.1	1.1
Lytle Creek	7.5	11.8	0.7	0.7

Table 3.7 Maximum displacement response of transmission lines with Tower II due to vertical excitation

Event	Tower displacement (cm)		Cable mid-point displacement (cm)	
	Free tower	Transmission line	Single cable	Transmission line
Mexico	0.1	0.1	150.9	150.9
San Fernando	0.1	0.1	31.5	31.5
Monte Negro	0.1	0.1	14.6	14.7
Imperial Valley	0.1	0.1	8.5	8.6
Parkfield	0.1	0.1	7.4	7.4
Lytle Creek	0.1	0.1	3.9	4.0

Table 3.8 Maximum forces of transmission lines with Tower II due to vertical excitation

Event	Tower internal force (kN)		Cable tension (kN)	
	Free tower	Transmission line	Single cable	Transmission line
Mexico	3.1	3.7	17.1	17.1
San Fernando	2.6	3.8	4.4	4.4
Monte Negro	2.1	3	2.1	2.1
Imperial Valley	4.3	6.1	1.7	1.7
Parkfield	2.9	4.4	1.1	1.1
Lytle Creek	3.1	3.9	0.7	0.7

Table 3.9 Effect of the suspension insulator on cable response to transverse excitation

Event	Maximum cable tension (kN)			Maximum cable displacement (cm)		
	No suspension	Suspension length = 1.0 m	Suspension length = 2.0 m	No suspension	Suspension length = 1.0 m	Suspension length = 2.0 m
Mexico	2.7	2.9	3.0	209.8	178.1	182.5
San Fernando	1.9	1.7	1.6	97.9	98.1	93.5

Table 3.10 Effect of the suspension insulator on cable response to vertical excitation

Event	Maximum cable tension (kN)			Maximum cable displacement (cm)		
	No suspension	Suspension length = 1.0 m	Suspension length = 2.0 m	No suspension	Suspension length = 1.0 m	Suspension length = 2.0 m
Mexico	17.1	17.1	17.1	150.8	150.8	150.8
San Fernando	4.4	4.4	4.4	150.8	150.8	150.8

Table 3.11 Ice and wind loading factors (NESC, 1993)

	Loading districts (for use in the case of combined wind and ice loading)			Extreme wind loading
	Heavy	Medium	Light	
Radial thickness of ice (mm)	12.5	6.5	0.0	0.0
Horizontal wind pressure (Pa)	190	190	430	see figure 3.18
Additional wind pressure (N/m)	4.4	2.5	0.7	0.0

Table 3.12 Overload capacity factors for metal towers (NESC, 1993)

	Overload capacity factors	
	Grade B construction	Grade C construction
Vertical strength	1.50	1.50
Transverse strength (wind load)	2.50	2.20

Table 3.13 Maximum forces in tower members in kN due to wind on cables (Case I)

(a) Light loading district

Cable diameter (cm)	Cable span (m)		
	300	400	500
2.0	40.8	54.4	67.9
2.5	51.0	67.9	84.9
3.0	61.0	81.4	101.9
3.5	71.2	95.0	118.9

(b) Medium loading district

Cable diameter (cm)	Cable span (m)		
	300	400	500
2.0	63.2	84.5	105.4
2.5	73.0	97.4	121.8
3.0	83.1	110.8	138.3
3.5	93.0	123.8	154.8

(c) Heavy loading district

Cable diameter (cm)	Cable span (m)		
	300	400	500
2.0	92.7	123.1	154.2
2.5	103.3	137.3	172.2
3.0	113.8	152.0	189.7
3.5	124.6	166.2	207.7

Table 3.14 Maximum forces in tower members in kN due to wind on tower (Case I)

(a) Light loading district

Tower base width (m)	Solidity ratio			
	0.05	0.10	0.15	0.20
6.5	15.4	30.9	46.3	61.7
7.0	16.6	33.2	49.9	66.5
7.5	17.8	35.6	53.4	71.2

(b) Medium and heavy loading district

Tower base width (m)	Solidity ratio			
	0.05	0.10	0.15	0.20
6.5	6.8	13.6	20.4	27.2
7.0	7.4	14.8	22.2	29.6
7.5	7.9	15.8	23.7	31.6

Table 3.15 Maximum forces in tower members in kN due to wind pressure of 0.60 kPa on cables (Case II)

Cable diameter (cm)	Cable span (m)		
	300	400	500
2.0	58.6	78.1	97.5
2.5	73.2	97.5	121.9
3.0	87.7	117.0	146.3
3.5	102.3	136.5	170.7

Table 3.16 Maximum forces in tower members in kN due to wind pressure of 0.60 kPa on tower (Case II)

Tower base width (m)	Solidity ratio			
	0.05	0.10	0.15	0.20
6.5	22.2	44.6	66.9	89.1
7.0	24.0	48.0	72.1	96.1
7.5	25.7	51.4	77.1	102.8

Table 3.17 Maximum forces in tower members in kN due to the 1940 Imperial Valley earthquake (cable diameter = 3.5 cm)

Peak ground acceleration (g)	Cable span (m)		
	300	400	500
0.20	113.0	111.2	110.1
0.35	195.4	193.6	191.6
0.50	282.1	277.5	274.6

Table 3.18 Maximum forces in tower members in kN due to the 1940 Imperial Valley earthquake (cable diameter = 2.0 cm)

Peak ground acceleration (g)	Cable span (m)		
	300	400	500
0.20	115.0	112.7	111.2
0.35	197.8	196.5	193.2
0.50	284.0	279.1	277.2

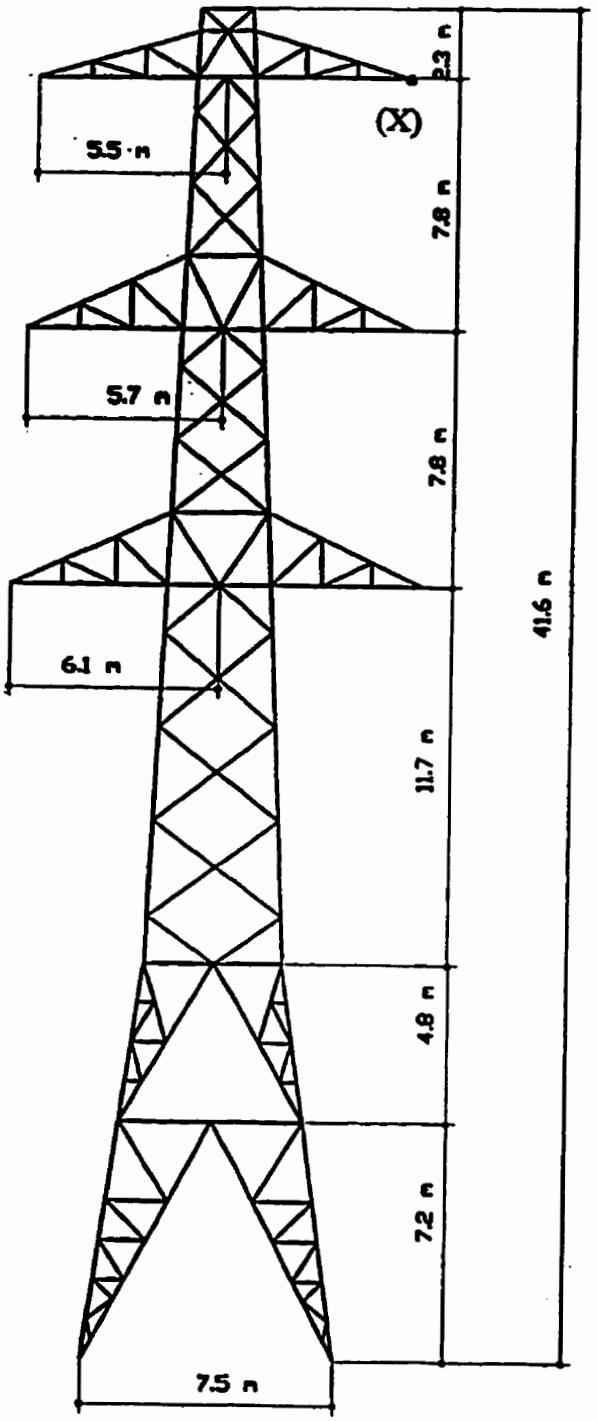

Figure 3.1 Transmission Tower I

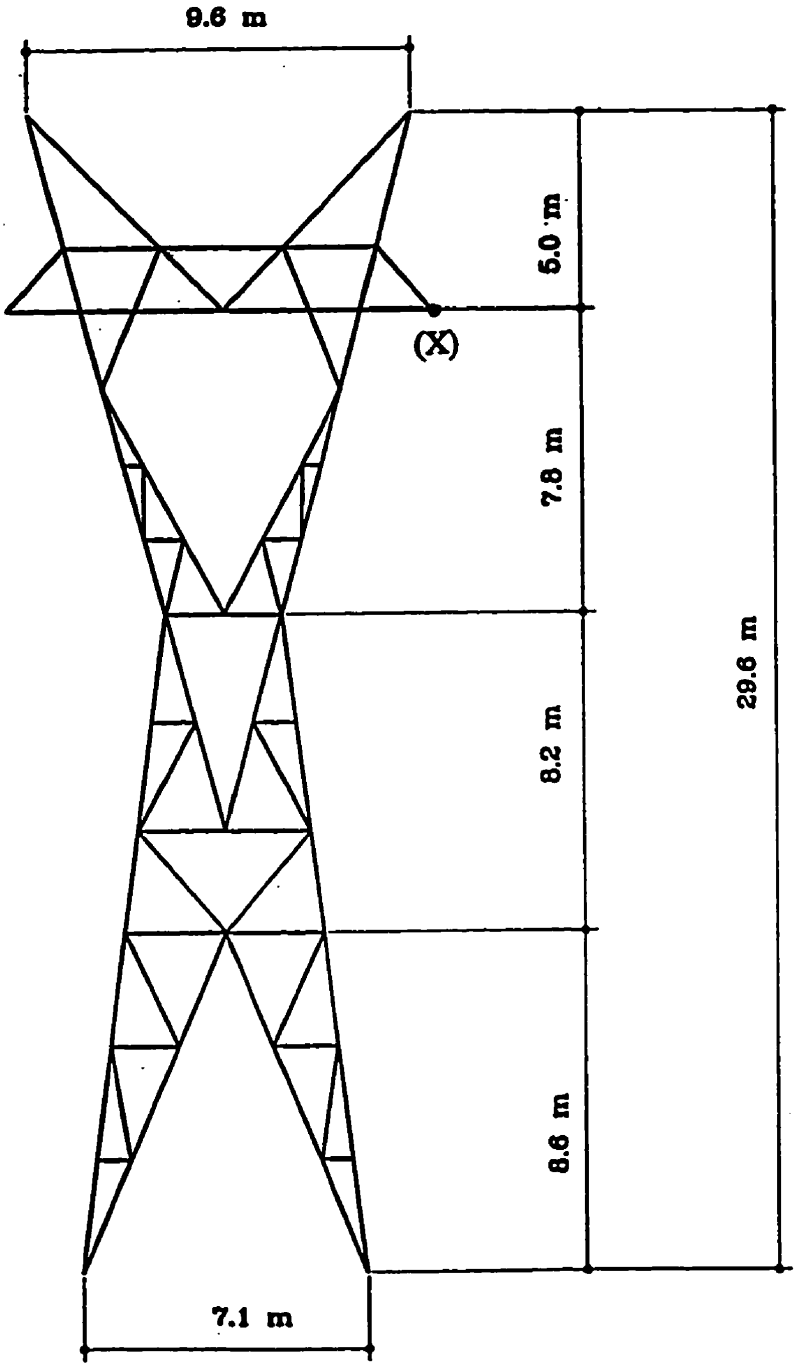

Figure 3.2 Transmission Tower II

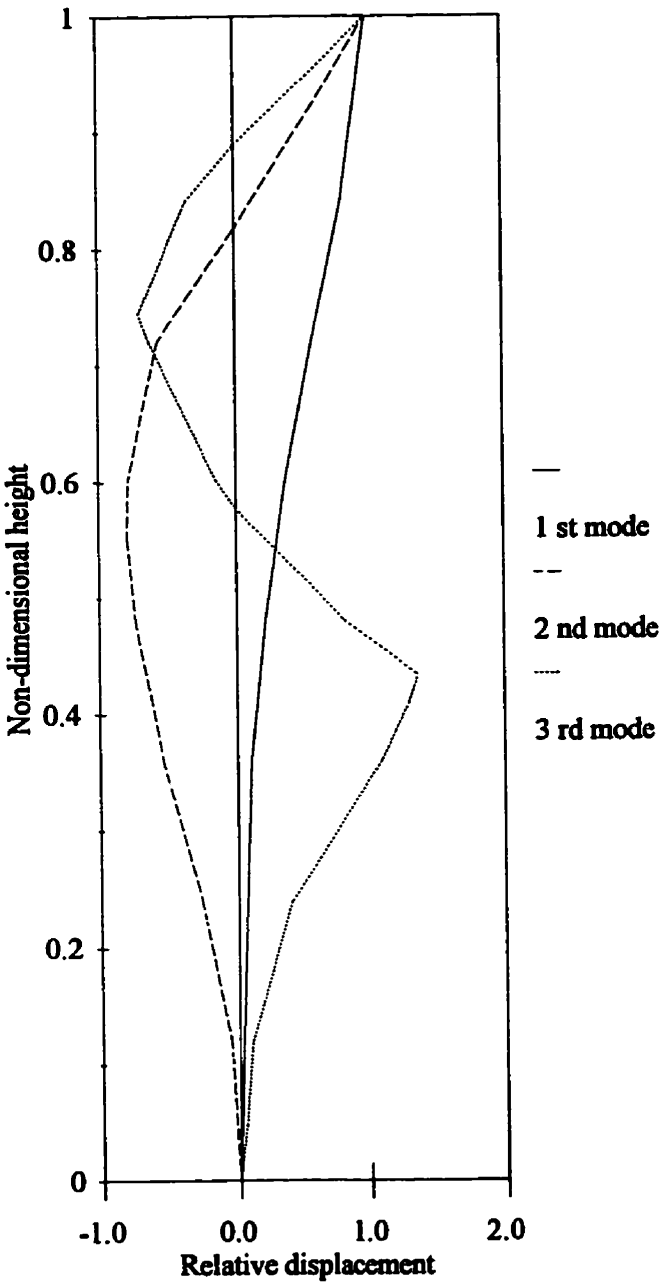

Figure 3.3 First three mode shapes for Tower I and Tower II

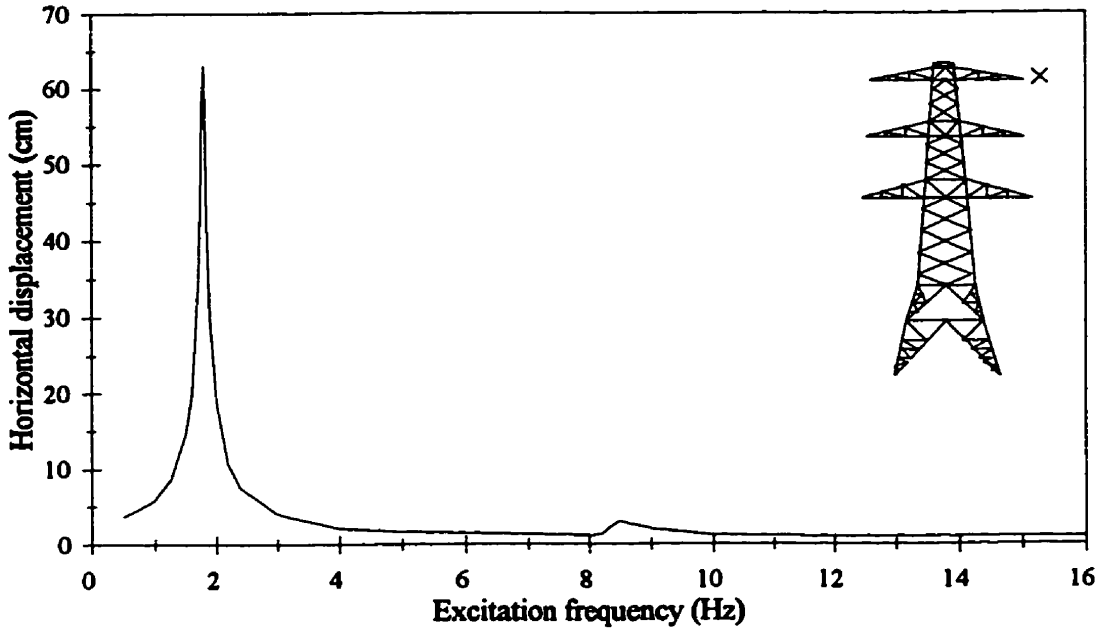

Figure 3.4 Displacement of point (X) in Tower I for different values of excitation frequency

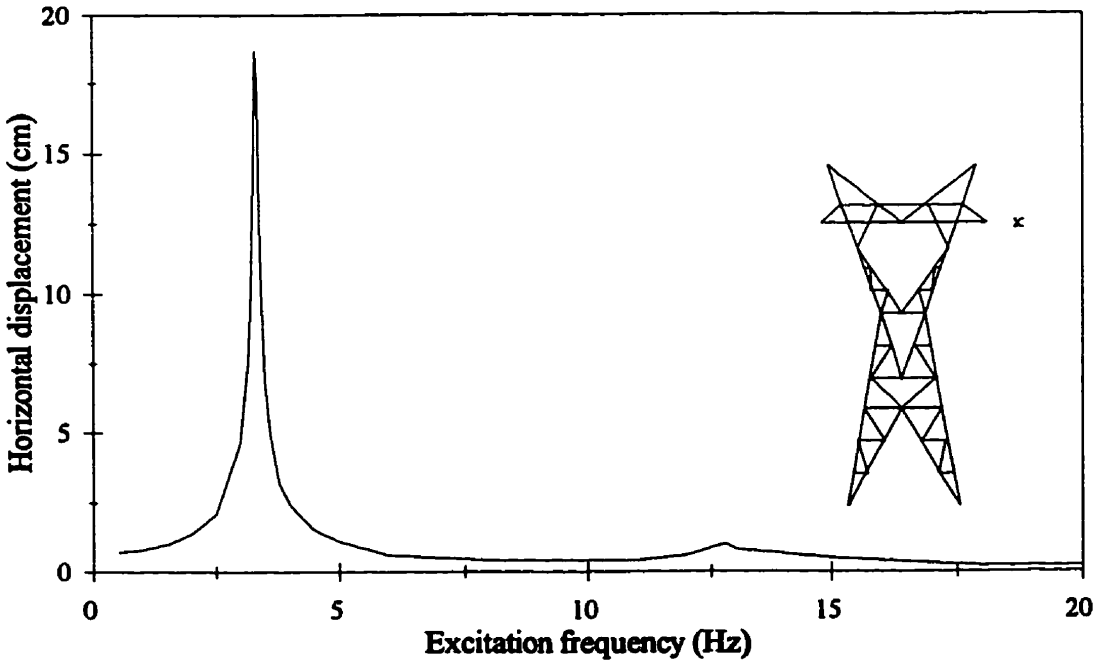

Figure 3.5 Displacement of point (X) in Tower II for different values of excitation frequency

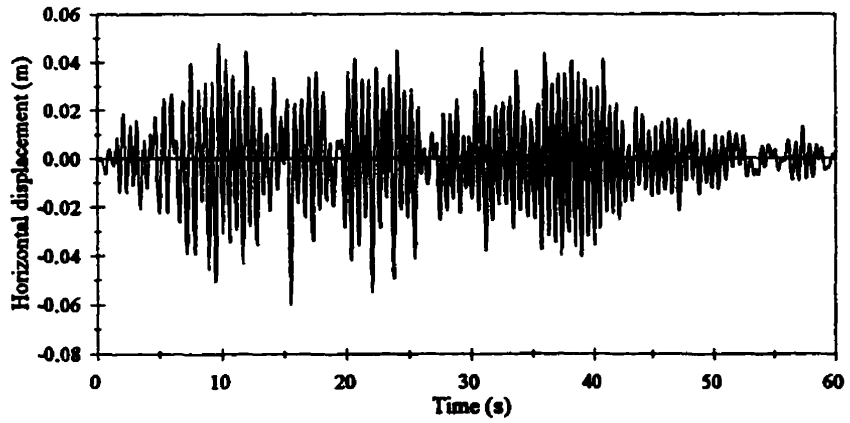

(a) Mexico Earthquake

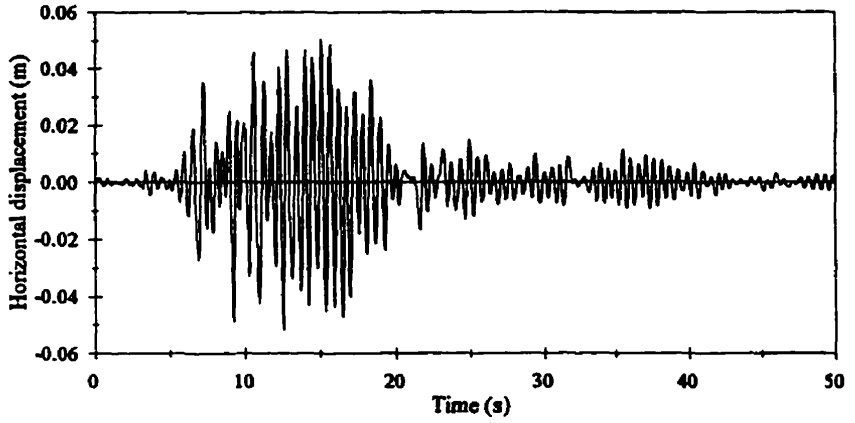

(b) San Fernando Earthquake

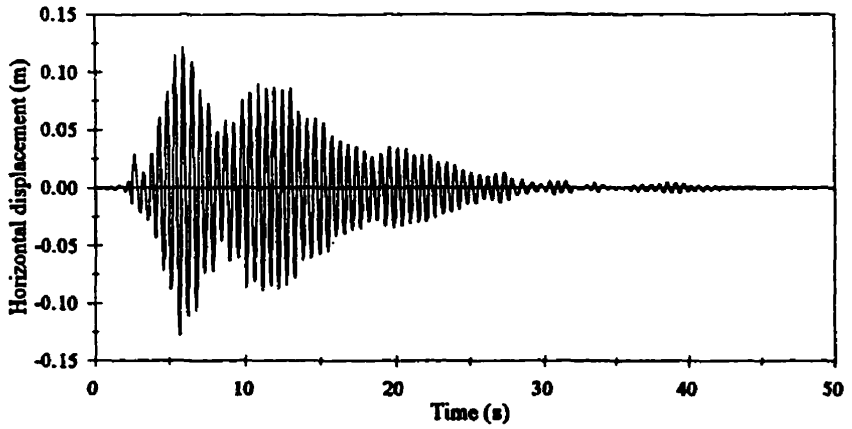

(c) Monte Negro Earthquake

Figure 3.6 Displacement of point (X) in transmission Tower I due to horizontal ground motion

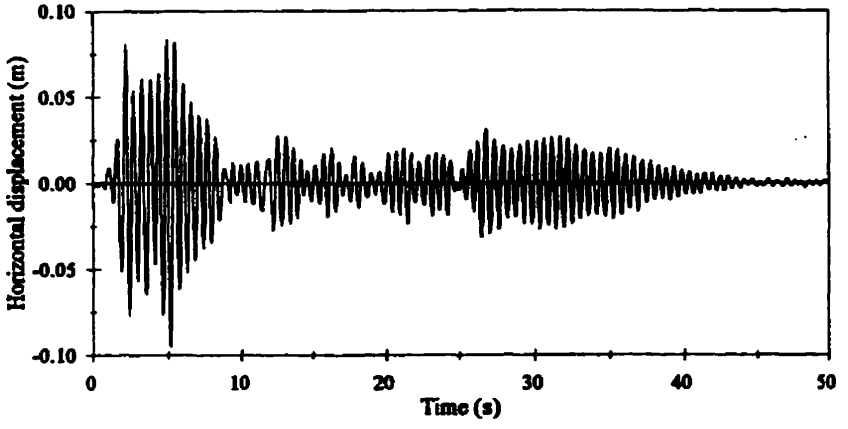

(d) Imperial Valley Earthquake

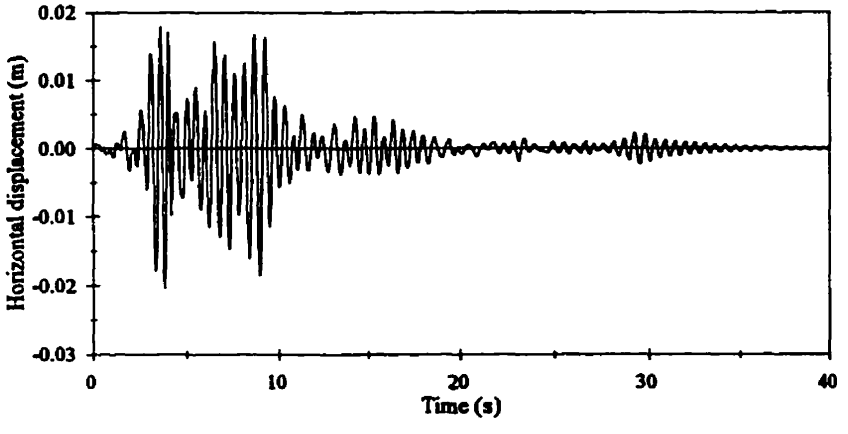

(e) Parkfield Earthquake

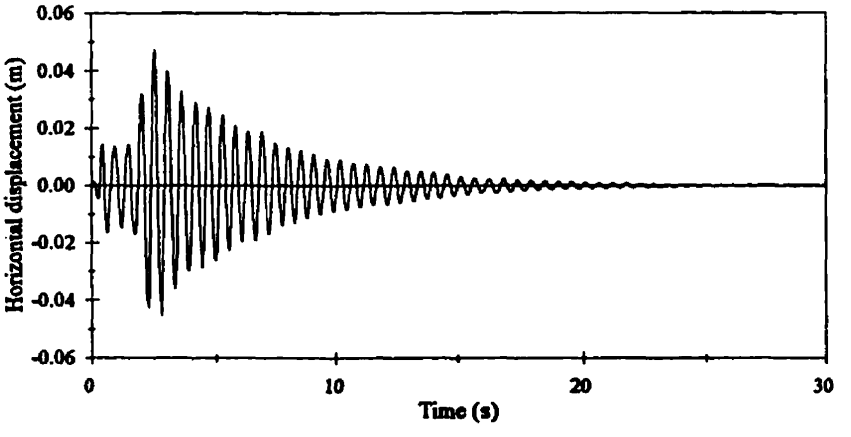

(f) Lytle Creek Earthquake

Figure 3.6 (cont.) Displacement of point (X) in transmission Tower I due to horizontal ground motion

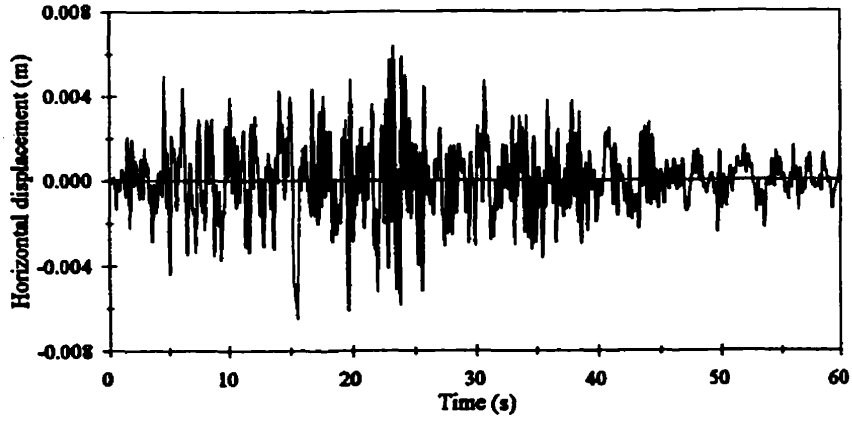

(a) Mexico Earthquake

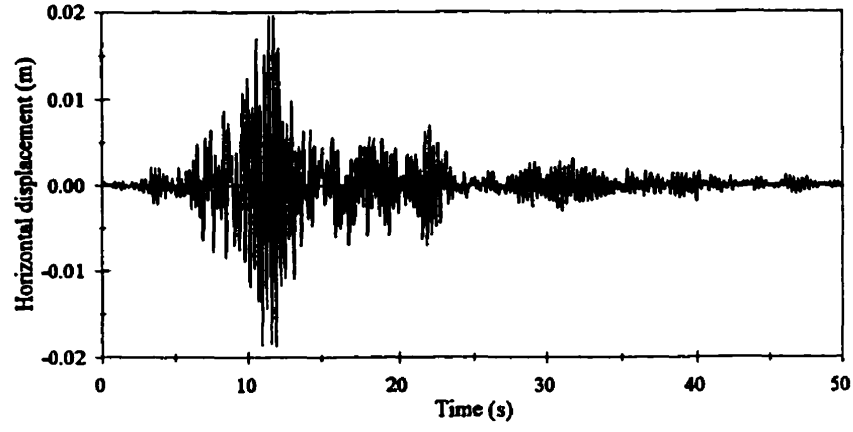

(b) San Fernando Earthquake

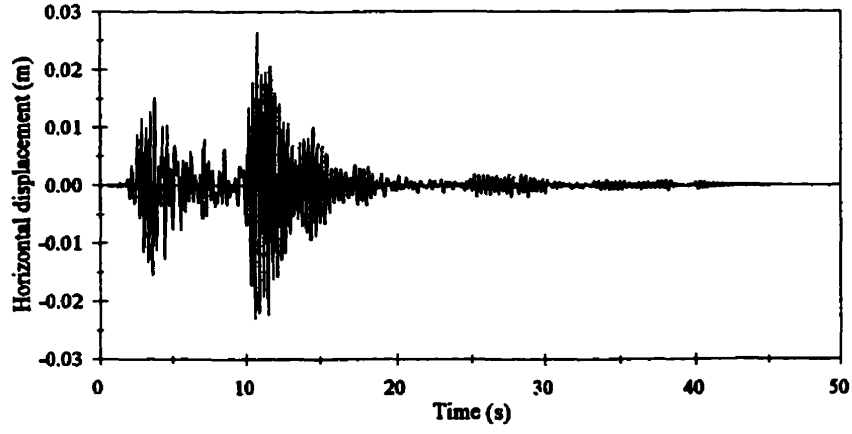

(c) Monte Negro Earthquake

Figure 3.7 Displacement of point (X) in transmission Tower II due to horizontal ground motion

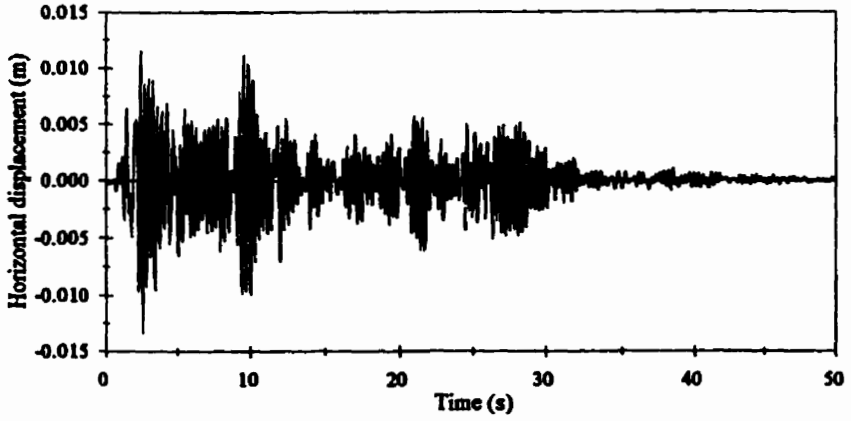

(d) Imperial Valley Earthquake

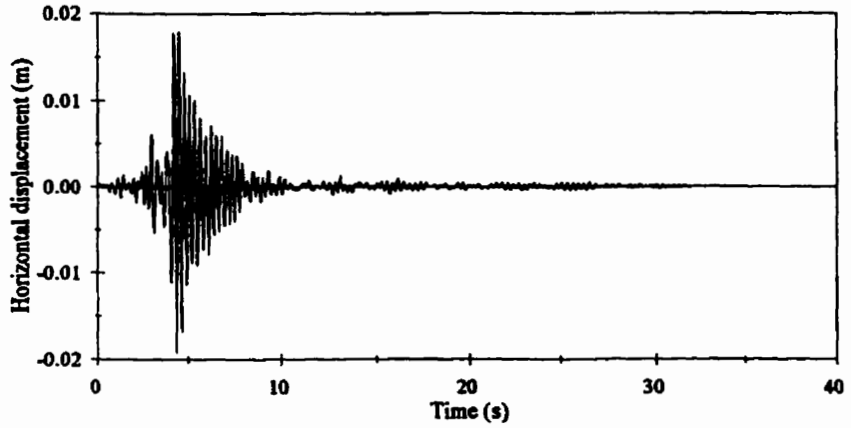

(e) Parkfield Earthquake

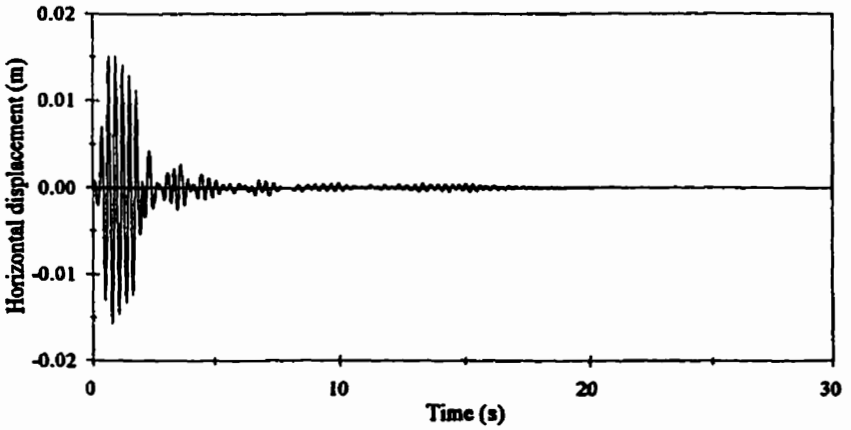

(f) Lytle Creek Earthquake

Figure 3.7 (cont.) Displacement of point (X) in transmission Tower II due to horizontal ground motion

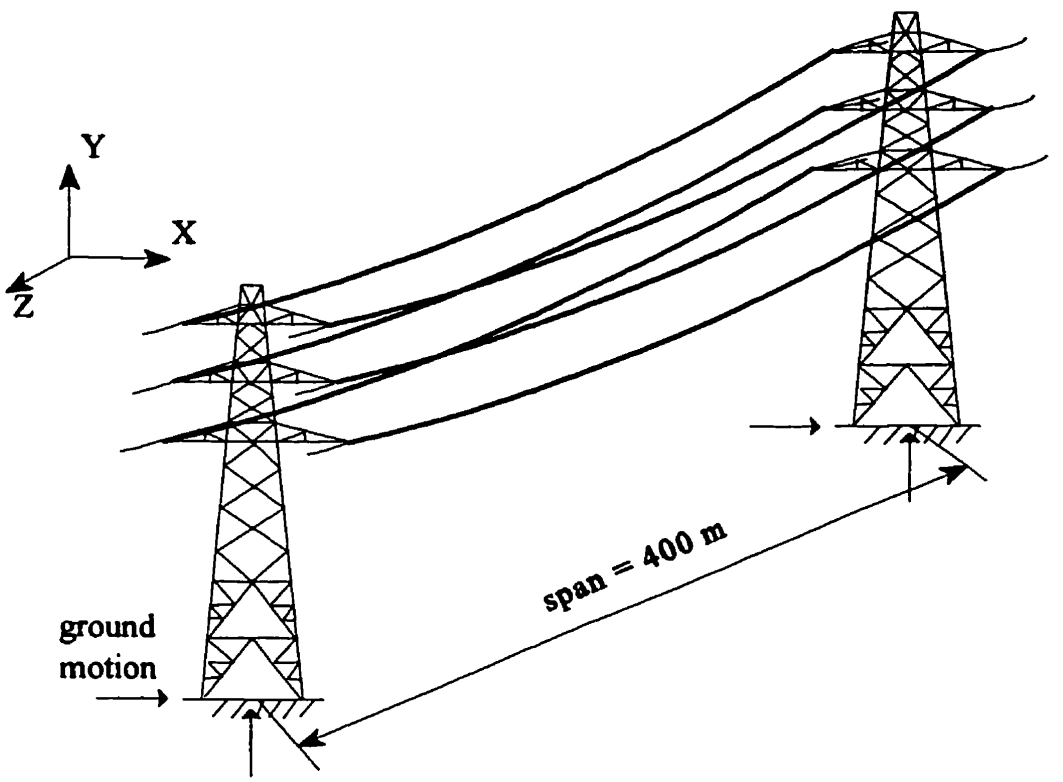

Figure 3.8 Transmission line system

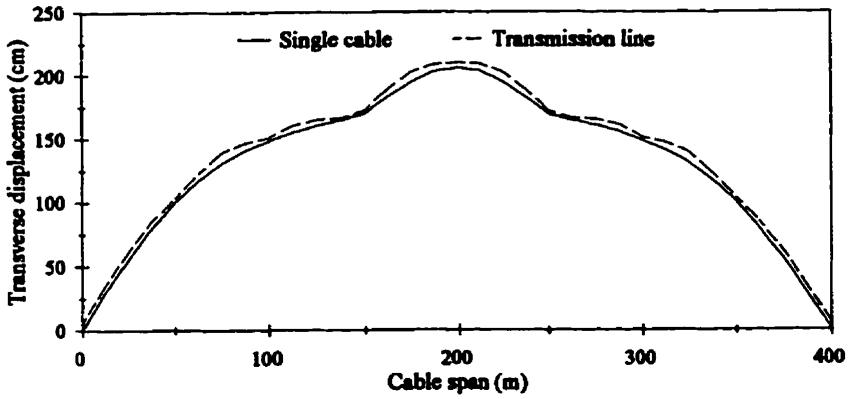

(a) Mexico Earthquake

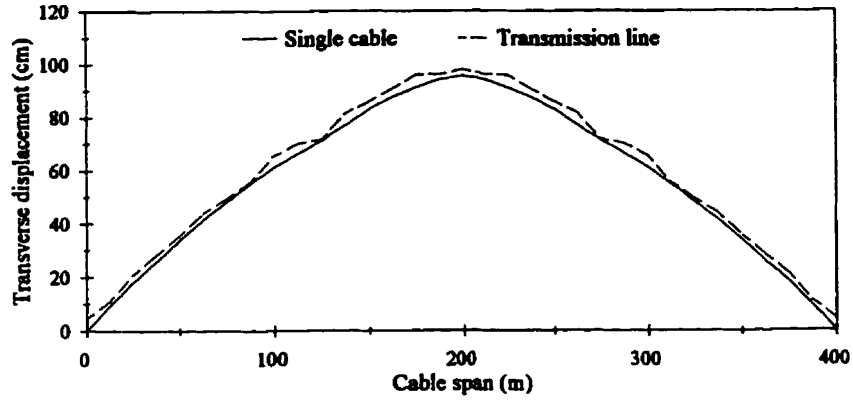

(b) San Fernando Earthquake

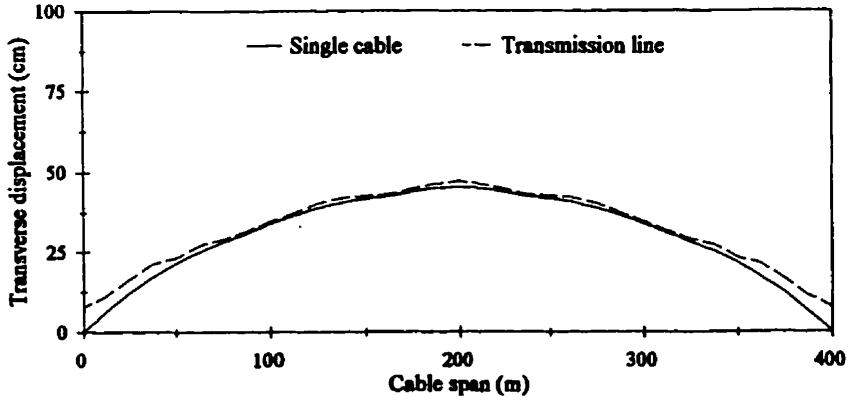

(c) Imperial Valley Earthquake

Figure 3.9 Envelopes of maximum response to transverse excitation for transmission lines with Tower I

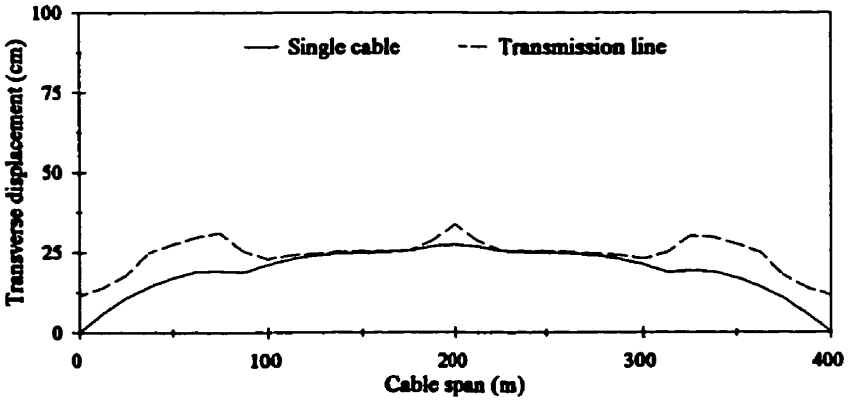

(d) Monte Negro Earthquake

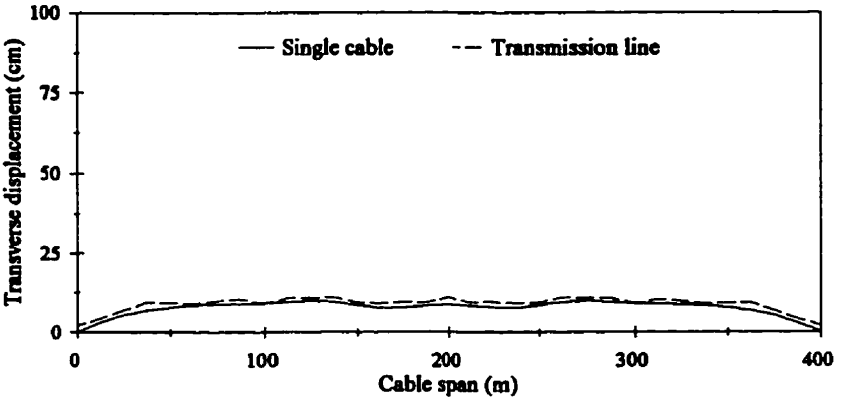

(e) Parkfield Earthquake

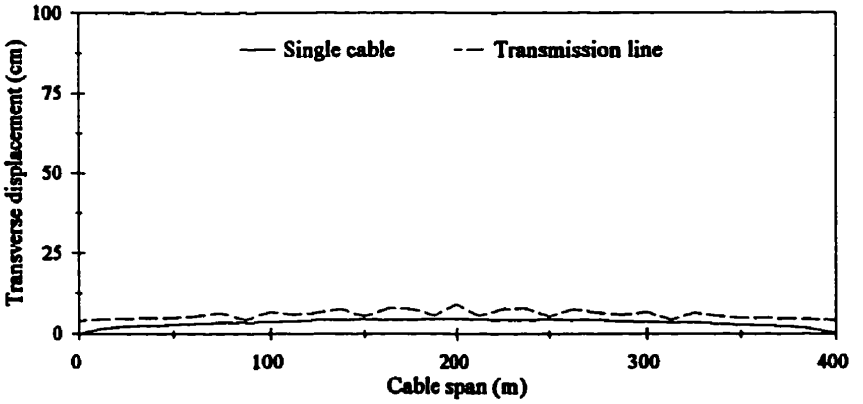

(f) Lytle Creek Earthquake

Figure 3.9 (cont.) Envelopes of maximum response to transverse excitation for transmission lines with Tower I

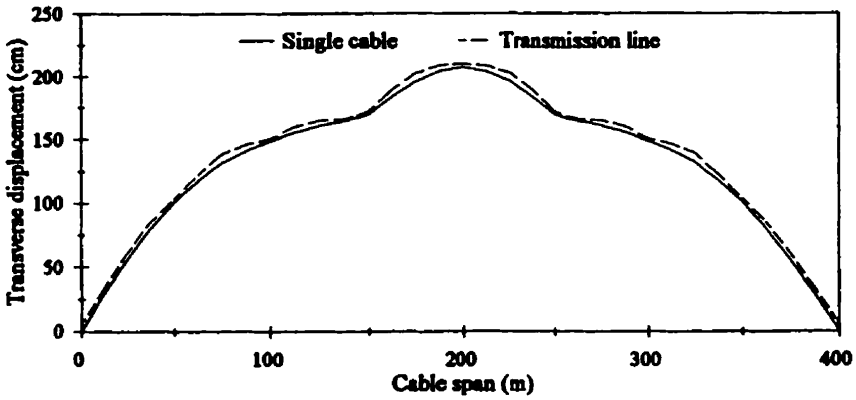

(a) Mexico Earthquake

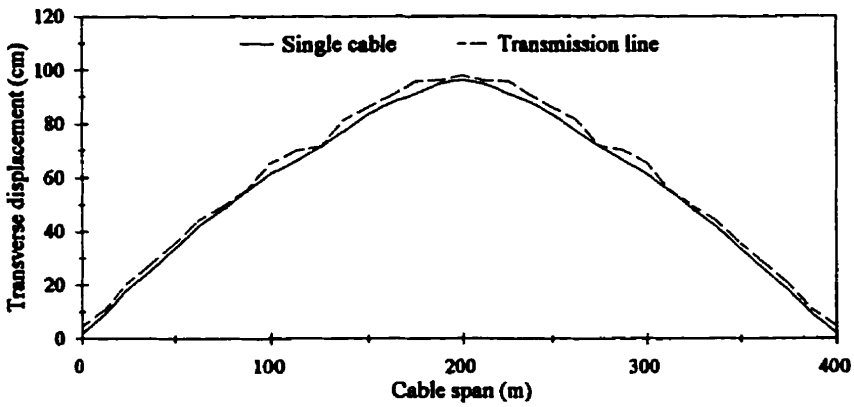

(b) San Fernando Earthquake

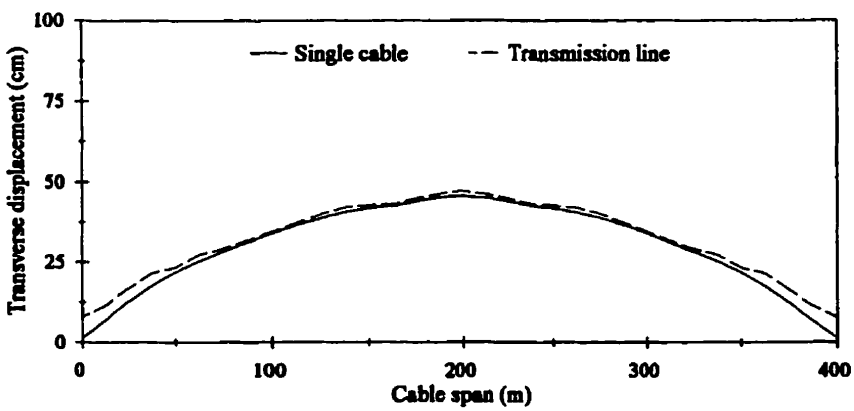

(c) Imperial Valley Earthquake

Figure 3.10 Envelopes of maximum response to transverse excitation for transmission lines with Tower II

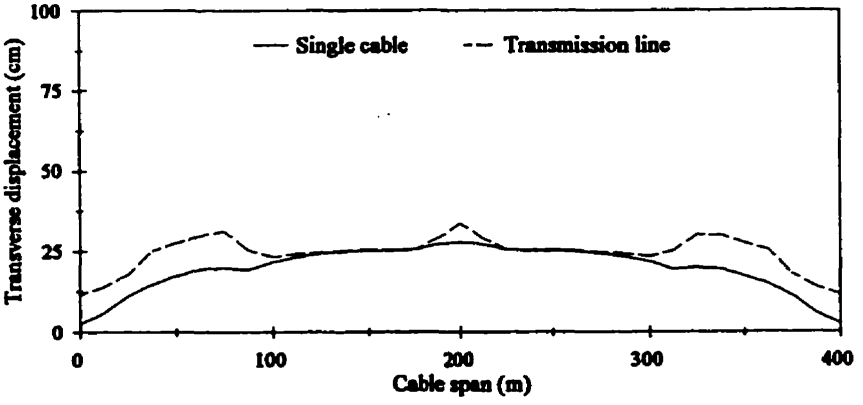

(d) Monte Negro Earthquake

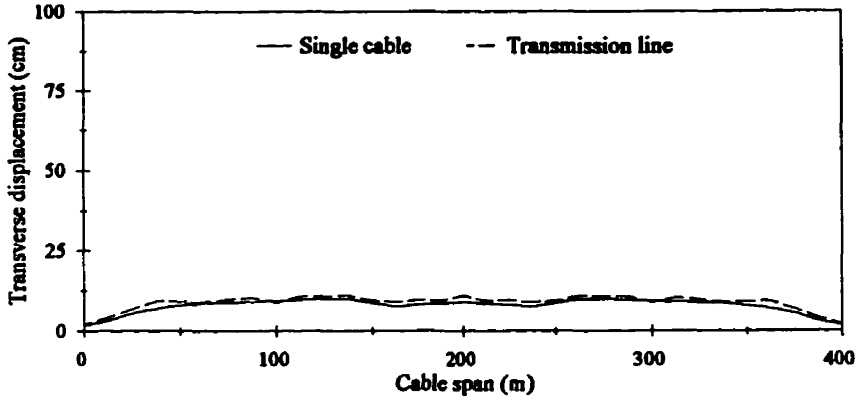

(e) Parkfield Earthquake

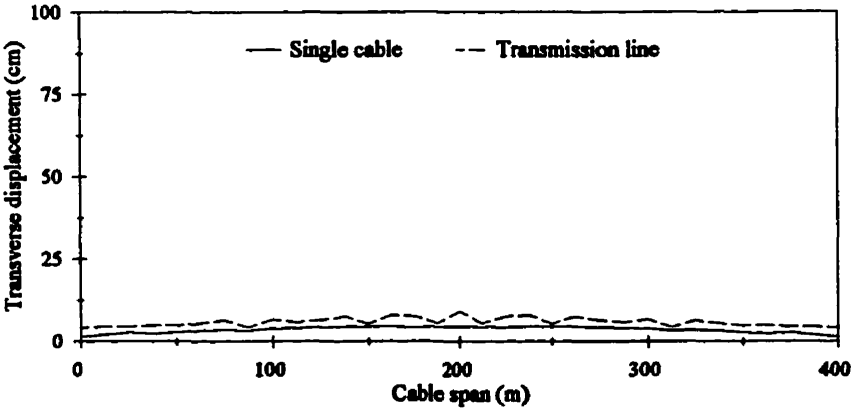

(f) Lytle Creek Earthquake

Figure 3.10 (cont.) Envelopes of maximum response to transverse excitation for transmission lines with Tower II

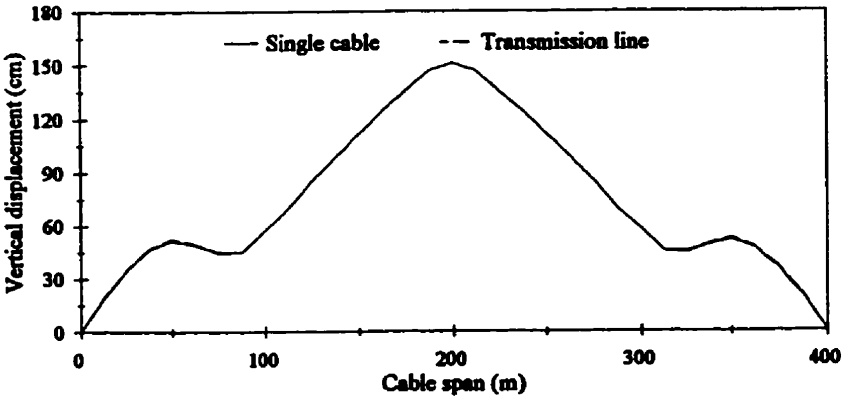

(a) Mexico Earthquake

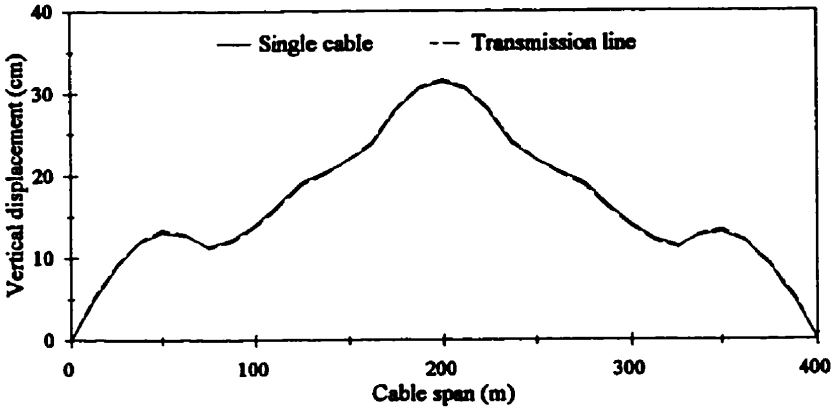

(b) San Fernando Earthquake

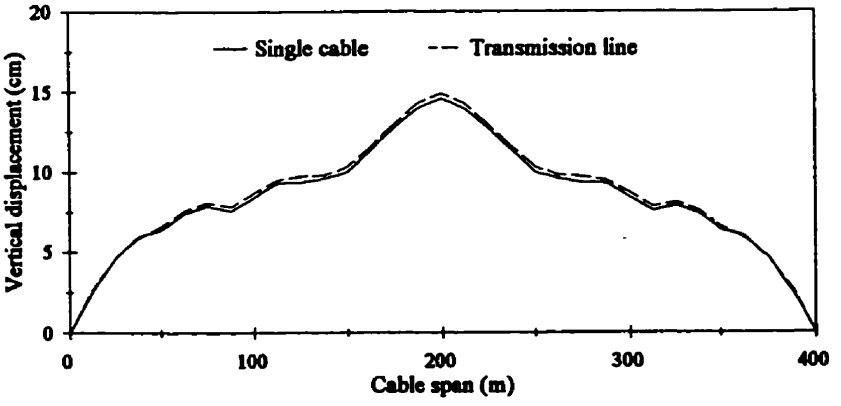

(c) Monte Negro Earthquake

Figure 3.11 Envelopes of maximum response to vertical excitation for transmission lines with Tower I

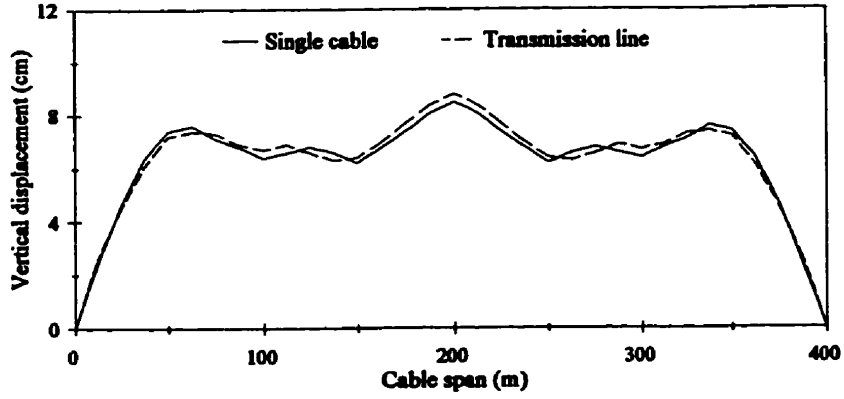

(d) Imperial Valley Earthquake

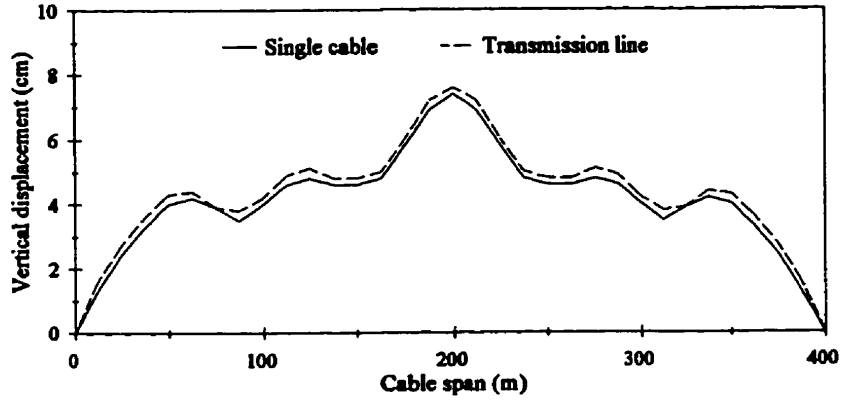

(e) Parkfield Earthquake

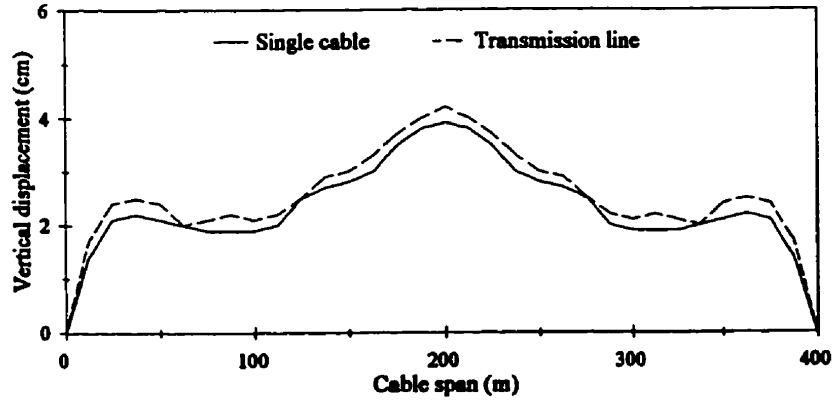

(f) Lytle Creek Earthquake

Figure 3.11 (cont.) Envelopes of maximum response to vertical excitation for transmission lines with Tower I

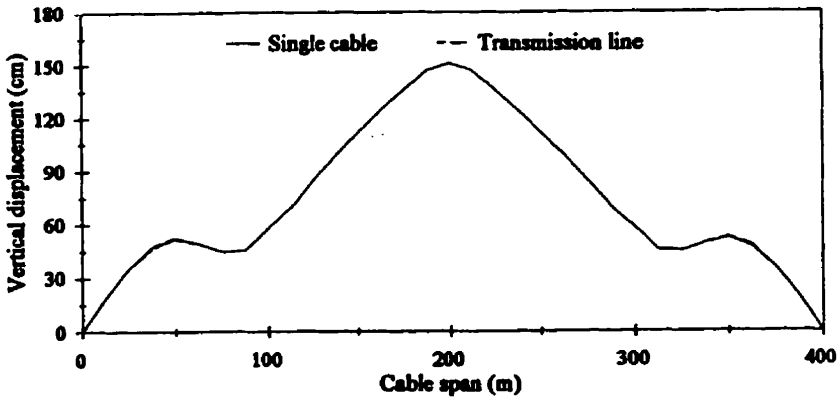

(a) Mexico Earthquake

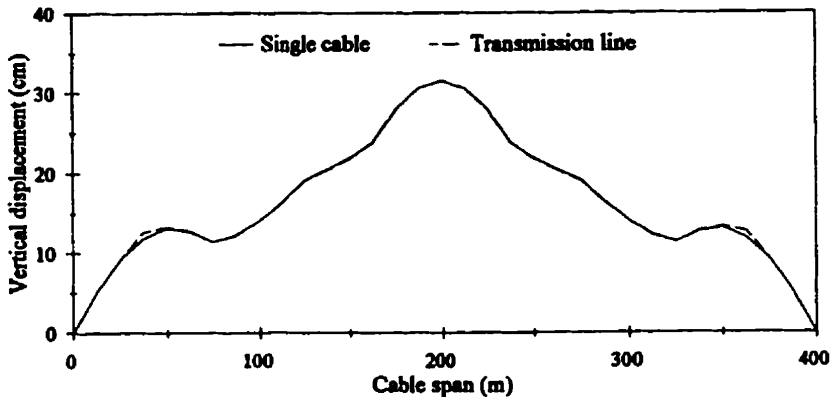

(b) San Fernando Earthquake

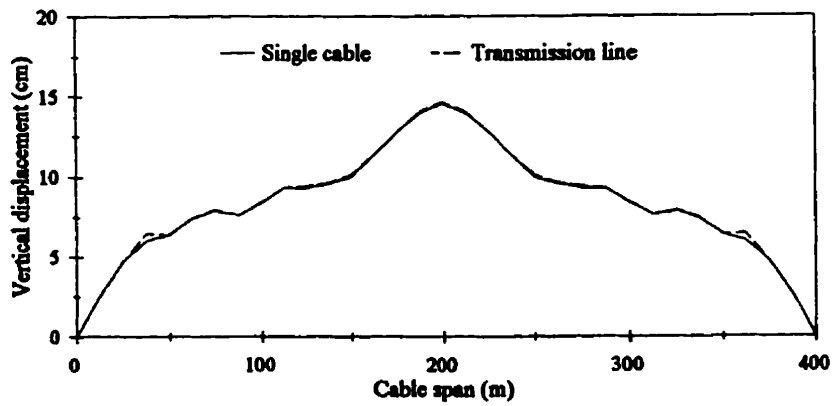

(c) Monte Negro Earthquake

Figure 3.12 Envelopes of maximum response to vertical excitation for transmission lines with Tower II

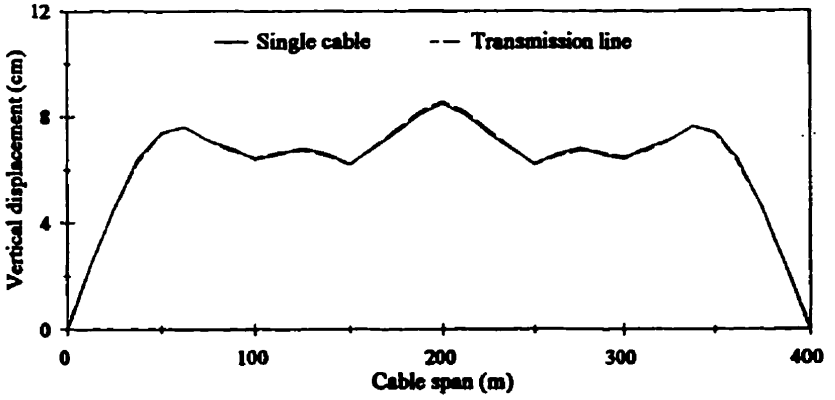

(d) Imperial Valley Earthquake

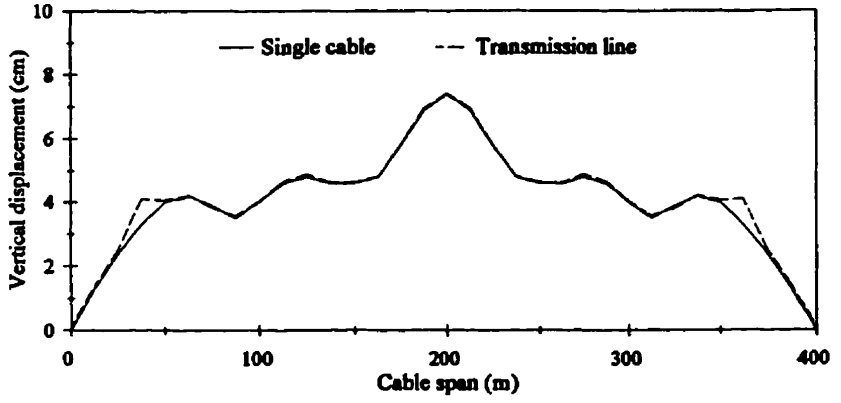

(e) Parkfield Earthquake

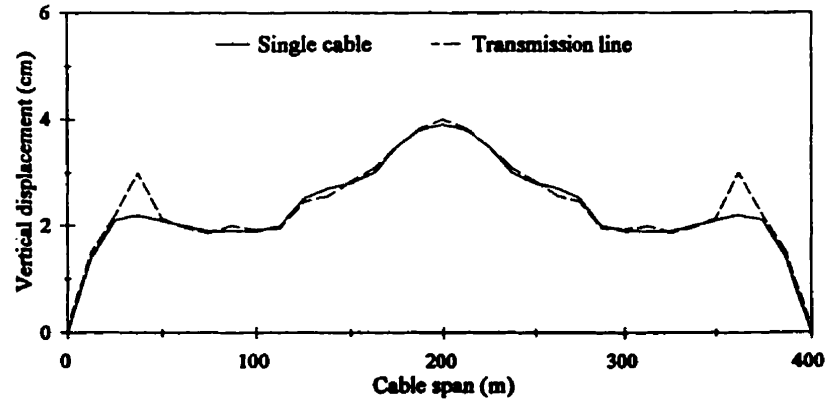

(f) Lytle Creek Earthquake

Figure 3.12 (cont.) Envelopes of maximum response to vertical excitation for transmission lines with Tower II

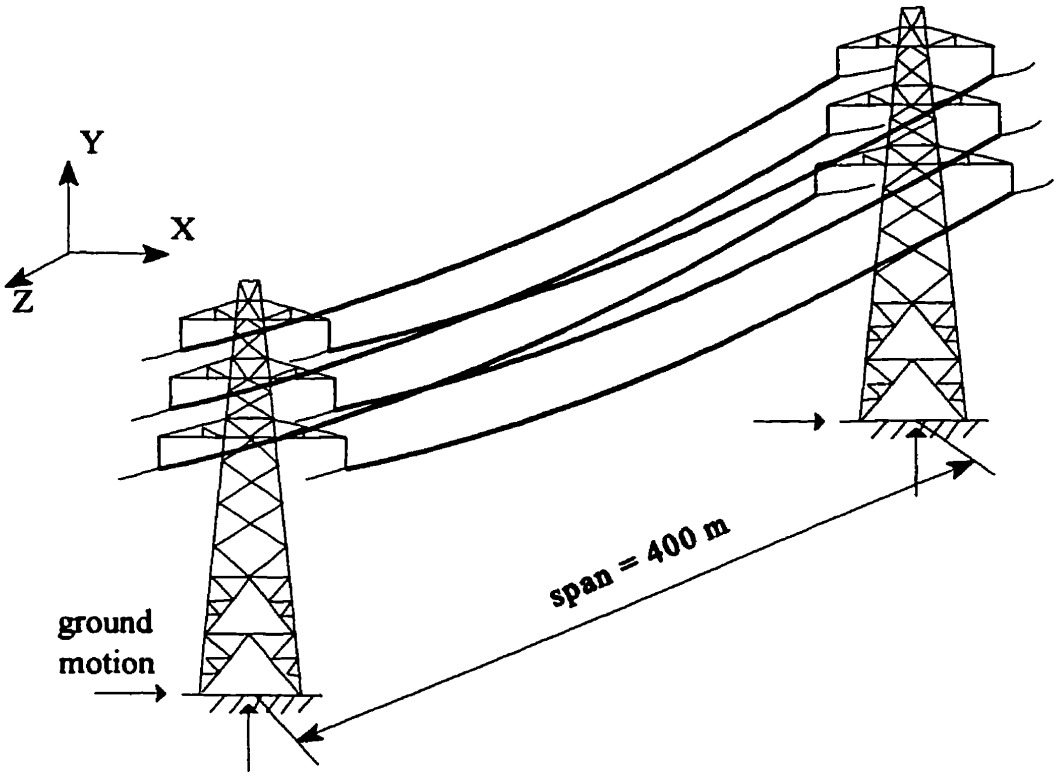

Figure 3.13 Transmission line system with suspension insulators

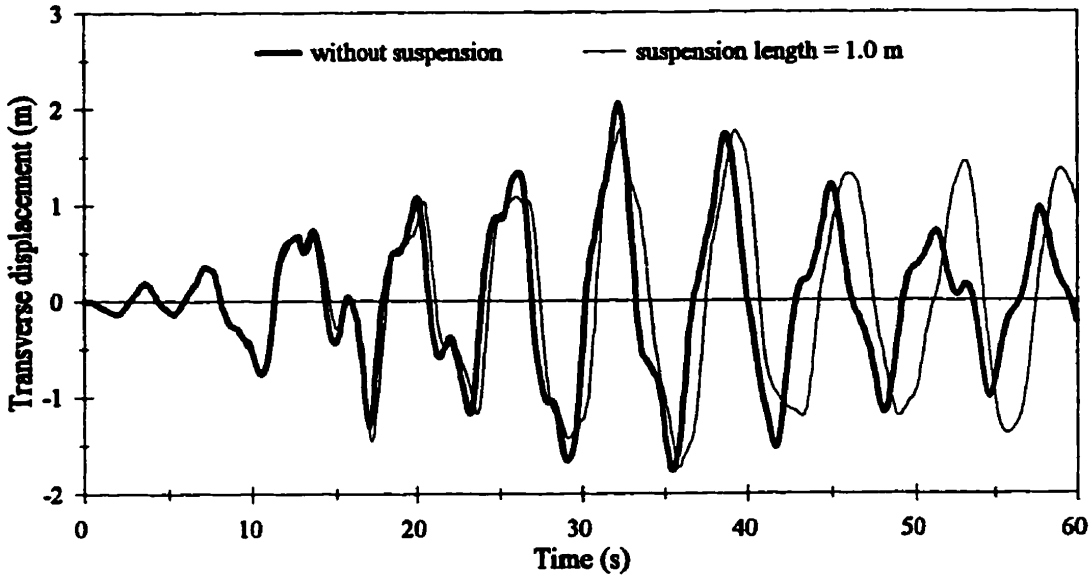

(a)

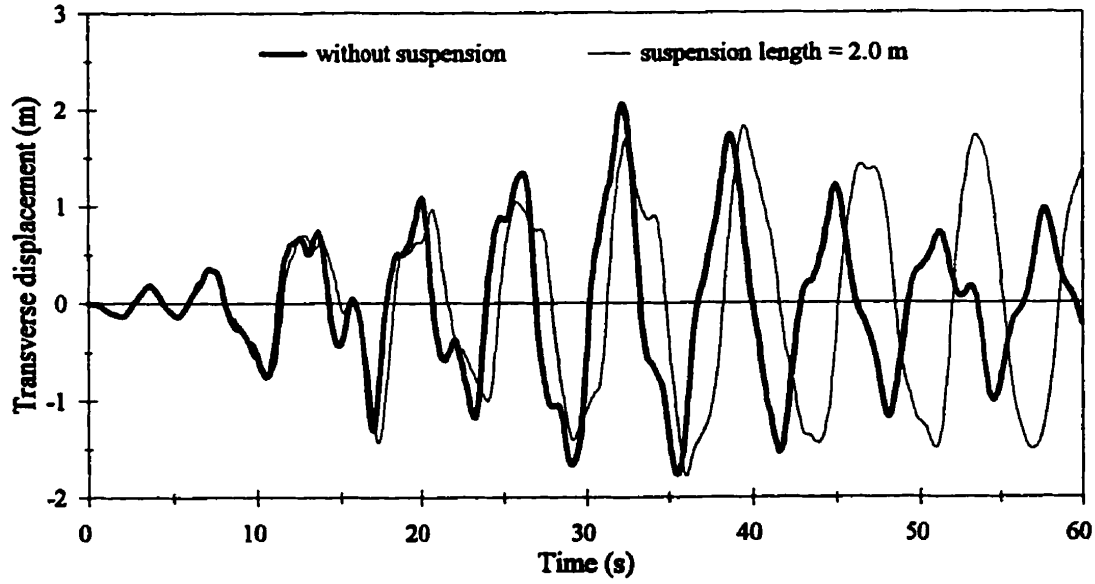

(b)

Figure 3.14 Effect of suspension insulator on the vibration of cable mid-point due to the horizontal component of the 1985 Mexico earthquake

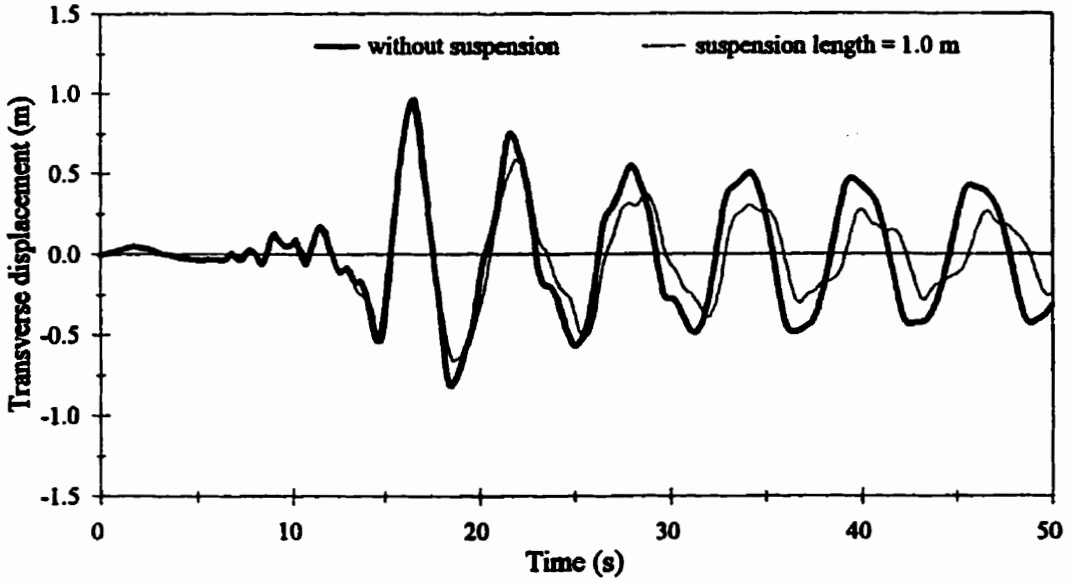

(a)

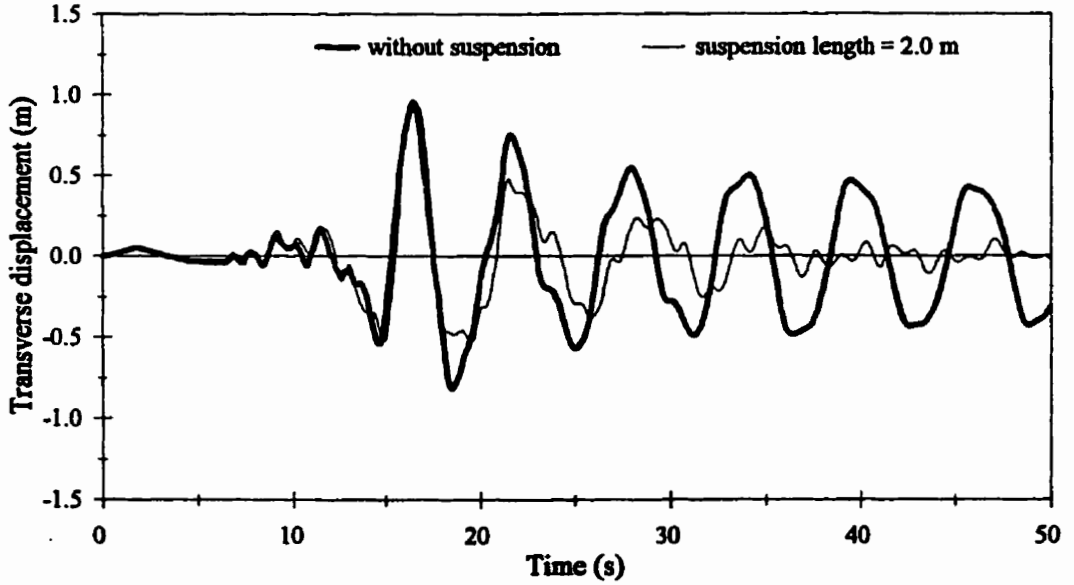

(b)

Figure 3.15 Effect of suspension insulator on the vibration of cable mid-point due to the horizontal component of the 1971 San Fernando earthquake

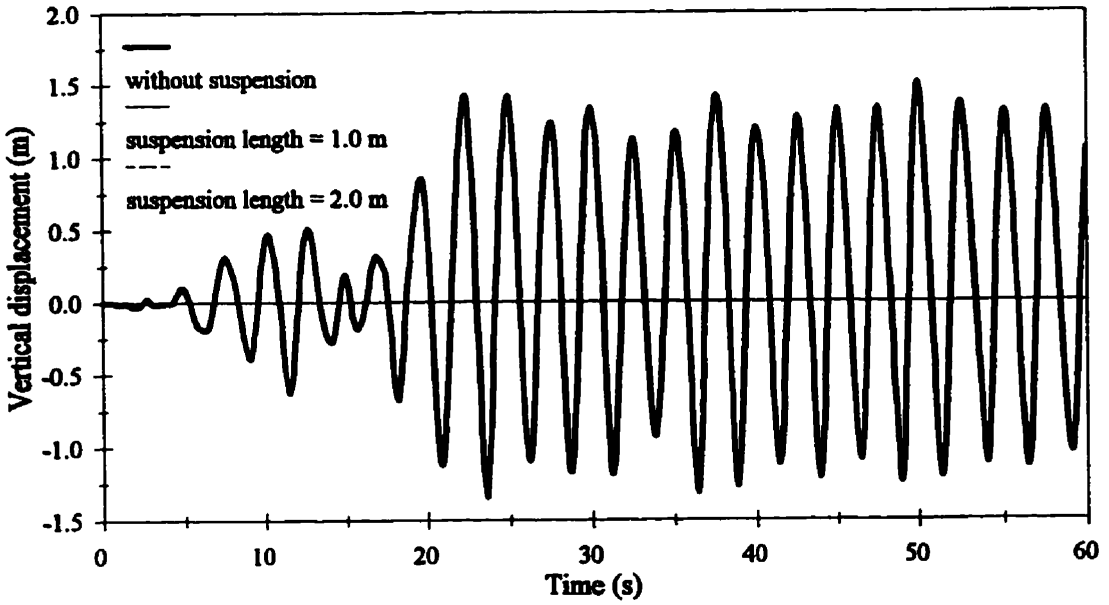

(a) Mexico Earthquake

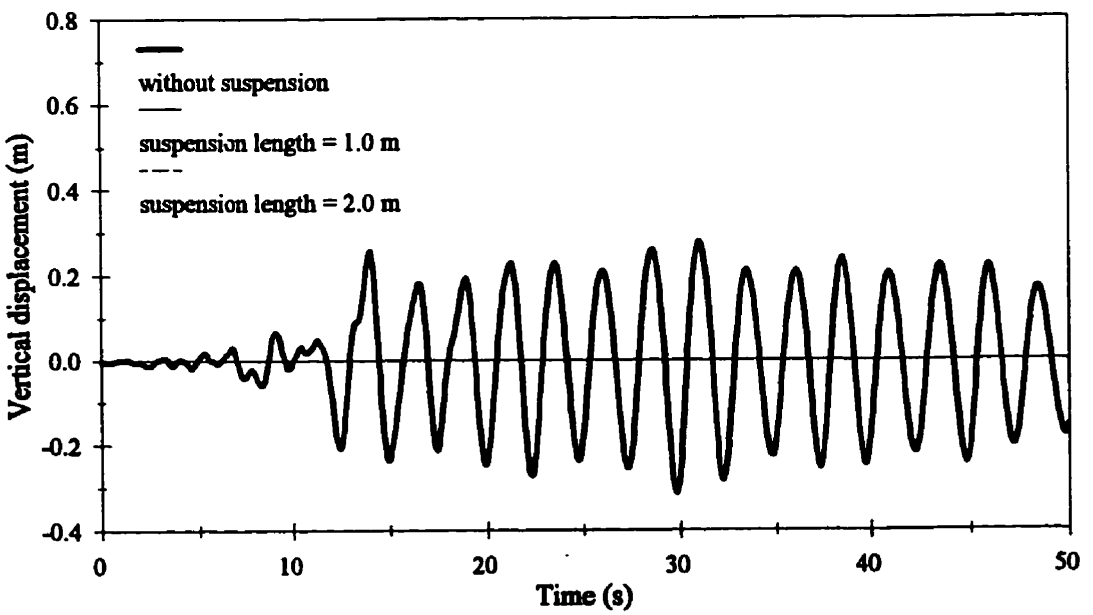

(b) San Fernando Earthquake

Figure 3.16 Effect of suspension insulator on the vibration of cable mid-point due to the vertical component of ground motion

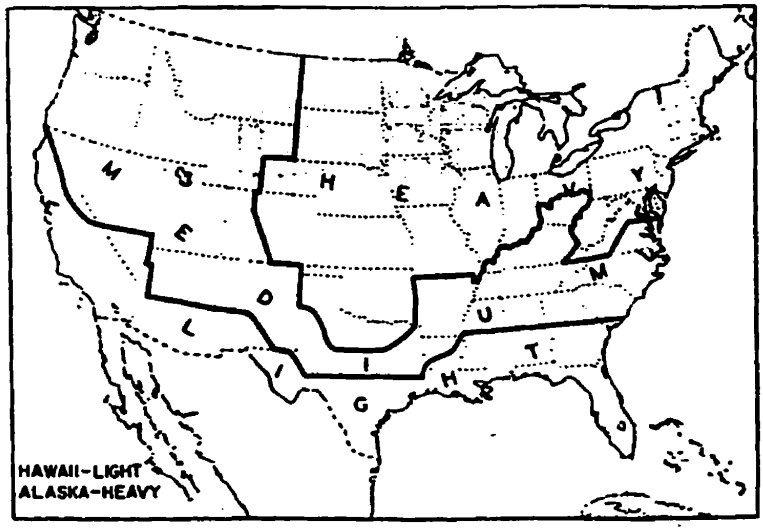

Figure 3.17 General loading map of the United States for transmission lines (NESC, 1993)

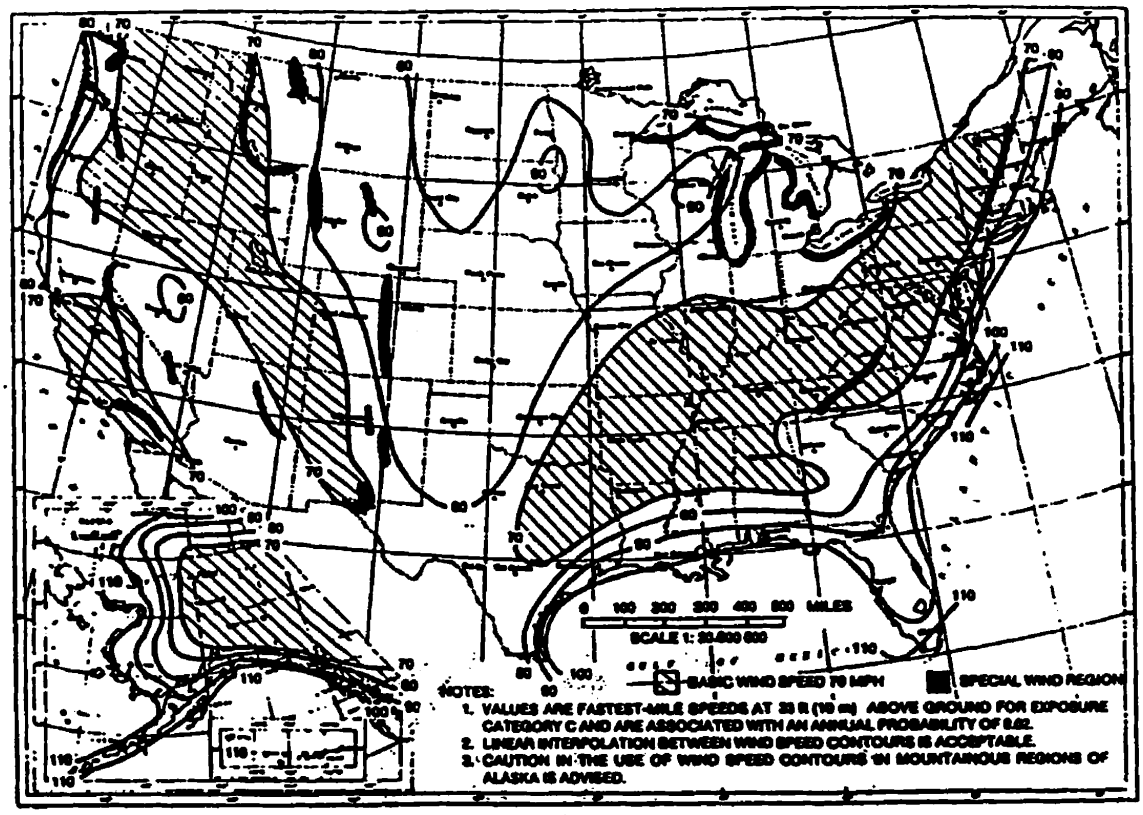

Figure 3.18 Basic wind speed in miles per hour (NESC, 1993)

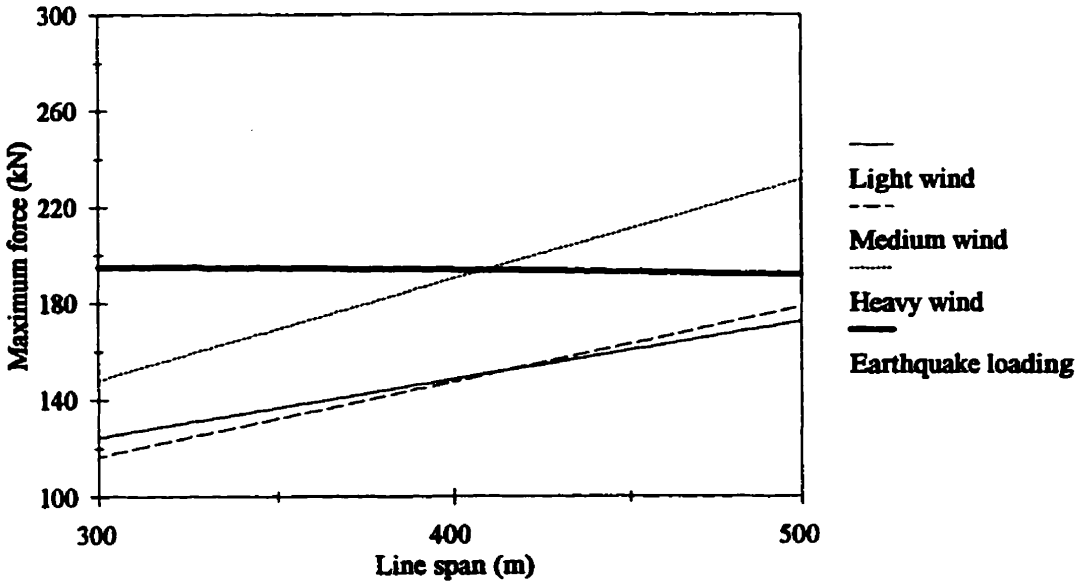

(a) Combined wind and ice loading

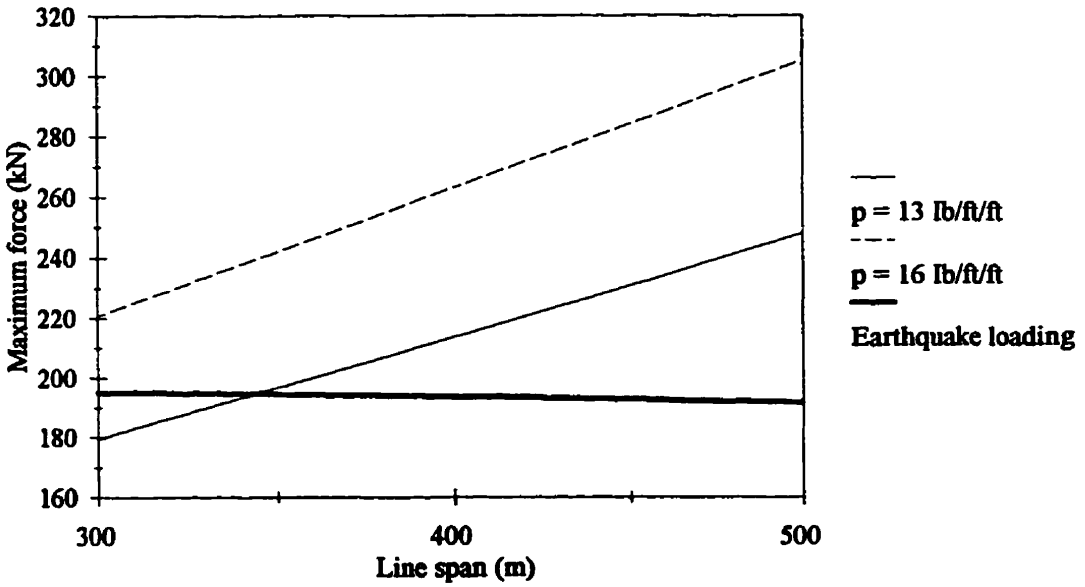

(b) Extreme wind loading

Figure 3.19 Maximum forces in tower members for different load combinations and for cable diameter of 3.5 cm

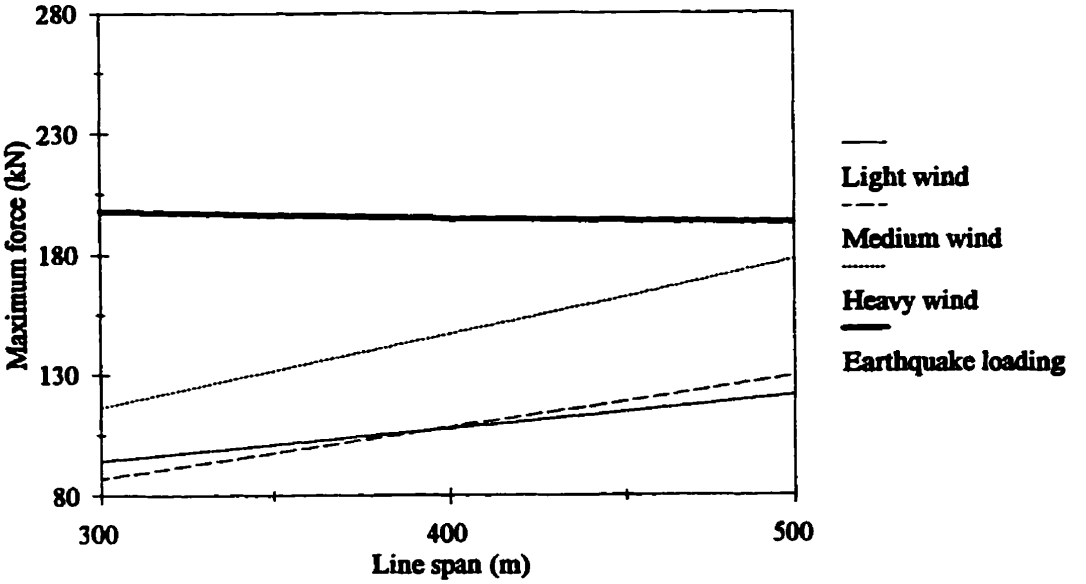

(a) Combined wind and ice loading

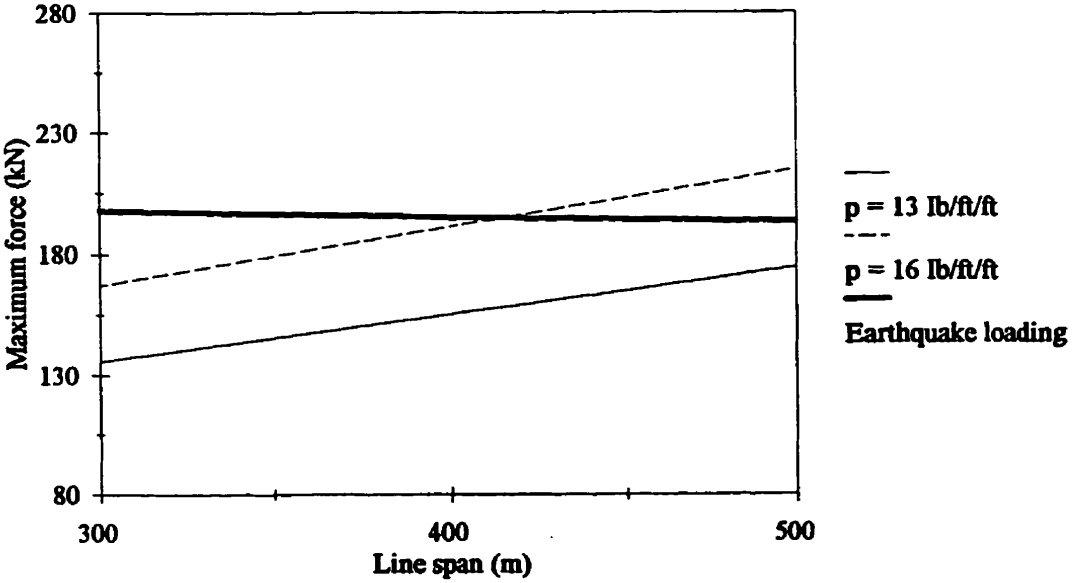

(b) Extreme wind loading

Figure 3.20 Maximum forces in tower members for different load combinations and for cable diameter of 2.0 cm

CHAPTER 4

MULTIPLE SUPPORT EXCITATION OF TRANSMISSION LINES

4.1 GENERAL

Transmission lines extend for long distances over different site conditions in areas of high seismicity. One major difficulty that arises during the seismic analysis of transmission line is its long span. Because of the long distances between transmission towers, they may be subjected to different input ground motions.

In the dynamic analysis of long span structures, multiple support excitation may be accounted for using several approaches. One approach is to use the travelling wave method where the input ground motions at all the supports are similar but with a phase shift that depends on the velocity of the seismic wave and the distance between supports. The second approach is the use of spatially correlated ground motions. This approach takes into account the wave travel effect as well as the incoherency of the seismic waves.

Several problems arise during the study of multiple support excitation of structures. Most of the commonly available computer programs for seismic analysis of structures do not allow the introduction of multiple acceleration time histories. The use of the displacement time history of the ground motion instead of the acceleration time history may be more appropriate for long span structures as suggested by Fenves (1992).

In this chapter, ground displacement time histories for vertical and horizontal ground motions are generated. Both the incoherency of seismic waves and the wave travel effects are accounted for. Various coherency models and seismic wave velocities are considered in the analysis. The transmission line is subjected to the generated ground motions. The equations of motion for the structure due to the multiple support excitation are derived. A simplified approach is described to obtain the response of the transmission line system to multiple support excitation.

The results of the analysis are presented in the form of cable displacement, cable tension, and tower internal forces. The system response using uniform support excitation is compared with the response using multiple support excitation which is a more realistic assumption. The effects of wave propagation velocity and coherency model on the response are also investigated.

4.2 GENERATION OF ARTIFICIAL GROUND DISPLACEMENT

The ground motion travels from the earthquake epicentre to a specific site at a speed that varies between 250 and 2000 m/s depending on the type of rock or soil through which the seismic waves travel. During this travel, the amplitude and the frequency of the seismic waves are affected. For short span structures, the input motion is assumed the same at all supports. However, this assumption is not true for long span structures such as transmission lines.

The variation in seismic ground motion affecting different supports of a long span structure is influenced by three main factors. The first factor is the wave travel effect that

results from the finite speed of the seismic waves. The second factor is the incoherency effect that results from the reflection and refraction of seismic waves. The third factor is the local site effect. The first two factors are accounted for in this analysis while the site effect is beyond the scope of this research.

To account for the variation in seismic ground motion, a seismological approach based on the seismic wave propagation from the epicentre to the supporting structure may be used. Alternatively, a stochastic approach based on random vibration analysis may be adopted. The ground motion cross spectral density $S_r(\omega)$ between an arbitrary point and a station at a distance r apart is given by:

$$S_r(\omega) = S(\omega)\, R(r,\omega) \tag{4.1}$$

where, $S(\omega)$ is the power spectral density of the ground displacement, and $R(r, \omega)$ is the coherency function.

To define the ground motion at a specific site, the power spectral density function and the coherency function should be defined.

4.2.1 Power Spectral Density of Ground Motion

The power spectral density of a ground motion is a distinctive characteristic of that ground motion as it is assumed constant at any location on the ground surface. An appropriate power spectrum density function that is commonly used by researchers is that presented by Clough and Penzien (1975) with the appropriate parameters to fit different kinds of soil. The Clough-Penzien power spectral density for ground displacement is given as:

$$S(\omega) = S_0 \frac{1 + 4\,\xi_g^2\,(\frac{\omega}{\omega_g})^2}{[1 - (\frac{\omega}{\omega_g})^2]^2 + 4\,\xi_g^2\,(\frac{\omega}{\omega_g})^2} \frac{(\frac{1}{\omega_f})^4}{[1 - (\frac{\omega}{\omega_f})^2]^2 + 4\,\xi_f^2\,(\frac{\omega}{\omega_f})^2} \qquad (4.2)$$

where S_0 is a scale factor; ω_g, ξ_g are the first ground filter parameters. The second ground filter parameters are ω_f, ξ_f. Values of different parameters depend on the actual earthquake data, on the type of the soil and on the component of the earthquake considered in the analysis. For the horizontal component of ground motion, Der Kiureghian and Neuenhofer (1991) provided values for the filter parameters for different soil types as given in table 4.1. The power spectral density function for the medium soil is used to generate the corresponding ground displacement. The medium soil is used because the predominant frequency of the ground motion is near the range of significant cable frequencies. The shape of the power spectral density of the ground displacement for the horizontal component of the earthquake is shown in figure 4.1. In this analysis S_0 is taken equal to 0.01 m^2/s^3.

The power spectral density function of the vertical component of ground motion is different from that of the horizontal component. Limited research was done to determine the shape of this function. Elghadamsi et al. (1988) and Hao et al. (1989) used the Clough-Penzien power spectrum to represent the vertical component of ground motion with the appropriate filter parameters.

Based on the results of about 120 vertical accelerograms, Elghadamsi et al. (1988) estimated the average value of the filter parameters for different site conditions as presented in table 4.2. Based on this table, the following values of filter parameters are used in the

present analysis: ω_g = 25.0 rad/s , ξ_g = 0.46 , ω_f = 0.1 ω_g , and ξ_f = ξ_g . The value of S_0 is taken 0.0075 m^2/s^3 to represent ¾ its value in the horizontal direction. The shape of the power spectral density function of the vertical component of the earthquake is shown in figure 4.2.

4.2.2 Coherency Models

Different coherency models were developed based on actual sets of earthquake records. From the available data in the literature, two different coherency models are used in this analysis. The first model was used by Hindy and Novak (1980), and will be denoted as model I. The second model was developed by Harichandran and Vanmarcke (1986), and will be denoted to as model II. The choice of these two models is based on their wide use in seismic response of long span structures [e.g., Ramadan and Novak (1992) and Zerva (1990)]. The purpose of using two different coherency models in the analysis is to investigate the effect of choosing a specific coherency model on the response of transmission lines.

Model I is a simplified function that works well in other random fields and is given by:

$$R(r,\omega) = \exp\left[-c\left(\frac{\omega\,|r|}{V}\right)^{\gamma}\right] \tag{4.3}$$

where, c is a constant that depends on the epicentral distance and the magnitude of the earthquake; V is seismic wave propagation velocity; and γ is a constant. The parameters γ = 1.0 and c = ½ are used as suggested by Hindy and Novak (1980). The wave propagation velocity is varied between 250 m/s and 2000 m/s to cover a wide range of possible wave propagation velocities.

This model was developed in 1980 by Hindy and Novak and was later found (Novak, 1987) to be in good agreement with the SMART-1 data. The change in the coherency with the frequency for various wave propagation velocities is shown in figure 4.3. It appears from this figure that at low propagation velocities (V = 250 m/s), the coherency at frequencies greater than 5.0 rad/s is almost zero which represent uncorrelated ground motions.

Model II was developed by Harichandran and Vanmarcke (1986) based on the analysis of the recorded data of Event 20 of the SMART-1 array. The coherency function is given by:

$$R(r,\omega) = A \exp\left[-\frac{2r}{\zeta\,\theta(\omega)}(1 - A + \zeta A)\right] + (1 - A)\exp\left[-\frac{2r}{\theta(\omega)}(1 - A + \zeta A)\right] \quad (4.4)$$

where,

$$\theta(\omega) = k\left[1 + \left(\frac{\omega}{2\pi f_0}\right)^b\right]^{-0.5} \quad (4.5)$$

The values of the constants were determined based on Event 20 as follows:

$A = 0.736$ $\qquad$ $\zeta = 0.147$

$k = 5210\ m$ $\qquad$ $f_0 = 1.09\ Hz$

$b = 2.78$

The coherency function of model II is represented by the solid line in figure 4.4.

There are some differences between model I and model II. Model I represents fully correlated ground motions at very low frequencies ($\omega = 0$), then the correlation decays rapidly at higher frequencies. Meanwhile, model II represents records that are not fully correlated

at low frequencies, however, the decrease in coherency with increasing frequency is slower than model I. This means that the variability in earthquake time histories generated by model I is due to the higher frequency components. Meanwhile, the variability in the time histories generated by model II is due to the lower frequency components.

The coherency function for the vertical component of ground motion can be considered similar to that of the horizontal component with different values for the constants. In the current analysis, the same coherency models are used for the horizontal and vertical components of ground motion for two reasons. First, the data available on the vertical component of ground motion in the literature is very limited. Second, the objective of this analysis is to evaluate the importance of considering multiple support excitation in the seismic analysis of transmission lines. This objective can be achieved by using the same coherency models.

4.2.3 Method for Generating Ground Displacement

Ramadan and Novak (1993) presented an asymptotically accurate technique to generate stationary random ground displacement. Considering only the incoherency effect between two or more stations, the generated ground displacement is given by:

$$u_r(t) = \sum_{k=0}^{N} \sum_{i=1}^{M} a_k \left[\sqrt{S(\omega_{ik})\,\Delta\omega}\, \cos\left(\omega_{ik}\, t + \phi_{ik} + \frac{\pi\, k\, r}{L_i}\right) + \sqrt{S(\omega'_{ik})\,\Delta\omega}\, \cos\left(\omega'_{ik}\, t + \phi'_{ik} + \frac{\pi\, k\, r}{L_i}\right) \right] \tag{4.6}$$

where,

r is the distance from an arbitrary point to the station;

ϕ_{ik} and ϕ'_{ik} are two random phase angles uniformly distributed between 0 and 2π;

ω_{ik}, ω'_{ik} are two circular frequencies given by $\omega_{ik} = i\,(\Delta\omega) - k\,(\Delta\omega) / N$, and ω'_{ik} $= i\,(\Delta\omega) - (k - \frac{1}{2})\,(\Delta\omega) / N$, $i = 1, 2, \ldots\ldots$, M with $\Delta\omega = \omega_{max} / M$;

M is the number of frequencies in the analysis. It is taken equal to 200;

a_k, $k = 0, 1, \ldots\ldots$, N are constants that will be defined later;

L_i is a frequency dependent characteristic length.

Ramadan and Novak (1993) presented the concept of the correlation length l_ω as:

$$l_\omega = \int_0^\infty R(r,\omega)\, dr \tag{4.7}$$

The correlation length is a frequency dependent length and it is used in evaluating the displacement time history of the ground motion through the relation $L_i = \alpha\, l_\omega$. The constant "α" depends on the distance over which the ground motion is simulated and it is assumed equal to 3.0 in this analysis.

To use equation (4.6) to generate ground motion records, the coherency of the simulated motion should be given as a Fourier series in the form:

$$R'(r,\omega) = \sum_{k=0}^{N} a_k^2 \cos\left(\frac{\pi k r}{L_\omega}\right) \tag{4.8}$$

The accuracy of the simulated motion depends on the number of Fourier terms used "N".

However, for N = 3 to 10 enough accuracy can be achieved. For the first coherency model, the correlation length l_ω equals to:

$$l_\omega = \frac{V}{c\ \omega} \tag{4.9}$$

To satisfy the target coherency function, the factors a_k in model I are defined by Ramadan and Novak (1993) as:

$$a_0^2 = \frac{1}{2\ L_\omega} \int_{-L_\omega}^{L_\omega} R(r,\omega)\ dr = \frac{1}{\alpha}\ (1 - e^{-\alpha}) \tag{4.10}$$

$$a_k^2 = \frac{1}{L_\omega} \int_{L_\omega}^{L_\omega} R(r,\omega) \cos\ (\frac{\pi k r}{L_\omega})\ dr = \frac{2\ [1 - (-1)^k\ e^{-\alpha}]}{\alpha\ [1 + (\frac{\pi k}{\alpha})^2]} \tag{4.11}$$

For coherency model II, the correlation length l_ω is chosen by Ramadan and Novak (1993) as:

$$l_\omega = \frac{\theta(\omega)\ \zeta}{2\ (1 - A - \zeta\ A)} \tag{4.12}$$

Therefore, the Fourier coefficients a_k are given by:

$$a_0^2 = \frac{1}{\alpha}\ [\ A\ (1 - e^{-\alpha}) + \frac{(1 - A)\ (1 - e^{-\zeta\alpha})}{\zeta}\ ] \tag{4.13}$$

$$a_k^2 = \frac{2}{\alpha} \left\{ \frac{A\,[1 - (-1)^k e^{-\alpha}]}{1 + (\frac{\pi k}{\alpha})^2} + \frac{(1 - A)\,[1 - (-1)^k e^{-\zeta\alpha}]}{\zeta\,[\,1 + (\frac{\pi k}{\alpha\zeta})^2\,]} \right\} \qquad (4.14)$$

Figure 4.4 shows the coherency function of model II, both the target coherency defined by equation (4.4) and the simulated coherency using equation (4.8) with the coefficients given by equations (4.13) and (4.14), for value of N = 10. The accuracy of the method developed by Ramadan and Novak is demonstrated.

The ground displacement generated by equation (4.6) is developed using a stationary random process. The nonstationary characteristics of ground motion are introduced by imposing a suitable time function on the ground displacement. In this research, for simplicity, a half sine wave is used. The nonstationary ground displacement $u_m(t)$ is given by:

$$u_{rn}(t) = u_r(t) \sin (\frac{\pi t}{T}) \qquad (4.15)$$

where T is the duration of the generated ground displacement which is taken equal to 40 s in this analysis.

4.2.4 Wave Travel Effect

The phase difference due to wave travel can be accounted for by introducing a time lag in equation (4.6). The time lag τ between any two stations is given by $\tau = r / V$ where r is the separation distance between the two stations and V is the wave velocity in the same

direction. Therefore, equation (4.6) can be modified to become:

$$u_r(t) = \sum_{k=0}^{N} \sum_{i=1}^{M} a_k \left[\sqrt{S(\omega_{ik})\,\Delta\omega}\, \cos\left\{\omega_{ik}\,(t-\tau) + \phi_{ik} + \frac{\pi\, k\, r}{L_i}\right\} + \sqrt{S(\omega'_{ik})\,\Delta\omega}\, \cos\left\{\omega'_{ik}\,(t-\tau) + \phi'_{ik} + \frac{\pi\, k\, r}{L_i}\right\} \right] \tag{4.16}$$

4.2.5 Generated Ground Displacement

The Clough-Penzien power spectrum for the horizontal and vertical components of ground motion shown in figures 4.1 and 4.2, are used to generate the ground displacement. The records are generated at two locations at distances of zero and 400 m, which is the typical span of the line. Four appropriate wave propagation velocities are used in the analysis: 2000, 1000, 500, and 250 m/s, to cover a wide range of expected wave propagation velocities. Model I and model II for the coherency are used in the analysis.

The generated horizontal ground displacements are shown in figures 4.5 through 4.8 for different assumptions and different coherency models. The generated vertical ground displacements are shown in figures 4.9 through 4.12 for different assumptions and different coherency models. Figures 4.5c, 4.5d, 4.9c, 4.9d show that for model I, the two generated records, 400 m apart, are well correlated at high velocities, 1000 m/s and 2000 m/s. On the other hand, at the low velocity of 250 m/s, the generated ground displacements are almost uncorrelated. It is also clear from figures 4.7 and 4.11 that using model II results in a ground motion that is not coherent at both stations.

4.3 ANALYSIS APPROACH

Multiple support excitation of long span structures is a complex problem. Most commonly available computer programs for the seismic analysis of structures do not allow more than one acceleration or displacement time histories as input data. This section is devoted to presenting different techniques to solve this problem.

4.3.1 Equations of Motion

The equation of motion of a structure subjected to seismic ground motion is in the form of equation (2.1). Differentiating between the response degrees of freedom denoted by "s" and the degrees of freedom where the ground motion is applied (ground degrees of freedom) denoted by "g", the following matrix equation is obtained:

$$\begin{bmatrix} M_{ss} & M_{sg} \\ M_{gs} & M_{gg} \end{bmatrix} \begin{Bmatrix} \ddot{u}_s \\ \ddot{u}_g \end{Bmatrix} + \begin{bmatrix} C_{ss} & C_{sg} \\ C_{gs} & C_{gg} \end{bmatrix} \begin{Bmatrix} \dot{u}_s \\ \dot{u}_g \end{Bmatrix} + \begin{bmatrix} K_{ss} & K_{sg} \\ K_{gs} & K_{gg} \end{bmatrix} \begin{Bmatrix} u_s \\ u_g \end{Bmatrix} = \begin{Bmatrix} 0 \\ 0 \end{Bmatrix} \quad (4.17)$$

The equation defining the response degrees of freedom is given by:

$$M_{ss}\,\ddot{u}_s + C_{ss}\,\dot{u}_s + K_{ss}\,u_s = -M_{sg}\,\ddot{u}_g - C_{sg}\,\dot{u}_g - K_{sg}\,u_g \quad (4.18)$$

The solution of equation (4.18) depends on how the earthquake is defined in the right-hand side of the equation. The ground motion can be introduced in the form of either an acceleration or a displacement time history. Each method has its own advantages and disadvantages.

If the support acceleration is defined, then the total displacement u_s is separated into two parts, the dynamic displacement u_{ds} and the pseudo-static displacement u_{ps}. The dynamic part of the displacement exists even if the structure is subjected to similar ground motions at all supports, while the pseudo-static displacement exists because of the differential movements between different supports of the structure. The total displacement is then given by:

$$\begin{Bmatrix} u_s \\ u_g \end{Bmatrix} = \begin{Bmatrix} u_{ds} \\ u_{dg} \end{Bmatrix} + \begin{Bmatrix} u_{ps} \\ u_{pg} \end{Bmatrix} \tag{4.19}$$

where $u_{dg} = 0.0$

Using equations (4.18) and (4.19) and removing all the time dependent terms, the static equilibrium equations are obtained:

$$K_{ss}\, u_{ps} = - K_{sg}\, u_{pg} \tag{4.20}$$

$$u_{ps} = - K_{ss}^{-1}\, K_{sg}\, u_{pg} = - R_{sg}\, u_{pg} \tag{4.21}$$

Finally, considering a lumped mass matrix and a Rayleigh damping, and making use of equations (4.19) to (4.21), equation (4.18) can be reduced to:

$$M_{ss}\, \ddot{u}_{ds} + C_{ss}\, \dot{u}_{ds} + K_{ss}\, u_{ds} = - M_{ss}\, R_{sg}\, \ddot{u}_{pg} \tag{4.22}$$

The generated support acceleration time histories are introduced in equation (4.22). However, the use of this equation is difficult because it involves matrix partitioning and

matrix inversion. Moreover, for a nonlinear system, where the stiffness changes after every time step, the whole matrix operations should be carried out after every stiffness change.

The second possibility is to specify the support displacement time histories. Starting with equation (4.18) and assuming a diagonal mass matrix and a stiffness proportional Rayleigh damping, the following equation is obtained:

$$M_{ss}\,\ddot{u}_s + C_{ss}\,\dot{u}_s + K_{ss}\,u_s = -K_{sg}\,u_g \tag{4.23}$$

Considering the initial conditions for the dynamic displacement to be zero, the initial conditions for the total displacement are given by:

$$\begin{aligned} u_s(0) &= R_{sg}\,u_g(0) \\ \dot{u}_s(0) &= R_{sg}\,\dot{u}_g(0) \end{aligned} \tag{4.24}$$

Equation (4.23) is applicable in the analysis of nonlinear systems. Defining support displacement instead of support acceleration is more appropriate for long span structures. However, the problem remains that most of the commonly used computer programs do not allow the specification of different displacement time histories at the different supports of the long span structures.

4.3.2 Simplified Approach for the Analysis

Fenves (1992) proposed a simplified technique for replacing the different support displacement by dynamic forces. The technique is based on adding stiff springs at the supports in the direction of the specified support displacement. A dynamic load, equal to the

spring stiffness multiplied by the support displacement, is then applied in the direction of each support displacement as shown in figure 4.13 for horizontal ground motion. If the spring is stiff enough, the displacement at the support point should be equal to the ground displacement time history. This approach is presented by Ghobarah et al. (1996).

To verify the accuracy of the simplified method, an example is solved for cable I using the data given in Chapter 2. The cable is fixed at both ends and subjected to a horizontal and a vertical sine-shaped ground motion. The response of the cable to a uniform excitation is evaluated using both the acceleration time history and the simplified approach. The ground motion has a frequency of 1.0 Hz and an amplitude of 0.3 g. The transverse displacement time history of the cable mid-point due to transverse ground motion is shown in figure 4.14. In figure 4.15, the vertical displacement time history of the cable mid-point due to vertical ground motion is plotted. Both figures show complete agreement between the simplified approach and the case of acceleration time history specified as uniform excitation. This is expected since the simplified approach is an exact solution.

4.4 RESPONSE OF TRANSMISSION LINES TO TRANSVERSE GROUND MOTION

To analyze the response of transmission lines to transverse ground motion, the model shown in figure 3.8 for the transmission line is used in the analysis. In this model, the typical span between transmission towers is taken 400 m. The cable used is Cable I with the properties given in Chapter 2.

The transmission line is subjected to the artificially generated ground motions (figures 4.5 through 4.8). The supports of the first tower are subjected to the generated ground displacement at zero m, while the supports of the second tower are subjected to the generated ground displacement at 400 m. Four different wave propagation velocities are considered in the analysis 250, 500, 1000, and 2000 m/s. The effect of the coherency model (model I and model II) is also studied.

The results of the analysis are shown in figures 4.16 to 4.22. Figures 4.16 to 4.19 show the envelopes of the peak cable displacement of the top cable in figure 3.8 using different coherency models and different assumptions in generating the ground motion. Figures 4.20 through 4.22 show the displacement time history of the cable mid-point using different assumptions to generate the ground motion records.

4.4.1 Transverse Cable Displacement

Figure 4.16 shows the envelopes of maximum total cable displacement considering the incoherency effect only. The envelopes of maximum cable displacement for the case of ground motion with wave travel effect only are plotted in figure 4.17. Both the incoherency and wave travel effects are included in the analysis of maximum cable displacement shown in figures 4.18 and 4.19 using model I and model II for the coherency, respectively.

It is evident from these figures that for most of the cases of input ground motion considered, the assumption of uniform ground motion at all supports ($V = \infty$ for model I) does not represent the most critical case for cable displacement. Considering the incoherency effect only, for example, the total displacement at the cable mid span equals to 87.9 cm for

uniform ground motion, while for multiple support excitation using model I with a wave propagation velocity of V = 500 m/s the response equals to 95.7 cm. The magnification at ¾ span point is larger for this case as the response increases from 58.2 cm for uniform ground motion to 82.8 cm for V = 500 m/s.

The same conclusion was arrived at by Abdel-Ghaffar and Stringfellow (1984a and b) and by Dumanoglu and Severn (1987) in their analysis of seismic behaviour of suspension bridges and by Rao and Iyengar (1991) in their study of the seismic behaviour of long span cables. The reason is that the antisymmetric modes are not excited by the uniform excitation case. It should be noted that figures 4.18 and 4.19 are not the sum of figures 4.16 and 4.17 as the maximum values do not occur at the same time and the problem under consideration is nonlinear in nature where the principle of superposition does not apply.

Figures 4.20 and 4.21 show the displacement time histories of the cable mid-point due to transverse ground motion considering the incoherency effect only and using model I and model II, respectively. Figure 4.20 shows that, using model I for the coherency, for higher propagation velocities ($V \geq 1000$ m/s) which is the case of the firm soil, the response approaches that of the case of uniform excitation. On the other hand, figure 4.21 shows that, using model II for the coherency, the response is different from the case of uniform excitation. This is mainly due to the uncorrelation between the seismic waves at the low frequency content using this model (figure 4.4). Figure 4.22 shows the transverse displacement time history of cable mid-point considering the wave travel effect only. The figure indicates that as the velocity of propagation increases the response becomes similar to the case of uniform excitation which is expected since $V = \infty$ represents the uniform excitation case.

Considering the incoherency effect only, the wave propagation velocity has a significant effect on the transverse cable displacement if model I for the coherency is used. The second lowest velocity (V = 500 m/s) results in the highest response specially from the cable mid point to the end of the cable as shown in figure 4.16. The lowest velocity (V = 250 m/s) does not result in the maximum displacement in this case as the two generated ground motions are almost uncorrelated and this might reduce the pseudo-static response. However, if model II is used, the wave propagation velocity has no effect on the results since the coherency function defined by model II does not depend on the wave velocity.

Considering the wave travel effect alone (figure 4.17), the lowest velocity (V = 250 m/s) results in the highest response in the last quarter of the cable span. The same observation was made by Dumanoglu and Severn (1987) in their study of suspension bridge cables. However, in the first half of the span the effect of the propagation velocity is not significant except for the case V = 250 m/s where the response is reduced dramatically. This large difference indicates that phasing between the input ground motion can have a significant effect on the response.

4.4.2 Internal Forces in Transmission Line Elements

The maximum forces in the tower members for different propagation velocities and different assumptions regarding the earthquake ground motion are shown in table 4.3. The maximum force in the tower members in the case of uniform ground motion at all supports is 95.9 kN. It is evident from the results that considering multiple support excitation increases the internal forces in tower members for all cases. The maximum increase is approximately

35% for wave propagation velocity of 500 m/s and considering the incoherency effect only using model I. These conclusions are particular to the numerical example selected and may vary with the tower dimensions, cable geometry and generated ground motion.

The maximum value of cable tension for different cases of input ground motion is shown in table 4.4. The maximum tension in the cable due to the effect of uniform ground motion is 1.08 kN. The tension in the cable due to the transverse component of ground motion is insignificant and the change in the tension due to multiple support excitation is very small. This result is expected since the transverse vibration of cables is mainly swinging and does not incorporate significant change in cable length and therefore does not produce significant stresses

4.4.3 Effect of the Coherency Model

Several coherency models are available to model the ground motion. Therefore, it is important to study the effect of choosing a specific coherency model on the response of transmission lines. The purpose of this study is not to recommend the use of a specific coherency model. The choice of a specific coherency model depends on the specific site conditions and the nature of the expected ground motion. However, the purpose of this study is to identify the characteristics of the selected models that has a significant effect on the response of transmission lines.

Considering the incoherency effect only, figure 4.16 shows that model II produces the highest total cable transverse displacement throughout most of the span. The reason is that

model II represents uncorrelated ground motions at the low frequency range which is the range of the cable predominant frequency.

Figure 4.23 shows that, considering both effects, at high propagation speeds there is almost no difference between the response using the two models. It was found by Zerva (1994) that the type of the coherency model has a significant effect on the dynamic and pseudo-static responses. However, concerning the total response, which is the summation of the pseudo-static and the dynamic responses, no general conclusion can be derived.

Table 4.2 shows that the differences in tower internal forces using different coherency models are in the range of 10% which suggest also that the differences in the internal forces using different coherency models are not significant.

4.4.4 Incoherency Versus Wave Travel Effects

It is a common approach in multiple support excitation analysis of long span structures to consider only the wave travel effect and neglect the incoherency effect. The purpose of this section is to examine the effect of these assumptions on the response. Figure 4.23 shows the maximum transverse displacement of the cable for various wave propagation velocities.

Figure 4.23 shows that considering the wave travel effect alone reduces the maximum cable displacement for all propagation speeds. However, at high propagation velocities, considering the incoherency effect in addition to the wave travel effect increases the response regardless of the coherency model considered in the analysis. It is also shown from table 4.3 that considering the incoherency effect may in some cases increase the internal forces in the tower members.

4.5 RESPONSE OF TRANSMISSION LINES TO VERTICAL GROUND MOTION

The analysis of the response of transmission lines to vertical ground motion is carried out in the same way as for the transverse ground motion. The transmission line is subjected to the artificially generated ground motions shown in figures 4.9 to 4.12. The supports of the first tower are subjected to a dynamic force based on the ground displacement developed at zero m, while the second tower supports are subjected to a dynamic force based on the ground displacement developed at 400 m. The results are presented for the top cable of the tower-cable system shown in figure 3.8.

4.5.1 Vertical Cable Displacement

Figure 4.24 shows the envelopes of the total peak cable displacement considering the incoherency effect only and using either model I or model II to model the coherency function. The envelopes of the total peak cable displacement considering the wave travel effect only are shown in figure 4.25. Both the incoherency and the wave travel effects are considered in the analysis shown in figures 4.26 and 4.27.

Figures 4.24 to 4.27 show that in many cases the response of the multiple support excitation cases may exceed that of the uniform excitation case, specially when the incoherency effect is considered alone. For example, considering the incoherency effect only with model I and velocity 500 m/s results in a peak vertical cable displacement of 41.0 cm, where the uniform support excitation results in a peak cable displacement of 28.6 cm. It is

evident from these figures also that the response is governed by the first and second symmetric modes which is related to the frequency of the generated ground motion.

Figures 4.28 and 4.29 show the vertical displacement time history of the cable mid-point considering the incoherency effect only and using model I and model II, respectively. These figures show that using model I, as the propagation velocity increases the response approaches that of the uniform excitation case. On the other hand, using model II results in a response that has a slight difference from the uniform excitation case regardless of the propagation velocity. Figure 4.30 shows the vertical displacement time history of the cable mid-point considering the wave travel effect only. Similar to the transverse displacement of the cable shown in figure 4.22, the response approaches the uniform excitation case as the velocity approaches infinity.

The wave propagation velocity has a significant effect on the cable displacement. Considering the incoherency effect alone and using model I, for example, the maximum displacement near the towers corresponds to V = 500 m/s. Near the middle of the cable, the maximum response corresponds to V = 1000 m/s.

4.5.2 Internal Forces in Transmission Line Elements

Table 4.5 shows the maximum forces developed in transmission tower members due to the vertical component of ground motion. This table indicates that the forces in the transmission tower members are very small as compared to those developed by the horizontal component of ground motion. The variation in these forces due to multiple support excitation is very small and insignificant.

The maximum tension developed in the cable due to vertical ground motion is shown in table 4.6. The maximum tension in the cable due to the effect of uniform ground motion is 5.00 kN. The maximum tension developed in the cable in case of multiple support excitation is 6.18 kN for the case of incoherency effect only using model I. However, these values are less than 20% of the tension developed in the cable due to its own weight which equals to 37.08 kN.

4.5.3 Effect of the Coherency Model

The type of coherency model used to generate the ground motion may have an influence on the response of transmission lines for small values of wave propagation velocities. Figure 4.31 shows the maximum value of vertical cable displacement using different coherency models and different propagation velocities. It is evident from this figure that at high propagation velocities, if both the incoherency and wave travel effects are considered in the analysis, then the value of the maximum total cable displacement is not affected by the type of the coherency model. Tables 4.5 and 4.6 show that the type of coherency model used has no specific effect on the internal forces in the tower and the cables.

4.5.4 Incoherency Versus Wave Travel Effects

The purpose of this section is to examine the effect of considering the wave travel effect alone or in addition to the incoherency effects in analyzing the response of transmission lines to vertical ground motion. Figure 4.31 shows that considering the wave travel effect alone reduces the maximum vertical displacement of cables, as compared to the uniform

support excitation case, for V > 250 m/s. For V = 250 m/s, the wave travel effect increases the cable displacement.

Considering the incoherency effect with the wave travel increases the response than the uniform excitation case for all coherency models and for V ≥ 1000 m/s. For the lower wave propagation speeds (V = 250 or 500 m/s), the vertical cable displacement is less than that of the uniform support excitation case.

4.6 SUMMARY

In this chapter the procedure to analyze the effect of multiple support excitation on the response of transmission line systems is presented. The method is used to analyze the response of the transmission line to transverse as well as vertical excitations. An artificially generated ground motion is developed, using random vibration approach, and used in the analysis.

The generated ground motion takes into account the incoherency of seismic waves as well as the wave travel effect. Two different coherency models are used in the analysis. Clough-Penzien power spectrum is used in the analysis with the appropriate coefficients. Ground displacements are generated at distances 400 m apart which represents the typical span of the line in the considered example.

A simplified approach to predict the structural response to multiple support excitation is presented. The approach is based on the use of displacement time histories at the structure supports. The approach is verified against the traditional approach where acceleration time histories are specified. The results show complete agreement between the two approaches.

The results of the analysis carried out on the transmission lines are presented. The following are the main findings:

1. The case of uniform support excitation does not produce the maximum response in the transmission line. Multiple support excitation, which is a more realistic assumption, can result in larger displacements and internal forces.
2. The assumed velocity of propagation of seismic waves has a significant effect on the response of transmission lines to seismic ground motion. In order to obtain a representative analysis of the transmission line, an accurate estimation of the wave velocity is required.
3. Considering the wave travel effect only, may reduce the displacement of the cable as compared to the uniform excitation case. However, if the incoherency effect is considered with the wave travel effect, the cable displacement increases over the case of uniform excitation.
4. The additional tension in transmission line cables due to transverse ground motion is small. Moreover, the change in the tension when considering multiple support excitation is negligible. On the other hand, the vertical component of ground motion produces higher values of tension in the cable but it is still less than 20% of the tension developed in the cable due its own weight.
5. The variation in member forces in transmission towers due to multiple support excitation in the transverse direction can be as high as 35%. On the other hand, the vertical component of ground motion produces negligible forces in transmission towers and therefore, the variation in these forces is insignificant.
6. The type of the coherency model used does not have a significant effect on the total response of transmission lines.

Table 4.1 Power spectral density filter parameters for horizontal ground motion (Der Kiureghian and Neuenhofer 1991)

Soil type	ω_g (rad/s)	ξ_g	ω_f (rad/s)	ξ_f
Firm	15.0	0.6	1.5	0.6
Medium	10.0	0.4	1.0	0.6
Soft	5.0	0.2	0.5	0.6

Table 4.2 Power spectral density filter parameters for vertical ground motion (Elghadamsi et al. 1988)

Soil type	ω_g (Hz)	ξ_g
Alluvium	4.17	0.46
Alluvium / Rock	4.63	0.46
Rock	6.18	0.46

Table 4.3 Maximum forces in tower members due to transverse ground motion (kN)

Effect considered		Propagation velocity (m/s)			
		250	500	1000	2000
Considering wave travel only		104.5	112.8	107.6	111.9
Considering incoherency only	Model I	114.8	129.5	109.1	98.1
	Model II	103.4			
Considering both effects	Model I	118.2	116.6	102.8	115.7
	Model II	102.7	111.4	101.2	113.0

Table 4.4 Maximum tension in cables due to transverse ground motion (kN)

Effect considered		Propagation velocity (m/s)			
		250	500	1000	2000
Considering wave travel only		0.78	0.88	0.88	0.98
Considering incoherency only	Model I	0.78	0.98	1.08	1.08
	Model II	1.18			
Considering both effects	Model I	0.78	0.88	0.88	0.98
	Model II	0.78	1.08	1.08	1.08

Table 4.5 Maximum forces in tower members due to vertical ground motion (kN)

Effect considered		Propagation velocity (m/s)			
		250	500	1000	2000
Considering wave travel only		4.22	4.02	4.22	4.32
Considering incoherency only	Model I	4.22	4.52	4.32	4.42
	Model II	4.41			
Considering both effects	Model I	4.32	3.83	4.12	4.42
	Model II	4.22	3.92	4.32	4.51

Table 4.6 Maximum tension in cables due to vertical ground motion (kN)

Effect considered		Propagation velocity (m/s)			
		250	500	1000	2000
Considering wave travel only		3.83	2.16	4.12	4.81
Considering incoherency only	Model I	4.51	6.18	6.08	5.10
	Model II	5.69			
Considering both effects	Model I	3.14	2.75	4.61	4.91
	Model II	4.22	2.55	4.71	5.49

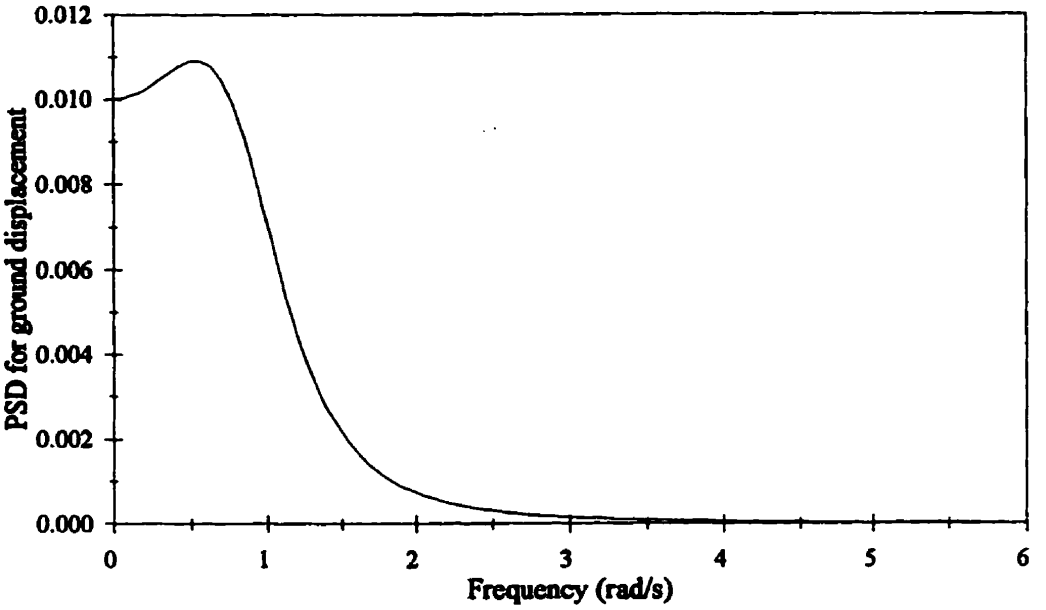

Figure 4.1 Power spectral density function for the horizontal component of ground motion

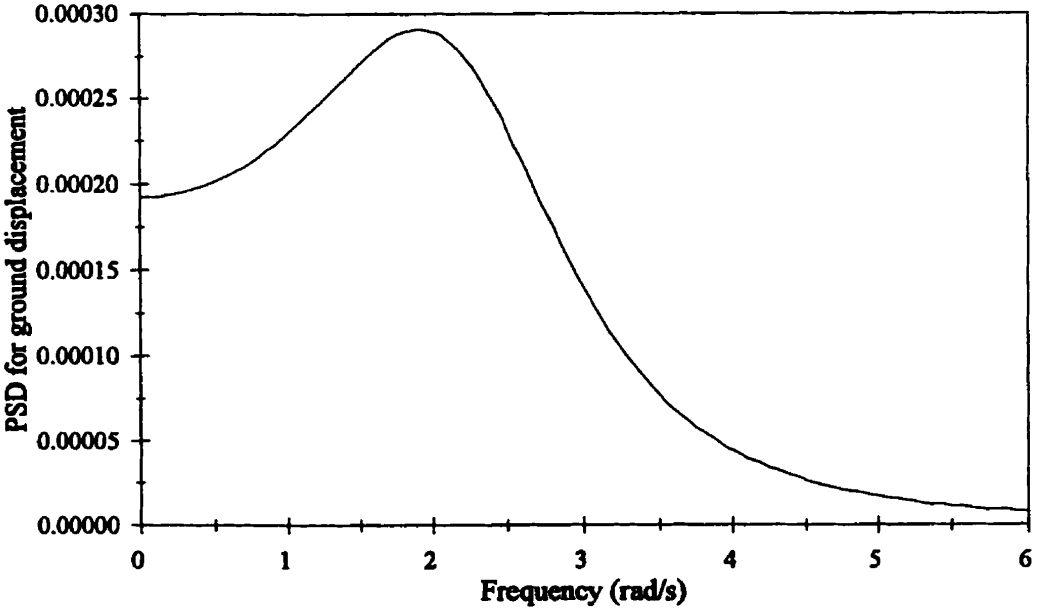

Figure 4.2 Power spectral density function for the vertical component of ground motion

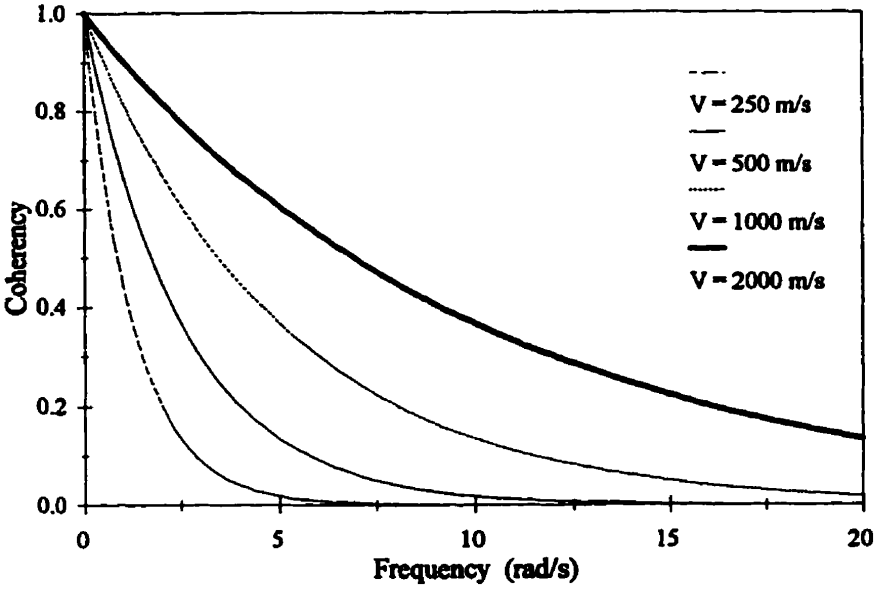

Figure 4.3 Change in coherency with the frequency of ground motion using model I

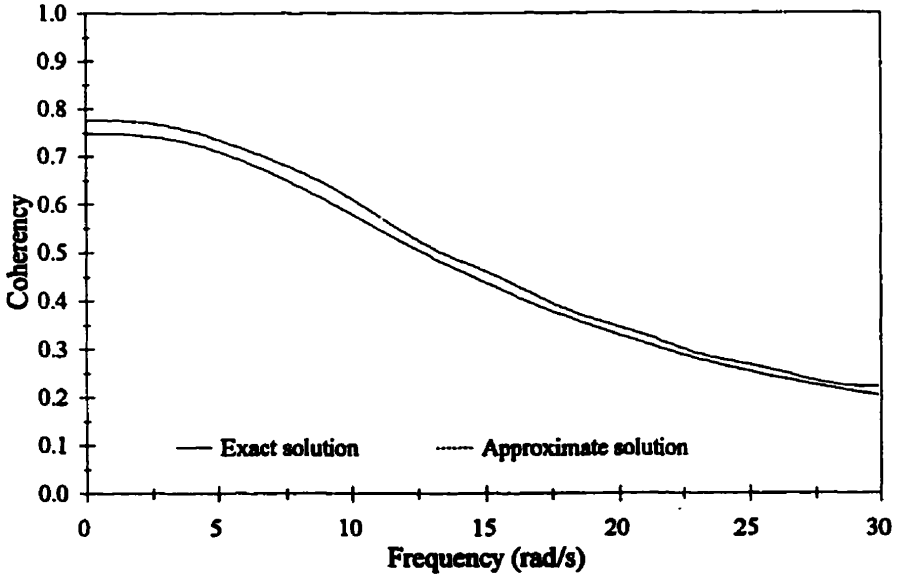

Figure 4.4 Change in coherency with the frequency of ground motion using model II

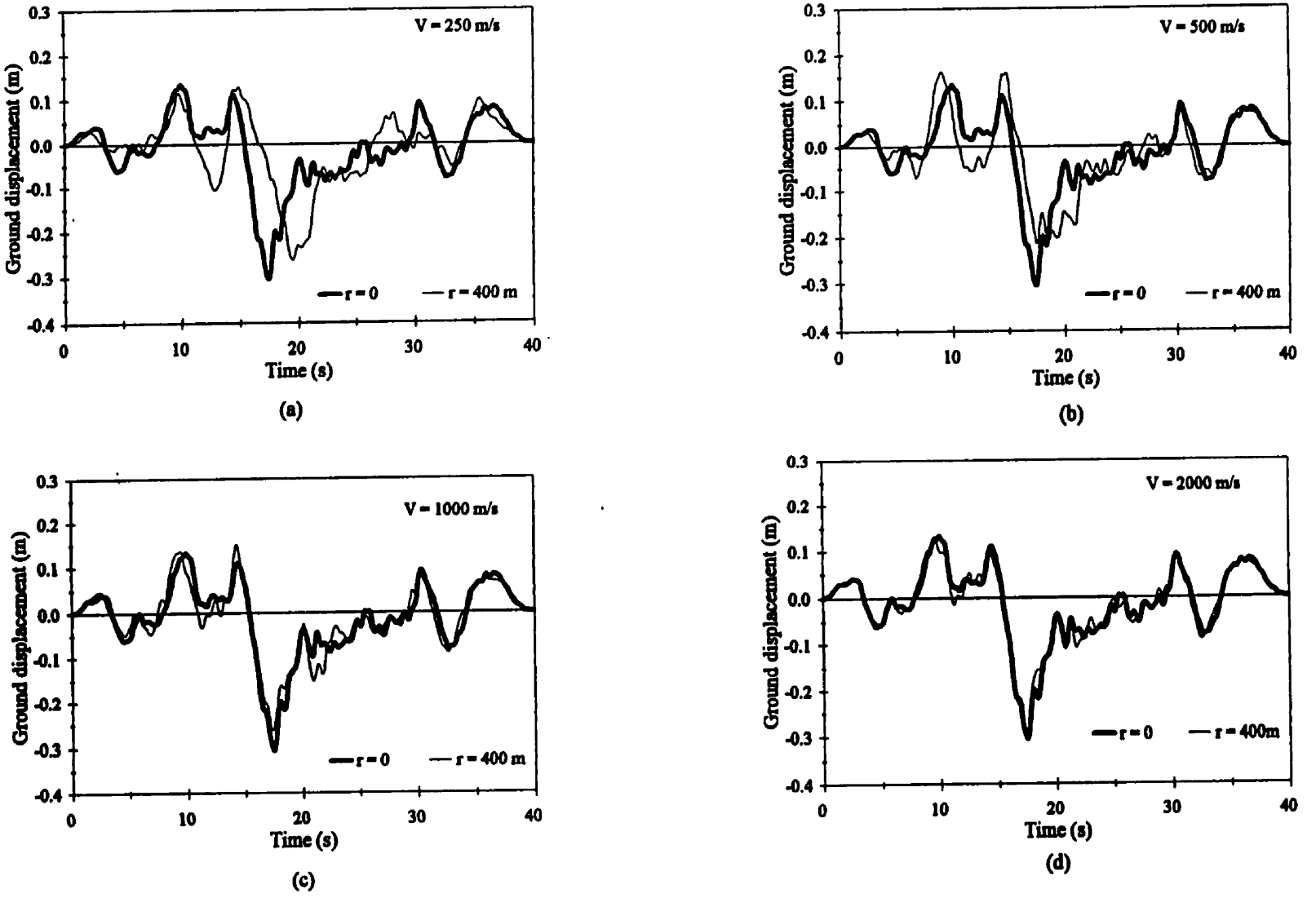

Figure 4.5 Generated horizontal ground displacement using model I and considering incoherency effect only: (a) V = 250 m/s ; (b) V = 500 m/s ; (c) V = 1000 m/s ; and (d) V = 2000 m/s

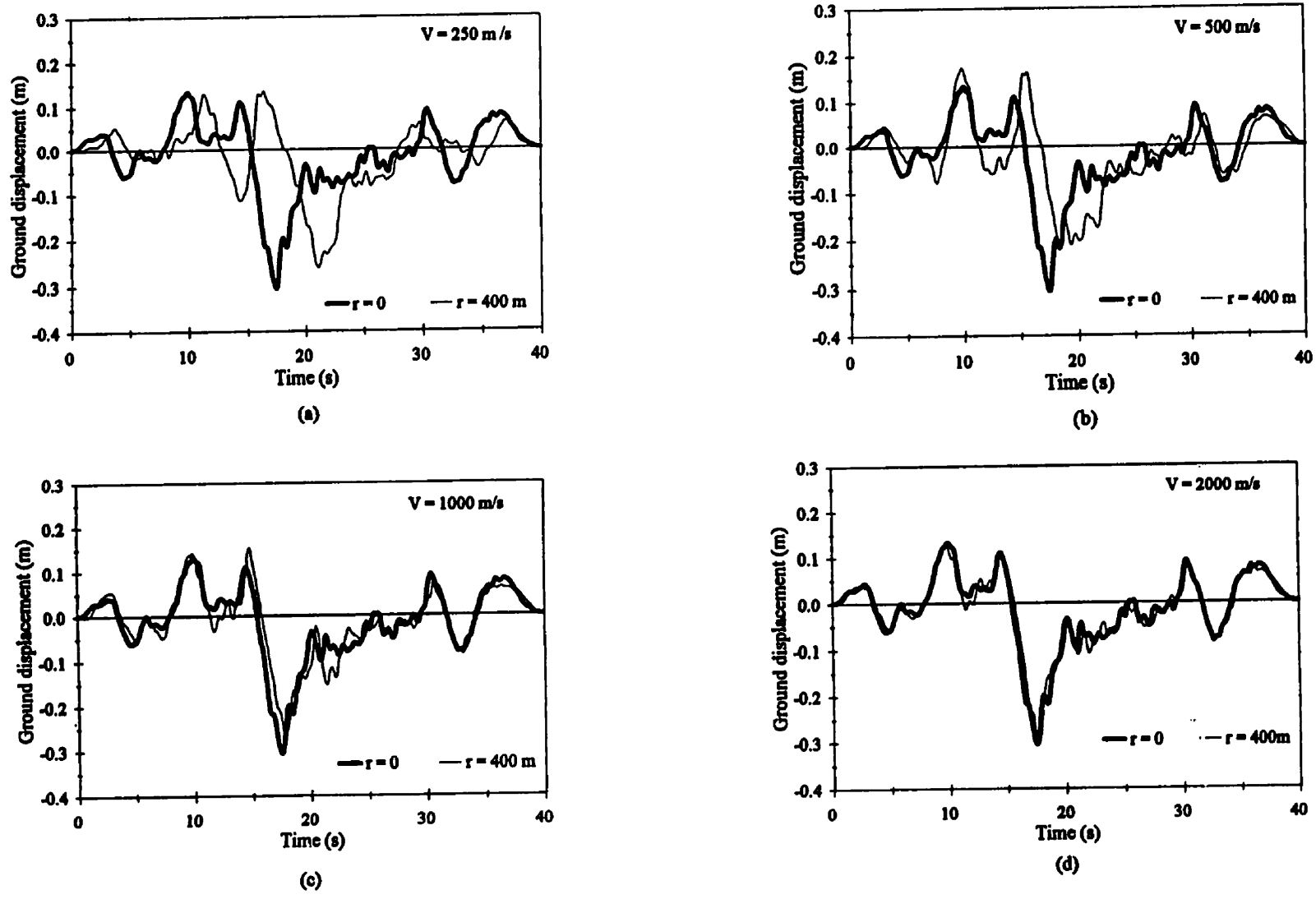

Figure 4.6 Generated horizontal ground displacement using model I and considering both incoherency and wave travel effects: (a) V = 250 m/s ; (b) V = 500 m/s ; (c) V = 1000 m/s ; and V = 2000 m/s

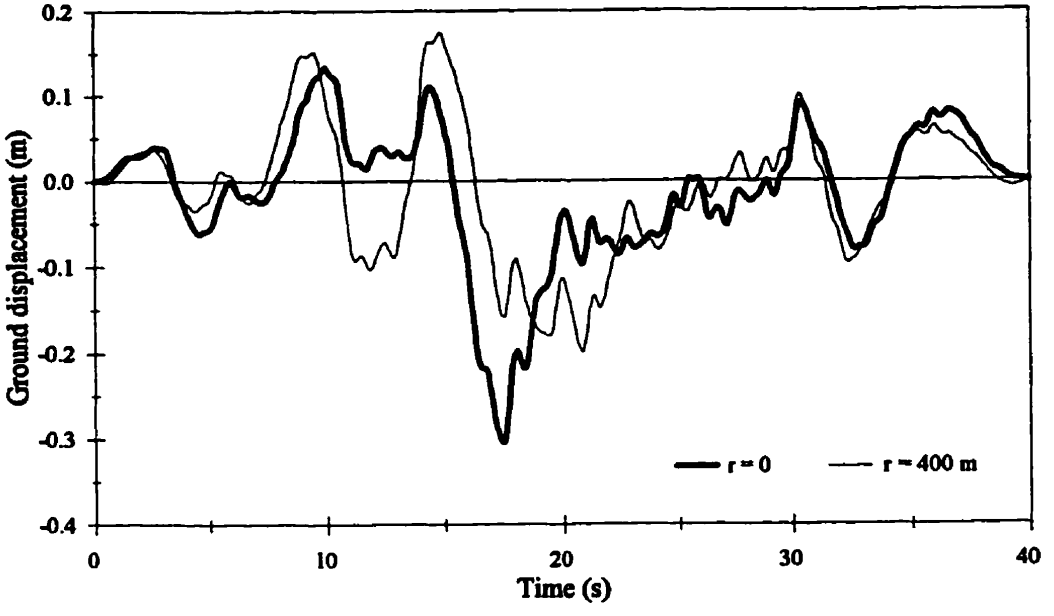

Figure 4.7 Generated horizontal ground displacement using model II and considering incoherency effect only

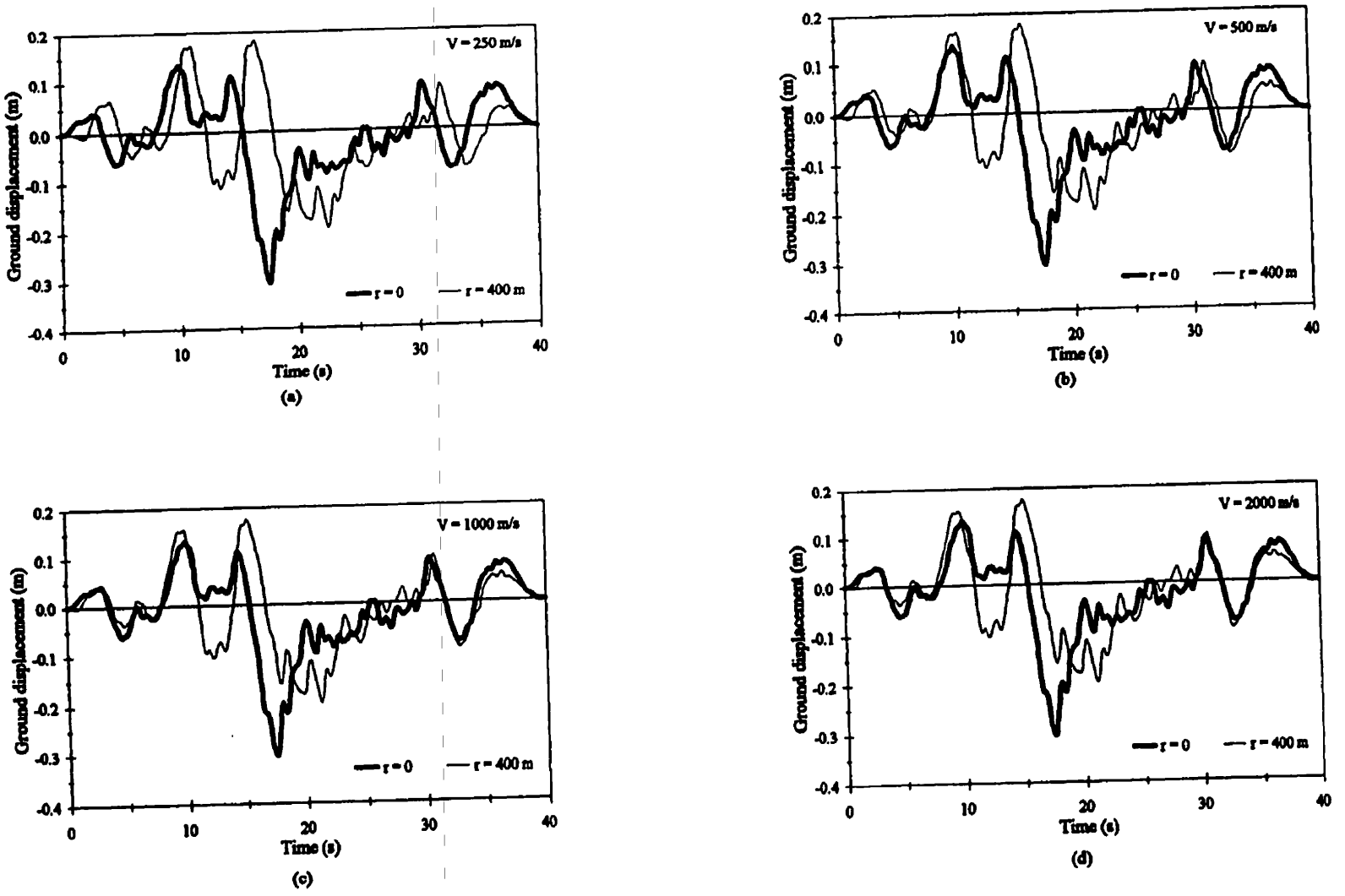

Figure 4.8 Generated horizontal ground displacement using model II and considering both incoherency and wave travel effects: (a) V = 250 m/s; (b) V = 500 m/s; (c) V = 1000 m/s; and V = 2000 m/s

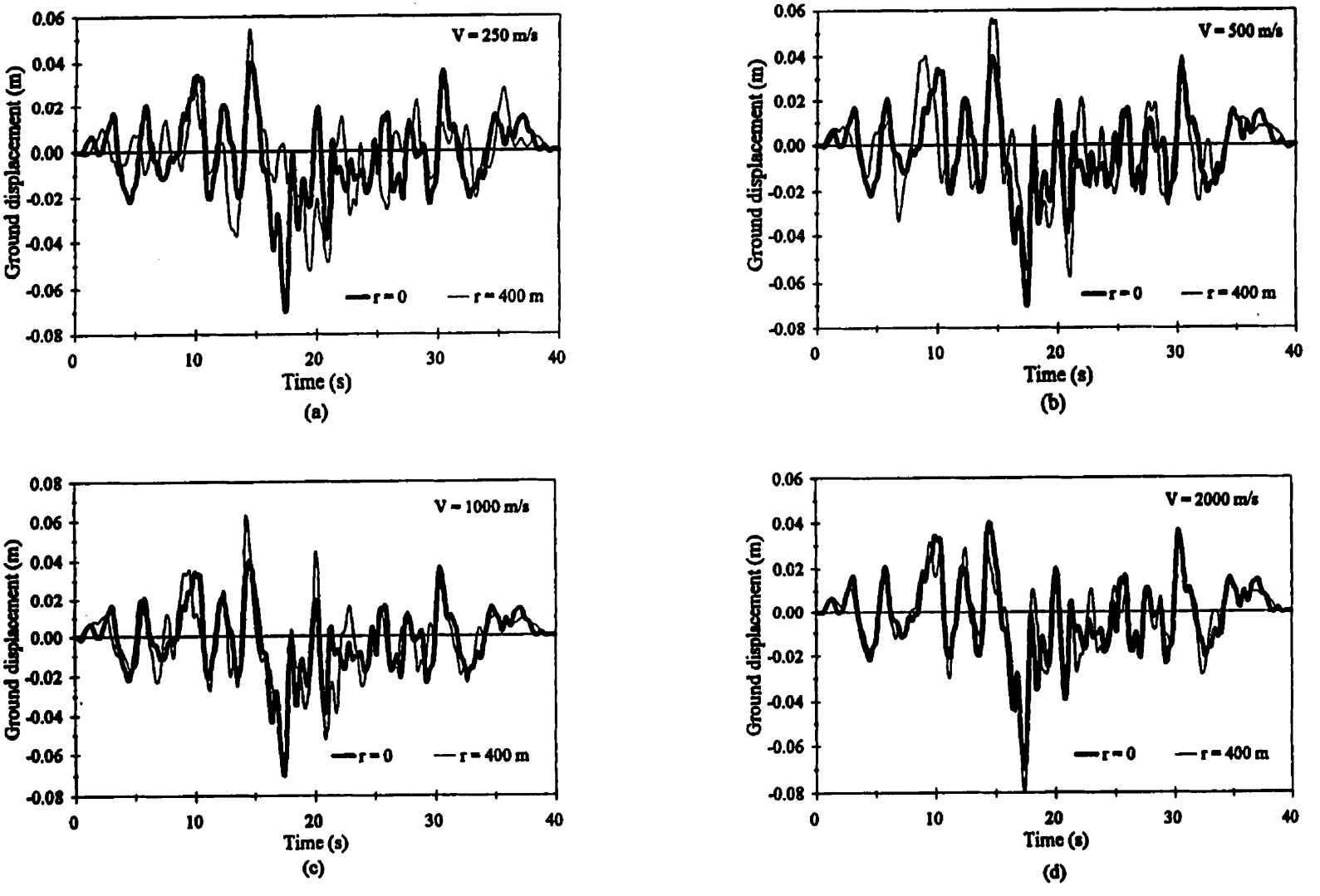

Figure 4.9 Generated vertical ground displacement using model I and considering incoherency effect only: (a) V = 250 m/s ; (b) V = 500 m/s ; (c) V = 1000 m/s ; and V = 2000 m/s

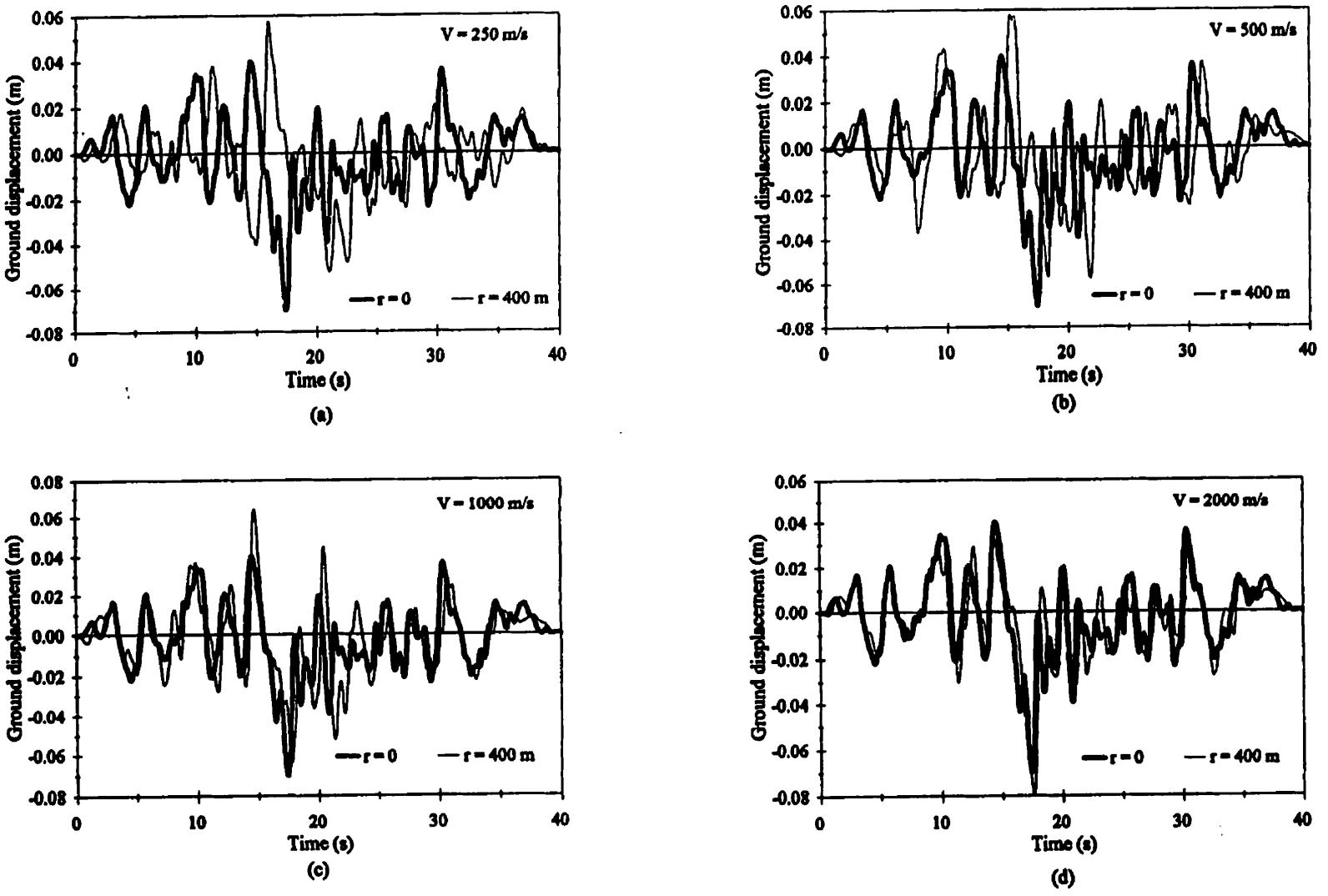

Figure 4.10 Generated vertical ground displacement using model I and considering both incoherency and wave travel effects: (a) V = 250 m/s ; (b) V = 500 m/s ; (c) V = 1000 m/s ; and (d) V = 2000 m/s

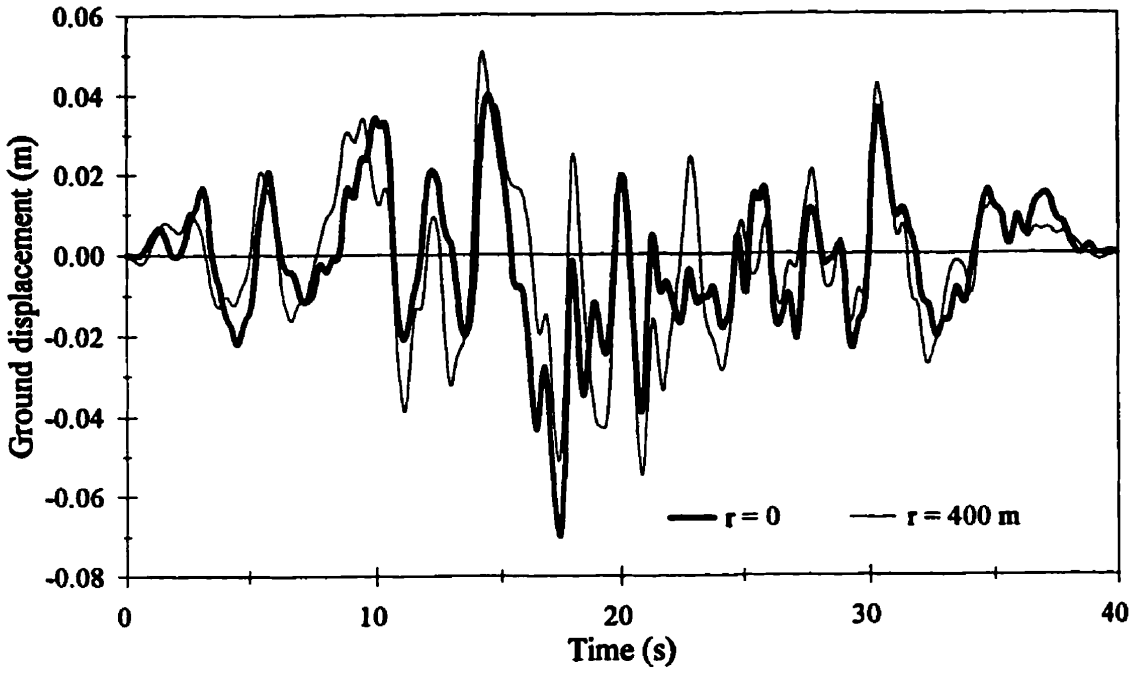

Figure 4.11 Generated vertical ground displacement using model II and considering incoherency effect only

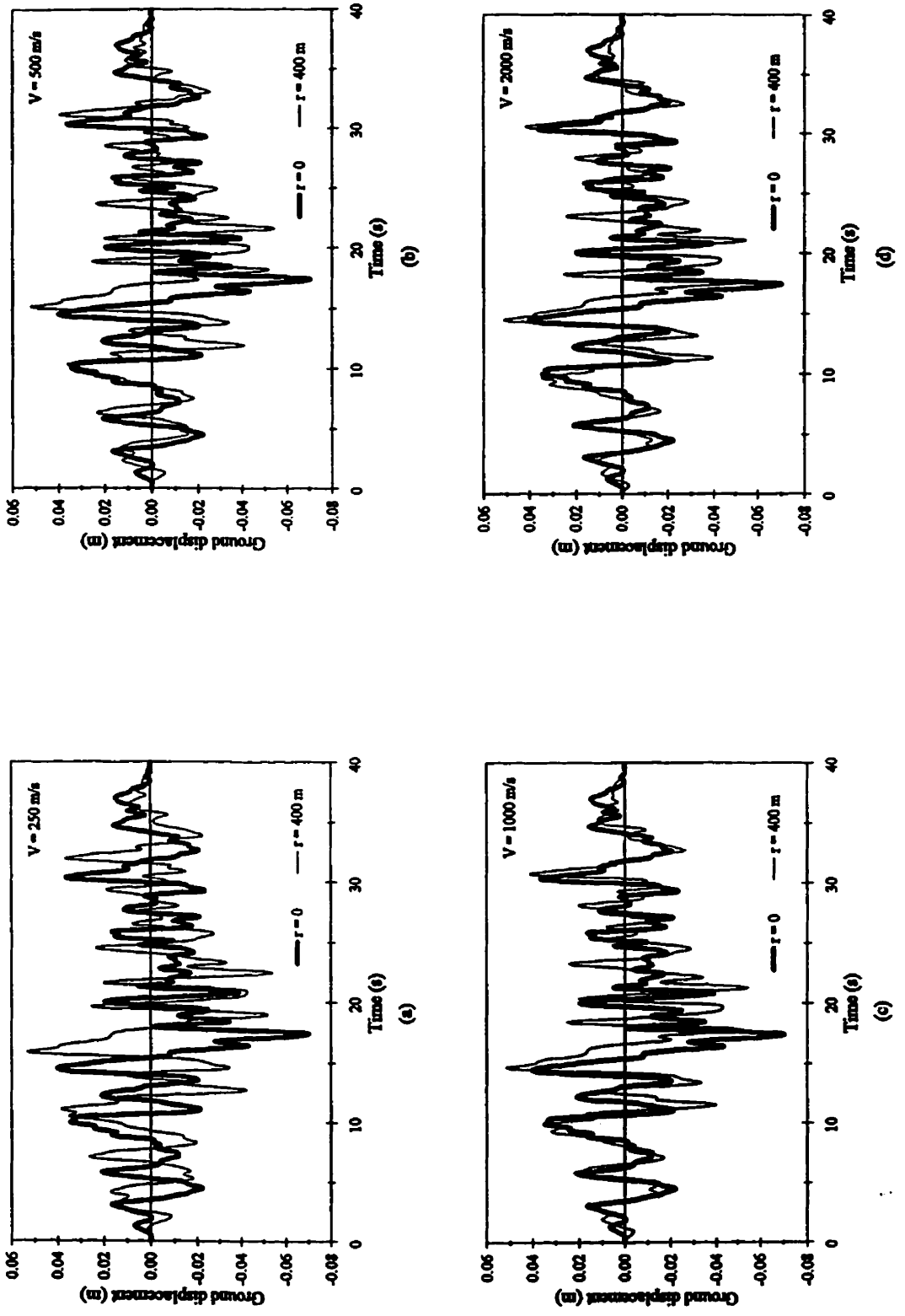

Figure 4.12 Generated vertical ground displacement using model II and considering both incoherency and wave travel effects: (a) V = 250 m/s; (b) V = 500 m/s; (c) V = 1000 m/s; and V = 2000 m/s

First tower support

Second tower support

(a) Specified support displacement

First tower support

Second tower support

(b) Specified dynamic forces

Figure 4.13 Simplified approach for ground motion application

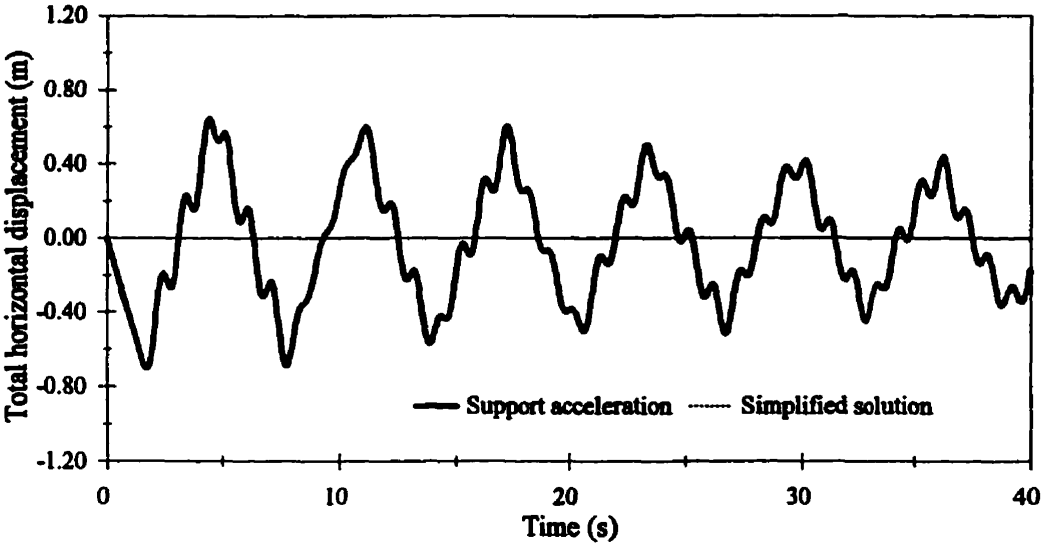

Figure 4.14 Transverse displacement time history of the cable mid-point due to sinusoidal ground motion with 1 Hz frequency

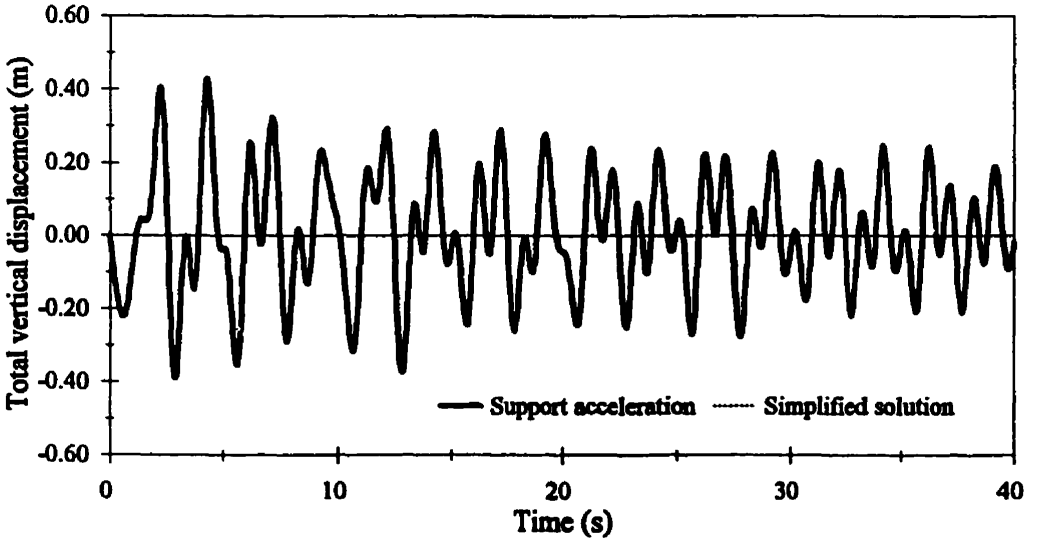

Figure 4.15 Vertical displacement time history of the cable mid-point due to sinusoidal ground motion with 1 Hz frequency

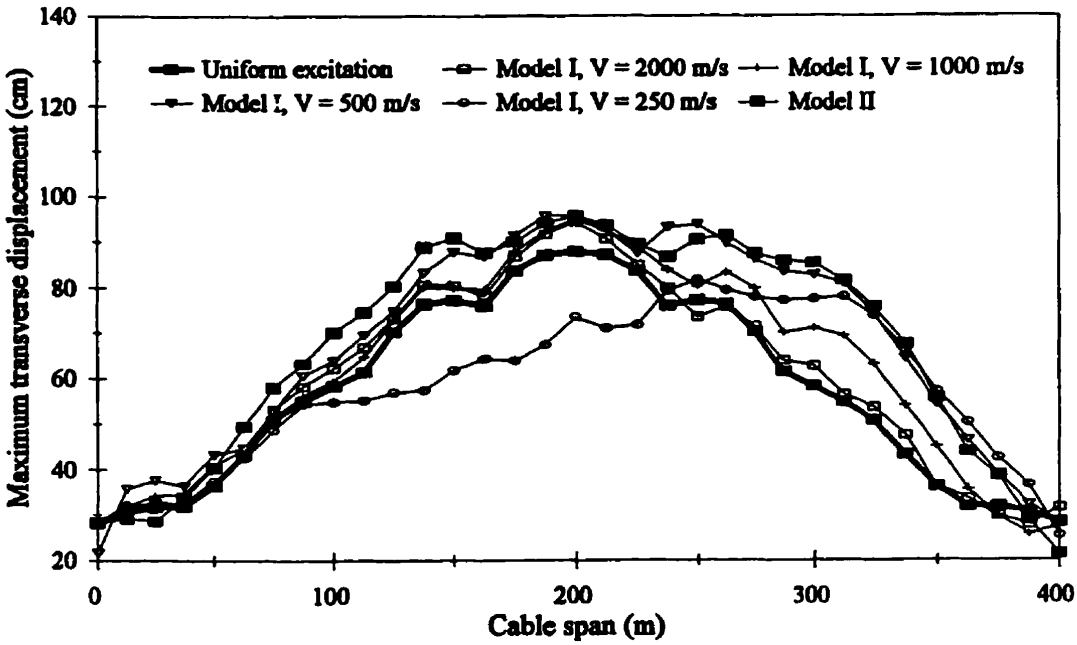

Figure 4.16 Envelopes of total peak cable transverse displacement considering incoherency effect only

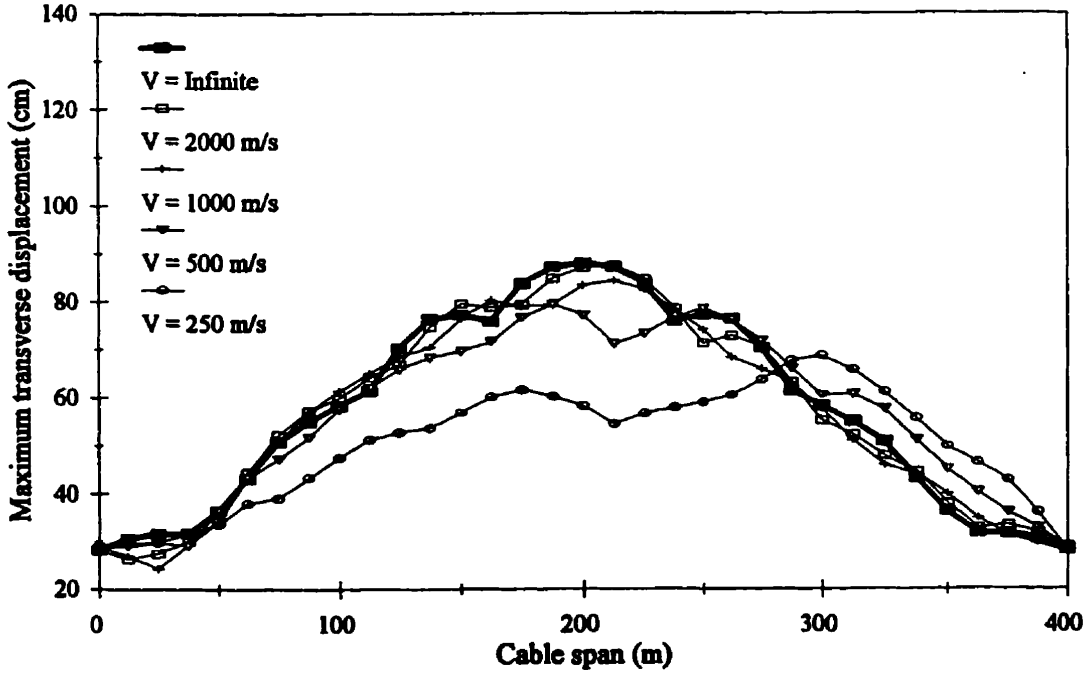

Figure 4.17 Envelopes of total peak cable transverse displacement considering wave travel effect only

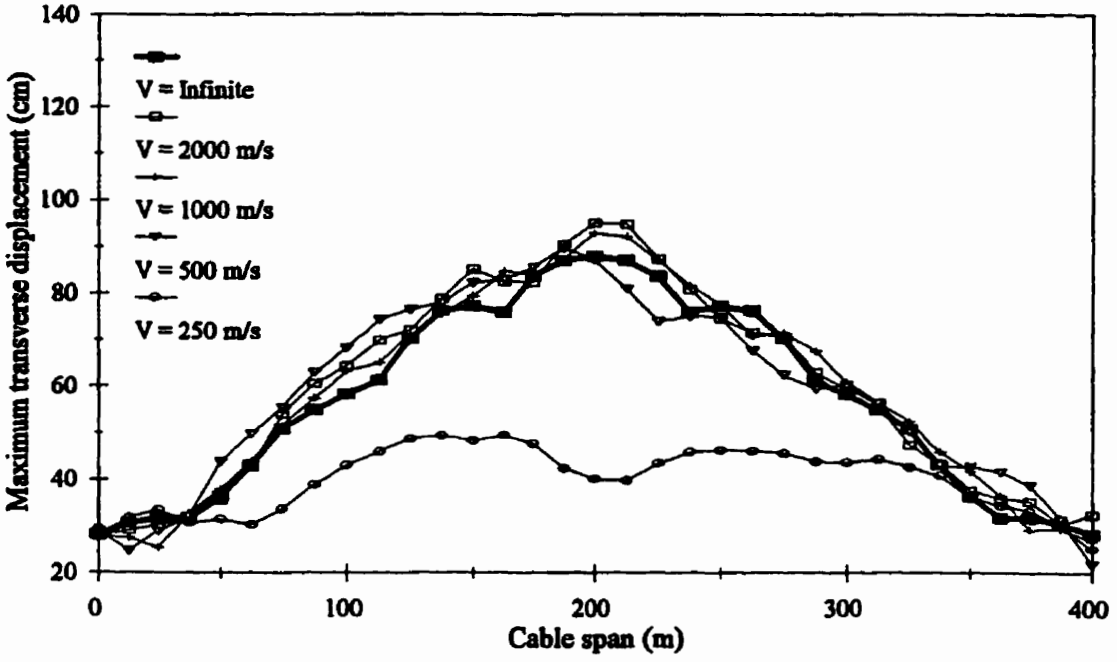

Figure 4.18 Envelopes of total peak cable transverse displacement considering incoherency and wave travel effects (model I)

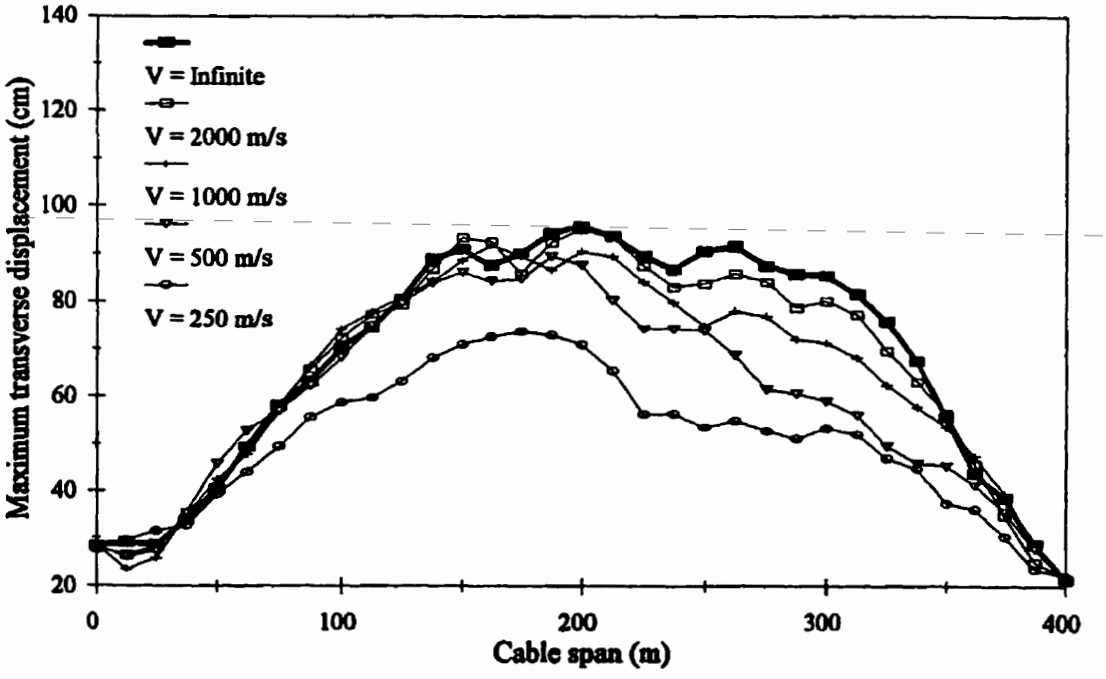

Figure 4.19 Envelopes of total peak cable transverse displacement considering incoherency and wave travel effects (model II)

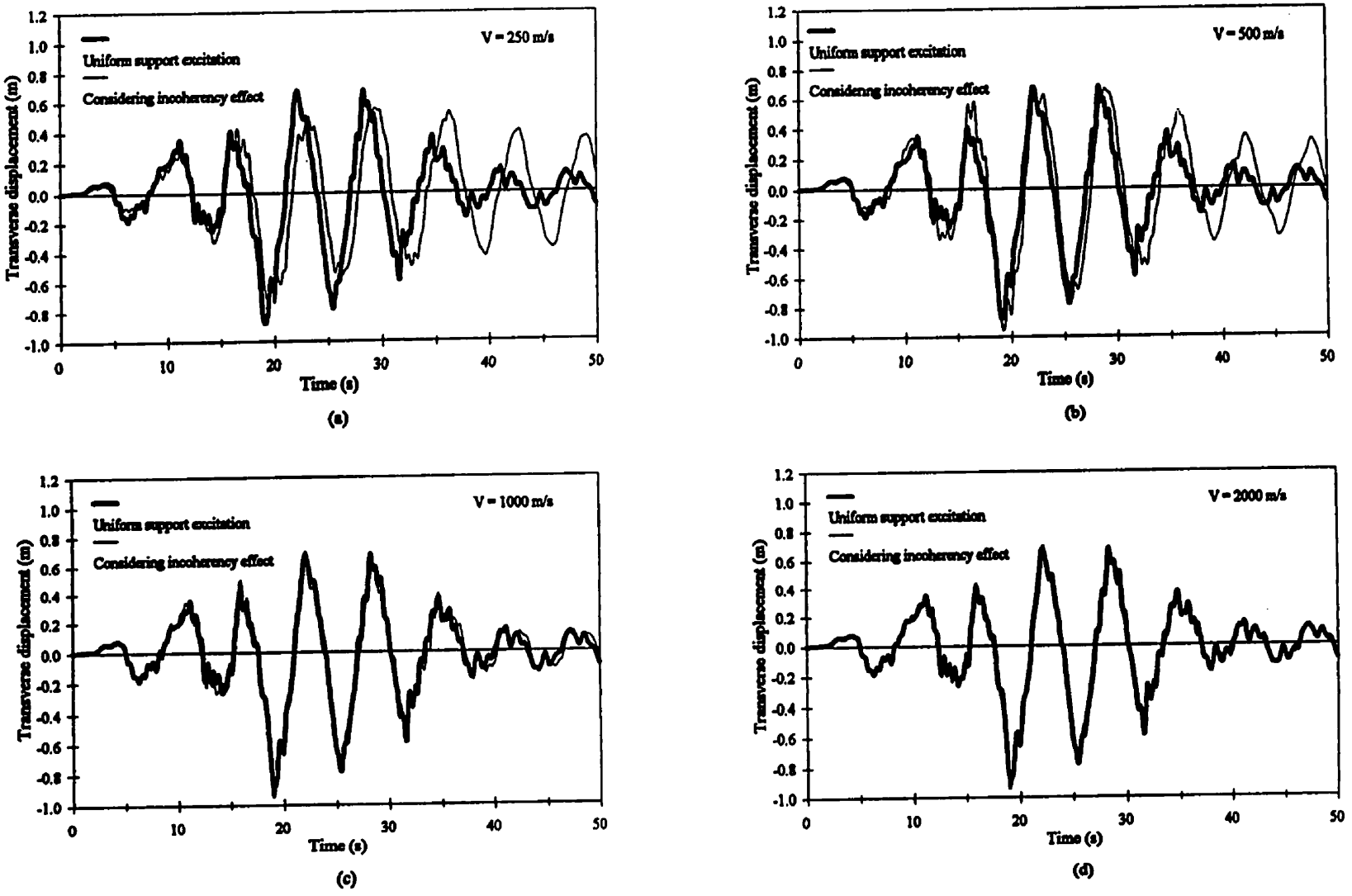

Figure 4.20 Transverse displacement of cable mid-point considering incoherency effect only (model I) : (a) V = 250 m/s; (b) V = 500 m/s; (c) V = 1000 m/s; and (d) V = 2000 m/s

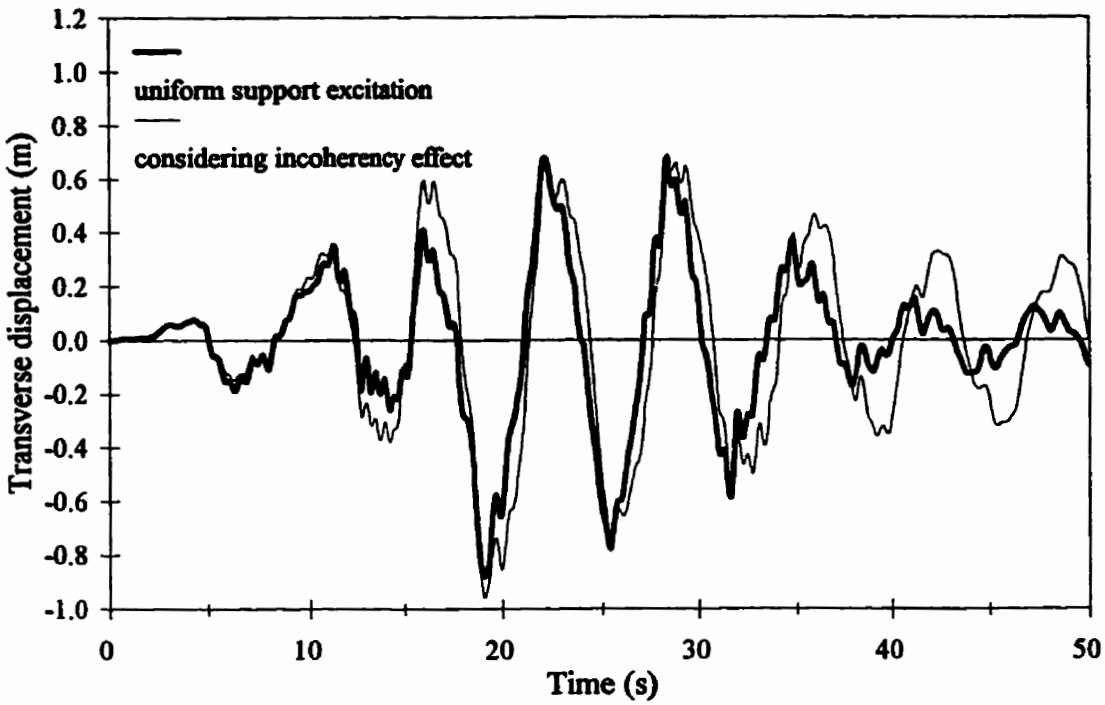

Figure 4.21 Transverse displacement of cable mid-point considering incoherency effect only (model II)

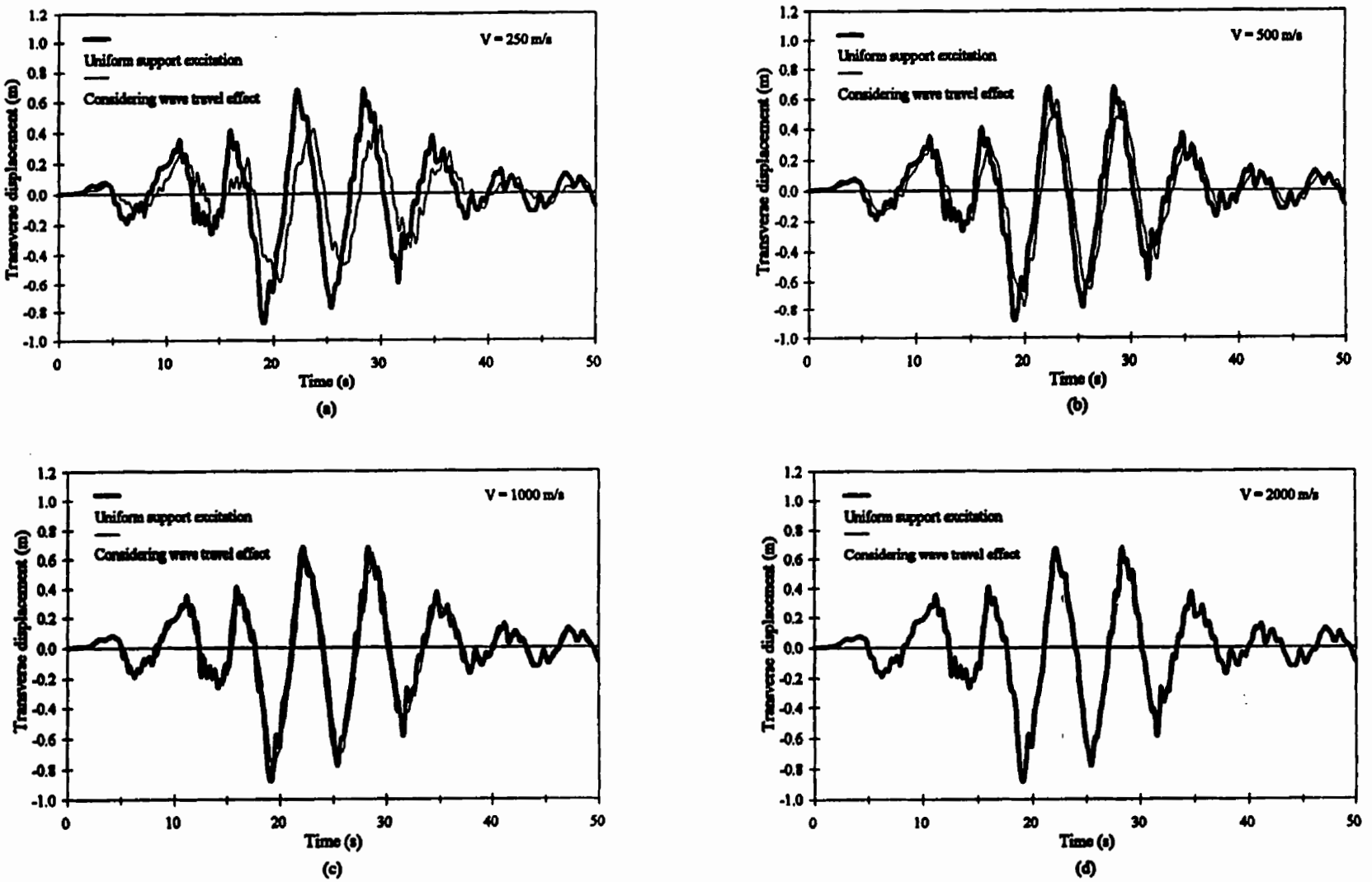

Figure 4.22 Transverse displacement of cable mid-point considering wave travel effect only: (a) V = 250 m/s; (b) V = 500 m/s; (c) V = 1000 m/s; and (d) V = 2000 m/s

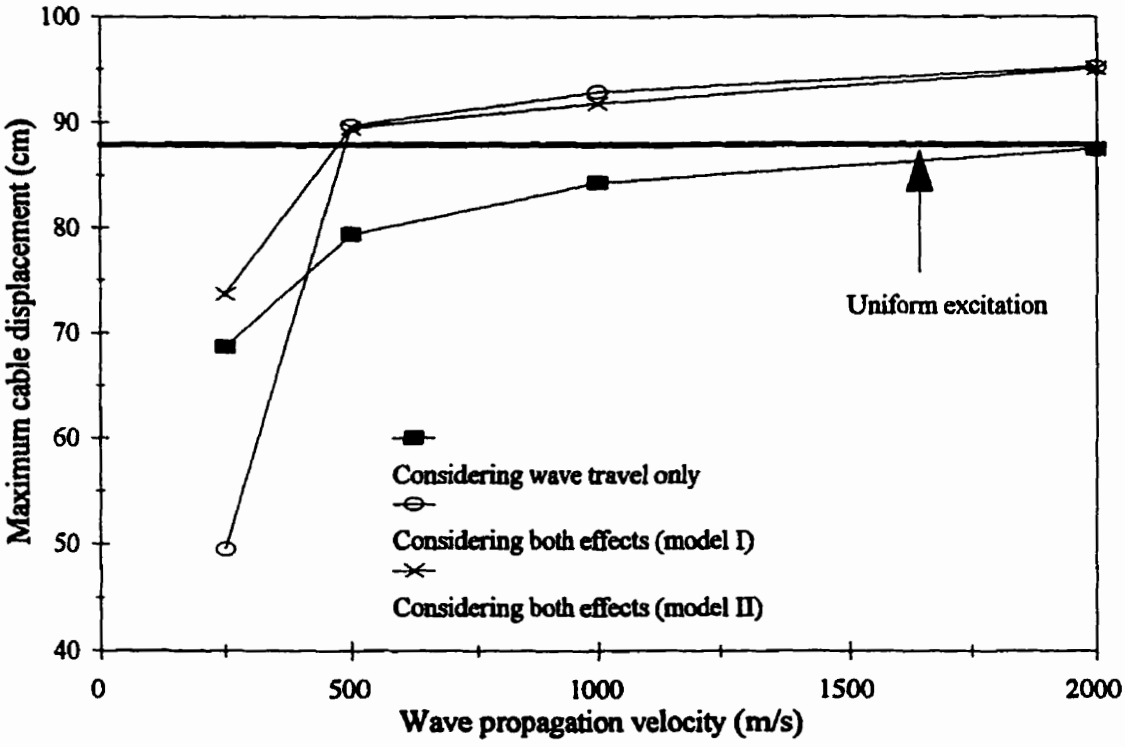

Figure 4.23 Effect of propagation velocity and coherency model on the maximum cable displacement due to transverse ground motion

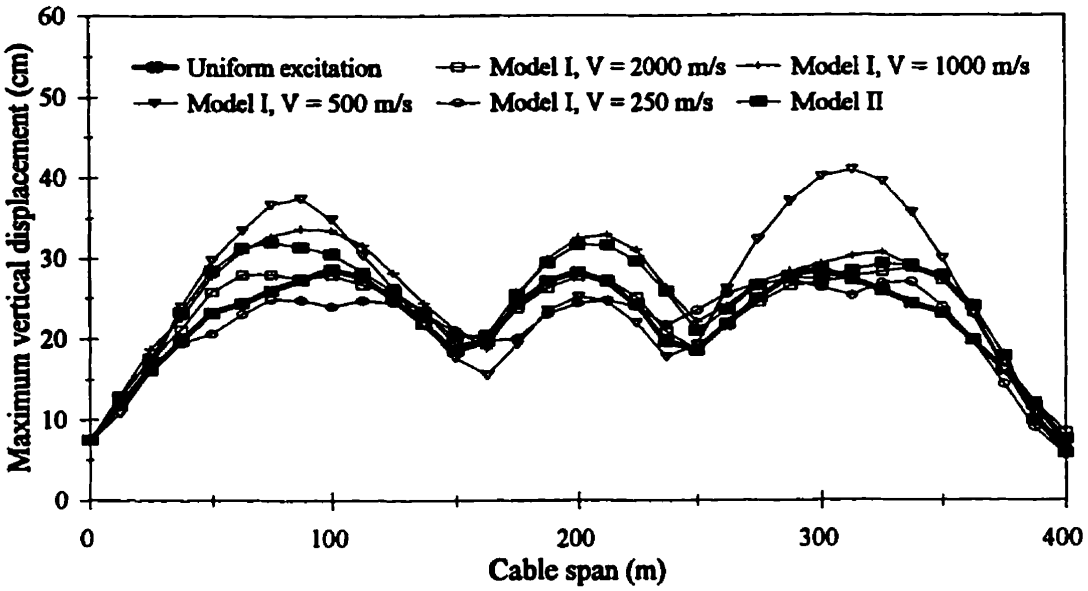

Figure 4.24 Envelopes of total peak cable vertical displacement considering incoherency effect only

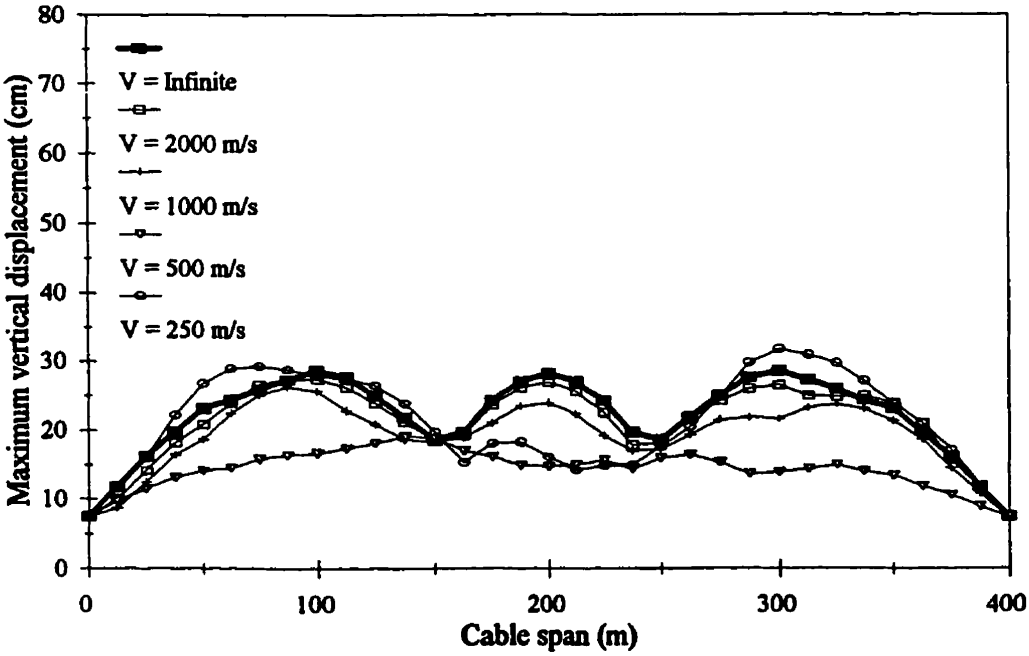

Figure 4.25 Envelopes of total peak cable vertical displacement considering wave travel effect only

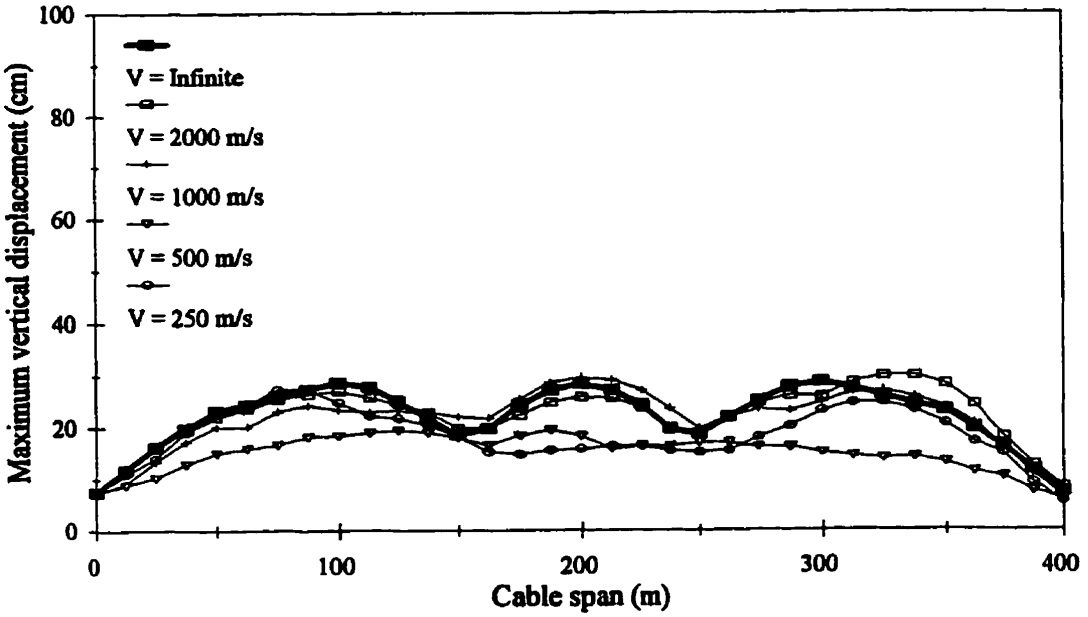

Figure 4.26 Envelopes of total peak cable vertical displacement considering incoherency and wave travel effects (model I)

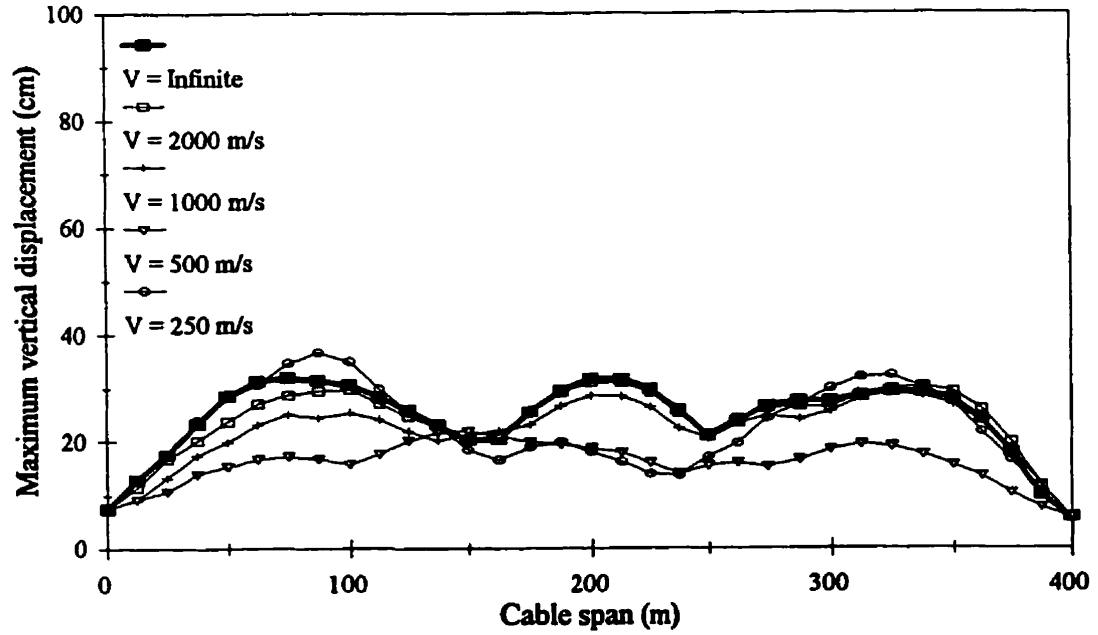

Figure 4.27 Envelopes of total peak cable vertical displacement considering incoherency and wave travel effects (model II)

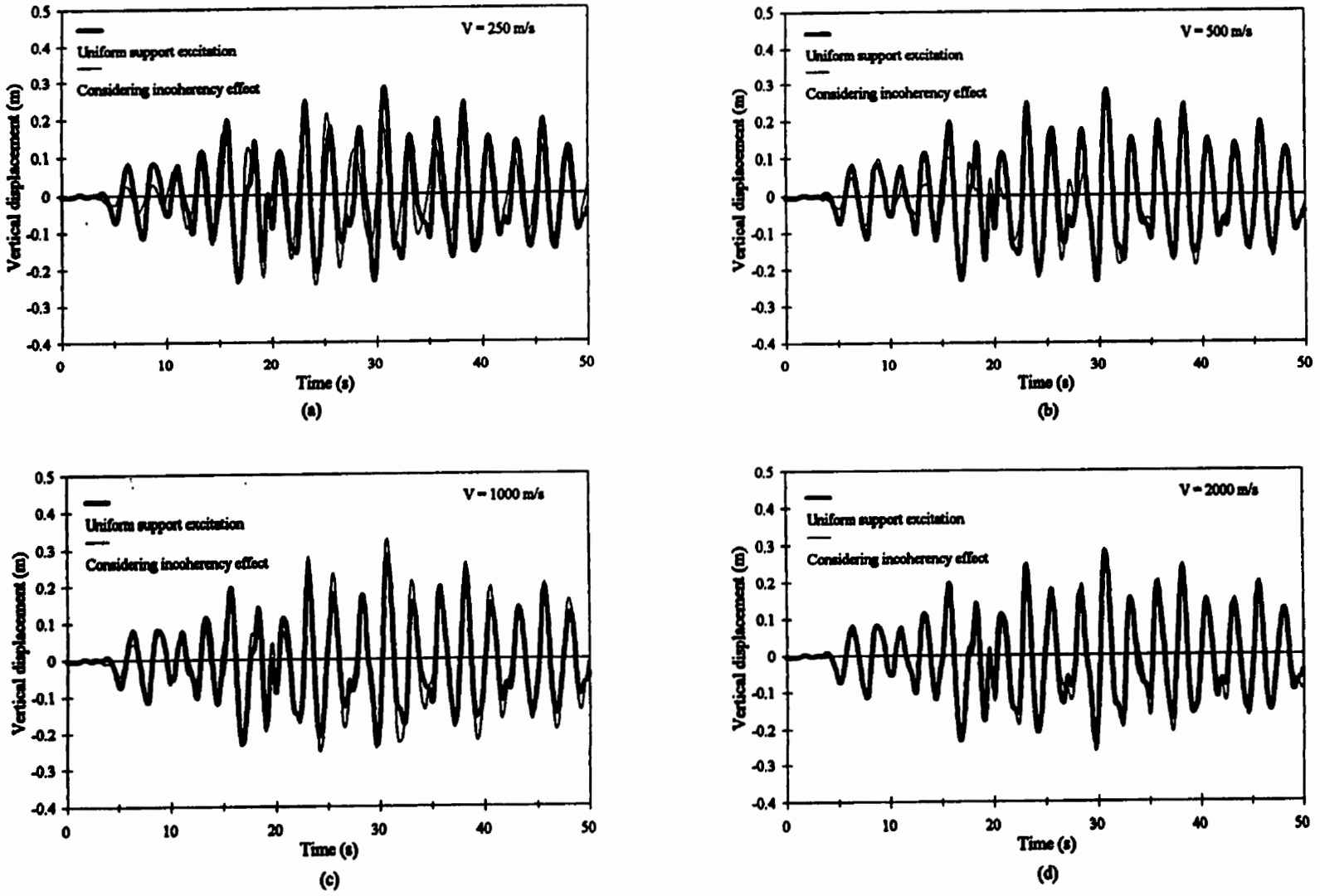

Figure 4.28 Vertical displacement of cable mid-point considering incoherency effect only (model I) : (a) V = 250 m/s; (b) V = 500 m/s; (c) V = 1000 m/s; and (d) V = 2000 m/s

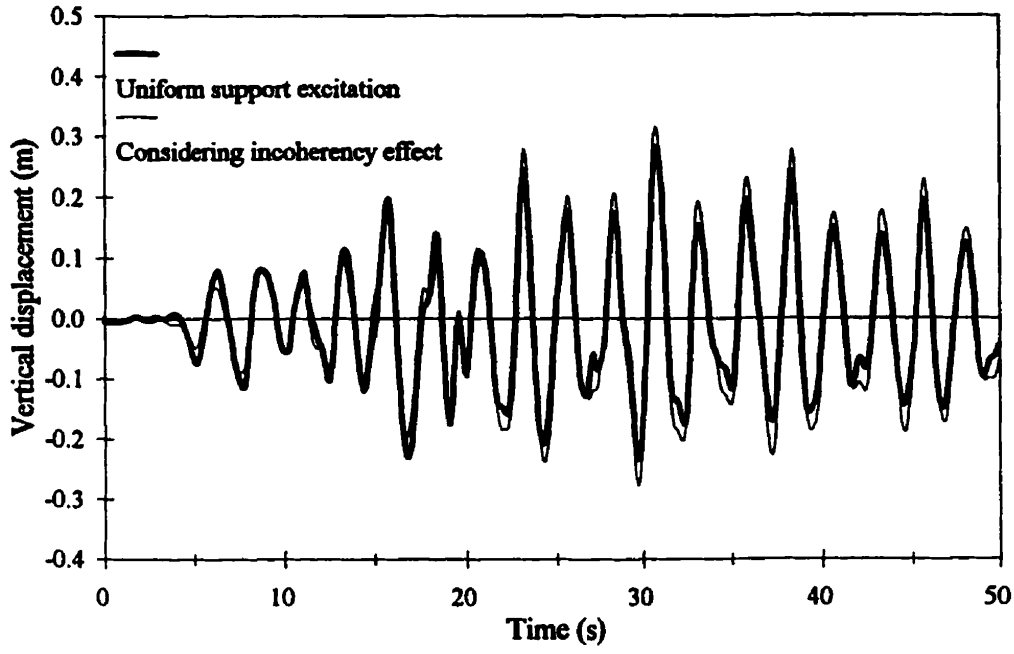

Figure 4.29 Vertical displacement of cable mid-point considering incoherency effect only (model II)

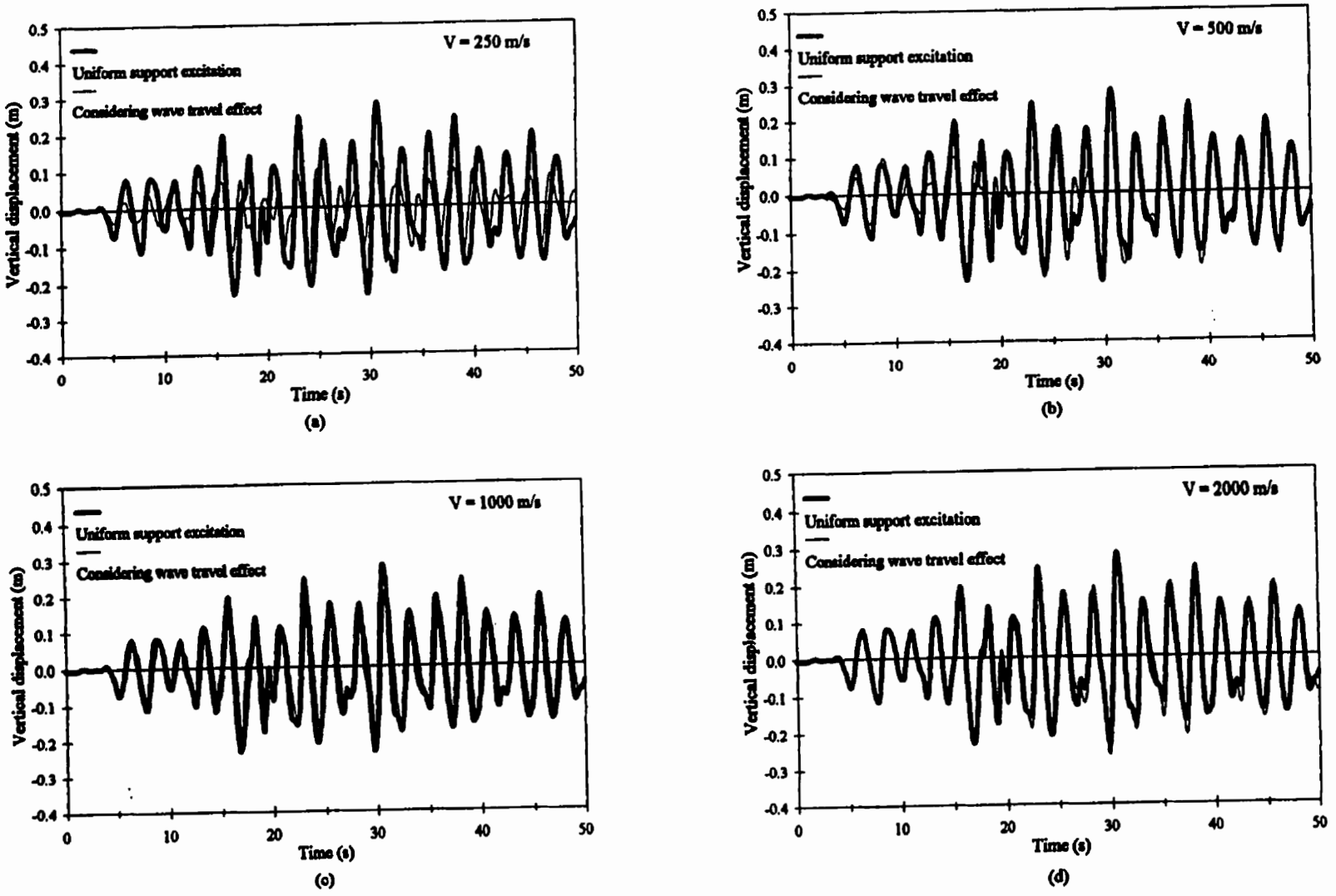

Figure 4.30 Vertical displacement of cable mid-point considering wave travel effect only: (a) V = 250 m/s; (b) V = 500 m/s; (c) V = 1000 m/s; and (d) V = 2000 m/s

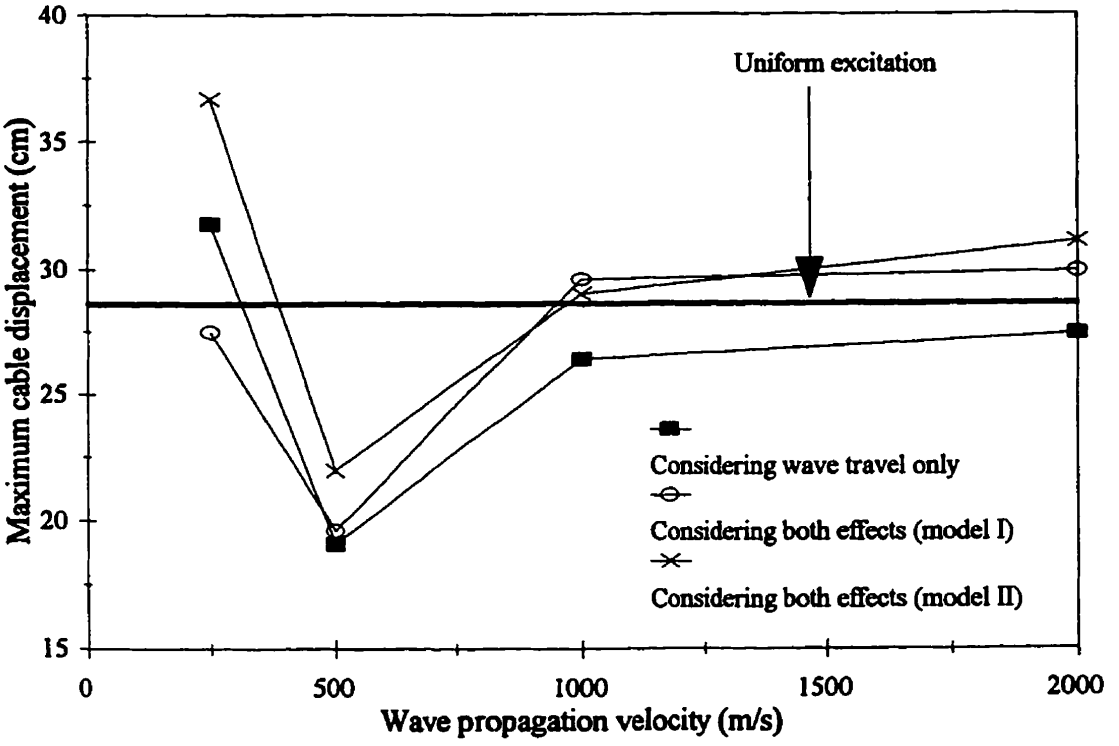

Figure 4.31 Effect of propagation velocity and coherency model on the maximum cable displacement due to vertical ground motion

CHAPTER 5

ANALYTICAL SOLUTION OF CABLE VIBRATION

5.1 GENERAL

Analytical solutions for nonlinear systems such as asymptotic methods yield satisfactory approximate solutions specially when the nonlinearity is small. Numerical techniques such as the finite element and the finite difference methods, although powerful tools in the analysis and design of nonlinear systems, still fail to reveal important features of the nonlinear cable behaviour (subharmonic and superharmonic oscillations, for example). It is therefore important to obtain as much information as possible from the analytical solution beside using the numerical methods.

The free vibration characteristics of cables were determined analytically in two and three dimensions. In earlier studies, Irvine and Caughey (1974) treated the cable dynamics as a linear problem in order to determine its frequencies of free vibration. Later on, the nonlinear nature of the problem was addressed by Hagedorn and Schafer (1980). The three dimensional free vibrations of cables were analyzed by Benedettini et al. (1986). Rao and Iyengar (1991b) and Al-Noury and Ali (1985) studied the three dimensional nonlinear forced vibrations of cables under in-plane periodic loads and out-of-plane static loads. Limited research work was conducted on the response of cables to support excitation. Perkins (1992)

used the first order perturbation method to study the case of parametric resonance due to longitudinal support excitation.

A major difficulty that is encountered in the dynamic analysis of long span cables, such as transmission line cables, is that during earthquakes there will be a time lag between the input earthquake ground motions at different supports. The system is subjected to multiple support excitation. The tower was found to respond to the seismic excitation mainly in its own fundamental mode of vibration (El-Attar et al., 1995a). Therefore, the transmission line problem can be reduced to a cable which is subjected to a harmonic excitation with a phase difference between both supports. Rao and Iyengar (1991a) studied the response of long span cables to seismic excitation using the normal modes approach. This approach may not be accurate enough for sagged cables as is the case in transmission lines.

In this chapter, the three-dimensional equations of cable vibration are developed considering the coupling between the in-plane and out-of-plane vibrations. This formulation is applicable to cables with small sag to span ratios where a parabolic approximation of the static equilibrium position can be assumed. This represents the majority of transmission line cables. The support motion is applied in both the vertical and transverse directions. The equations of motion are solved using Galerkin method for the spatial problem and the method of multiple time scales for the temporal problem.

The solution is verified by comparing the results to that of the finite element analysis presented earlier. The stability of the steady state solution is examined. A parametric study is conducted to investigate the effect of the cable sag to span ratio on the amplitude of oscillations and zones of instability. The effect of cable damping is also analyzed. Finally, the

effect of the phase difference between different support excitations on the cable response in the symmetric and anti-symmetric modes is studied.

5.2 EQUATIONS OF CABLE VIBRATION

Consider the dynamic equilibrium of a single cable with weight per unit length, mg, hanging in a vertical plane between two supports at the same level as shown in figure 5.1. If the element length is dS_0, then under tension its length becomes dS where,

$$dS = (1 + \frac{T}{EA})\, dS_0 \tag{5.1}$$

where,

T is the cable tension; E is Young's modulus of the cable material; and A is the cable cross sectional area.

The change in tension across an element of length dS in the x and y directions is given by:

$$\begin{aligned} dT_x &= \frac{\partial}{\partial S}(T\frac{\partial x}{\partial S})\, dS = \frac{\partial}{\partial S_0}(\frac{T}{1 + T/EA}\frac{\partial x}{\partial S_0})\, dS_0 \\ dT_y &= \frac{\partial}{\partial S}(T\frac{\partial y}{\partial S})\, dS = \frac{\partial}{\partial S_0}(\frac{T}{1 + T/EA}\frac{\partial y}{\partial S_0})\, dS_0 \end{aligned} \tag{5.2}$$

The condition of static equilibrium of the cable is that $dT_x = 0$ and $dT_y = -mg$. Using this condition with equation (5.2) and for cables with small sag to span ratios, the position of cable static equilibrium is given by:

$$y = \frac{mgL^2}{2H}\left[\frac{x}{L} - \left(\frac{x}{L}\right)^2\right] \tag{5.3}$$

where L is the distance between supports and H is the horizontal component of static cable tension.

The nonlinear equations of equilibrium of cable motion in space can be written as:

$$\frac{\partial}{\partial S}\left[(T + R)\frac{\partial}{\partial S}(x + u)\right] = m\frac{\partial^2 u}{\partial t^2} \tag{5.4}$$

$$\frac{\partial}{\partial S}\left[(T + R)\frac{\partial}{\partial S}(y + v)\right] = -mg + m\frac{\partial^2 v}{\partial t^2} \tag{5.5}$$

$$\frac{\partial}{\partial S}\left[(T + R)\frac{\partial w}{\partial S}\right] = m\frac{\partial^2 w}{\partial t^2} \tag{5.6}$$

where u, v, and w are small displacements in the x, y, and z directions as shown in figure 5.1, respectively, R is the additional dynamic cable tension and S is the tangent to the cable coordinate at the point of interest.

Assuming small sag to span ratio, which is the actual case in transmission line cables, then $dS \approx dx$ and $T \approx H$. Rao and Iyengar (1991b) found that the additional dynamic cable tension "R" is given by:

$$R = EA\left(\frac{\partial u}{\partial x} + \frac{dy}{dx}\frac{\partial v}{\partial x} + \frac{1}{2}\left(\frac{\partial v}{\partial x}\right)^2 + \frac{1}{2}\left(\frac{\partial w}{\partial x}\right)^2\right) \tag{5.7}$$

Introducing equation (5.7) into equations (5.4), (5.5), and (5.6) and taking into account the static equilibrium of the cable, the following three dynamic equilibrium equations are derived:

$$\frac{\partial}{\partial x}\left[H\frac{\partial u}{\partial x} + EA\left\{\frac{\partial u}{\partial x} + \frac{dy}{dx}\frac{\partial v}{\partial x} + \frac{1}{2}\left(\frac{\partial v}{\partial x}\right)^2 + \frac{1}{2}\left(\frac{\partial w}{\partial x}\right)^2\right\}\right] = m\,\ddot{u} \qquad (5.8)$$

$$\frac{\partial}{\partial x}\left[H\frac{\partial v}{\partial x} + EA\left(\frac{dy}{dx} + \frac{\partial v}{\partial x}\right)\left\{\frac{\partial u}{\partial x} + \frac{dy}{dx}\frac{\partial v}{\partial x} + \frac{1}{2}\left(\frac{\partial v}{\partial x}\right)^2 + \frac{1}{2}\left(\frac{\partial w}{\partial x}\right)^2\right\}\right] = m\ddot{v} \qquad (5.9)$$

$$\frac{\partial}{\partial x}\left[H\frac{\partial w}{\partial x} + EA\,\frac{\partial w}{\partial x}\left\{\frac{\partial u}{\partial x} + \frac{dy}{dx}\frac{\partial v}{\partial x} + \frac{1}{2}\left(\frac{\partial v}{\partial x}\right)^2 + \frac{1}{2}\left(\frac{\partial w}{\partial x}\right)^2\right\}\right] = m\,\ddot{w} \qquad (5.10)$$

Neglecting the longitudinal inertia term ($\ddot{u}$), equation (5.8) takes the form:

$$\frac{\partial u}{\partial x} + \frac{dy}{dx}\frac{\partial v}{\partial x} + \frac{1}{2}\left(\frac{\partial v}{\partial x}\right)^2 + \frac{1}{2}\left(\frac{\partial w}{\partial x}\right)^2 = g(t) \qquad (5.11)$$

where g(t) is a function of time only.

The implication of neglecting the contribution of the longitudinal inertia is that the tension along the cable is a function of time only which agrees with the results of the finite element analysis carried out by Aziz et al. (1996).

Integrating equation (5.11) with respect to x, with the boundary conditions u(0, t) = u(L,t) = 0, results in

$$g(t) = \frac{1}{L}\int_0^L \left[\frac{dy}{dx}\frac{\partial v}{\partial x} + \frac{1}{2}\left(\frac{\partial v}{\partial x}\right)^2 + \frac{1}{2}\left(\frac{\partial w}{\partial x}\right)^2\right] dx \qquad (5.12)$$

Using equation (5.12), equations (5.9) and (5.10) can be simplified to the following form:

$$\frac{\partial}{\partial x}\left[H\frac{\partial v}{\partial x} + EA\left(\frac{dy}{dx} + \frac{\partial v}{\partial x}\right) g(t)\right] = m\,\ddot{v} \tag{5.13}$$

$$\frac{\partial}{\partial x}\left[H\frac{\partial w}{\partial x} + EA\,\frac{\partial w}{\partial x}\, g(t)\right] = m\,\ddot{w} \tag{5.14}$$

5.2.1 Response of Cables to Support Excitation

Since the cable response to seismic ground motion acting in the longitudinal direction is negligible compared to its response to the vertical and transverse components of ground motion, the longitudinal component of ground motion is not considered in this analysis. The two components of displacement v(x, t) and w(x, t) of a cable subjected to a ground motion at both supports acting in the y and z directions as shown in figure 5.1, are given by:

$$\begin{aligned} v(x,t) &= v_s(x,t) + v_d(x,t) \\ w(x,t) &= w_s(x,t) + w_d(x,t) \end{aligned} \tag{5.15}$$

where $v_s(x, t)$ and $w_s(x, t)$ are the pseudo-static displacements in the y and z directions respectively, and $v_d(x, t)$ and $w_d(x, t)$ are the dynamic displacements in the y and z directions respectively.

The pseudo-static displacements are given by:

$$\begin{aligned} v_s(x,t) &= \left(1 - \frac{x}{L}\right) v_1(t) + \frac{x}{L}\, v_2(t) \\ w_s(x,t) &= \left(1 - \frac{x}{L}\right) w_1(t) + \frac{x}{L}\, w_2(t) \end{aligned} \tag{5.16}$$

where $v_1(t)$ and $w_1(t)$ are the displacement time histories at the left support in the y and z directions, and $v_2(t)$ and $w_2(t)$ are the displacement time histories at the right support. For the special case of short span cables, uniform support excitation may be assumed where $v_1(t) = v_2(t)$ and $w_1(t) = w_2(t)$.

In the solution for the vertical and transverse motions of the cable, the following non-dimensional parameters are introduced:

$$v_n = \frac{v_d}{L}, \qquad w_n = \frac{w_d}{L}, \qquad X = \frac{x}{L} \tag{5.17}$$

It was shown from the finite element analysis that the cable displacements in the vertical and transverse directions are dominated by the first mode. Therefore, only one degree of freedom is required to represent the cable vibration in each direction, and a two-degree of freedom model would be accurate enough to evaluate the displacement of any point along the cable. The dynamic displacement of the cable in the vertical and transverse directions are modelled in the form:

$$\begin{aligned} v_n(x,t) &= V(t)\,\Phi(x) \\ w_n(x,t) &= W(t)\,\Theta(x) \end{aligned} \tag{5.18}$$

where $\Phi(x)$ is the first in-plane mode of vibration and $\Theta(x)$ is the first out-of-plane mode of vibration

From the static equilibrium shape of the cable,

$$\frac{dy}{dX} = \frac{\beta L}{2}(1 - 2X) \tag{5.19}$$

where $\beta = mgL / H$,

Integrating equation (5.12) and using equations (5.15) to (5.19), the following is obtained:

$$g(t) = \beta I_3 V + 0.5 I_4 V^2 + 0.5 I_5 W^2 + \frac{0.5}{L^2}(v_2 - v_1)^2 + \frac{0.5}{L^2}(w_2 - w_1)^2 \tag{5.20}$$

where,

$$\begin{aligned} I_1 &= \int_0^1 \Phi^2 \, dX, & I_2 &= \int_0^1 \Theta^2 \, dX, & I_3 &= \int_0^1 \Phi \, dX \\ I_4 &= \int_0^1 \Phi'^2 \, dX, & I_5 &= \int_0^1 \Theta'^2 \, dX, & I_6 &= \int_0^1 \Theta \, dX \end{aligned} \tag{5.21}$$

Using equations (5.15) to (5.20), adding the damping term and applying Galerkin method, equations (5.13) and (5.14) can be reduced to two coupled nonlinear ordinary differential equations in the following form:

$$\begin{aligned} &\ddot{W} + 2\eta\omega_3\dot{W} + \omega_3^2 W + c_1 W V + c_2 W V^2 + c_3 W^3 + \\ &F_1 \ddot{w}_1 + F_3(\ddot{w}_2 - \ddot{w}_1) + F_4 W (w_2 - w_1)^2 + F_4 W (v_2 - v_1)^2 = 0 \end{aligned} \tag{5.22}$$

$$\ddot{V} + 2\eta\omega_2\dot{V} + \omega_2 V + c_4 V + c_5 W + c_6 V + c_7 V W + (F_2 - F_7)\ddot{v}_1 + F_7\ddot{v}_2 + F_5 V (v_2 - v_1)^2 + F_6 (v_2 - v_1)^2 + F_5 V (w_2 - w_1)^2 + F_6 (w_2 - w_1)^2 = 0 \quad (5.23)$$

where the constants c_1 to c_7 are given by equation (5.24) and the constants F_1 to F_7 are given by equation (5.25) as follows:

$$c_1 = \alpha\gamma\beta (I_3 I_5 / I_2) \qquad c_2 = 0.5\,\alpha\gamma (I_4 I_5 / I_2)$$
$$c_3 = 0.5\,\alpha\gamma (I_5^2 / I_2) \qquad c_4 = 1.5\,\alpha\gamma\beta (I_3 I_4 / I_1)$$
$$c_5 = 0.5\,\alpha\gamma\beta (I_3 I_5 / I_1) \qquad c_6 = 0.5\,\alpha\gamma (I_4^2 / I_1) \quad (5.24)$$
$$c_7 = 0.5\,\alpha\gamma (I_4 I_5 / I_1)$$

$$F_1 = \frac{1}{L}(I_6 / I_2) \qquad F_2 = \frac{1}{L}(I_3 / I_1)$$
$$F_3 = \frac{1}{L}\left(\int_0^1 X\,\Theta\,dX\right) / I_2 \qquad F_4 = \frac{0.5\,\alpha\gamma}{L^2}(I_5 / I_2)$$
$$F_5 = \frac{0.5\,\alpha\gamma}{L^2}(I_4 / I_1) \qquad F_6 = \frac{0.5\,\alpha\gamma\beta}{L^2}(I_3 / I_1) \quad (5.25)$$
$$F_7 = \frac{1}{L}\left(\int_0^1 X\Phi\,dX\right) / I_1$$

where $\gamma = E A / H$ and $\alpha = H / m L^2$.

Equations (5.22) and (5.23) indicate that there are two kinds of nonlinearities in the system, quadratic and cubic nonlinearities. The quadratic nonlinearity terms are due to the initial curvature of the cable and the cubic nonlinearity terms are due to stretching of the cable under tension.

5.2.2 Solution of the Equations of Motion

The method of multiple time scales by Nayfeh and Mook (1979) is adopted in the solution of the equations of motion of the cable. Assume that $T_i = \epsilon^i t$ where ϵ is a small quantity of the order of the amplitude of the response. The time scale T_1 is slower than the time scale T_0 and more generally, T_n is slower than T_{n-1}. The derivatives with respect to t are given by:

$$\begin{aligned} \frac{d}{dt} &= D_0 + \epsilon D_1 + \epsilon^2 D_2 + \ldots\ldots \\ \frac{d^2}{dt^2} &= D_0^2 + 2\epsilon D_0 D_1 + \epsilon^2 (D_1^2 + 2 D_0 D_1) + \ldots\ldots \end{aligned} \tag{5.26}$$

where $D_i = \partial/\partial T_i$

The following scaling scheme is considered: $W(t) = \epsilon W^*(t)$; $V(t) = \epsilon V^*(t)$; $v_i(t) = \epsilon^3 v_i^*(t)$; $w_i(t) = \epsilon^3 w_i^*(t)$ where i = 1, 2 and $\eta = \epsilon^2 \eta^*$. The reason for this scaling scheme is to have the effect of damping and load appear in the perturbation solution at the same time the effect of nonlinearity appears in it. Dropping the asterisks, the time dependent component of the response V(t) and W(t) are expanded in the form:

$$\begin{aligned} W(T_0,T_1,T_2) &= W_0(T_0,T_1,T_2) + \epsilon W_1(T_0,T_1,T_2) + \epsilon^2 W_2(T_0,T_1,T_2) \\ V(T_0,T_1,T_2) &= V_0(T_0,T_1,T_2) + \epsilon V_1(T_0,T_1,T_2) + \epsilon^2 V_2(T_0,T_1,T_2) \end{aligned} \tag{5.27}$$

Applying the expansions given in equations (5.26) and (5.27) to equations (5.22) and (5.23), two differential equations with different powers of ϵ are arrived at. Equating the sum of the coefficients of the same power of ϵ to zero, the following equations are obtained:

ϵ^0 Coefficient:

$$D_0^2 W_0 + \omega_3^2 W_0 = 0 \qquad (5.28a,b)$$
$$D_0^2 V_0 + \omega_2^2 V_0 = 0$$

ϵ^1 Coefficient:

$$D_0^2 W_1 + \omega_3^2 W_1 = -2 D_0 D_1 W_0 - c_1 W_0 V_0 \qquad (5.29a,b)$$
$$D_0^2 V_1 + \omega_2^2 V_1 = -2 D_0 D_1 V_0 - c_4 V_0^2 - c_5 W_0^2$$

ϵ^2 Coefficient:

$$D_0^2 W_2 + \omega_3^2 W_2 = -2D_0D_2W_0 - D_1^2 W_0 - 2D_0D_1W_1 - c_1W_0V_1 - c_1W_1V_0 - c_2W_0V_0^2 - c_3W_0^3 - (F_1 - F_3)\ddot{w}_1 - F_3\ddot{w}_2 - 2\eta\omega_3 D_0 W_0 \qquad (5.30a,b)$$

$$D_0^2 V_2 + \omega_2^2 V_2 = -2D_0D_2V_0 - D_1^2 V_0 - 2D_0D_1V_1 - 2c_4V_0V_1 - 2c_5W_0W_1 - c_6V_0^3 - c_7V_0W_0^2 - (F_2 - F_7)\ddot{v}_1 - F_7\ddot{v}_2 - 2\eta\omega_2 D_0$$

The solution of equations (5.28a and b) for the out-of-plane and the in-plane motions takes the form:

$$W_0 = A_1(T_1,T_2)\, e^{-i\omega_3 T_0} + cc \qquad (5.31a,b)$$
$$V_0 = A_2(T_1,T_2)\, e^{-i\omega_2 T_0} + cc$$

where cc represents the complex conjugate of all the terms before the plus sign.

Introducing equations (5.31) into equation (5.29a), the following is obtained:

$$D_0^2 W_1 + \omega_3^2 W_1 = 2\, i\, \omega_3 D_1 A_1 e^{-i\omega_3 T_0} - c_1 A_1 A_2 e^{-i(\omega_2+\omega_3)T_0} - c_1 A_2 \bar{A}_1 e^{-i(\omega_2-\omega_3)T_0} + cc \qquad (5.32)$$

where $\overline{A}_i$ is the complex conjugate of A_i, i = 1, 2.

Eliminating the secular term results in $D_1A_1 = 0$; and the solution for equation (5.32) is given by:

$$W_1(t) = \frac{c_1 A_1 A_2}{\omega_2^2 + 2\omega_2\omega_3} e^{-i(\omega_2+\omega_3)T_0} + \frac{c_1 A_2 \overline{A}_1}{\omega_2^2 - 2\omega_2\omega_3} e^{-i(\omega_2-\omega_3)T_0} + cc \qquad (5.33)$$

Similarly, substituting equation (5.31a and b) into equation (5.29b), gives:

$$D_0^2 V_1 + \omega_2^2 V_1 = 2 i \omega_2 D_1 A_2 e^{-i\omega_2 T_0} - c_4 A_2^2 e^{-2i\omega_2 T_0} - c_4 A_2 \overline{A}_2 - c_5 A_1^2 e^{-2i\omega_3 T_0} - c_5 A_1 \overline{A}_1 + cc \qquad (5.34)$$

Eliminating the secular term results in $D_1A_2 = 0$; and the solution for equation (5.34) is given by:

$$V_1(t) = \frac{1}{3}\frac{c_4}{\omega_2^2} A_2^2 e^{-2i\omega_2 T_0} - c_4 \frac{A_2\overline{A}_2}{\omega_2^2} - \frac{c_5 A_1^2}{\omega_2^2 - 4\omega_3^2} e^{-2i\omega_3 T_0} - c_5 \frac{A_1\overline{A}_1}{\omega_2^2} + cc \qquad (5.35)$$

At this stage, it is appropriate to simplify the solution by differentiating between two cases. The first case is that when the excitation is in the transverse direction only, while the second case is that when the excitation is in the vertical direction only.

5.2.3 Transverse Excitation

The support excitations are defined as accelerations using the travelling wave approach in the following form:

$$\ddot{w}_1 = P_1 \cos \Omega t , \qquad \ddot{w}_2 = P_1 \cos (\Omega t + \tau) \tag{5.36}$$

The external resonance is defined by:

$$\Omega = \omega_n + \epsilon^2 \sigma \tag{5.37}$$

where n = 2, 3 for the vertical and transverse excitations, respectively, τ is the phase difference due to wave travel effect which is equal to the length between cable supports divided by the wave propagation velocity, σ is a detuning parameter. Resonance occurs when $\sigma = 0$.

Substituting equations (5.31a and b), (5.33), and (5.35) into equations (5.30a) and (5.30b) and eliminating the secular term, the following equations are obtained:

$$\begin{aligned} &2i\omega_3 D_2 A_1 + 2c_1 c_4 \frac{A_2 \overline{A}_2 A_1}{\omega_2^2} + c_1 c_5 \frac{A_1^2 \overline{A}_1}{\omega_2^2 - 4\omega_3^2} + 2c_1 c_5 \frac{A_1^2 \overline{A}_1}{\omega_2^2} - \\ &c_1^2 \frac{A_1 A_2 \overline{A}_2}{\omega_2^2 + 2\omega_2\omega_3} - c_1^2 \frac{A_1 A_2 \overline{A}_2}{\omega_2^2 - 2\omega_2\omega_3} - 2c_2 A_1 A_2 \overline{A}_2 - 3c_3 A_1^2 \overline{A}_1 - \\ &(F_1 - F_3) \frac{P_1}{2} e^{-i\epsilon^2\sigma T_0} - F_3 \frac{P_1}{2} e^{(-i\epsilon^2\sigma T_0 + \tau)} + 2 i \eta \omega_3^2 A_1 = 0 \end{aligned} \tag{5.38}$$

$$\begin{aligned} &2 i \omega_2 D_2 A_2 + \frac{10}{3} c_4^2 \frac{A_2^2 \overline{A}_2}{\omega_2^2} + 4 c_4 c_5 \frac{A_2 A_1 \overline{A}_1}{\omega_2^2} - 3 c_6 A_2^2 \overline{A}_2 - \\ &2 c_1 c_5 \frac{A_1 \overline{A}_1 A_2}{\omega_2^2 + 2 \omega_2\omega_3} - 2 c_1 c_5 \frac{A_1 \overline{A}_1 A_2}{\omega_2^2 - 2\omega_2\omega_3} - 2 c_7 A_1 \overline{A}_1 A_2 + \\ &2 i \eta \omega_2^2 A_2 = 0 \end{aligned} \tag{5.39}$$

A_1 and A_2 are expressed in the polar form as follows:

$$A_1 = \frac{1}{2} a\, e^{-i\phi_1} \qquad A_2 = \frac{1}{2} b\, e^{-i\phi_2} \tag{5.40}$$

where a, b and ϕ_1, ϕ_2 are the amplitudes and phase angles of A_1 and A_2.

Substituting equation (5.40) into equations (5.38) and (5.39), and equating the real and imaginary parts to zero, the following set of equations is arrived at:

$$\begin{aligned}
2\,\omega_3\,\epsilon^2\,\dot{a} &= -(F_1 - F_3)\epsilon^2 P_1 \sin\gamma_1 - F_3 P_1 \epsilon^2 \sin(\gamma_1 + \tau) - 2\epsilon^2 \eta \omega_3^2 a \\
2\,\omega_3\,a\,\epsilon^2\,\dot{\gamma}_1 &= 2\,\omega_3\,a\,\epsilon^2\,\sigma + S_1\,a^3 + S_2\,a\,b^2 - \\
&\quad (F_1 - F_3)\,P_1\,\epsilon^2 \cos\gamma_1 - F_3\,P_1\,\epsilon^2 \cos(\gamma_1 + \tau) \\
\dot{b} &= -\eta\,\omega_2\,b \\
2\,\omega_2\,b\,\epsilon^2\,\dot{\phi}_2 &= S_3\,b^3 + S_4\,b\,a^2
\end{aligned} \tag{5.41}$$

where:

$$\begin{aligned}
\gamma_1 &= \epsilon^2\,\sigma\,T_0 - \phi_1 \\
S_1 &= 0.25\,\epsilon^2 \left[\frac{2\,c_1\,c_5}{\omega_2^2} + \frac{c_1\,c_5}{\omega_2^2 - 4\,\omega_3^2} - 3\,c_3 \right] \\
S_2 &= 0.25\,\epsilon^2 \left[\frac{2\,c_1\,c_4}{\omega_2^2} - 2\,\frac{c_1^2}{\omega_2^2 - 4\,\omega_3^2} - 2\,c_2 \right] \\
S_3 &= 0.25\,\epsilon^2 \left[\frac{10}{3}\,\frac{c_4^2}{\omega_2^2} - 3\,c_6 \right] \\
S_4 &= 0.25\,\epsilon^2 \left[\frac{4\,c_4\,c_5}{\omega_2^2} - 4\,\frac{c_1\,c_5}{\omega_2^2 - 4\,\omega_3^2} - 2\,c_7 \right]
\end{aligned} \tag{5.42}$$

The steady state solution is given by the condition:

$$\dot{a} = \dot{b} = \dot{\gamma}_1 = \dot{\gamma}_2 = 0 \qquad (5.43)$$

Therefore, from equation (5.41), b = 0 and,

$$(F_1 - F_3)\, P_1 \sin \gamma_1 + F_3\, P_1 \sin(\gamma_1 + \tau) + 2\,\eta\,\omega_3^2\, a = 0 \qquad (5.44)$$

$$2\omega_3 \epsilon^2 a\sigma + S_1 a^3 - (F_1 - F_3)\, P_1 \epsilon^2 \cos\gamma_1 - F_3 P_1 \epsilon^2 \cos(\gamma_1 + \tau) = 0 \qquad (5.45)$$

Equation (5.45) shows that the system exhibits either softening or hardening behaviour depending on the value of S_1 which in turn depends on the terms of the quadratic and cubic nonlinearities. After solving equations (5.44) and (5.45) to determine the values of a and γ_1, the general solution of the non-dimensional time dependent component of the response V(t) and W(t) are given by substituting equations (5.31a and b), (5.33) and (5.35) into equation (5.27).

$$W(t) = a \cos(\omega_3 t + \phi_1)$$

$$V(t) = \epsilon \left\{ - \frac{c_5\, a^2}{2\,(\omega_2^2 - 4\,\omega_3^2)} \cos 2(\omega_3 t + \phi_1) - \frac{c_5\, a^2}{2\,\omega_2^2} \right\} \qquad (5.46)$$

Equation (5.46) shows that due to transverse excitation, the cable vibrates in the transverse direction with its natural frequency (ω_3). Meanwhile, there is a vertical vibration of order ϵ and frequency $2\omega_3$ coupled with the transverse vibration. Moreover, there is a non-zero amplitude term in the vertical direction due to the quadratic nonlinearity.

5.2.4 Vertical Excitation

The support excitations are defined in the following form:

$$\ddot{v}_1 = P_2 \cos \Omega t , \qquad \ddot{v}_2 = P_2 \cos (\Omega t + \tau) \tag{5.47}$$

where Ω is given by equation (5.37).

Performing the analysis in a similar manner to the case of transverse excitation, the steady state solution is given by:

$$(F_2 - F_7) P_2 \sin \gamma_2 + F_7 P_2 \sin (\gamma_2 + \tau) + 2 \eta \omega_2^2 b = 0 \tag{5.48}$$

$$2\omega_2 \epsilon^2 b\sigma + S_3 b^3 - (F_2 - F_7) P_2 \epsilon^2 \cos\gamma_2 - F_7 P_2 \epsilon^2 \cos(\gamma_2 + \tau) = 0 \tag{5.49}$$

The solution of equations (5.48) and (5.49) simultaneously results in the values of b and γ_2. The solution for W(t) and V(t) is given by:

$$W(t) = 0$$

$$V(t) = b \cos (\omega_2 t + \phi_2) + \epsilon \left\{ \frac{c_4 b^2}{6 \omega_2^2} \cos 2 (\omega_2 t + \phi_2) - \frac{c_4 b^2}{2\omega_2^2} \right\} \tag{5.50}$$

Equation (5.50) shows that due to transverse excitation, no transverse vibration is associated with the vertical vibration. The cable vibrates in the vertical direction with its natural frequency ω_2. In addition, there is a vibration of order ϵ and frequency $2\omega_2$. The cable motion is also characterized by a non-zero amplitude term due to the quadratic nonlinearity.

5.3 STABILITY OF STEADY STATE SOLUTION

Due to the nonlinearity, the response may be multi-valued for the same amplitude and frequency of excitation. In some cases, there are three possible amplitudes of the response. However, not all possible solutions are stable. It is necessary to examine the stability of the steady state solution. For the case of support excitation in the transverse direction, consider equation (5.41) with b = 0 and a and γ_1 expressed in the following form:

$$\begin{aligned} a(t) &= a + a_{11}(t) \\ \gamma_1(t) &= \gamma_1 + \gamma_{11}(t) \end{aligned} \tag{5.51}$$

where a and γ_1 are the steady state solution and a_{11} and γ_{11} are small perturbations of the steady state solution.

Substituting equation (5.51) into the steady state solution given by equations (5.44) and (5.45), the following expressions are obtained:

$$\begin{aligned} \dot{a}_{11} &= h_1 a_{11} + h_2 \gamma_{11} \\ \dot{\gamma}_{11} &= h_3 a_{11} + h_4 \gamma_{11} \end{aligned} \tag{5.52}$$

where

$$\begin{aligned} h_1 &= h_4 = -\eta \omega_3 , \\ h_2 &= \frac{-2 \epsilon^2 \omega_3 a \sigma - S_1 a^3}{2 \epsilon^2 \omega_3} , \\ h_3 &= \frac{3 S_1 a^2 + 2 \epsilon^2 \omega_3 \sigma}{2 \epsilon^2 \omega_3 a} \end{aligned} \tag{5.53}$$

The stability of the solution depends on the eigen values of equation (5.52). The position of the points separating the stable and unstable regions is given by the characteristic equation $h_1 h_4 - h_2 h_3 = 0$, which in the case of no damping can be written as:

$$\sigma^2 + \frac{2 S_1 a^2}{\epsilon^2 \omega_3} \sigma + \frac{3 S_1^2 a^4}{4 \epsilon^4 \omega_3^2} = 0 \qquad (5.54)$$

Equation (5.54) has two possible solutions given by:

$$\sigma^*_1 = - \frac{S_1 a^2}{2 \epsilon^2 \omega_3} \qquad \sigma^*_2 = - \frac{3 S_1 a^2}{2 \epsilon^2 \omega_3} \qquad (5.55)$$

The solution given by σ^*_1 is the backbone curve which is the solution of equation (5.45) without the loading term.

The stability of the solution due to support motion in the vertical direction is obtained in a similar way to the stability analysis in the transverse direction. The position of the points separating the stable and unstable regions for the case of zero damping is given by the equation:

$$\sigma^*_1 = - \frac{S_3 b^2}{2 \epsilon^2 \omega_2} \qquad \sigma^*_2 = - \frac{3 S_3 b^2}{2 \epsilon^2 \omega_2} \qquad (5.56)$$

5.4 NUMERICAL EXAMPLES

In the numerical examples, unless otherwise stated, only the first out-of-plane mode and the first in-plane symmetric mode are considered. Three cable examples are analyzed

with the properties shown in table 5.1. These cables cover a wide range of sag to span ratios from 0.03 to represent sagged cables to 0.003 to represent taut cables. The first symmetric mode shapes are those given by Irvine and Caughey (1974):

$$\Theta(X) = \sin \pi X$$
$$\Phi(X) = 1 - \tan\frac{\mu}{2} \sin\mu X - \cos\mu X \qquad (5.57)$$

where,

$$\mu = \omega_2 \sqrt{\frac{m}{H}}\, L$$

Based on equation (5.57), the constants c_1 to c_7 and F_1 to F_7 given by equations (5.24) and (5.25), respectively are evaluated. The calculated values of some important constants are given in table 5.2. The non-dimensional solutions for the displacements W(t) and V(t) are given by equations (5.46) and (5.50) for the transverse and vertical excitations, respectively. The dimensional solution can be found by using equations (5.17) and (5.18) and considering the scaling scheme used in the analysis.

5.4.1 Verification of the Results

The results of the analytical solution may be compared with the results obtained using numerical integration of the equations of motion (5.22) and (5.23) (Benedettini and Rega, 1987). However, the numerical integration of these equations does not verify the validity of using a two-degree of freedom model to represent the cable vibration. Therefore, the results of the analytical solution are compared to those of the finite element analysis.

The accuracy of the perturbation solution depends on two factors: the number of terms carried in the perturbation solution and the number of modes of vibration considered in the analysis. Since the solution is carried only up to the ϵ order terms, then the accuracy of the perturbation solution is somewhat reduced. Using one mode in each direction is adequate only if the modes are widely separated, as the accuracy of the solution is reduced away from the resonance frequency. Since the finite element analysis yields the total solution (transient response and steady state response), the transient response is added to the steady state solution developed by the multiple time scales.

Figures 5.2 and 5.3 show the displacement time history of the cable mid-point of Cable I to uniform transverse and vertical support excitation, respectively. The support excitation is a cosine function scaled to a peak acceleration of 0.1 g. The results of Cable II are shown in figures 5.4 and 5.5, while those of cable III are shown in figures 5.6 and 5.7.

These figures show good agreement between the perturbation solution and the finite element approach. While the frequencies are almost identical, the difference in amplitude is reasonably small. As expected, the accuracy of the results increases near the resonance amplitude. Comparing figures 5.4a and 5.4b, for example, shows that, for Cable II, the accuracy of the perturbation solution for an excitation with 0.4 Hz frequency is better than the accuracy for an excitation with 0.5 Hz frequency (resonance frequency = 0.32 Hz). Moreover, the accuracy increases for cables with small sag to span ratios (Cables II and III) because the effect of quadratic nonlinearity is reduced. For taut cables (Cable III), since the modes are widely separated, the perturbation solution can be extended for a wider range of

frequencies around the resonance frequency. It is expected that if enough terms are included in the perturbation solution, the results would approach those of the finite element analyses.

5.4.2 Effect of the Cable Sag to Span Ratio

The sag in the cable creates quadratic nonlinearity in addition to the cubic nonlinearity. In the numerical examples, the first cable with a sag to span ratio of 0.03 represents a sagged cable while the third cable with a sag to span ratio of 0.003 approaches the behaviour of a string. Figure 5.8 shows the frequency-amplitude relationship of different cables to vertical support excitation scaled to peak acceleration values of 0.1 g and 0.2 g. Figure 5.8a shows a softening behaviour for Cable I (sagged cable) due to the vertical ground motion. The softening characteristics of the cable are due to the quadratic nonlinearity. Multi-valued response of the cable is obtained for certain values of the detuning parameter σ. However, only two of these three solutions are stable and either one of them can be reached depending on the initial conditions. Reducing the sag to span ratio, as in Cable III (Figure 5.8c), results in hardening characteristics of the cable due to the cubic nonlinearity.

Regarding the stability region, Figure 5.8b also indicates that for Cable II the solution is almost linear and stable in all regions. The reason for that is due to the interaction between the quadratic and cubic nonlinearity terms. The amplitude of vibration of Cable III is generally smaller than that of Cables I and II which is the case for taut cables.

5.4.3 Effect of Damping Ratio on the Response

Figure 5.9 shows the effect of cable damping on the frequency amplitude relationship for Cable I as an example. This figure indicates that the effect of the damping on the cable vertical vibration is significant. With higher damping ratios, finite peak amplitudes occur as can be seen by comparing the curve corresponding to a damping ratio of 0% to that corresponding to a damping ratio of 5%.

5.5 EFFECT OF PHASE DIFFERENCE BETWEEN SUPPORT EXCITATIONS

One of the distinctive features of long span cables is the possible difference in the support excitations acting at cable ends due to the wave travel effect. In simplistic form, the wave travel effect can be accounted for by a phase shift between the motions affecting different ends of the cable. The phase shift in support excitations influences different modes of cable vibration. For simplicity, the effect of multiple support excitation is analyzed for zero damping, however the same formulation can be used for the damped case.

5.5.1 Transverse Excitation

5.5.1.1 Symmetric modes

Consider the first symmetric mode given by equation (5.57) and for the three cases of cables considered, $F_3 = 0.159 = \frac{1}{2} F_1$. Solving equation (5.44) results in $\gamma_1 = -\tau / 2$. Equation (5.45) takes the form:

$$2 \omega_3 \epsilon^2 a \sigma + S_1 a^3 - 2 F_3 P_1 \epsilon^2 \cos \frac{\tau}{2} = 0 \qquad (5.58)$$

5.5.1.2 Anti-symmetric modes

The first transverse anti-symmetric frequency and mode of vibration of the cable are given by Irvine and Caughey (1974) as:

$$\omega_3 = \frac{2\pi}{L}\sqrt{\frac{H}{m}} \qquad (5.59)$$

$$\Theta(X) = \sin 2\pi X$$

For this mode, $I_6 = 0$, $F_1 = 0$, and equation (5.44) gives $\gamma_1 = (\pi - \tau) / 2$. Equation (5.45) takes the form:

$$2\,\omega_3\,\epsilon^2\,a\,\sigma + S_1\,a^3 + 2\,F_3\,P_1\,\epsilon^2 \sin\frac{\tau}{2} = 0 \qquad (5.60)$$

5.5.2 Vertical Excitation

5.5.2.1 Symmetric modes

Following a similar analysis to the transverse vibration case, equation (5.49) for the vertical vibration takes the form:

$$2\,\omega_2\,\epsilon^2\,b\,\sigma + S_3\,b^3 - 2\,F_7\,P_2\,\epsilon^2 \cos\frac{\tau}{2} = 0 \qquad (5.61)$$

5.5.2.2 Anti-symmetric modes

The first vertical anti-symmetric frequency and mode of vibration of the cable are given by Irvine and Caughey (1974) as:

$$\omega_2 = \frac{2\pi}{L}\sqrt{\frac{H}{m}} \qquad (5.62)$$

$$\Phi(X) = \sin 2\pi X$$

Similarly, for this mode, $I_3 = 0$ and therefore $F_2 = 0$. Equation (5.48) gives $\gamma_2 = (\pi - \tau) / 2$. Equation (5.49) takes the form:

$$2\,\omega_2\,\epsilon^2\,b\,\sigma + S_3\,b^3 + 2\,F_7\,P_2\,\epsilon^2 \sin\frac{\tau}{2} = 0 \qquad (5.63)$$

5.5.3 Discussion

The effect of the phase shift in support excitation on the frequency-response relationship for Cable I is shown in figures 5.10 and 5.11 for transverse and vertical excitations, respectively. The support excitation is in the form of a cosine wave scaled to a peak acceleration of 0.1 g. These figures show that, for the first symmetric mode, the amplitude of the dynamic response is reduced when considering the phase shift. For the case of $\tau = \pi$ (i.e., the two components of ground motion are completely out-of-phase) there is no stable solution for the cable equation of motion. The response being discussed is the dynamic response component. To obtain the total response, the pseudo-static component of the response should be added to the dynamic component.

For the first anti-symmetric mode, the effect of different phase shifts on the frequency response relationship of Cable I for 0.1 g peak support acceleration is shown in figures 5.10b and 5.11b. These figures show that for uniform excitation ($\tau = 0$), the anti-symmetric modes

are not excited. As the phase shift increases, the anti-symmetric mode response increases until it reaches its maximum value at $\tau = \pi$ (i.e., the two components of ground motion are completely out-of-phase). This emphasizes the importance of considering the phase shift in the support input motion. This represents the case when the anti-symmetric modes are excited which, depending on the specific cable characteristics, may result in a higher overall response of the cable.

5.6 SUMMARY

The analysis of nonlinear cable response to support excitation in the vertical and transverse directions is presented in this chapter. The coupled nonlinear equations of motion are formulated and solved. The spatial problem is solved using Galerkin method for a two-degree of freedom model. The temporal problem is solved using the method of multiple time scales. The stability of the steady state solution is developed and discussed. Different cable examples with different sag to span ratios and damping ratios are used in the analysis to demonstrate aspects of the solution and stability phenomenon. The effect of the phase difference between the support excitation at different cable ends on the response is examined.

The analysis shows that the analytical solution with a two-degree of freedom model yields accurate results as compared to the finite element approach. The accuracy of the analytical solution increases for cables with small sag to span ratio where the modes of vibration become widely separated. The results show that due to vertical excitation, only vertical vibration exists, while due to transverse excitation, both vertical and transverse vibrations exist. The analysis shows a softening behaviour for sagged cables due to the

quadratic nonlinearity resulting from the initial curvature of the cable. Taut cables show hardening behaviour due to the stretching of the cable. It is also demonstrated from the analysis that the uniform support motion excites only the symmetric cable modes. The anti-symmetric modes are excited due to the phase difference between the input motions at cable ends.

Table 5.1 Properties of the example cables

Cable type	d / L	α (S^{-2})	β	γ	ω_2 (Hz)	ω_3 (Hz)
Cable I	0.03	0.102	0.240	1495.00	0.15	0.28
Cable II	0.01	0.306	0.080	498.33	0.30	0.32
Cable III	0.003	1.020	0.024	149.50	0.50	0.51

Table 5.2 Important constants for different cable types

Cable type	c_1	c_2	c_3	c_4	c_5	c_6	c_7	$F_1 \times 10^{-2}$	$F_2 \times 10^{-2}$
Cable I	268	46394	3720	1548	41.4	178877	14346	0.318	0.1153
Cable II	458	120640	3721	603	6.2	105851	327	0.318	0.0514
Cable III	4285	1.54×10^8	3721	7694	0.062	1.84×10^8	4454	0.318	0.0017

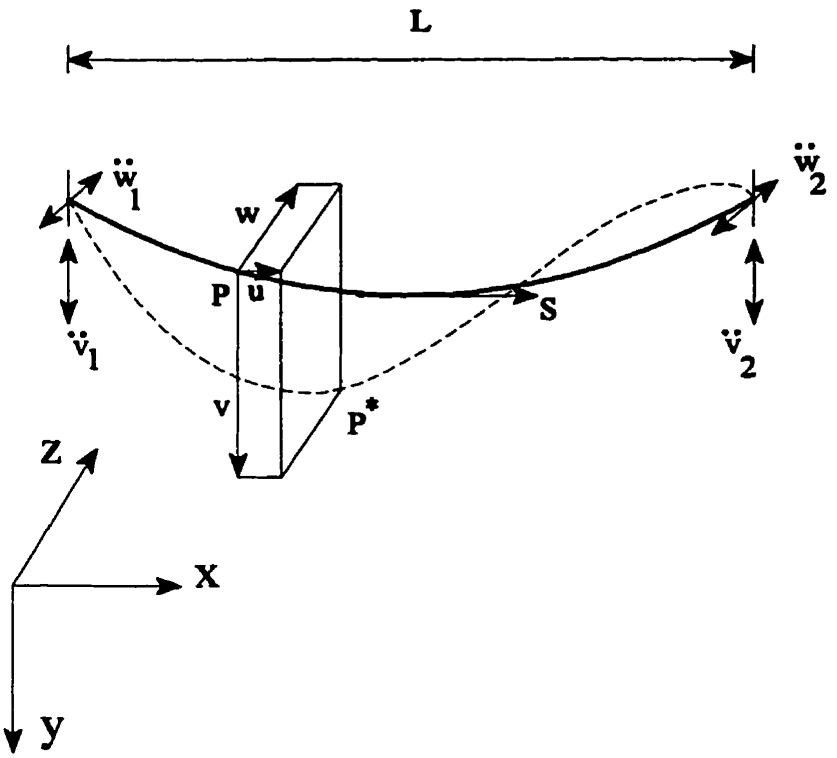

Figurre 5.1 Coordinate axes and components of cable motion

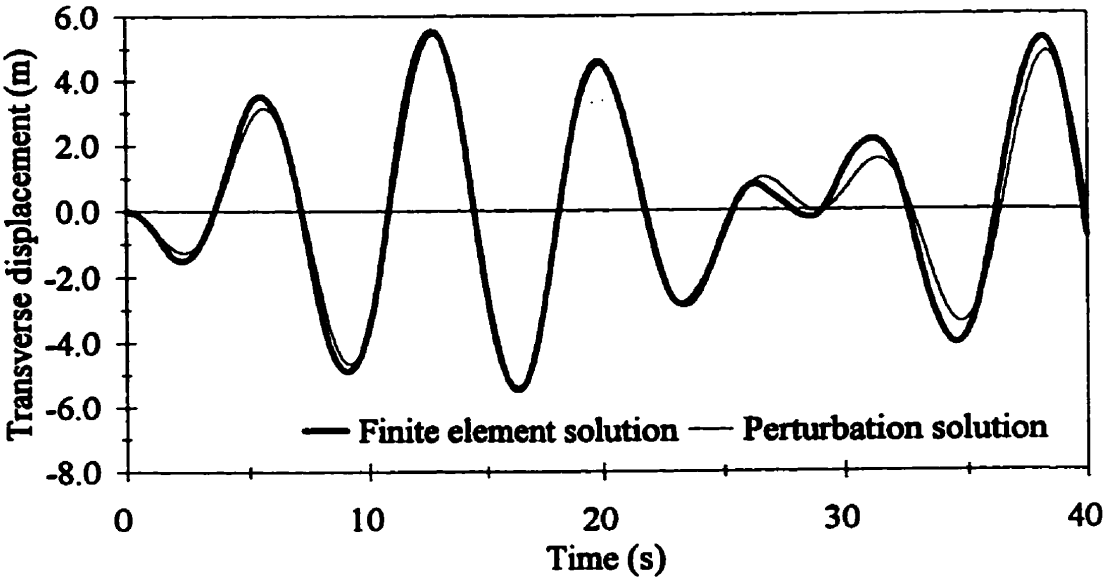

(a) f = 0.12 Hz

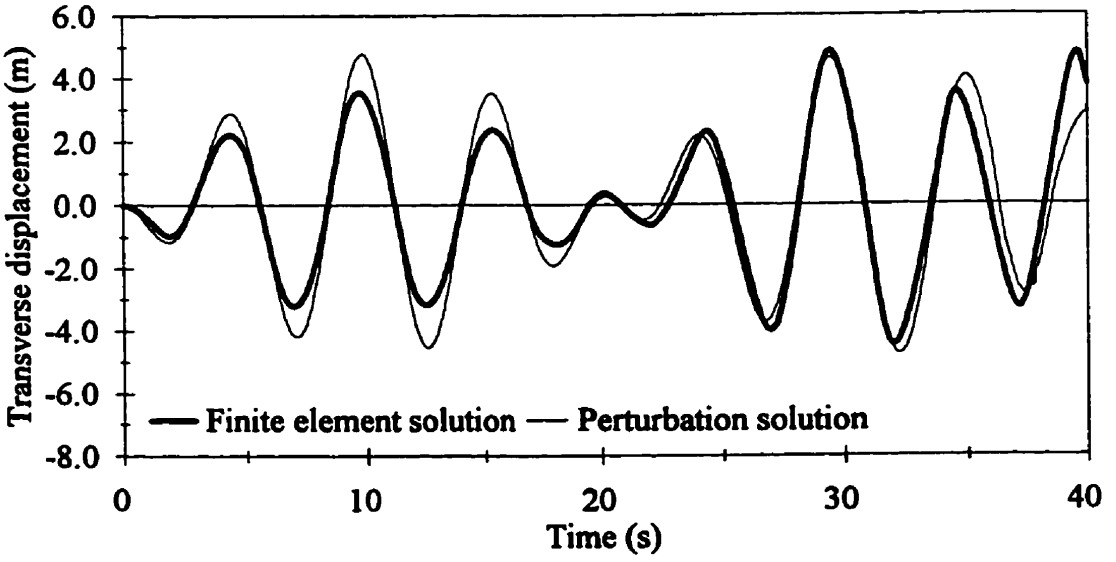

(b) f = 0.20 Hz

Figure 5.2 Transverse displacement time history of Cable I mid-point due to transverse excitation

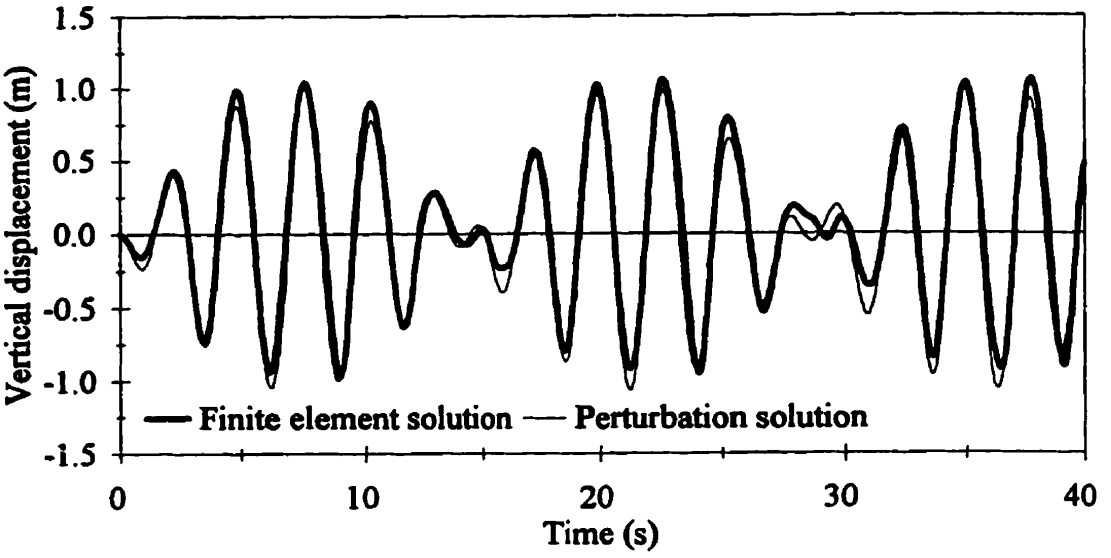

(a) f = 0.33 Hz

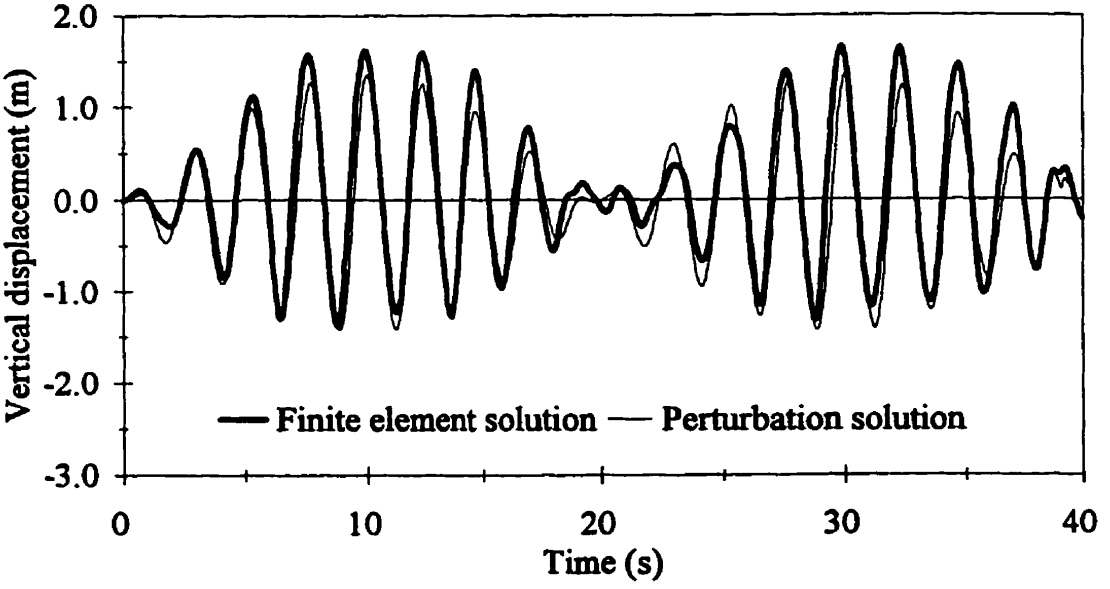

(b) f = 0.45 Hz

Figure 5.3 Vertical displacement time history of Cable I mid-point due to vertical excitation

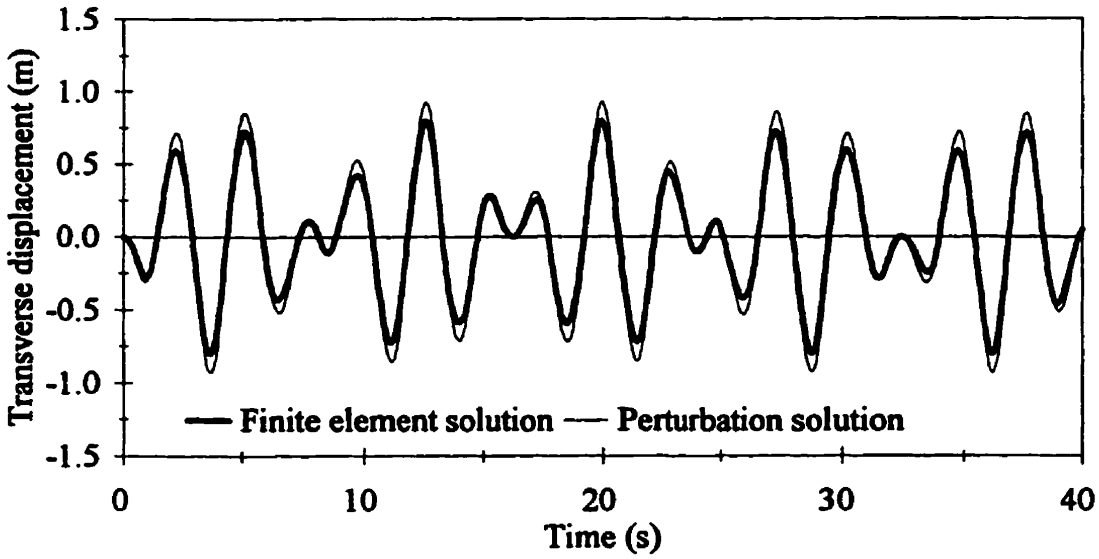

(a) f = 0.40 Hz

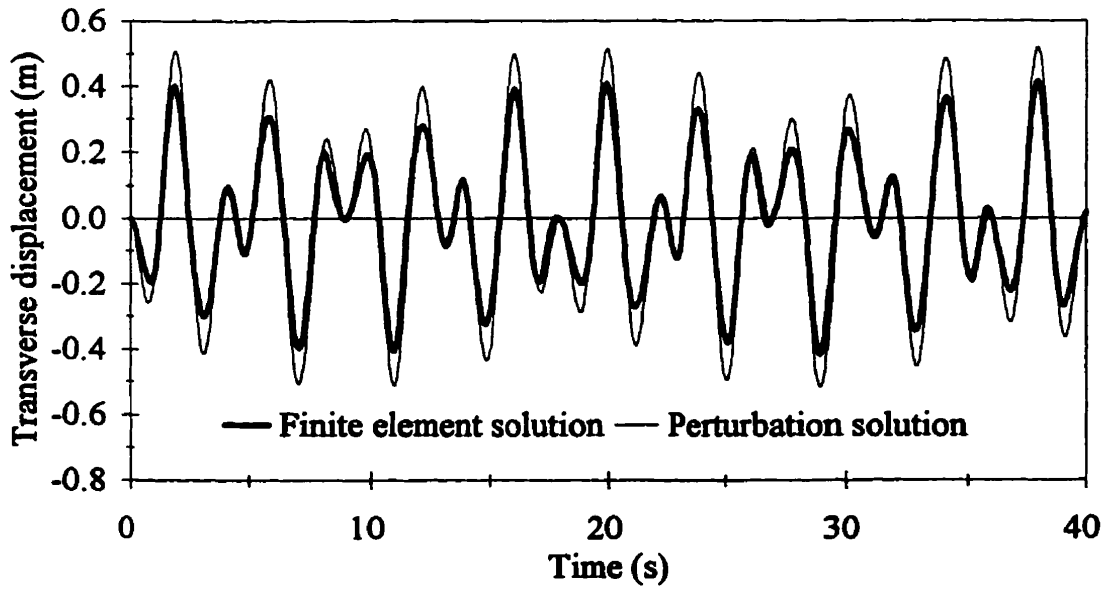

(b) f = 0.50 Hz

Figure 5.4 Transverse displacement time history of Cable II mid-point due to transverse excitation

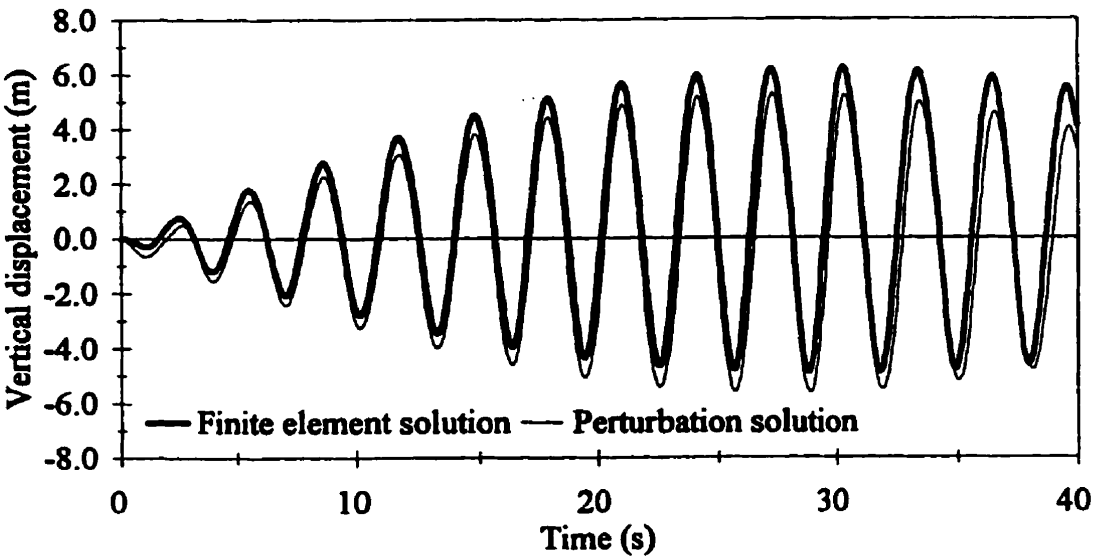

(a) f = 0.33 Hz

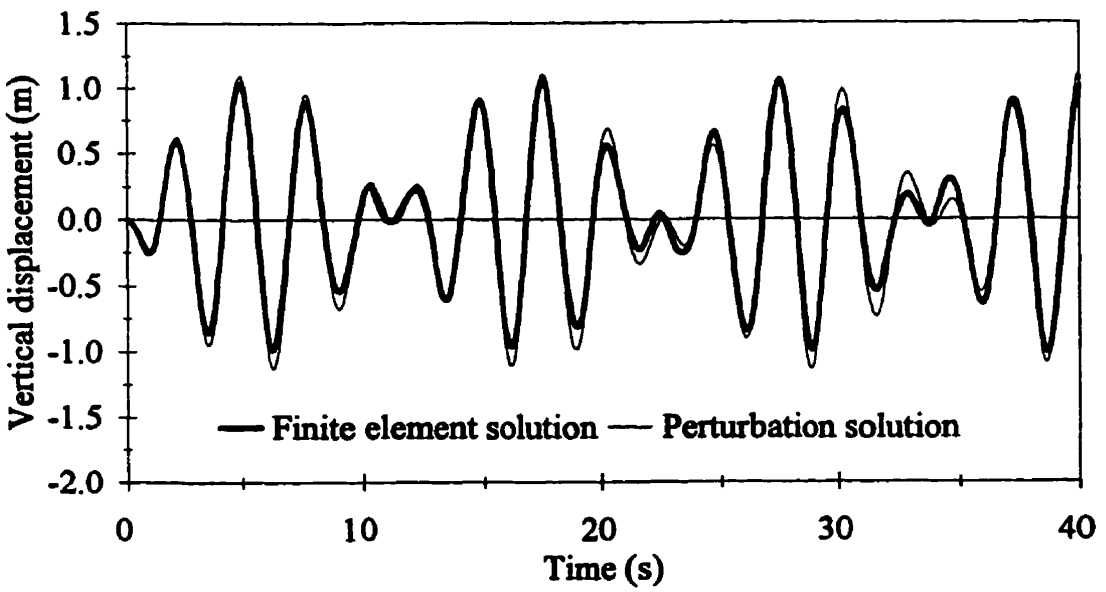

(b) f = 0.40 Hz

Figure 5.5 Vertical displacement time history of Cable II mid-point due to vertical excitation

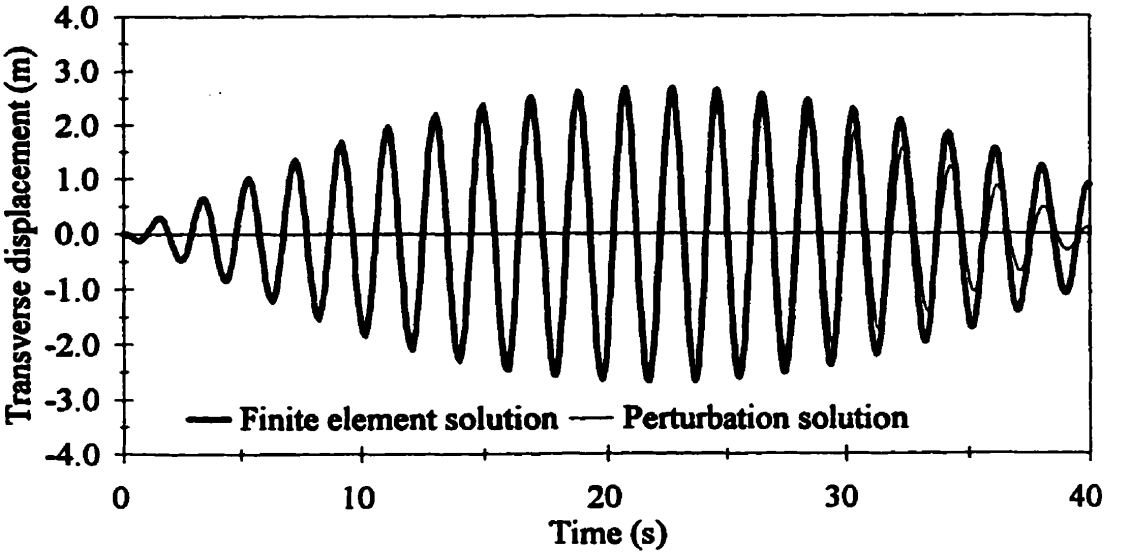

(a) f = 0.53 Hz

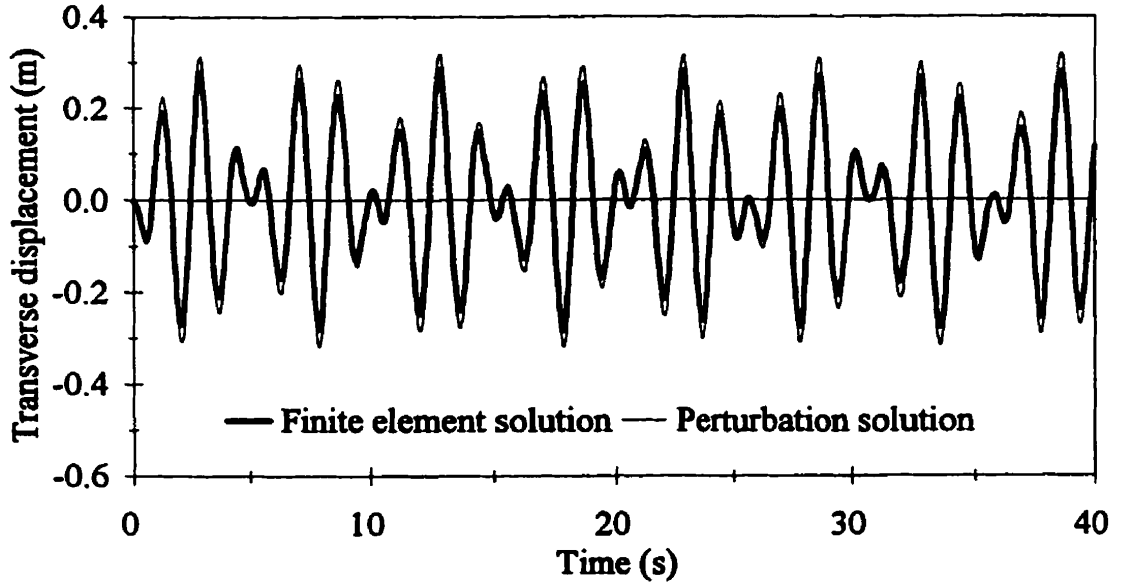

(b) f = 0.70 Hz

Figure 5.6 Transverse displacement time history of Cable III mid-point due to transverse excitation

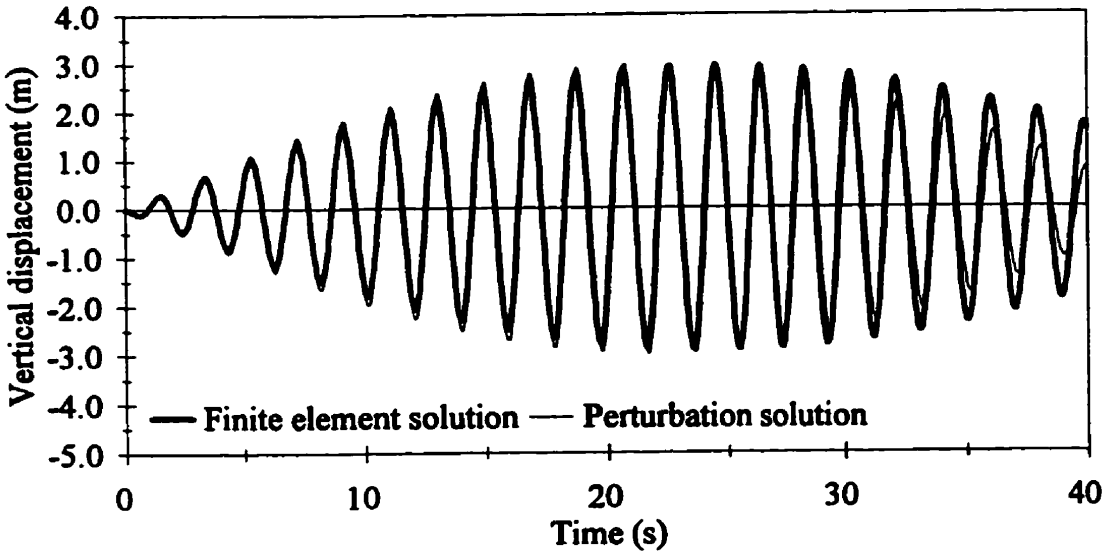

(a) f = 0.53 Hz

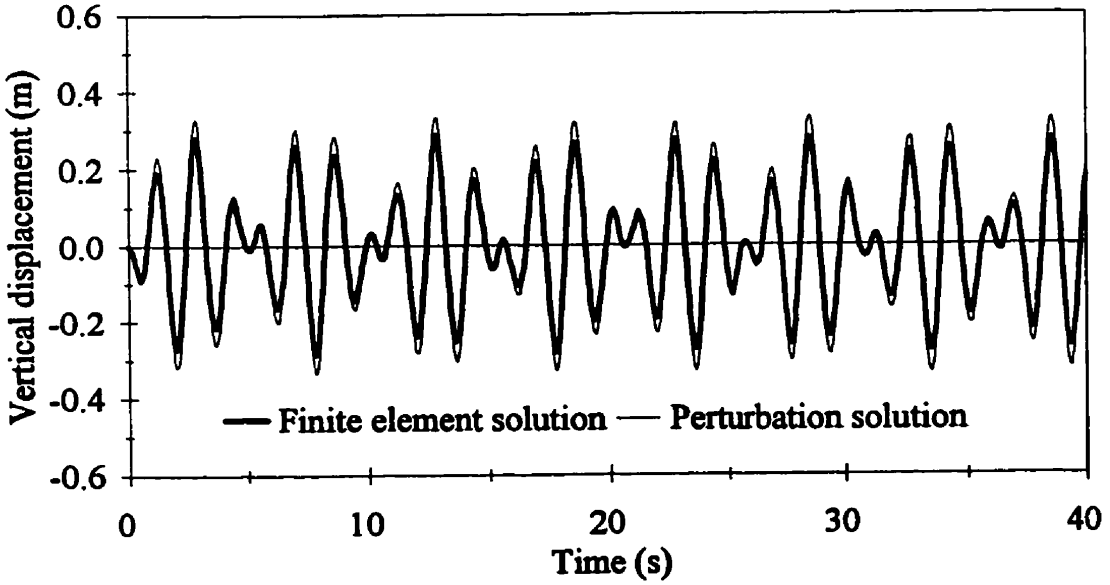

(b) f = 0.70 Hz

Figure 5.7 Vertical displacement time history of Cable III mid-point due to vertical excitation

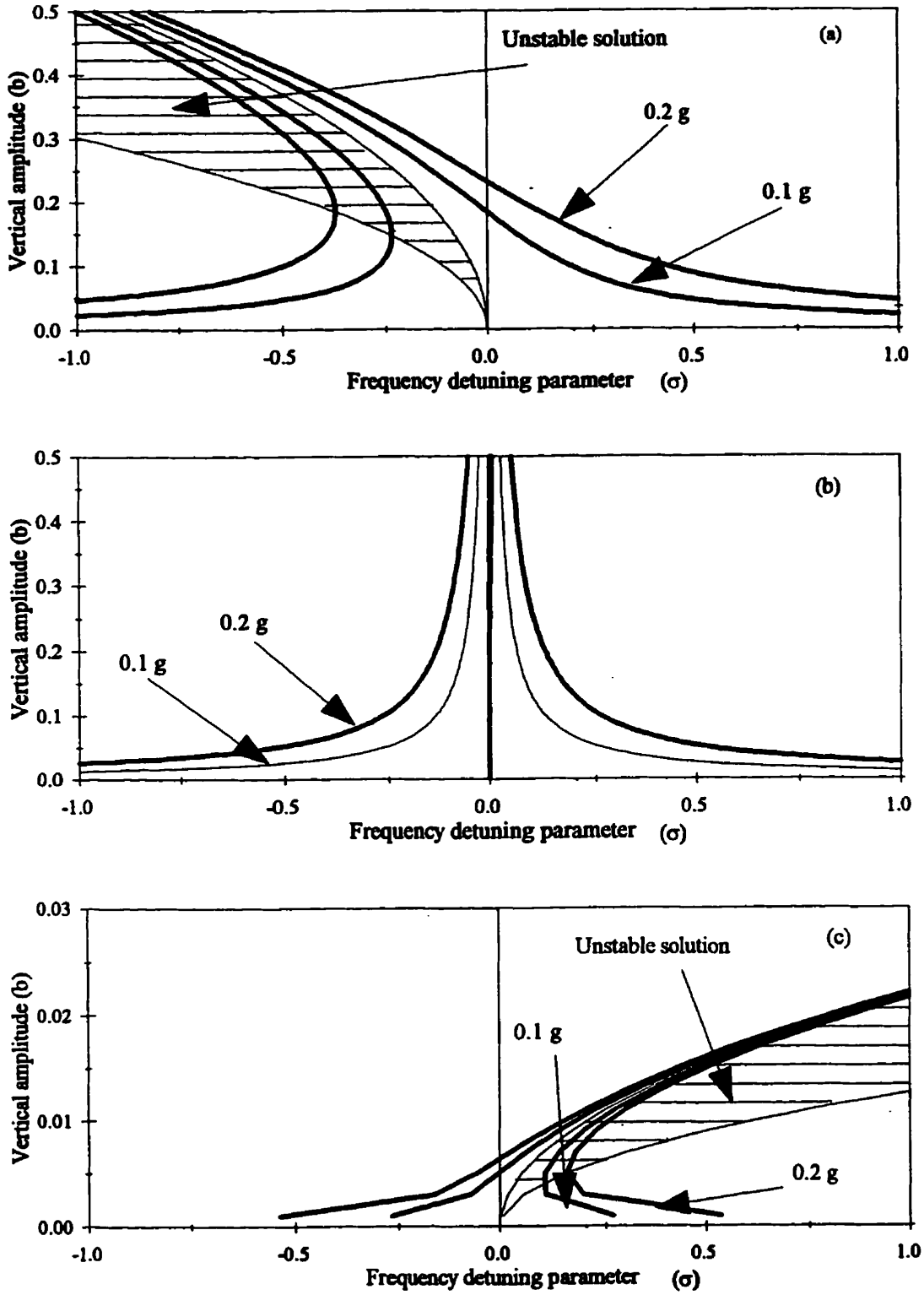

Figure 5.8 Frequency response curve for different cables due to vertical excitation, (a) Cable I, (b) Cable II and (c) Cable III

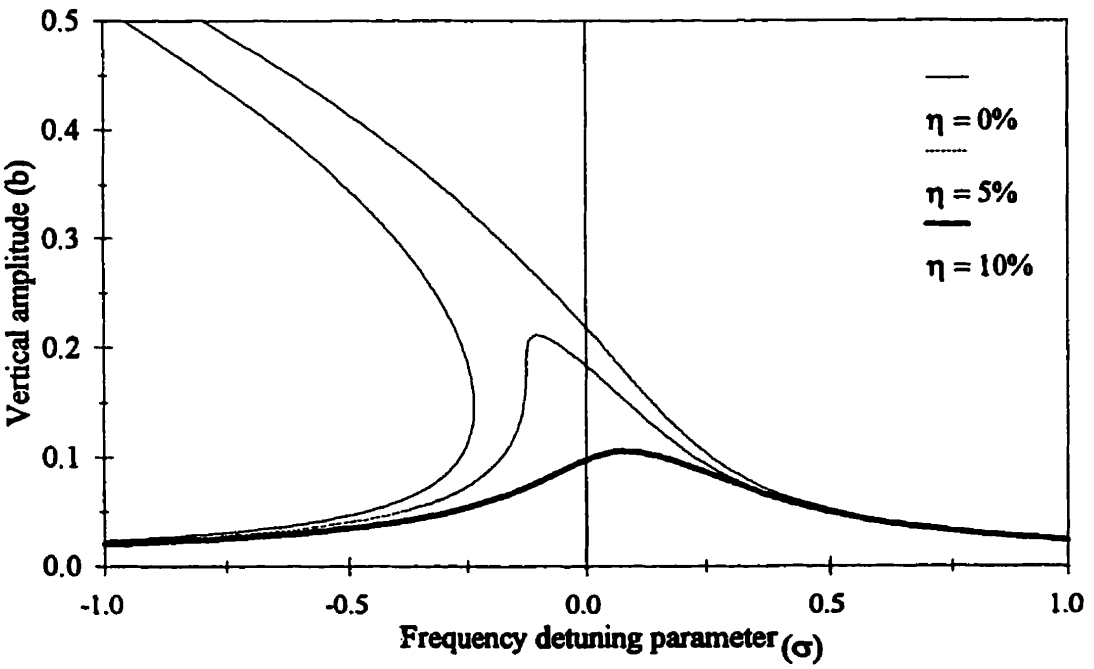

Figure 5.9 Effect of damping on the frequency response relationship of Cable I due to vertical excitation

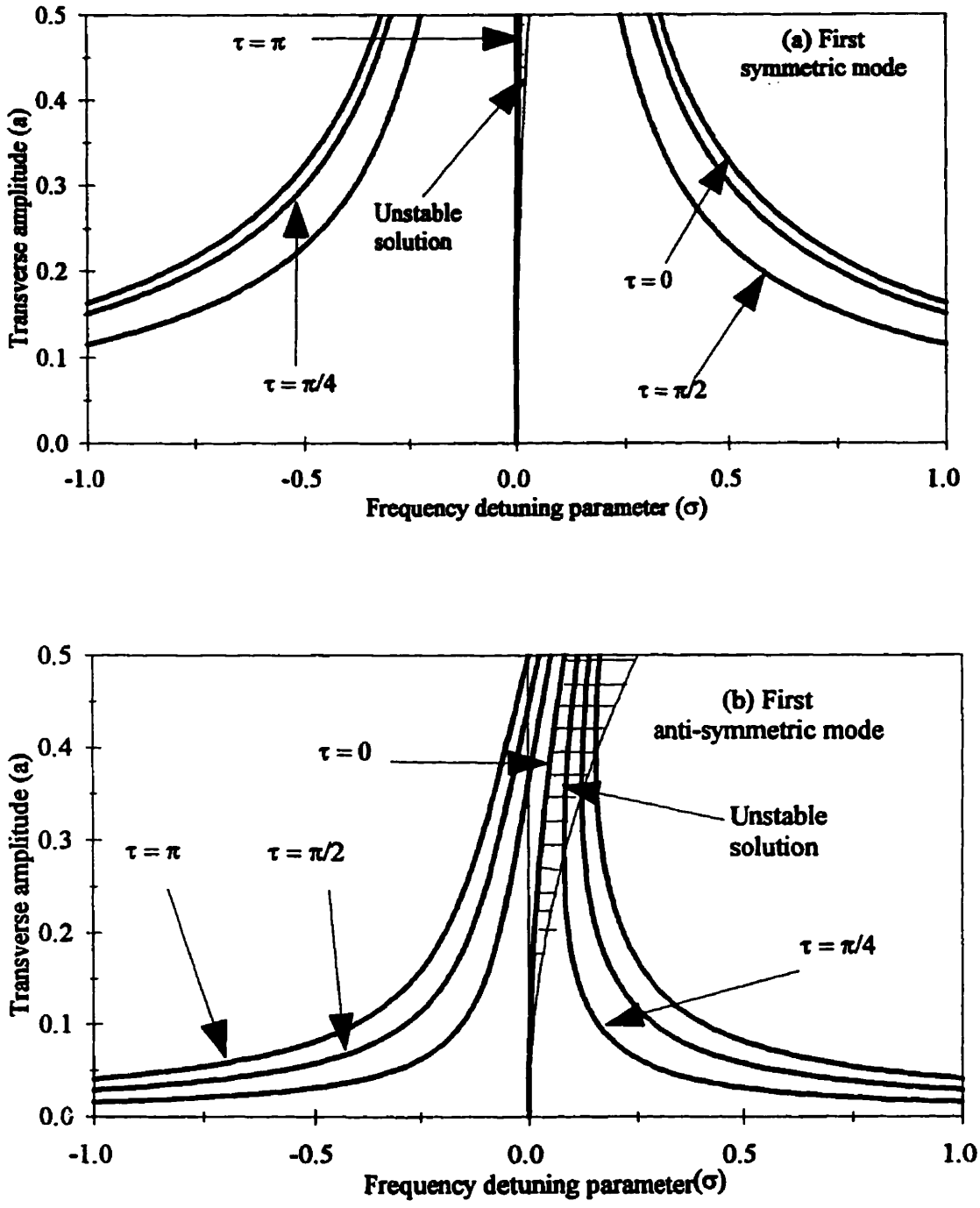

Figure 5.10 Effect of phase difference between transverse support excitation on the frequency response relationship of Cable I

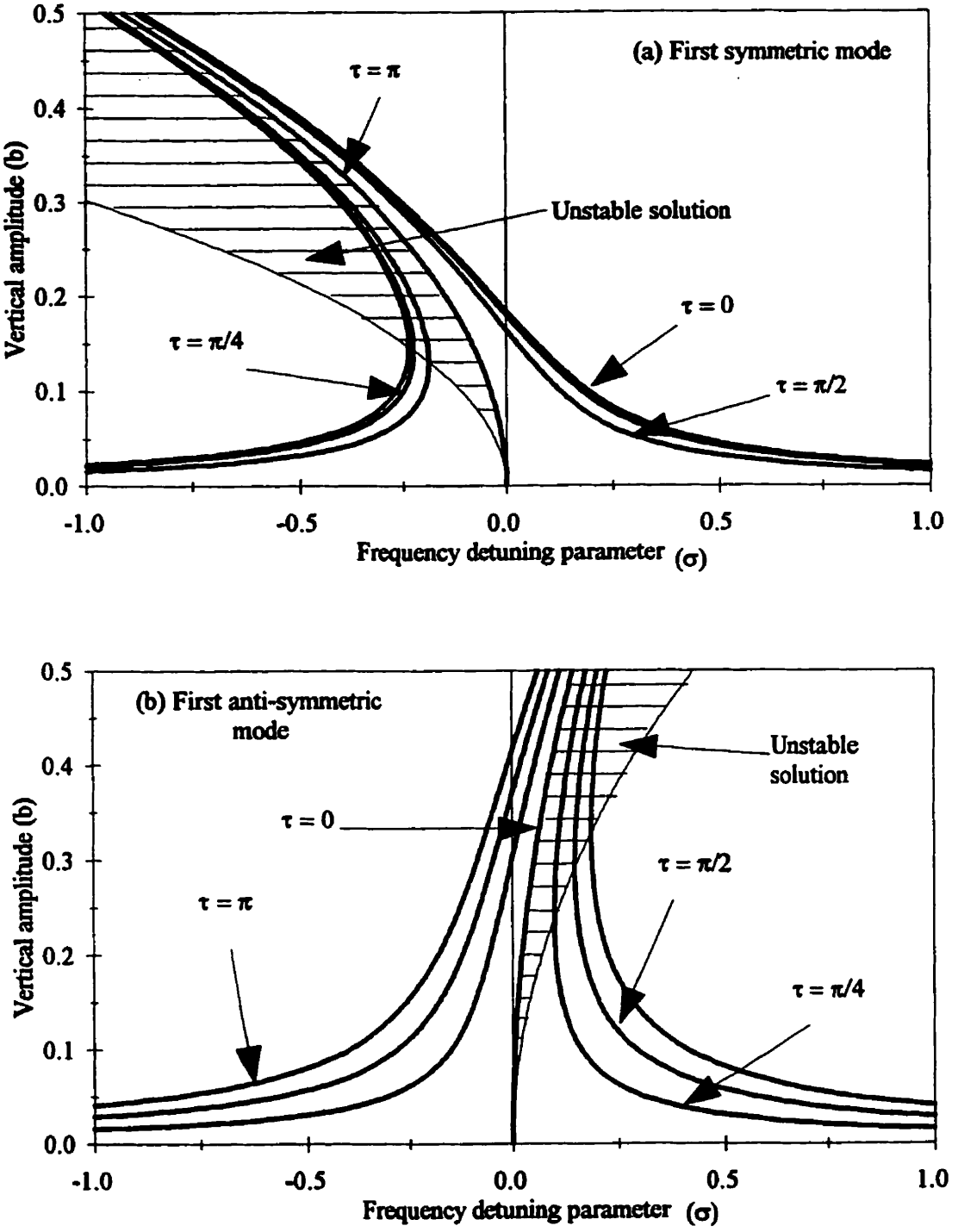

Figure 5.11 Effect of phase difference between vertical support excitation on the frequency response relationship of Cable I

CHAPTER 6

RELIABILITY ASSESSMENT OF CABLE VIBRATION

6.1 GENERAL

Transmission lines typically extend in areas of high seismicity and sometimes cross active faults. There have been several cases of line burn-out due to cable vibration during the 1994 Northridge earthquake (EERI, 1995). The current practice in the design of transmission lines is to account for wind and ice loads without consideration for seismic loading. The cable clearances specified for transmission lines by the National Electrical Safety Code (NESC, 1993) have not been checked for earthquake loading conditions. The NESC (1993) limits the initial cable tension to 35% of the breaking strength and limits the tension in the cable due to wind and ice loading to 60% of its breaking strength. This implies that the tension caused by wind and ice loading does not exceed the value of the initial static tension in the cable. However, there has been no attempt to check the magnitude of cable tension caused by earthquake ground motion.

The analysis of transmission line systems showed that there is a wide separation in the frequencies of free vibration between the towers and cables in the transverse direction (Aziz et al., 1996). Therefore, the tower vibration has little, or no, effect on the cable vibration. In the vertical direction, the tower is very stiff and again it has negligible effect on the cable

vibration. On this basis, an intermediate span of the line can be modelled by separate cables with the ground motion applied directly at the cable ends.

In this study, Monte Carlo simulation method is used to determine the probability that the cable displacement and cable tension will exceed a certain limit. The transmission line is subjected to vertical and transverse ground motions. The analysis is performed using both actual and artificial ground motion records. The results of the analysis are verified by comparing the mean values of the response quantities caused by artificial earthquakes to those caused by a sample of actual earthquakes. The strong ground motion duration and the parameters of the power spectrum function are considered as random variables. The generated ground motion records are scaled to different values of peak ground acceleration. Cable examples with varying sag to span ratios are used in the analysis. Sensitivity analysis is performed to examine the effects of various modelling assumptions on the results.

6.2 GROUND MOTION MODELLING

Several attempts have been made to generate artificial ground motion records using both stationary and nonstationary approaches. The procedure of generating ground motion records from a prescribed power spectral density function, as explained in Chapter 4, will be used in this analysis. Multiple support excitation is not considered to simplify the analysis.

The stationary acceleration time history can be generated in a similar way as described in Chapter 4 but for the case of uniform support excitation. The generated stationary ground acceleration is defined as:

$$\ddot{u}_g(t) = \sum_{k=1}^{N} \sqrt{2\, S_g(\omega_k)\, \Delta\omega}\, \sin(\omega_k t + \phi_k) \qquad (6.1)$$

where,

ω_k is the frequency corresponding to the power spectral ordinate;

k = 1, 2,....., n is the number of frequencies considered in the analysis. Typically this is taken equal to 200;

$S_g(\omega_k)$ is the value of the power spectral function for the ground acceleration, as defined by equation 6.2, calculated at ω_k;

$\Delta\omega = \omega_{k+1} - \omega_k$; and

ϕ_k is a random phase angle uniformly distributed between 0 and 2π.

6.2.1 Power Spectral Density

The power spectrum of the earthquake record is a distinctive characteristic of the ground motion. The Clough-Penzien (1975) power spectral density for the ground displacement , $S_g(\omega)$, is used to generate the ground motion. It is defined as:

$$S_g(\omega) = S_0 \frac{1 + 4\,\zeta_g^2 \left(\frac{\omega}{\omega_g}\right)^2}{\left[1 - \left(\frac{\omega}{\omega_g}\right)^2\right]^2 + 4\,\zeta_g^2 \left(\frac{\omega}{\omega_g}\right)^2} \frac{\left(\frac{\omega}{\omega_f}\right)^4}{\left[1 - \left(\frac{\omega}{\omega_f}\right)^2\right]^2 + 4\,\zeta_f^2 \left(\frac{\omega}{\omega_f}\right)^2} \qquad (6.2)$$

where S_0 is a scale factor; ω_g, ζ_g are the first filter parameters for the ground motion and the second filter parameters are ω_f and ζ_f. The statistical values of the first filter parameter for

the horizontal component of ground motion were given by Lai (1982) based on the study of 118 soil-site records and 22 rock-site records, as shown in table 6.1

From the analysis of the vertical component records of 161 soil sites and 26 rock sites, Elghadamsi et al. (1988) found that the mean value of ω_g is 4.17 Hz for soil-site records and 6.18 Hz for rock-site records. They also found that the mean value of ζ_g is 0.46 for all sites. Since the coefficients of variation of these parameters are not provided, in this study they will be assumed equal to those of the horizontal component of ground motion. The value of ω_f is taken equal to 0.1 ω_g and ζ_f is considered equal to ζ_g. The probability distribution of the filter parameters is assumed to be normal distribution. The effect of this assumption on the results is examined later.

6.2.2 Temporal Shape of the Ground Motion

To model the time varying intensity of a typical earthquake, the stationary acceleration time history generated by equation 6.1 is typically multiplied by a suitable envelope nonstationary function. One form for this envelope function $\psi(t)$, is defined by Sues et al. (1985) as:

$$\begin{aligned} \psi(t) &= \left(\frac{t}{t_1}\right)^2 \quad ; \quad 0 \le t \le t_1 \\ &= 1 \quad ; \quad t_1 \le t \le t_2 \\ &= e^{-c(t - t_2)} \quad ; \quad t_2 \le t \end{aligned} \tag{6.3}$$

where t_1 and t_2 are the rise and decay times of the ground motion, t_2-t_1 is the strong shaking duration and c is a decay parameter as shown in figure 6.1. Sues et al. (1985) used values of

t_1 = 1.5 s and c = 0.18. They also recommended a mean duration of the strong ground shaking of 10.0 s for soft soil and 5.5 s for rock with a coefficient of variation of almost 0.9 for all cases. The duration of strong ground motion shaking is assumed to be normally distributed.

6.3 ANALYSIS PROCEDURE

The cable vibration problem is nonlinear due to the geometric nonlinearity of the cable. To determine the statistical characteristics of cable vibration, it is not possible to use a closed form mathematical formulation and a simulation procedure is required to be used in the analysis. The selected method is the Monte Carlo simulation which is a powerful tool for the statistical analysis of uncertainty in complex engineering problems.

The analysis carried out by several researchers such as Gambhir and Batchelor (1978), suggested that the cable sag to span ratio is the most important parameter that affects the cable's natural frequencies and response to dynamic loading. On this basis, all other cable characteristics will be maintained constant in the analysis. The following properties are assumed to represent a typical cable:

Span	= 400 m	Weight	= 22.23 N/m
Young's modulus	= 55×10^3 MPa	Damping ratio	= 0.01
Cable cross section area	= 10^{-3} m^2		

The simulation method can be summarized in the following steps:

1. Five cable examples are used with sag to span ratios in the range normally used in the construction of transmission lines (3.0%, 3.5%, 4.0%, 4.5% and 5.0%).

2. Using the mean, the coefficient of variation, the probability distribution of the ground motion parameters and the strong shaking duration, one hundred artificial records are generated for the horizontal ground acceleration for soil-sites and 100 records for rock sites. Similar number of records are generated for the vertical ground acceleration for soil and rock sites.
3. Each record is scaled up to different values of peak ground acceleration of 0.25 g, 0.50 g, 0.75 g and 1.0 g.
4. Each point of the results represents the effect of one hundred earthquakes on the five cables which total five hundred cable response analysis calculations.
5. The mean and standard deviation of the maximum displacement and the maximum tension in the cable are calculated.

6.4 CABLE RESPONSE

The cable response is evaluated in terms of two quantities; the maximum displacement of the cable in either the vertical or the transverse directions and the maximum dynamic cable tension as a ratio of the initial static tension in the cable due to its own weight. The statistical properties of the response quantities are presented first, then design guidance and probability distribution curves are plotted.

6.4.1 Statistical Properties

Figures 6.2 and 6.3 show the mean value (μ) and the mean $\pm$ one standard deviation ($\mu \pm \sigma$) of the cable displacement in the transverse and vertical directions for different soil

conditions. Values of the mean and coefficient of variation of the transverse and vertical displacements are listed in tables 6.2 and 6.3, respectively. The results show that the mean of the maximum displacement in the transverse direction is larger than that in the vertical direction. For example, for a peak ground acceleration of 1.0 g, the mean of the maximum lateral displacement is 260.4 cm for soil sites, while the mean of the maximum vertical displacement is 174.2 cm for the same soil site.

The mean of the maximum displacement in the transverse and vertical directions are larger for ground motion on soil sites than for ground motion on rock sites as shown in figures 6.2 and 6.3. For example, for a peak ground acceleration of 0.5 g, the mean maximum transverse displacement for soil sites is 138.7 cm while it is equal to 72.5 cm for rock sites. For the same value of peak ground acceleration, the mean of the maximum vertical displacement is 76.2 cm for soil sites and 63.2 cm for rock sites. The reason for the smaller values of displacement for rock sites is that the ground motion records on rock sites have higher frequency content than the records on soil sites. The cable fundamental frequencies in the transverse and vertical directions are low as shown in Chapter 2. For the case of the cable considered in the analysis and for a sag to span ratio of 0.03, the fundamental frequency of free vibration in the vertical direction is 0.38 Hz and the fundamental frequency of free vibration in the transverse direction is 0.15 Hz.

The coefficient of variation of the vertical displacement is less than that of the transverse displacement as shown in tables 6.2 and 6.3. The modes of vibration in the transverse direction are widely separated and the response is governed by the first mode which increases the number of the relatively high and the relatively low values of transverse

displacements. Consequently, the coefficient of variation of the transverse displacement increases. On the other hand, in the vertical direction the modes of vibration are closely spaced which reduces the possibility of extreme values of the response and hence the coefficient of variation of the maximum vertical displacement is reduced.

Figures 6.4 and 6.5 show the mean and the mean ± one standard deviation of the ratio of the maximum dynamic to the static tension in the cable due to transverse and vertical excitations, respectively. Values of the mean of the dynamic to static tension and the coefficient of variation are given in tables 6.4 and 6.5 for transverse and vertical excitations, respectively. The results show that the mean of the tension due to vertical excitation is much larger than the mean value of the tension due to transverse excitation. For example, for a peak ground acceleration of 1.0 g on soil sites, the mean of the ratio of dynamic to static tension is 0.822 due to vertical excitation and 0.316 due to transverse excitation. The reason for this reduction in mean tension is the fact that the transverse vibration of cables is usually of a swinging type that causes little change in the cable length and consequently does not produce significant strains and stresses.

Similar to the displacement response of the cable, the tension in the cable due to seismic excitation on soil sites is larger than the tension in the cable due to seismic excitation on rock sites. Moreover, the coefficient of variation of cable tension due to seismic ground motion in the vertical direction is less than that due to seismic ground motion in the transverse direction.

The results in figures 6.2 to 6.5 show that the relationship between the peak ground acceleration and the mean value of the maximum cable response can be approximated by a

straight line. The reason is that the nonlinear behaviour of the cable results mainly from the large displacement which is limited to the case of resonance. Otherwise, there is no large displacement in the cable and the response is almost linear.

6.4.2 Recorded and Generated Earthquakes

The use of actual earthquake records in the proposed simulation procedure involves a number of difficulties. Many of the available records are not well identified for being on soil or rock sites. In addition, many of the available records are not free field time histories but rather modified by the response of a structure. For these reasons, the number of available and usable earthquake records is not large enough to obtain sufficiently accurate results.

The current analysis is based on 100 generated time histories for each case of horizontal and vertical motions for rock and soil sites. In order to evaluate the effect of using generated versus actual earthquake records, the mean values of the maximum displacement of the cable due to artificial ground motion are compared to the similar values of the response using a smaller sample of actual earthquake ground motion. The vertical and horizontal components of a sample of 45 actual ground motion records are used in the analysis (Naumoski et al., 1988). The sample consists of 24 rock-site records and 21 stiff soil-site records as shown in table 6.6.

Figures 6.6 and 6.7 show the mean value of cable displacement in the transverse and vertical directions, respectively. These figures show a reasonable agreement between the cable displacement using actual records and generated ground motion. For example in the transverse direction, using actual records scaled to a peak ground acceleration of 1.0 g results

in a mean value of maximum cable displacement of 240.0 cm for soil sites and 151.2 cm for rock sites. Using artificial earthquakes, the cable displacement is 260.4 cm for soil sites and 142.3 for rock sites with a percentage difference of 7.8% for soil sites and 6.3% for rock sites. These differences are mainly due to the small size of actual earthquakes sample.

For the vertical component of ground motion, the differences between the cable response to actual and generated time histories are larger than the case of the horizontal ground motion. For example, using actual earthquakes scaled to a peak ground acceleration of 1.0 g results in a mean maximum vertical displacement of 197.1 cm for soil sites and 153.8 cm for rock sites. Using artificial earthquakes, the cable displacement is equal to 174.2 cm for soil sites and 132.0 cm for rock sites. The percentage difference is 13.1% for soil sites and 16.5% for rock sites. The reason for the larger difference is due to the lack of comprehensive representative statistical data for the vertical component of ground motion. However, the differences are still small enough as compared to the uncertainty in the analysis.

6.4.3 Probability Distribution for Cable Response

Figures 6.8 and 6.9 show the probability of exceedance of the cable maximum transverse and vertical displacements, respectively for different values of peak ground acceleration and for different site conditions. Small probabilities of less than 10% as indicated by the horizontal line in the figures, should be treated with caution because of their low degree of reliability. To increase the accuracy of the solution, the sample size may be increased. These curves can be used as a basis to design the clearances of transmission lines for seismic requirements along with other loads and functional requirements.

Using figures 6.8 and 6.9 to design the clearance of transmission lines in a specific area is a straightforward process. First, the design peak ground acceleration should be defined for the area under consideration for a specific return period. Then the designer should specify a specific probability of exceedance for the design of the power transmission line. Finally, using these figures, the maximum displacement corresponding to the defined peak ground acceleration and the specified probability of exceedance can be determined.

Figures 6.8 and 6.9 indicate that the probability of exceedance for the transverse displacement can be considerable and illustrate the need to take seismic loading into consideration in the design of transmission lines. For example, for soil sites and for a peak ground acceleration of 1.0 g, there is a probability of 78% that the cable displacement exceeds 1.0 m, a probability of 29% that it exceeds 3.0 m and a probability of 16% that the displacement exceeds 5.0 m. These high probability values should be addressed in the design process.

The probability that the ratio between the dynamic and the static tension of the cable exceeds a certain limit due to vertical excitation is shown in figure 6.10. This figure indicates that the probability that the dynamic tension exceeds the static tension may reach 22% for soil sites and 17% for rock sites. These probabilities are high which suggest that the seismic loading should be taken into consideration in the design of transmission line cables.

6.5 SENSITIVITY ANALYSIS

Several assumptions have been made in the analysis concerning the cable sag to span ratio and the ground motion parameters. The effect of different assumptions on the cable

response is studied using a sensitivity analysis. Since the cable response to soil-site records is larger than its response to rock-site records, only the results for soil-site records are presented.

6.5.1 Cable Sag to Span Ratio

The results shown in figures 6.2 to 6.10 represent the average of five cable examples with sag to span ratios of 3.0%, 3.5%, 4.0%, 4.5% and 5.0%. This range of cable sag to span ratio represents the practical range of cable sag that is commonly used for transmission lines. Figure 6.11 shows the maximum values of cable displacements in the vertical and transverse directions for cables with different sag to span ratios. The differences between the response of the cable with a sag to span ratio of 3% and that of the cable with a sag to span ratio of 5% are relatively small. Cables with sag to span ratio 3% and 5% represent the limits of the considered range of cable sag. The response of the taut cable (sag to span ratio of 1%) is less than the response of the sagged cables. Taut cables are outside the range of interest because it is used less frequently in transmission lines due to their high initial tension. The effect of the cable sag on its displacement in the vertical direction is much smaller than that in the transverse direction which results mainly from the correlation between the natural frequencies of different cables and the predominant frequency of the ground motion.

6.5.2 Ground Motion Duration

To study the effect of the mean value of strong ground motion duration ($t_2 - t_1$) on the cable response, the mean value of the duration for soil-site records is reduced from 10.0 s to

5.0 s. Figures 6.12 and 6.13 show the effect of reducing the mean value of the duration on the cable maximum displacement and tension, respectively. The difference in the maximum displacement in both directions is relatively small. For example, for a peak ground acceleration of 1.0 g, the mean value of the maximum cable transverse displacement is reduced from 260.4 cm to 230.2 cm with a percentage change of 11.5% when the duration is reduced to the half. The maximum vertical displacement is reduced from 174.2 cm to 132.4 cm with a percentage change of 24% when the duration is reduced to the half. The reason is that the response is mainly governed by the first mode. Away from the first mode frequency, the cable response is very small and the duration has no effect on the response. The results in figures 6.12 and 6.13 suggest that there is confidence in the analysis using strong ground motion duration of 10.0 s.

6.5.3 Probability Distribution of the Ground Motion

The probability distribution of the ground motion predominant frequency ω_g was assumed to be normal. To examine the effect of this assumption on the results, the probability distribution of ω_g is assumed to be lognormal and the results are compared to that of the normal distribution as shown in figure 6.14. The results indicate that the effect of the difference in the probability distribution for ω_g is small and does not exceed 10% which endorses the use of normal distribution for its simplicity.

6.6 SUMMARY

The characteristics of the response of transmission line cables to seismic excitation are analyzed. The cables are modeled as fixed at both ends and the interaction effects with the towers are neglected. Generated ground acceleration time histories are used in the analysis. Monte Carlo simulation method is applied to determine the statistical properties of the cable response to transverse and vertical seismic ground motions.

The analysis shows that the cable response due to artificial ground motion is close to its response using actual earthquake records. It also shows that the local soil conditions have a significant effect on the response of cables to transverse and vertical ground motions. The soil site records where the frequencies of ground motion are relatively low, have larger effect on the cable vibration than the rock site records with a higher frequency content. The tension produced in the cable due to vertical ground motion is much larger than the tension produced due to transverse ground motion. The transverse vibration of cables is of a swinging type and does not produce significant stress.

The probability that the dynamic cable tension produced by vertical ground motion exceeds the static cable tension is high in several cases which suggests that the seismic loading needs to be considered in the design of the cable. The displacement of the cable due to transverse and vertical excitations can be significant and should be taken into account in examining the allowable clearances of transmission lines.

Table 6.1 Statistics for the Clough-Penzien power spectral density function

Ground condition		ω_g (Hz)		ζ_g	
		Mean	Coefficient of variation	Mean	Coefficient of variation
Rock	Horizontal	4.25[1]	0.398[1]	0.35[1]	0.391[1]
	Vertical	6.18[2]	0.398[3]	0.46[2]	0.391[3]
Soil	Horizontal	3.04[1]	0.425[1]	0.32[1]	0.426[1]
	Vertical	4.17[2]	0.425[3]	0.46[2]	0.426[3]

(1) Lai (1982)
(2) Elghadamsi (1988)
(3) assumed

Table 6.2 Maximum cable transverse displacement

Peak Ground Acceleration (PGA)	Soil sites		Rock sites	
	Mean (cm)	Coefficient of variation	Mean (cm)	Coefficient of variation
0.25 g	70.1	0.58	35.0	0.57
0.50 g	138.7	0.59	72.5	0.59
0.75 g	201.0	0.59	105.5	0.60
1.00 g	260.4	0.58	142.3	0.60

Table 6.3 Maximum cable vertical displacement

Peak Ground Acceleration (PGA)	Soil sites		Rock sites	
	Mean (cm)	Coefficient of variation	Mean (cm)	Coefficient of variation
0.25 g	35.0	0.43	30.2	0.47
0.50 g	76.2	0.44	63.2	0.48
0.75 g	122.7	0.43	91.5	0.49
1.00 g	174.2	0.43	132.0	0.50

Table 6.4 Dynamic to static cable tension ratio due to transverse excitation

Peak Ground Acceleration (PGA)	Soil sites		Rock sites	
	Mean	Coefficient of variation	Mean	Coefficient of variation
0.25 g	0.071	0.45	0.041	0.49
0.50 g	0.151	0.46	0.081	0.50
0.75 g	0.229	0.46	0.132	0.49
1.00 g	0.316	0.46	0.180	0.50

Table 6.5 Dynamic to static cable tension ratio due to vertical excitation

Peak Ground Acceleration (PGA)	Soil sites		Rock sites	
	Mean	Coefficient of variation	Mean	Coefficient of variation
0.25 g	0.180	0.34	0.152	0.41
0.50 g	0.392	0.38	0.306	0.43
0.75 g	0.605	0.37	0.487	0.45
1.00 g	0.822	0.36	0.670	0.45

Table 6.6 Description of the used ground motion records (Naumoski et al. 1988)

Rec. No.	Date & Event	Magn.	Station	Horizontal Component	Soil Condition
1	1966 Parkfield	5.6	Temblor No. 2	N65W	Rock
2	1966 Parkfield	5.6	Cholame, Shandon No. 5	N85E	Rock
3	1957 San Francisco	5.3	Golden Gate Park	S80E	Rock
4	1957 San Francisco	5.3	State Bldg.	S09E	Stiff Soil
5	1935 Helena	6.0	Carroll College	N00E	Rock
6	1970 Lytle Creek	5.4	Wrightwood, California	S25W	Rock
7	1975 Oroville	5.7	Seismogr. Station	N53W	Rock
8	1971 San Fernando	6.4	Pacoima Dam	S74W	Rock
9	1971 San Fernando	6.4	Lake Hughes, Station 4	S21W	Rock
10	1985 Nahanni	6.9	Site 1, Iverson	LONG	Rock
11	1971 Central Honshu, Japan	5.5	Yoneyama Bridge	TRANS	Stiff Soil
12	1972 Near E. Coast Japan	5.8	Kushiro Central Whraf	N00E	Stiff Soil
13	1966 Honshu, Japan	5.4	Hoshina-A	N00E	Stiff Soil

Table 6.6 (cont.) Description of the used ground motion records (Naumoski et al. 1988)

Rec. No.	Date & Event	Magn.	Station	Horizontal Component	Soil Condition
14	1979 Monte Negro	5.4	Albatros Hotel, Ulcinj	N00E	Rock
15	1981 Benja Luka	6.1	Seism. Station, Benja Luka	N90W	Rock
16	1940 Imperial Valley	6.6	El Centro	S00E	Stiff Soil
17	1951 Kern County	7.6	Taft Lincoln School Tunnel	S69E	Rock
18	1951 Kern County	7.6	Taft Lincoln School Tunnel	N21E	Rock
19	1968 Borrego Mtn.	6.5	San Onofre SCE Power Plant	N57W	Stiff Soil
20	1968 Borrego Mtn.	6.5	San Onofre SCE Power Plant	N33E	Stiff Soil
21	1971 San Fernando	6.4	3838 Lankershim Blvd., L.A.	S90W	Rock
22	1971 San Fernando	6.4	Hollywood Storage P.E. Lot	N90E	Stiff Soil
23	1971 San Fernando	6.4	3407 6th Street, L.A.	N90E	Stiff Soil
24	1971 San Fernando	6.4	Griffith Park Observatory, L.A.	S00W	Rock
25	1971 San Fernando	6.4	234 Figueroa St., L.A.	N37E	Stiff Soil
26	1974 Near E. Coast Honshu, Japan	6.1	Kashima Harbor Wharf	N00E	Stiff Soil

Table 6.6 (cont.) Description of the used ground motion records (Naumoski et al. 1988)

Rec. No.	Date & Event	Magn.	Station	Horizontal Component	Soil Condition
27	1971 Near S. Coast Honshu, Japan	7.0	Kushiro Central Wharf	N90E	Stiff Soil
28	1979 Monte Negro	7.0	Albatros Hotel, Ulcinj	N00E	Rock
29	1985 Mexico	8.1	El Suchil, Guerrero Array	S00E	Rock
30	1985 Mexico	8.1	La Villita, Guerrero Array	N90E	Rock
31	1933 Long Beach	6.3	Subway Terminal, L.A.	N51W	Rock
32	1933 Long Beach	6.3	Subway Terminal, L.A.	N39E	Rock
33	1934 Lower Calif.	6.5	El Centro	S00W	Stiff Soil
34	1971 San Fernando	6.4	2500 Wilshire Blvd., L.A.	N61W	Stiff Soil
35	1971 San Fernando	6.4	3550 Wilshire Blvd., L.A.	WEST	Stiff Soil
36	1971 San Fernando	6.4	222 Figueroa Street, L.A.	S37W	Stiff Soil
37	1971 San Fernando	6.4	3470 Wilshire Blvd., L.A.	S90W	Stiff Soil
38	1971 San Fernando	6.4	4680 Wilshire Blvd., L.A.	N15E	Stiff Soil
39	1971 San Fernando	6.4	445 Figueroa St., L.A.	S38W	Rock

Table 6.6 (cont.) Description of the used ground motion records (Naumoski et al. 1988)

Rec. No.	Date & Event	Magn.	Station	Horizontal Component	Soil Condition
40	1971 San Fernando	6.4	Hollywood Storage, L.A.	S00W	Stiff Soil
41	1968 Near E. Coast Honshu, Japan	7.9	Muroran Harbor	N00E	Stiff Soil
42	1973 Near E. Coast Honshu, Japan	7.4	Kushiro Central Wharf	N00E	Stiff Soil
43	1985 Mexico	8.1	Zihuatenejo, Guerrero Array	S00E	Rock
44	1985 Mexico	8.1	Teacalco, Guerrero Array	N00E	Rock
45	1985 Mexico	8.1	Mesa Vibradora C.U., Mexico City	N90W	Rock

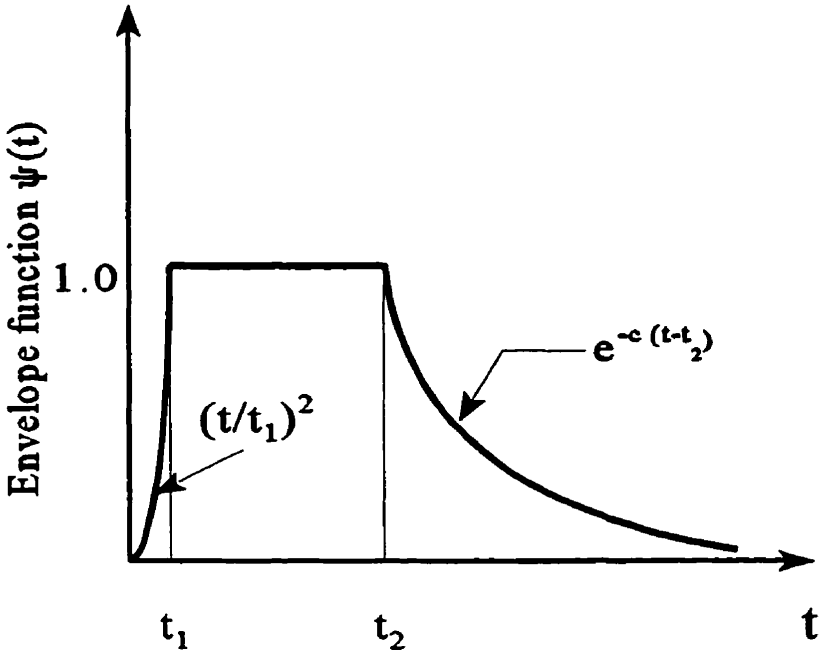

Figure 6.1 Envelope function for the ground motion acceleration time history

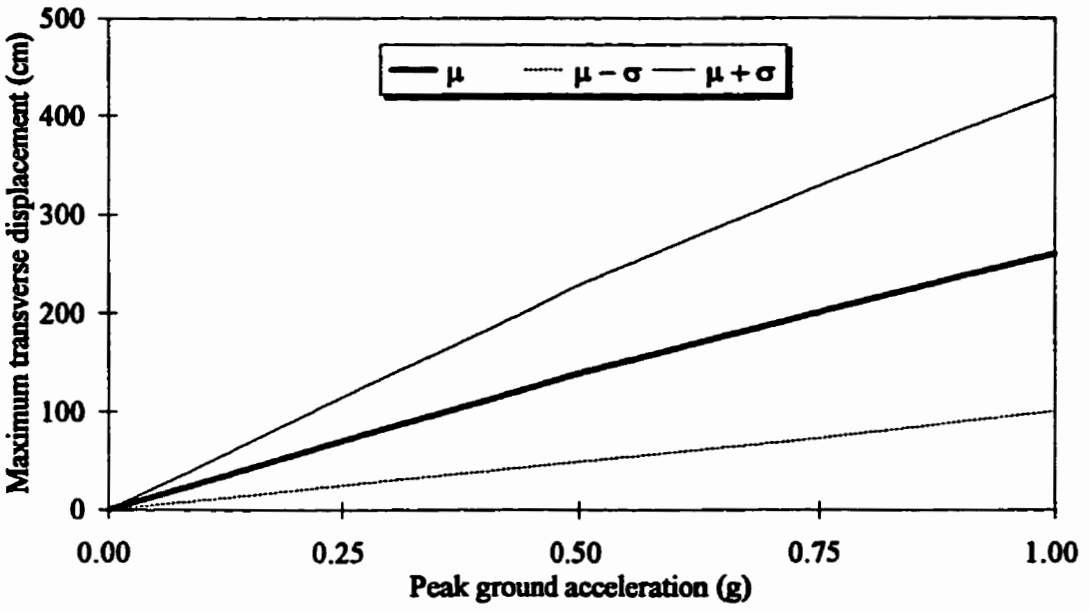

(a) Soil Sites

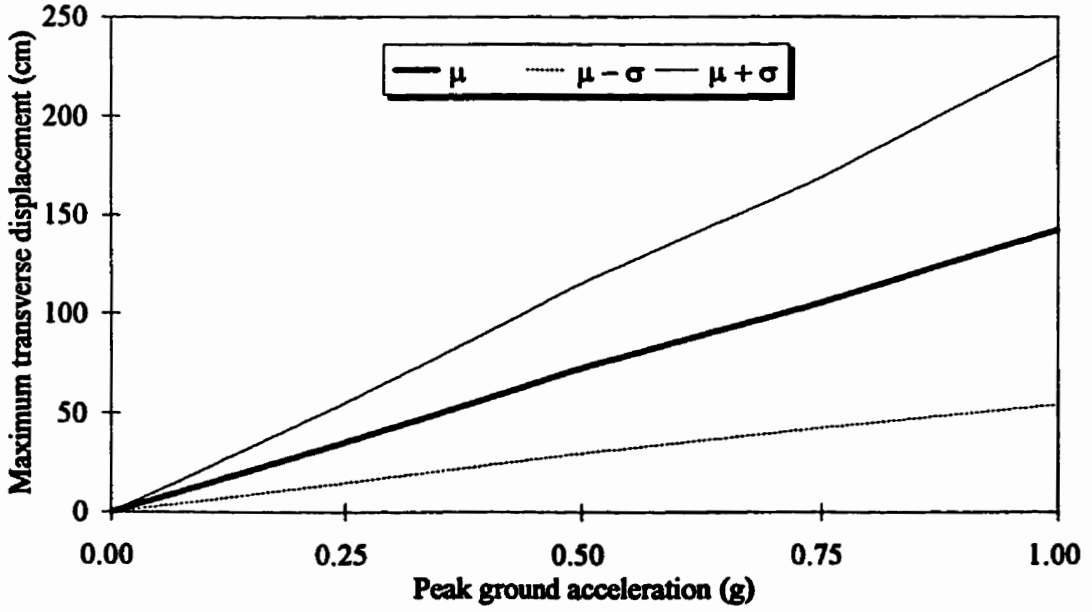

(b) Rock Sites

Figure 6.2 Maximum transverse displacement of cables due to transverse excitation

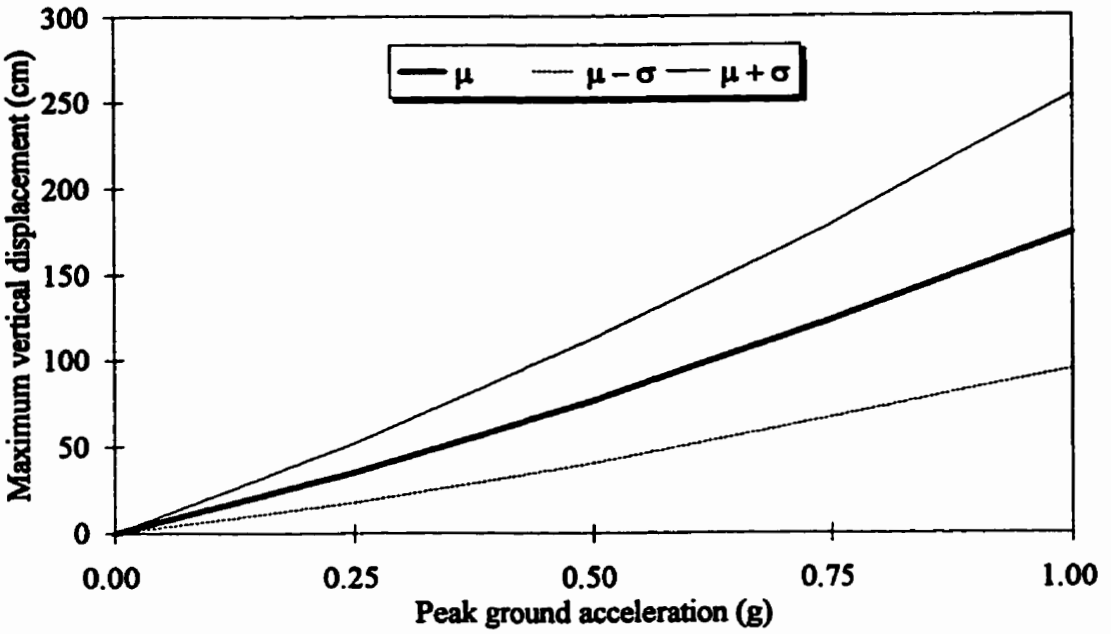

(a) Soil Sites

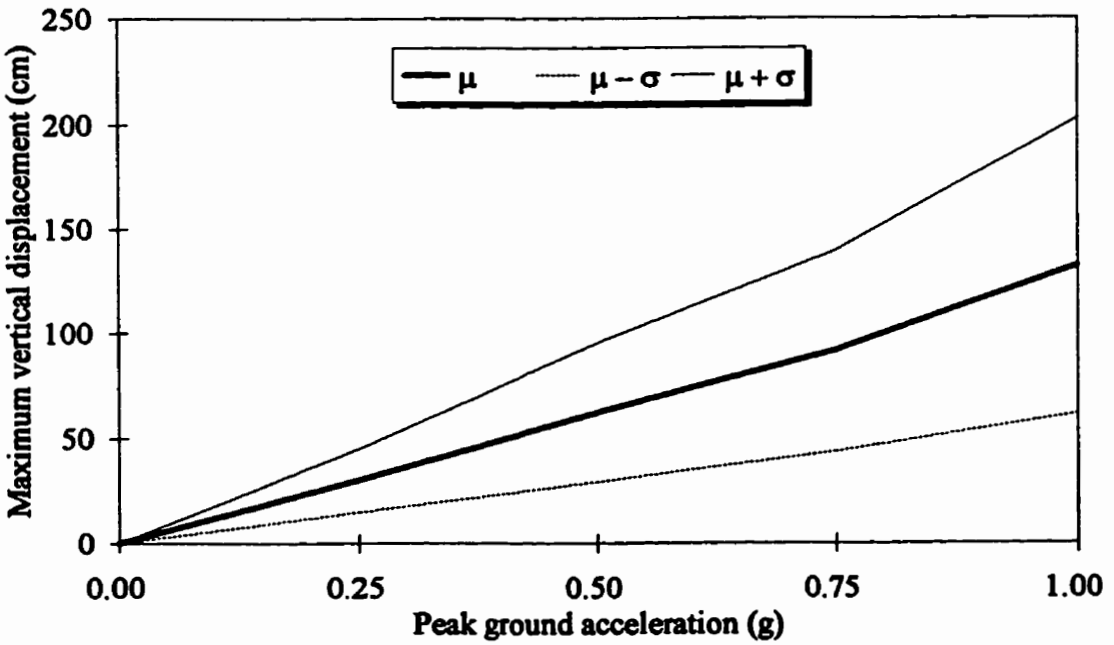

(b) Rock Sites

Figure 6.3 Maximum vertical displacement of cables due to vertical excitation

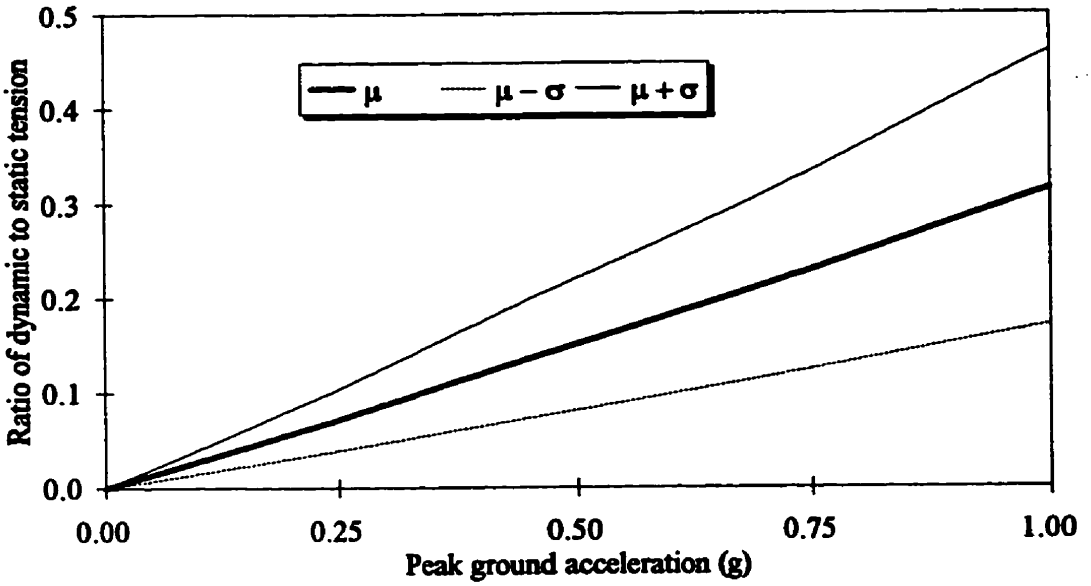

(a) Soil Sites

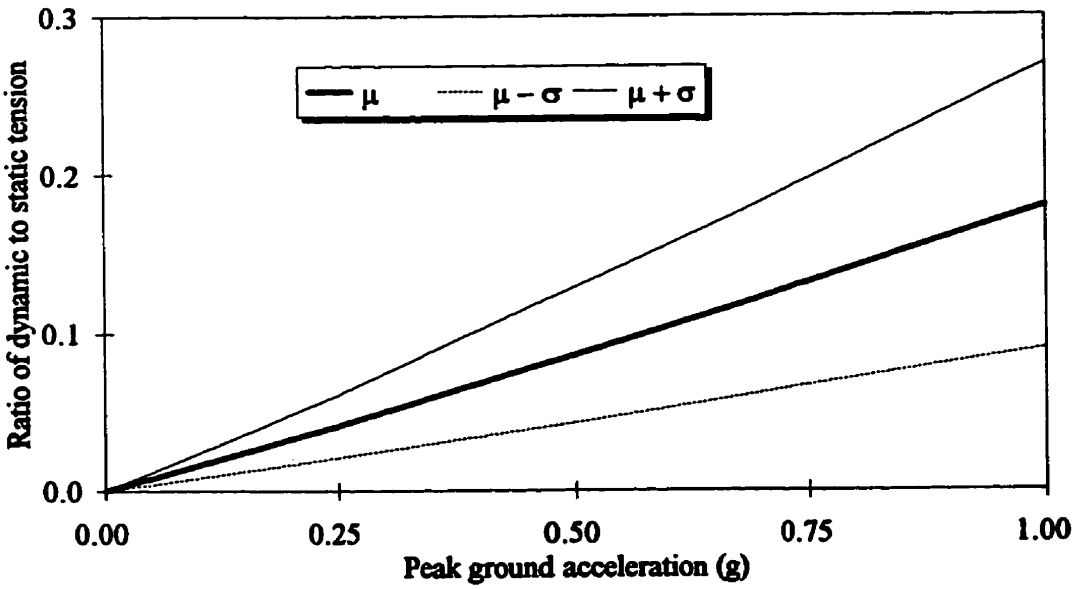

(b) Rock Sites

Figure 6.4 Maximum ratio of dynamic to static tension due to transverse excitation

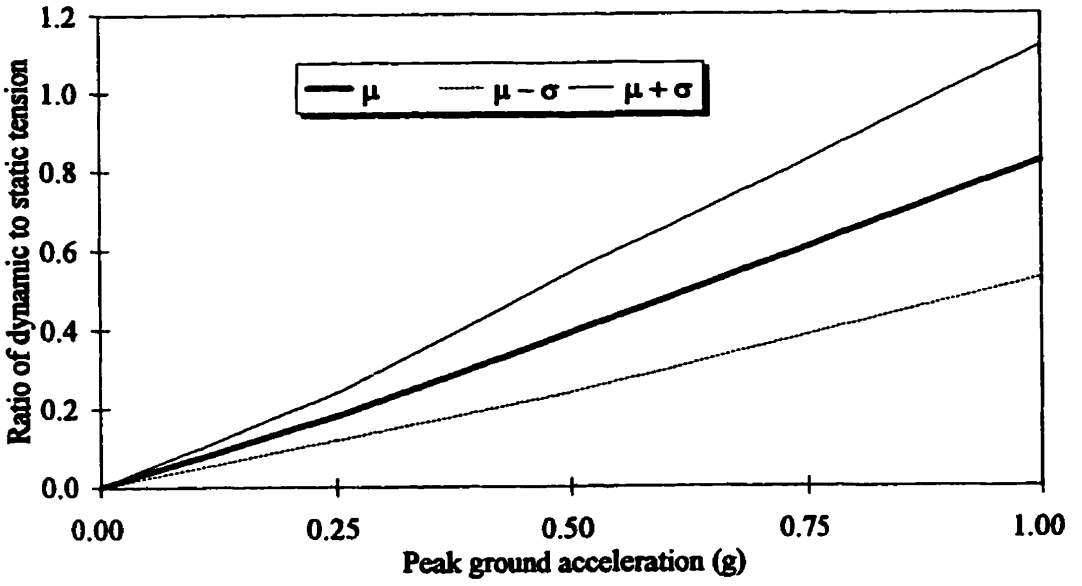

(a) Soil Sites

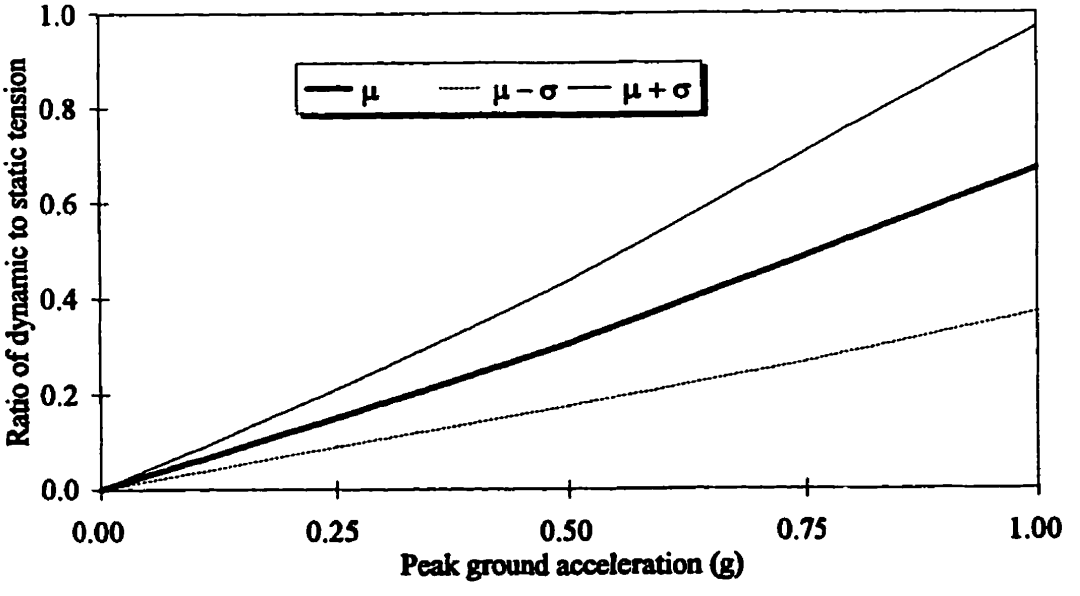

(b) Rock Sites

Figure 6.5 Maximum ratio of dynamic to static tension due to vertical excitation

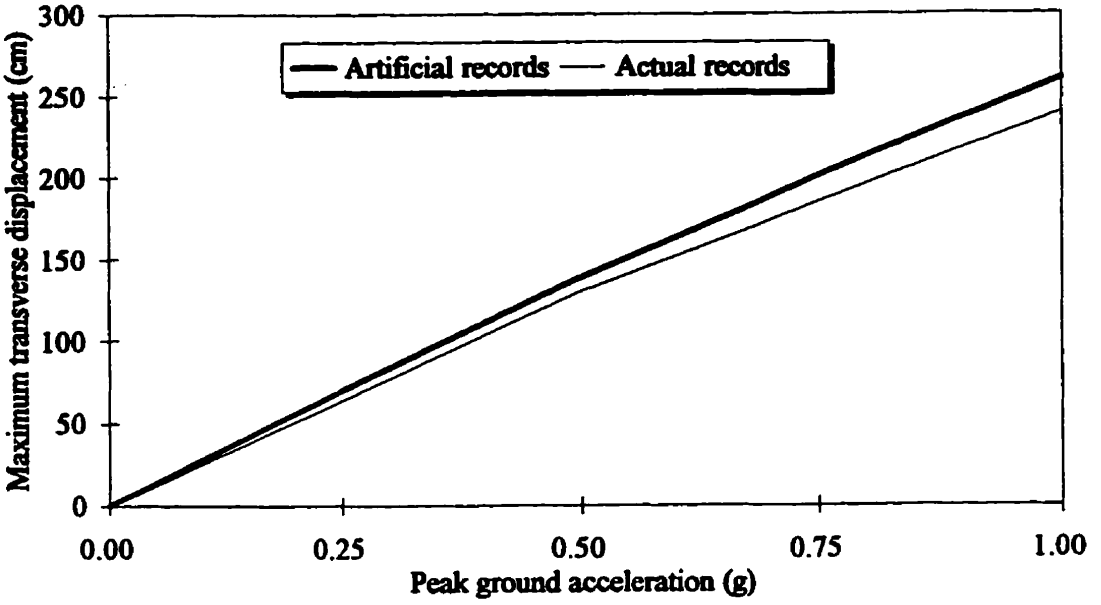

(a) Soil Sites

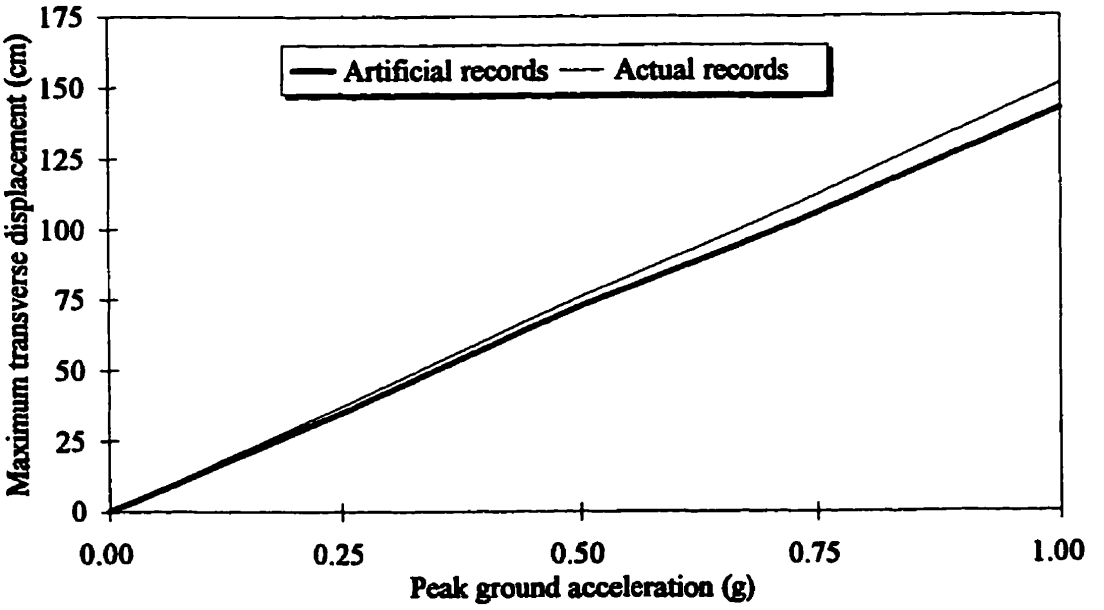

(b) Rock Sites

Figure 6.6 Comparison between the effect of the transverse component of actual and artificial ground motion

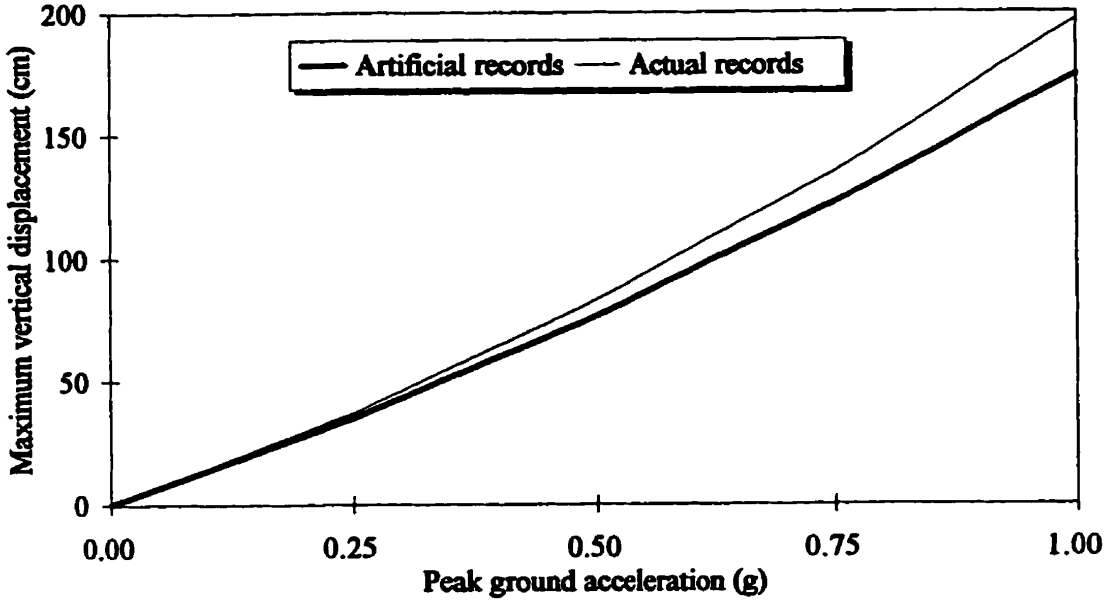

(a) Soil Sites

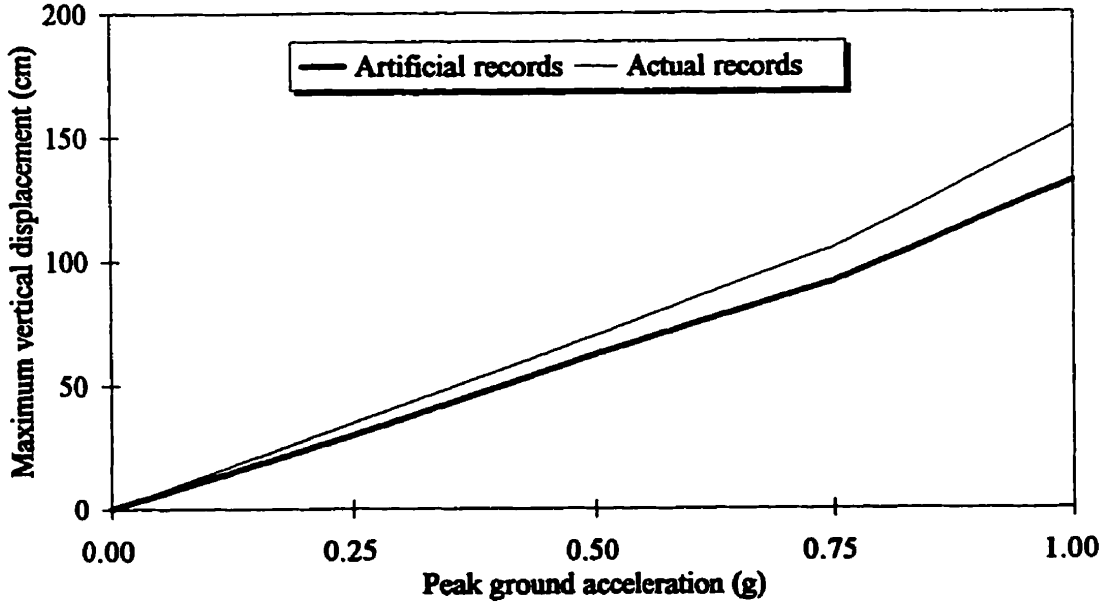

(b) Rock Sites

Figure 6.7 Comparison between the effect of the vertical component of actual and artificial ground motion

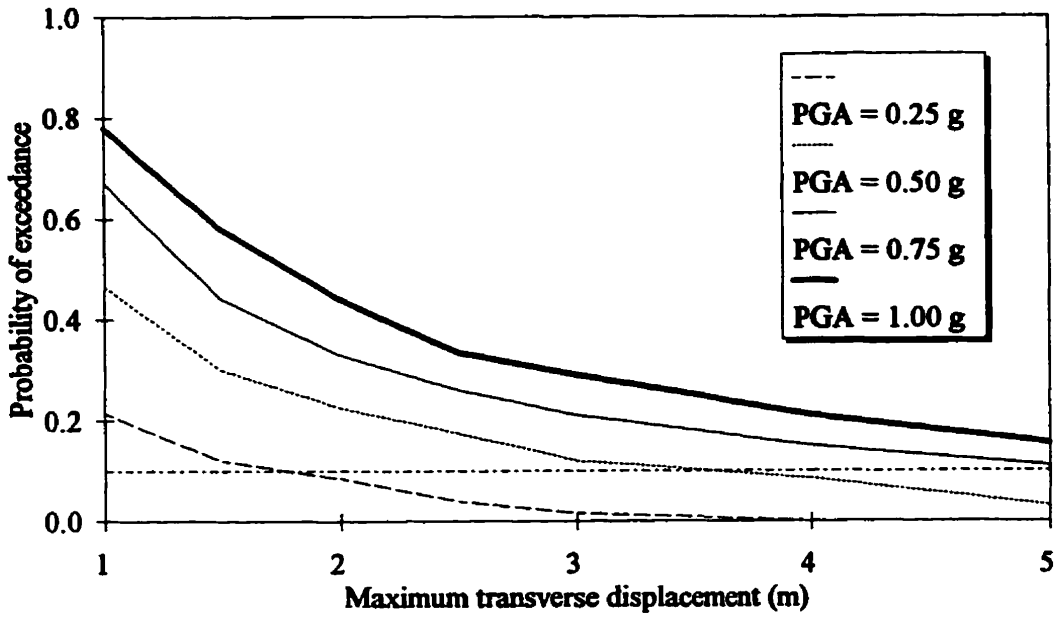

(a) Soil Sites

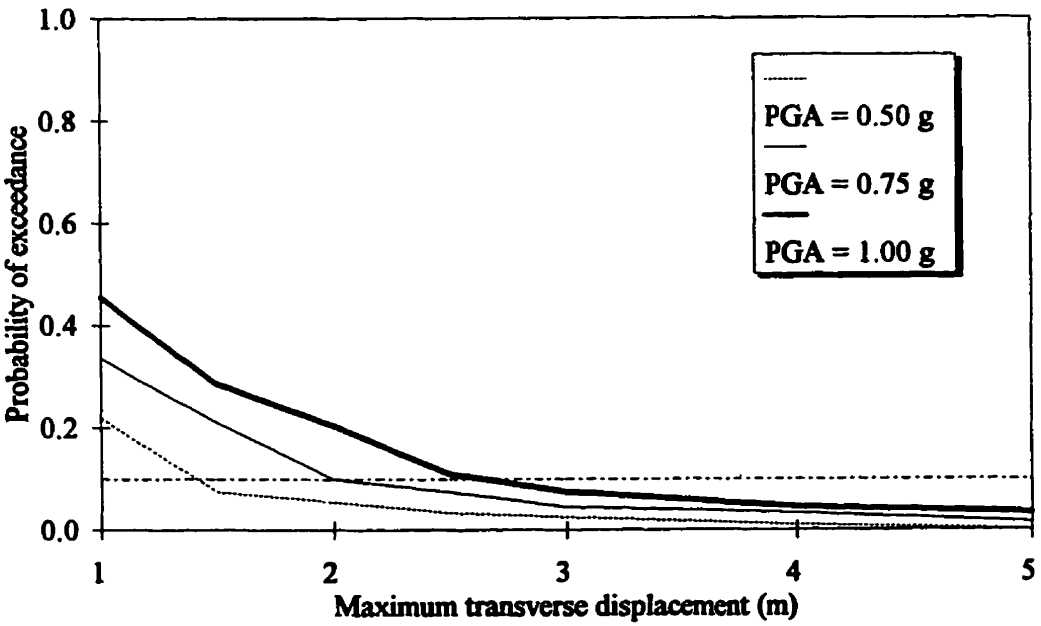

(b) Rock Sites

Figure 6.8 Probability of exceedance of maximum transverse cable displacement due to transverse excitation

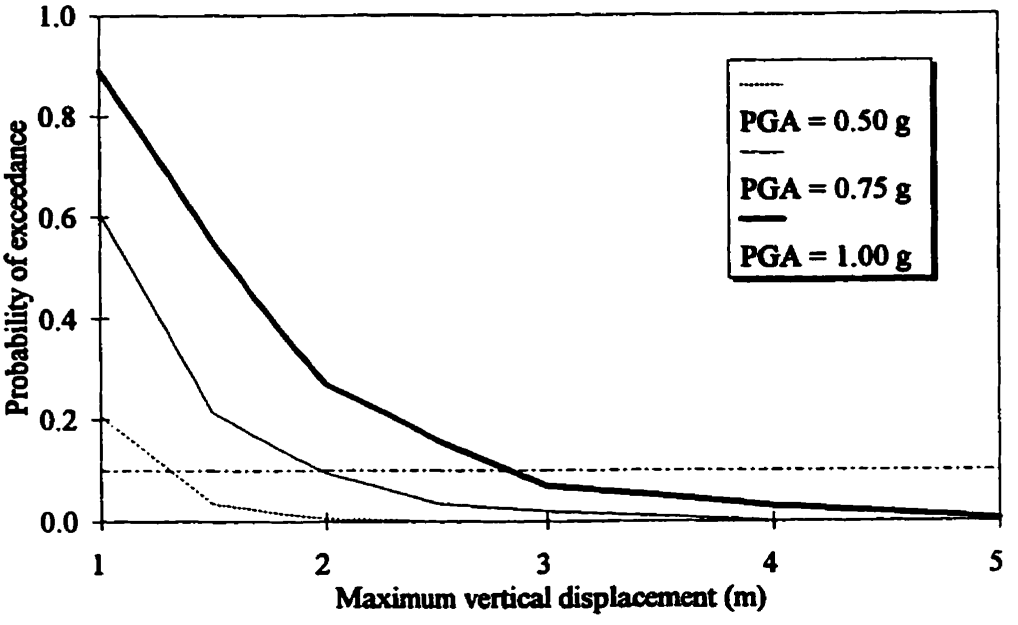

(a) Soil Sites

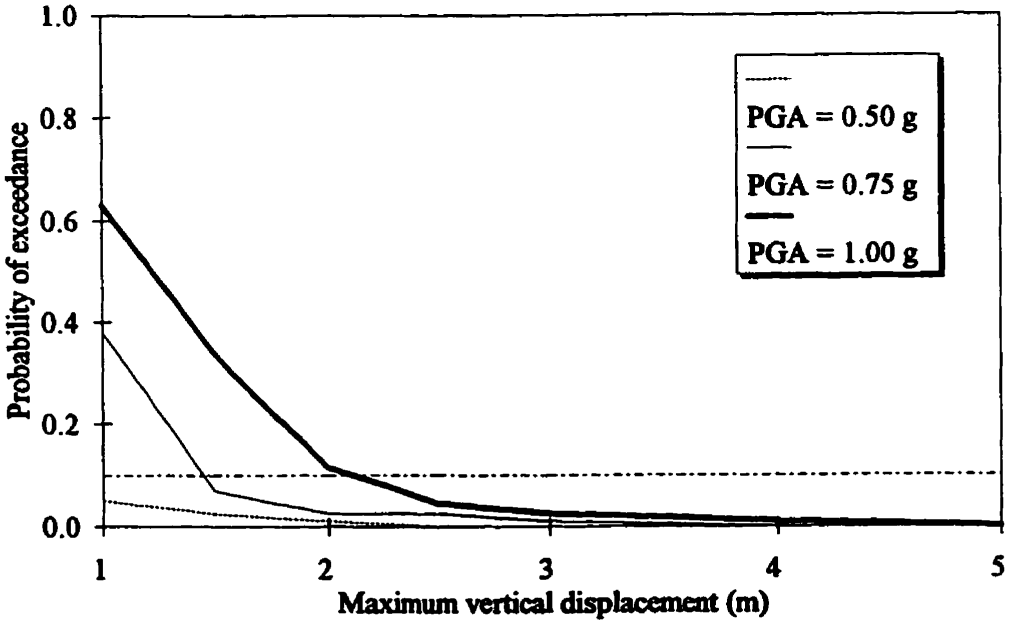

(b) Rock Sites

Figure 6.9 Probability of exceedance of maximum vertical cable displacement due to vertical excitation

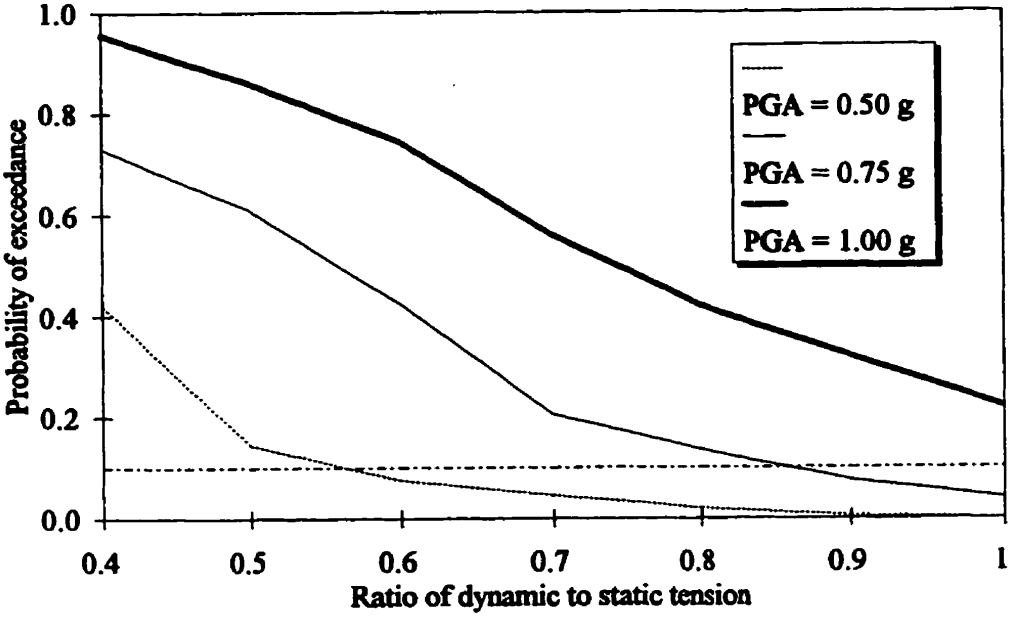

(a) Soil Sites

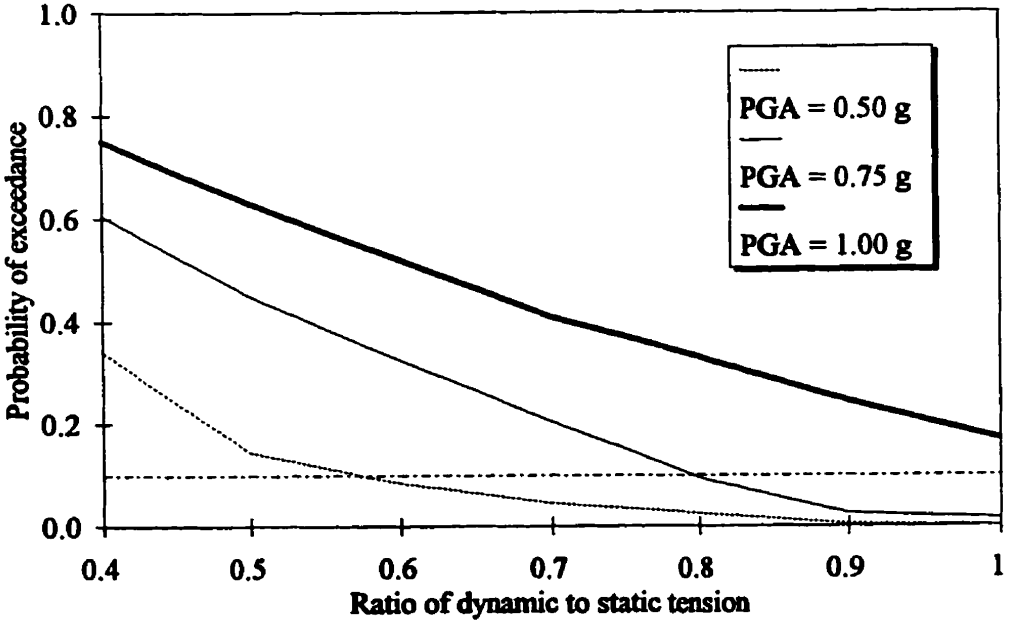

(b) Rock Sites

Figure 6.10 Probability of exceedance of maximum dynamic to static cable tension due to vertical excitation

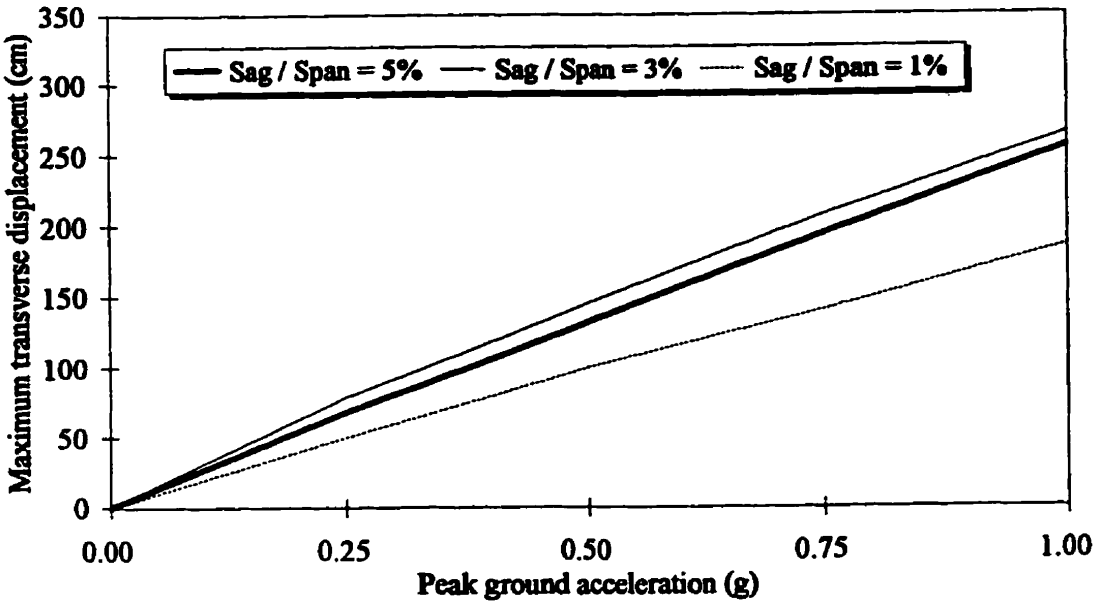

(a) Transverse excitation

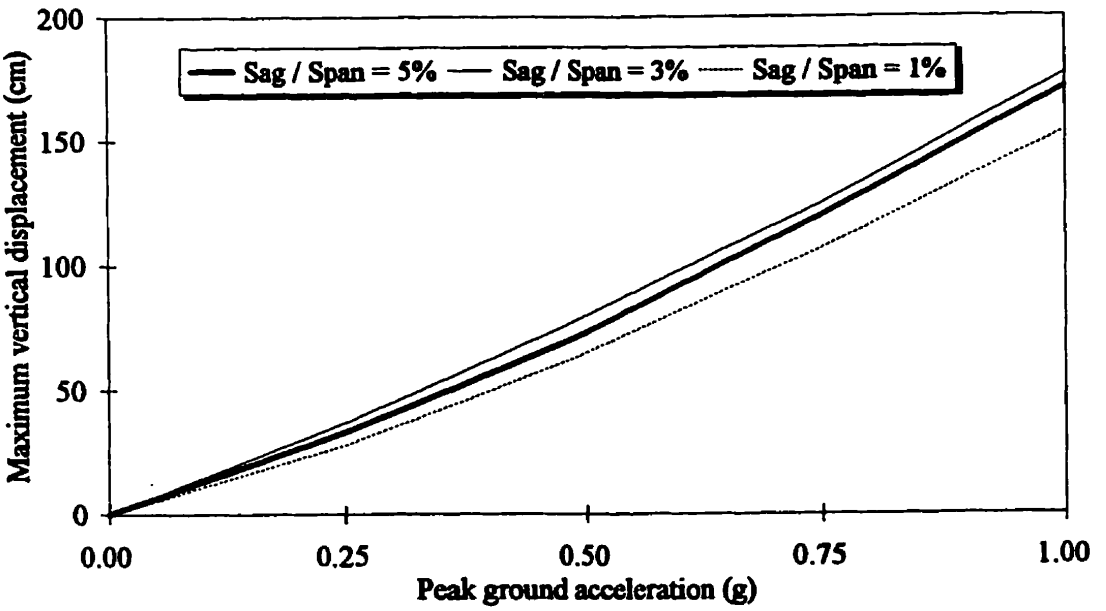

(b) Vertical excitation

Figure 6.11 Effect of cable sag to span ratio on the mean value of the maximum cable displacement

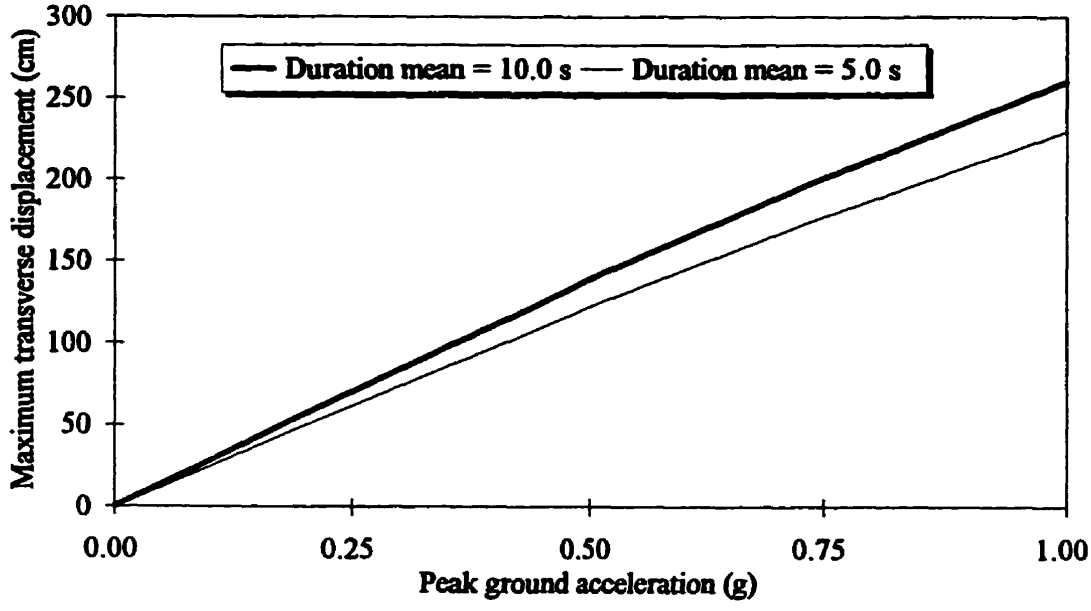

(a) Ttansverse excitation

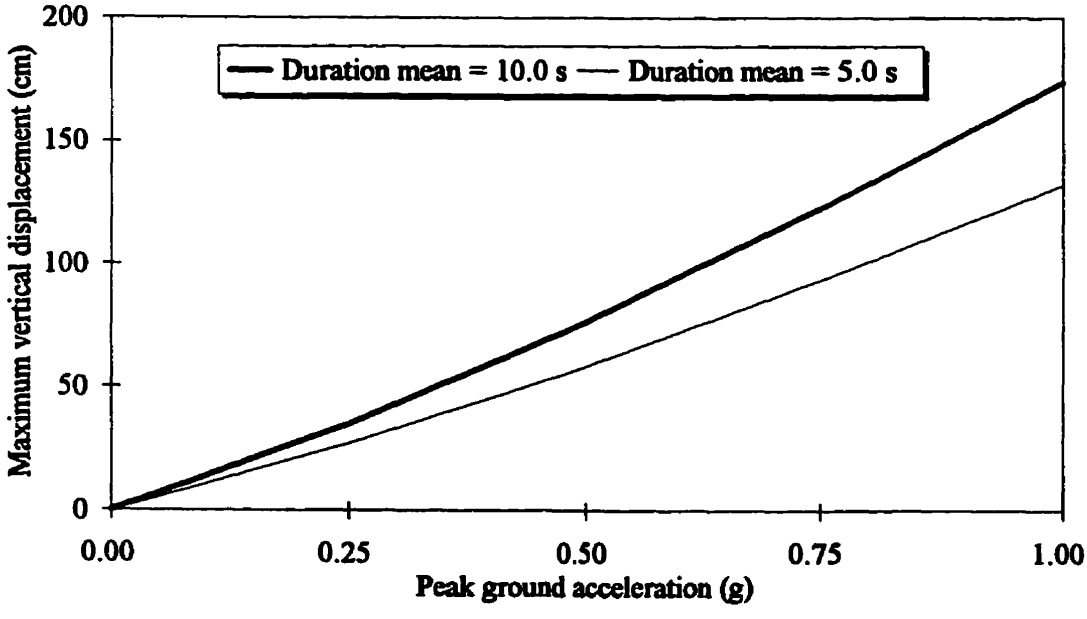

(b) Vertical excitation

Figure 6.12 Effect of strong ground motion duration on the mean value of the maximum cable displacement

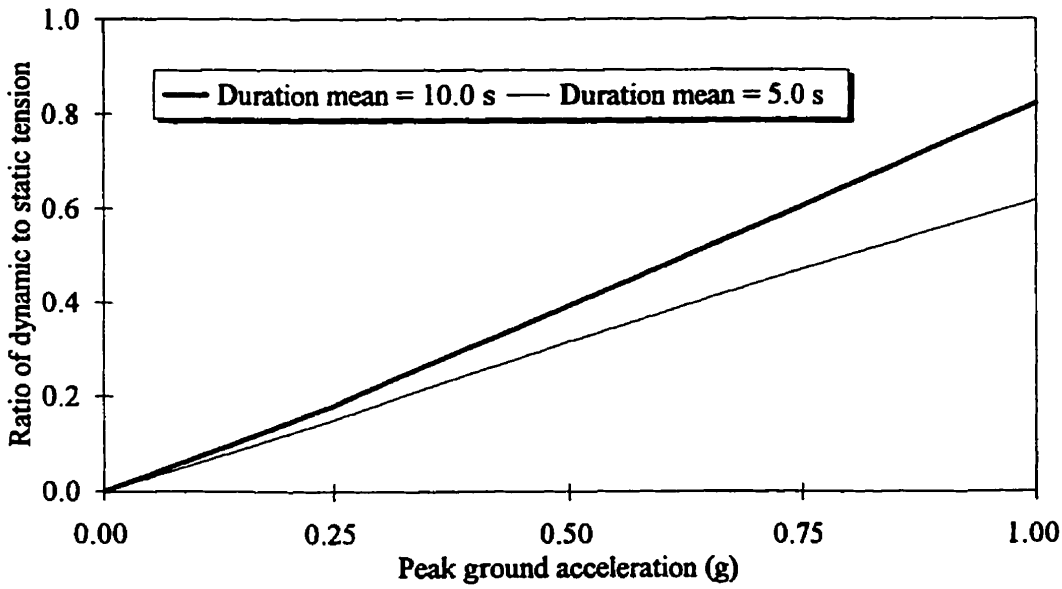

Figure 6.13 Effect of strong ground motion duration on the mean value of the ratio of dynamic to static cable tension due to vertical excitation

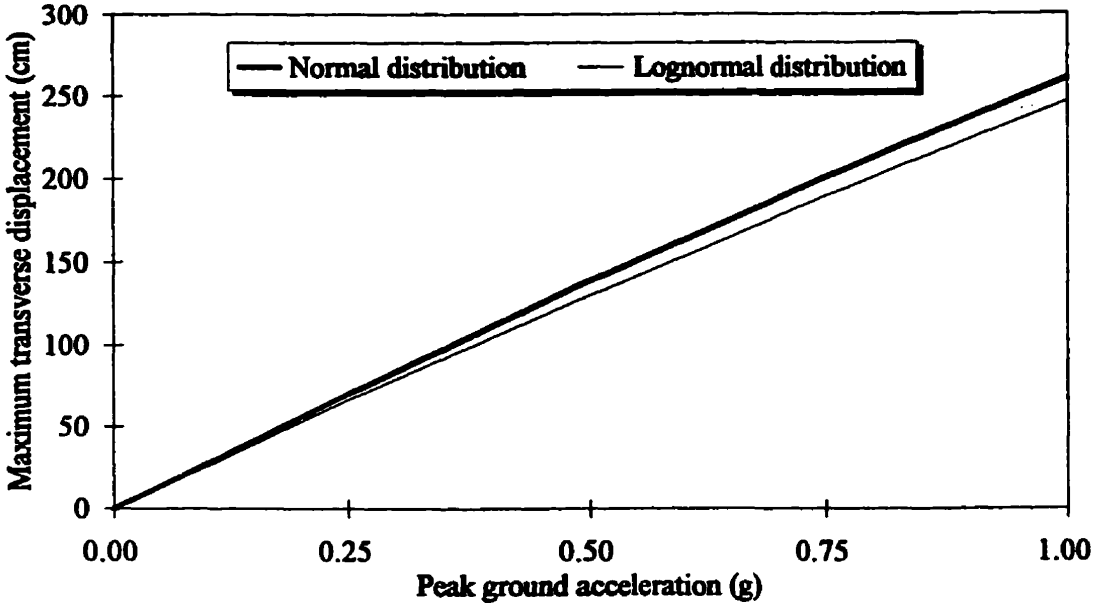

(a) Transverse excitation

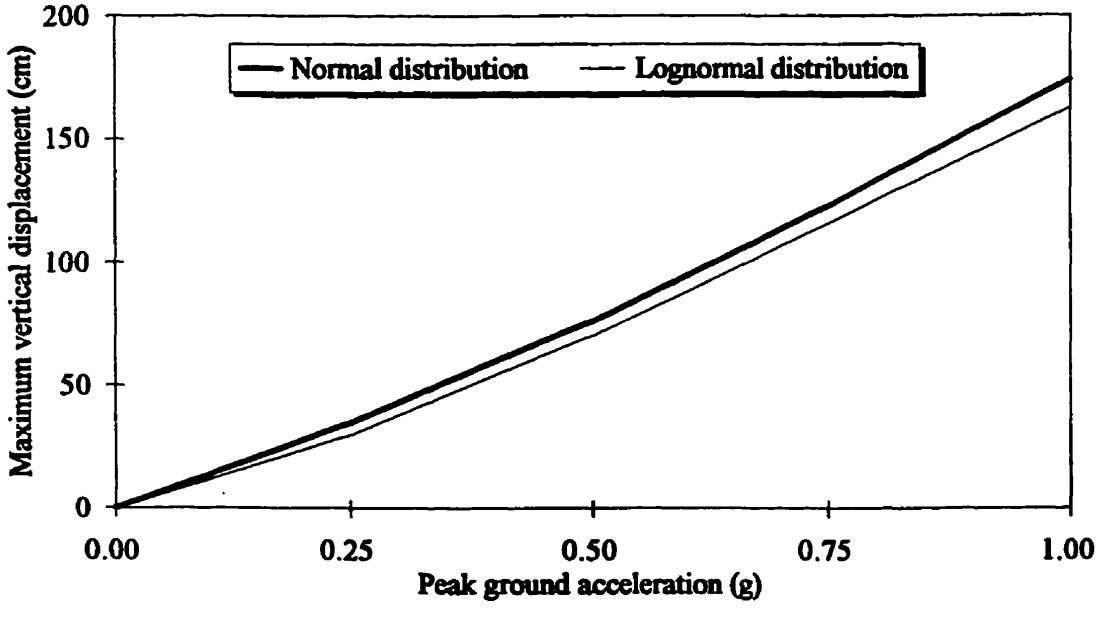

(b) Vertical excitation

Figure 6.14 Effect of the probability distribution type of the ground motion predominant frequency on the maximum cable displacement

CHAPTER 7

SUMMARY AND CONCLUSIONS

7.1 SUMMARY

A comprehensive study of the dynamic characteristics and seismic response of transmission lines is presented. The research is carried out in the following stages:

a) A finite element formulation for the cable dynamics is developed. The cable is modelled by a two-node straight element that allows for the cable geometric nonlinearity. The natural frequencies of the in-plane and the out-of-plane vibrations are evaluated and the cable response to seismic ground motion is determined.

b) The dynamic characteristics of steel latticed transmission towers are determined. The seismic response of an intermediate span of the transmission line is evaluated for the case of uniform support excitation. The effect of different modelling assumptions on the response is evaluated.

c) The internal forces in the tower members caused by the earthquake ground motion are computed and compared to those caused by the code defined wind and/or ice loads. The code considered in the analysis is the National Electrical Safety Code (NESC, 1993).

d) The effect of multiple support excitation on the response of transmission lines is investigated. The effects of both incoherency and wave travel are considered in the analysis.

e) A closed form solution for the cable response to multiple support excitation is presented. The cable is modelled by a two-degree of freedom model. The interaction between the in-plane and the out-of-plane vibrations is considered in the analysis. The effects of cable sag, cable damping and the phase difference between the ground motion excitations at various supports are investigated.

f) A probabilistic analysis of the cable seismic response is carried out. Probabilistic measures and probability of exceedance curves are presented for the cable tension and the cable maximum transverse and vertical displacements.

7.2 CONCLUSIONS

The following are the main conclusions arrived at from the analysis:

1. The analysis of the dynamic characteristics of transmission line elements indicates that for taut cables, both the in-plane and the out-of-plane frequencies are widely spaced and the response is mainly governed by the fundamental modes of vibration. For sagged cables, the in-plane frequencies of vibration are closely spaced and the higher modes contribute significantly to the response. The response of transmission towers to transverse excitation is dominated by the first mode contribution.

2. The study of the transmission line response to earthquake ground motion indicates that the cable response to earthquakes with low A/V ratio is much higher than their

response to earthquakes with high A/V ratio. Large displacements result in the cable due to transverse and vertical ground motions. The displacement caused by the longitudinal ground motion component is insignificant.

3. Due to the separation between the vertical and transverse fundamental frequencies of vibration for towers and cables, the contribution of the towers to the seismic behaviour of transmission lines is negligible. For the purpose of evaluating the cable displacement, the line can be modelled by cables fixed at both ends.

4. The forces developed in the transmission towers due to earthquake ground motion may exceed the forces caused by the code defined loads particularly in areas of high seismicity and low wind velocities. This suggests that earthquake loads should be considered in designing transmission towers.

5. The analysis of multiple support excitation of the transmission line indicates that the case of uniform support excitation does not necessarily cause the maximum forces and displacements in the line elements. The multiple support excitation which is a more accurate assumption can result in larger displacements and internal forces.

6. The analytical solution of the cable equations of motion produces accurate results as compared to the finite element solution. The accuracy of the solution increases for cables with a small sag to span ratio. The analytical solution can be used to examine the nonlinear cable behaviour near resonance. The analysis shows a softening behaviour for sagged cables and a hardening behaviour for taut cables.

7. The probabilistic analysis of cable vibration indicates that there is a reasonable probability that the cable tension due to seismic excitation exceeds the static cable

tension. Moreover, there is a high probability that the transverse and the vertical cable displacements exceed large displacement values depending on the site conditions and the peak ground acceleration. This suggests that the common approach in design to neglect the earthquake load and consider only wind and ice loads may not be a conservative design.

7.3 RECOMMENDATIONS

Based on the research presented in this thesis, the following recommendations for future work are suggested:

1. The results obtained from the current analysis shows that the forces produced in the transmission towers due to seismic ground motion may exceed those produced by the code specified wind and / or ice loads in seismically active areas. On the other hand, the overstrength design factors specified for the code loads are very high and result in a high cost for the design. It is recommended that the earthquake load is introduced in the design codes as a step to reduce the overstrength design factors and the line cost. If all the design loads are accounted for in the design, the overstrength factors can be reduced.
2. It is shown from the analysis that substantial displacements may result in the cable due to earthquake ground motion. It is therefore recommended to verify the line clearances indicated in the design codes against the seismic loads to ensure that during earthquakes, the cables do not touch each other or any other structures.

3. The analysis indicates that large cable displacements may result from earthquake ground motion which indicates the importance of developing a technique to damp these vibrations. One of the most promising techniques is the use of self damping conductors and more research is required in this area.

4. There is a lack of experimental work in the area of seismic behaviour of cables. It is recommended that shake table tests on cables be conducted to examine the effects of different parameters on the cable vibration.

REFERENCES

Abdel-Ghaffar, A.M. and Stringfellow, R.G., 1984a. Response of Suspension Bridges to Travelling Earthquake Excitations: Part I- Vertical Response. Soil Dynamics and Earthquake Engineering, Vol. 3, No. 4, pp. 62-72.

Abdel-Ghaffar, A.M. and Stringfellow, R.G., 1984b. Response of Suspension Bridges to Travelling Earthquake Excitations: Part II- Lateral Response. Soil Dynamics and Earthquake Engineering, Vol. 3, No. 4, pp. 73-81.

Ali, S.A., 1986. Dynamic Response of Sagged Cables. Computers and Structures, Vol. 23, No. 1, pp. 51-57.

Al-Noury, S.I. and Ali, S.A., 1985. Large-Amplitude Vibrations of Parabolic Cables. Journal of Sound and Vibration, Vol. 101, No. 4, pp. 451-462.

Argyris, J.H., Dunne, P.C., and Angelopoulos, T., 1973. Non-Linear Oscillations Using the Finite Element Technique. Computational Methods in Applied Mechanics and Engineering, Vol. 2, pp. 203-250.

ASCE, 1991. Guidelines for Transmission Line Structural Loading. Prepared by Committee on Electrical Transmission Structures of the Committee on the Analysis and Design of Structures, the Structural Division, the Americal Society of Civil Engineers.

Aziz, T.S., Ghobarah, A. and El-Attar, M., 1995. Effect of Spatially Incoherent Ground Motion on the Seismic Response of Overhead Transmission Lines. Proceedings of Al-Azhar Engineering Fourth International Conference, Vol. 3, pp. 191-200, Cairo, Egypt.

Aziz, T.S., Ghobarah, A., and El-Attar, M., 1996. Nonlinear Dynamics of Transmission Lines. Proceedings of Eleventh World Conference on Earthquake Engineering, Acapulco, Mexico.

Benedettini, F. and Rega, G., 1987. Non-Linear Dynamics of an Elastic Cable under Planar Excitation. Int. J. Non-Linear Mechanics, Vol. 22, No. 6, pp. 497-509.

Benedettini, F., Rega, G., and Vestroni, F., 1986. Modal Coupling in the Free Nonplanar Finite Motion of an Elastic Cable. Meccanica, Vol. 21, pp. 38-46.

CAN/CSA-C22.3 No. 1-M87, 1987. Overhead Systems. Canadian Standards Association, Rexdale, Ontario.

CSA S37-M86, 1986. Antenna Towers and Antenna Supporting Structures. Canadian Standards Association, Rexdale, Ontario.

Clough, R.W. and Penzien, J., 1975. Dynamics of Structures. McGraw-Hill, New York.

Committee on Wind Effects, 1987. Wind Loading and Wind-Induced Structural Response, A state-of-the-art report, ASCE, 207 p., 1987.

Currie, I.G., Havard, D.G., MacDonald, R. and Pon, C.J., 1989. Aeolian Vibration of Bundle Conductors. Proceedings of the spring meeting of the Engineering and Operation Section of the Canadian Electrical Association, Toronto, 22p.

Der Kiureghian, A. and Neuenhofer, A., 1991. A response Spectrum Method for Multiple-Support Seismic Excitations. Earthquake Engineering Research Center, Report UCB/ EERC-91-08, University of California, Berkeley, CA.

Desai, Y.M., Popplewell, N., Shah, A.H. and Buragohain, D.N., 1988. Geometric Nonlinear Static Analysis of Cable Supported Structures. Computers and Structures, Vol. 29, No. 6, pp. 1001-1009.

Dumanoglu, A.A and Severn, R.T., 1987. Seismic Response of Modern Suspension Bridges to Asynchronous Vertical Ground Motion. Proceedings of the Institution of Civil Engineers, Part 2, Vol. 83, pp. 701-730.

El-Attar, M., Ghobarah, A. and Aziz, T.S., 1995a. Dynamic Analysis of Overhead Transmission Lines. Proceedings of the Canadian Society of Civil Engineering Annual Conference, Ottawa, Canada, Vol. IV, pp. 605-614.

El-Attar, M., Aziz, T.S., Mansour, W.M. and Ghobarah, A., 1995b. A Nonlinear Approach to the Attenuation of Oscillations of Transmission Lines Subjected to Seismic Loading. Proceedings of the Ninth World Congress on the Theory of Machines and Mechanisms, Milano, Italy, Vol. 2, pp. 1118-1122.

El-Attar, M., Ghobarah, A. and Aziz, T.S., 1996. Nonlinear Cable Response to Multiple Support Periodic Excitation. Submitted to the Journal of Sound and Vibration.

Elghadamsi, F.E., Mohraz, B., Lee, C.T. and Moayyad, P., 1988. Time-Dependent Power Spectral Density of Earthquake Ground Motion. Soil Dynamics and Earthquake Engineering, Vol. 7, No. 1, pp. 15-21.

Fenves, G.L., 1992. Earthquake Analysis and Response of Multi-Span Bridges and Viaduct Structures. Seminar Proceedings, Seismic Design and Retrofit of Bridges, University of California at Berkeley, pp. 214-244.

Foata, M., Hardy, C., St-Louis, M. and Brunelle, J., 1989. Modeling of the Conductor Vibrations and Applications to the Grondines 450KV River Crossing. Proceedings of the spring meeting of the Engineering and Operation Section of the Canadian Electrical Association, Toronto, 15p.

Gambhir, M.L. and Batchelor, B., 1977. A Finite Element for 3-D Prestressed Cablenets. Int. Journal of Numerical Methods in Engineering, Vol. 11, pp. 1699-1718.

Gambhir, M.L. and Batchelor, B., 1978. Parametric Study of Free Vibration of Sagged Cables. Computers and Structures, Vol. 8, No. 5, pp. 641-648.

Ghobarah, A., Aziz, T.S. and El-Attar, M., 1996. Response of Transmission Lines to Multiple Support Excitation. Engineering Structures, Vol. 18, No. 12, pp. 936-946.

Hagedorn, P., 1981. Non-linear Oscillations. Clarendon Press., Oxford.

Hagedorn, P., 1982. On the Computation of Damped Wind-Excited Vibrations of Overhead Transmission Lines. Journal of Sound and Vibration, Vol. 83, No. 2, pp. 253-271.

Hagedorn, P. and Schafer, B., 1980. On Non-linear Free Vibrations of an Elastic Cable. Int. International Journal of Non-Linear Mechanics, Vol. 15, pp. 333-340.

Hao, H., Oliveira, C.S., and Penzien, J., 1989. Multiple-Station Ground Motion Processing and Simulation Based on SMART-1 Array Data. Nuclear Engineering and Design, Vol. 111, pp. 293-310.

Harichandran, R.S. and Vanmarcke, E.H., 1986. Stochastic Variation of Earthquake Ground Motion in Space and Time. Journal of Engineering Mechanics, ASCE, Vol. 112, No. 2, pp. 154-174.

Henghold, W.M. and Russell, J.J., 1976. Equilibrium and Natural Frequencies of Cable Structures (A Nonlinear Finite Element Approach.). Computers and Structures, Vol. 6, pp. 267-271.

Henghold, W.M., Russell, J.J. and Morgan, J.D., 1977. Free Vibrations of Cable in Three Dimensions. Journal of Structural Engineering, ASCE, Vol. 103, No. ST5, pp. 1127-1136.

Hindy, A. and Novak, M., 1980. Response of Pipelines to Random Ground Motion. Journal of Engineering Mechanics, ASCE, Vol. 106, pp. 339-360.

Hodhod, O.A., 1993. Dynamic and Seismic Characteristics of Cable-Stayed Bridges. Ph.D. Thesis, McMaster University, Hamilton, Ontario, Canada

Irvine, H.M., 1981. Cable Structures. The MIT Press, Cambridge, Massachusetts, 259p.

Irvine, H.M. and Caughey, T.K., 1974. The Linear Theory of Free Vibrations of a Suspended Cable. Proc. Royal Society, London, A.341, pp. 299-315.

Iyengar, R.N. and Rao, G.V., 1988. Free Vibrations and Parametric Instability of a Laterally Loaded Cable. Journal of Sound and Vibration, Vol. 127, No. 2 , pp. 231-243.

Jones , T.A., Cometa, E.T. and Chan, J.C., 1988. Comparative Stress-Strain Characteristics of ACSR and SDC Overhead Conductors. Proc. of the International Conference on Overhead Line Design and Construction : Theory and Practice (up to 150 kV), Publication Number 297, The Institute of Electrical Engineers, London, U.K.

Kempner, L., Stroud, R.C. and Smith, S., 1981. Transmission Line Dynamic/Static Structural Testing. Journal of Structural Engineering, ASCE, Vol. 107, No. ST10, pp. 1895-1906.

Kotsubo, S., Takanishi, T., Uno, K. and Sonoda, T., 1983. Dynamic Tests and Seismic Analysis of High Steel Towers of Electrical Transmission Line. Transactions of the Japan Society of Civil Engineering, Vol. 15, pp. 72-75.

Kravitz, R.A., 1982. Transmission Line Tower Analysis and Design in Review. IEEE Transactions on Power Apparatus and Systems, Vol. PAS-101, pp. 4350-4357.

Lai, S.-S. P., 1982. Statistical Chracterization of Strong Ground Motions Using Power Spectral Density Function. Bulletin Seismological Society of America, Vol. 72, pp. 259-274.

Lomas, C., 1993. Transmission tower development in the UK. Engineering Structures, Vol.15, No.4, pp. 277-288.

Leonard, J.W. and Recker, W.W., 1972. Nonlinear Dynamics of Cables with Low Initial Tension. Journal of Engineering Mechanics, ASCE, Vol. 98, No. EM2, pp. 293-310.

Loh, C.H. and Lin, S.G., 1990. Directionality and Simulation in Spatial Variation of Seismic Waves. Engineering Structures, Vol. 12, pp. 134-143.

Luo, T.H., Durrani, A. and Conte, J., 1995. Seismic Reliability Assessment of Existing R/C Flat-Slab Buildings. Journal of Structural Engineering, ASCE, Vol. 121, No. 10, pp. 1522-1530.

Luongo, A., Rega, G. and Vestroni, F., 1982. Monofrequent Oscillations of a Non-linear Model of a Suspended Cable. Journal of Sound and Vibration, Vol. 82, No. 2, pp. 247-259.

Luongo, A., Rega, G. and Vestroni, F., 1984. Planar Non-linear Free Vibrations of an Elastic Cable. International Journal of Non-Linear Mechanics, Vol. 19, pp. 39-52.

Maeno, Y., Hanada, K., Sakamoto, Y. and Yamagishi, H., 1984. Dynamic Properties of UHV Power Transmission Towers- Full Scale Tests and Numerical Investigation. Proceedings of the Eight World Conference on Earthquake Engineering, San Francisco, California, Vol. VI, pp. 929-936.

Maison, B.F., 1992. PC-ANSR, A Computer Program for Nonlinear Structural Analysis, University of California, Berkeley, CA.

McClure, G. and Tinawi, R., 1987. Mathematical Modeling of the Transient Response of Electric Transmission Lines due to Conductor Breakage. Computers and Structures, Vol. 26, pp. 41-56.

McCulloch, A.R., Pue-Gilchrist, A.C. and Kirkpatrick, L.A., 1980. Ten Years of Progress with Self-Damping Conductor. IEEE Transactions on Power Apparatus and Systems, Vol. PAS-99, pp. 998-1011.

Migliore, H.J. and Webster, R.L., 1979. Current Methods for Analyzing Dynamic Cable Response. Shock and Vibration, Vol. 11, No. 6, pp. 3-16.

Migliore, H.J. and Webster, R.L., 1982. Current Methods for Analyzing Dynamic Cable Response 1979 to the Present. Shock and Vibration, Vol. 14, No. 9, pp. 19-24.

Mondkar, D.P. and Powell, G.H., 1975. ANSR-I: General Purpose Program for Analysis of Nonlinear Structural Response. Earthquake Engineering Research Centre, Report UCB/ EERC- 75-37, University of California, Berkeley, CA.

Mondkar, D.P. and Powell, G.H., 1977. Finite Element Analysis of Non-linear Static and Dynamic Response. Int. J. for Numerical Methods in Engineering, Vol. 11, pp. 499-520.

Mote, S.H. and Chu, K-H., 1978. Cable Trusses Subjected to Earthquakes. Journal of Structural Engineering, ASCE, Vol. 104, No. ST4, pp. 667-680.

Myerscough, C.J., 1973. A Simple Model of the Growth of Wind-Induced Oscillations in Overhead Lines. Journal of Sound and Vibration, Vol. 28, No. 4, pp. 699-713.

Myerscough, C.J., 1975. Further Studies on the Growth of Wind-Induced Oscillations in Overhead Lines. Journal of Sound and Vibration, Vol .39, No .4, pp. 503-517.

Nayfeh, A.H. and Mook, D.T., 1979. Nonlinear Oscillations. Wiley Interscience, New York.

Nazmy, A.S. and Abdel-Ghaffar, A.M., 1992. Effects of Ground Motion Spatial Variability on the Response of Cable Stayed Bridges. Earthquake Engineering and Structural Dynamics, Vol. 21, No.1, pp. 1-20.

Naumoski, N., Tso, W.K. and Heidebrecht, A.C., 1988. A Selection of Representative Strong Motion Earthquake Records Having Different A/V Ratios. McMaster University, Earthquake Engineering Research Group, EERG Report 88-01.

NBCC 1995. National Building Code of Canada. National Research Council of Canada, Ottawa, Ontario.

NESC, 1993.National Electrical Safety Code. American National Standard, Institutes of Electrical and Electronics Engineers, Inc., NY.

Northridge Earthquake of January 17, 1994- Reconnaissance Report, Vol. 1, Earthquake Spectra, Supplement C to Volume 11, Earthquake Engineering Research Institute, Oakland, CA, 1995.

Novak, M., 1987. Discussion of "Stochastic Variation of Earthquake Ground Motion in Space and Time" by R.S. Harichandran and E.H.Vamareke. Journal of Engineering Mechanics, ASCE, Vol. 113, No. 8, pp. 1267-1270.

Ozono, S. and Maeda, J., 1992. In-Plane Dynamic Interaction between a Tower and Conductors at Lower Frequencies. Engineering Structures, Vol. 14, No. 4, pp. 210-216.

Ozono, S., Maeda, J., and Makino, M., 1988. Characteristic of In-Plane Free Vibration of Transmission Line Systems. Engineering Structures, Vol. 10, No. 4, pp. 272-280.

Perkins, N.C., 1992. Modal Interactions in the Non-linear Response of Elastic Cables Under Parametric/ External Excitation. Int. J. Non-Linear Mechanics, Vol. 27, No. 2, pp. 233-250.

Perkins, N.C. and Mote, C.D., 1987. Three-Dimensional Vibration of Travelling Elastic Cables. Journal of Sound and Vibration, Vol. 114, No. 2, pp. 325-340.

Ramadan, O. and Novak, M., 1992. Dam Response to Spatially Variable Seismic Ground Motions. Geotechnical Research Centre, GEOT-14-92, University of Western Ontario, London, Canada.

Ramadan, O. and Novak, M., 1993. Simulation of Spatially Incoherent Random Ground Motions. Journal of Engineering Mechanics, ASCE, Vol. 119, No. 5, pp. 997-1016.

Ramadan, O. and Novak, M., 1994. Simulation of Multidimensional, Anisotropic Ground Motion. Journal of Engineering Mechanics, ASCE, Vol. 120, No. 8, pp. 1773-1785.

Rao, G.V. and Iyengar, R. N., 1991a. Seismic Response of a Long Span Cable. Earthquake Engineering and Structural Dynamics, Vol. 20, pp. 243-258.

Rao, G.V. and Iyengar, R.N., 1991b. Internal Resonance and Non-Linear Response of a Cable Under Periodic Excitation. Journal of Sound and Vibration, Vol. 149, No.1, pp. 25-41.

Rassem, M., Ghobarah, A. and Heidebrecht, A.C., 1996. Site Effects on the Seismic Response of a Suspension Bridge. Engineering Structures, Vol. 18, No. 5, pp. 363-370.

Russell, J.J., Morgan, J.D. and Henghold, W.M., 1978. Cable Equilibrium and Stability in a Steady Wind. Journal of Structural Engineering, ASCE, Vol. 104, No. ST2, pp. 301-310.

Schafer, B., 1984. Dynamical Modelling of Wind-Induced Vibrations of Overhead Lines. Int. J. Non-Linear Mechanics, Vol. 19, No. 5, pp. 455-467.

Simpson, A., 1966. Determination of the In-Plane Natural Frequencies of Multi-Span Transmission Lines by a Transfer Matrix Method. Proc. IEEE, Vol. 113, No. 5, pp. 870-877.

Simpson, A., 1970. On the Oscillatory Motions of Translating Elastic Cables. Proc. of a Symposium on Structural Dynamics. Loughborough University of Technology, Paper No. B.4, 13p, U.K.

Sues, R.H., Wen, Y-K. and Ang, A. H.-S., 1985. Stochastic Evaluation of Seismic Structural Performance. Journal of Structural Engineering, ASCE, Vol. 111, No. 6, pp. 1204-1218.

Suzuki, T., Tamamatsu, K. and Fukasawa, T., 1992. Seismic Response Characteristics of Transmission Towers. Tenth World Conference on Earthquake Engineering, Madrid, Spain, pp. 4961-4967.

Takahashi, K., 1991. Dynamic Stability of Cables Subjected to an Axial Periodic Load. Journal of Sound and Vibration, Vol. 144, No. 2, pp. 323-330.

Takahashi, K. and Konishi, Y., 1987a. Non-Linear Vibrations of Cables in Three Dimensions, Part I: Non-Linear Free Vibrations. Journal of Sound and Vibration, Vol. 118, No. 1, pp. 69-84.

Takahashi, K. and Konishi, Y., 1987b. Non-Linear Vibrations of Cables in Three Dimensions, Part II: Out-Of-Plane Vibrations Under In-Plane Sinusoidally Time-Varying Load. Journal of Sound and Vibration, Vol. 118, No. 1, pp. 69-84.

Trainor, P.G.S., Shah, A.H. and Popplewell, N., 1986. Estimating the Fundamental Natural Frequency of Towers by Dunkerley's Method. Journal of Sound and Vibration, Vol. 109, No. 2, pp. 285-292.

Tso, W.K., Zhu, T.J. and Heidebrecht, A.C., 1992. Engineering Implication of Ground Motion A/V Ratio. Soil Dynamics and Earthquake Engineering, Vol. 11, pp. 133-144.

Winget, J.M. and Houston, R.L., 1976. Cable Dynamics- A Finite Segment Approach. Computers and Structures, Vol. 6, pp. 475-480.

Yamaguchi, H., Miyata, T., and Ito, M., 1982. Dynamics of a Suspended Cable in Three Dimensions. Transactions of Japan Society of Civil Engineering, Vol. 14, pp. 424-427.

Zerva, A., 1990. Response of Multi-Span Beams to Spatially Incoherent Seismic Ground Motions. Earthquake Engineering and Structural Dynamics, Vol. 19, pp. 819-832.

Zerva, A., 1994. On the Spatial Variation of Seismic Ground Motions and its Effects on Lifelines. Engineering Structures, Vol. 16, No. 7, pp. 534-546.

IMAGE EVALUATION TEST TARGET (QA-3)

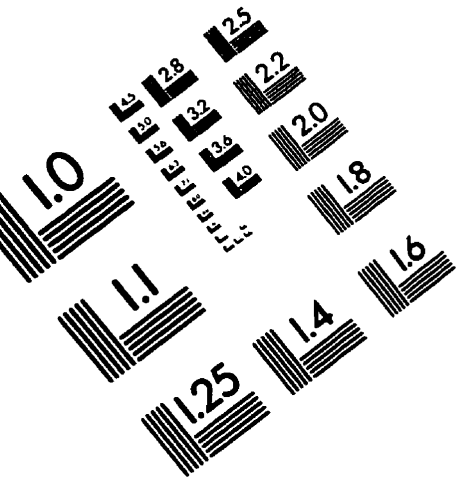

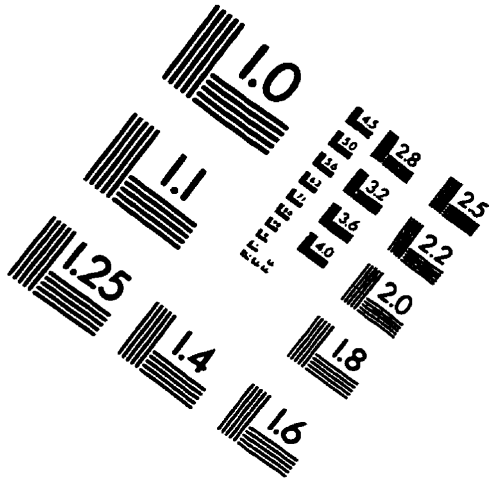

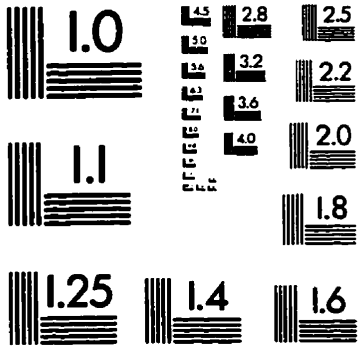

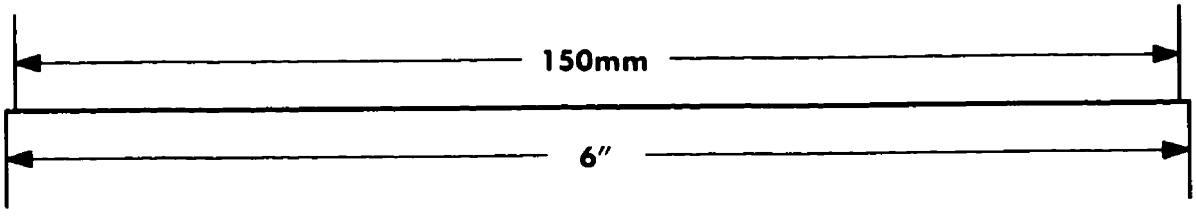

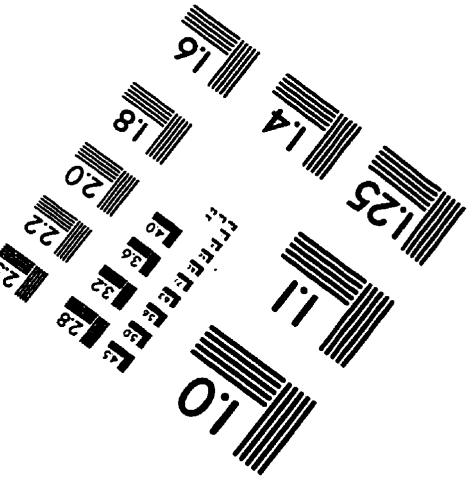

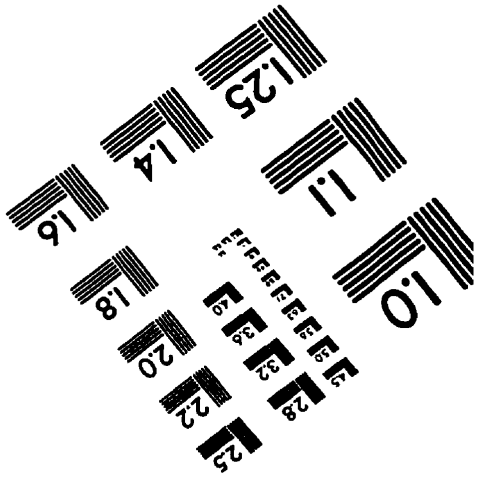

APPLIED IMAGE, Inc
1653 East Main Street
Rochester, NY 14609 USA
Phone: 716/482-0300
Fax: 716/288-5989